An Investigation of Phosphorous-Based Bioconjugation Techniques for Protein Modification

by

Maja Lopandic

A thesis

presented to the University of Waterloo

in fulfillment of the

thesis requirement for the degree of

Master of Science

in

Chemistry

Waterloo, Ontario, Canada, 2022

Author's Declaration

I hereby declare that I am the sole author of this thesis. This is a true copy of the thesis, including any final revisions, as accepted by my examiners.

I understand that my thesis may be made electronically available to the public.

Abstract

Bioconjugation is a powerful technique allowing for the modification of biomolecules such as proteins. Exposed amino acid residues on the surface of proteins act as chemical handles for the attachment of biomolecules or synthetic compounds including polymers, therapeutic agents, and fluorophores. Protein conjugates are commonly employed in drug delivery applications, as molecular probes, and in the assembly of biosensors and biomaterials. As these designs become increasingly complex, new bioconjugation chemistries are needed. In this thesis, novel phosphorous-based bioconjugation techniques were investigated. The phospha-Michael addition and Wittig reactions were the basis of the studied approaches. The reaction of triphenylphosphine (TPP) and tris(2-carboxyethyl)phosphine (TCEP) with maleimide results in the formation of a phosphonium adduct. These adducts were further used in the Wittig reaction involving aldehydes containing unique chemical moieties. A polymer-bound TPP resin was also successfully employed in the solid phase organic synthesis of Wittig olefin bioconjugation reagents using maleimide and an assortment of aldehydes for protein modification. Several functionalized polymer-supported resins were used in a chromatography-free purification protocol for these reagents.

Five different activated ester Wittig olefin reagents were successfully synthesized and purified with the solid phase approach. These reagents target residues containing primary amines. Each reagent was successfully attached to the surface of bovine carbonic anhydrase, the model protein. Electrospray ionization mass spectrometry (ESI MS) was used to detect these conjugates. An amine-functionalized Wittig olefin reagent was synthesized with the solid phase approach for the site-selective transglutaminase mediated modification of apomyoglobin. As the apomyoglobin-Wittig olefin conjugate was not detected by ESI MS, future studies will focus on the design of an appropriate Wittig olefin substrate for transglutaminase.

It is contemplated that the strategies demonstrated herein may allow for the synthesis of new molecular probes and therapeutic drug molecules for biomolecular applications. Additionally, the immobilization of enzymes onto solid surfaces and polymer-supported resins using our method may also be employed in the fabrication of novel catalytic biomaterials.

Acknowledgements

I would like to thank my supervisor Dr. John Honek for all of his guidance and support throughout my undergraduate and graduate studies. I would like to express my full appreciation for the time and effort he put into helping me learn and grow as a researcher.

I would like to thank Fatima Merza, a former graduate student in the Honek laboratory. We both started at the same time in the Honek research group and she provided immense help and encouragement while we worked together. I would also like to acknowledge and thank our undergraduate researchers: Amanda Ratto, Julian Marlyn, Ethan Solomon, and Claire Stoecker for their contributions to this project. Thank you to the former Honek research group members for their help as well.

I would like to express my sincerest thanks to Dr. Richard Smith and Valerie Goodfellow of the University of Waterloo Mass Spectrometry Facility for their help and training with the mass spectrometry techniques in this project. Thank you both for all of your guidance and support, both with respect to my project and academic advice during my graduate studies. I would also like to sincerely thank Jan Venne of the University of Waterloo NMR Facility for running the samples.

Thank you to my committee members, Dr. Subha Kalyaanamoorthy and Dr. Jean Duhamel for taking the time to review the work presented in this thesis.

Lastly, but certainly not least, I would like to thank all of my family and friends who have always been there to help me throughout my graduate studies. I sincerely appreciate the many ways they have expressed their support, allowing me to be successful during my time here.

Table of Contents

List of Figures

List of Tables

List of Schemes

List of Abbreviations

ACN	Acetonitrile
ADC	Antibody-drug conjugates
ApoMb	Apomyoglobin
BCA	Bovine carbonic anhydrase
BSTPP	Bis(*p*-sulfonatophenyl) phenylphosphine
CDCl$_3$	Deuterated chloroform
DCM	Dichloromethane
ddH$_2$O	Doubly distilled water
DMF	*N*, *N*-Dimethylformamide
DMSO	Dimethyl sulfoxide
DPPA	3-(Diphenylphosphino) propionic acid
ESI MS	Electrospray ionization mass spectrometry
EtOH	Ethanol
FA	Formic acid
HEPES	4-(2-Hydroxyethyl)-1-piperazineethanesulfonic acid
HSF	Horse spleen ferritin
K$_d$	Dissociation constant
KP	Potassium phosphate
MAL	Maleimide
MEK	Methyl ethyl ketone
MeOH	Methanol
MP	Macroporous polystyrene
MPA	3-Maleimidopropionic acid *N*-succinimidyl ester
mPEG$_4$BA	Methoxy-PEG$_4$-Benzaldehyde
MSTPP	3-(diphenylphosphino) monobenzenesulfonic acid
MTGase	Microbial transglutaminase
MWCO	Molecular weight cut-off
NaOH	Sodium hydroxide
NEM	N-Ethylmaleimide
NHS	N-Hydroxysuccinimide

NMR	Nuclear magnetic resonance
PEG	Poly(ethylene glycol)
PEG-TPP	Poly(ethylene glycol)-triphenylphosphine
PfFtn	*Pyrococcus furiosus* ferritin
pI	Isoelectric point
PNP	p-Nitrophenol
PS	Polystyrene-supported
PS-DIEA	Polystyrene-supported diisopropylethylamine
PS-TPP	Polystyrene-supported triphenylphosphine
PS-Ts-NHNH$_2$	Polystyrene-supported hydrazide
PS-TsOH	Polystyrene-supported *p*-toluenesulfonic acid
RP-HPLC	Reverse-phase high performance liquid chromatography
SPOS	Solid phase organic synthesis
t-Boc	Tert-butyloxycarbonyl
TCEP	Tris(2-carboxyethyl)phosphine
TEA	Triethylamine
TFA	Trifluoroacetic acid
TFP	2,3,5,6-Tetrafluorophenol
TGase	Transglutaminase
THF	Tetrahydrofuran
THPP	Tris(hydroxypropyl)phosphine
TLC	Thin layer chromatography
TPP	Triphenylphosphine
TSTPP	Tris(3-sulfophenyl)phosphine
UV	Ultraviolet

Chapter 1.0. Introduction to Protein Bioconjugation Strategies

Bioconjugation is a powerful chemical tool for biomolecule derivatization. This technique refers to the linkage between two molecules, at least one of which is a biomolecule. Lipids, carbohydrates, nucleic acids, and proteins can be modified with a variety of synthetic compounds including polymers, fluorophores, and drug compounds. From the four classes of biomolecules listed, proteins have the greatest versatility in terms of size, structure, and function.[1-5] Bioconjugation of synthetic components to proteins results in the creation of bioconjugates with novel functionalities and properties, depending on the desired application. Protein bioconjugation serves as a platform for the fabrication of antibody-drug conjugates (ADCs), polymer-protein therapeutic agents, molecular probes for diagnostics, enzymatic assays, immobilization of proteins, biosensors, and biomaterials.[6-9]

Surface amino acid residues, along with the N- and C-termini of proteins, act as chemical handles that are selectively targeted for derivatization (Figure 1.1). Commonly employed amino acid residues are nucleophilic and include lysine, cysteine, tyrosine and histidine.[10] Unique chemical strategies exist for each amino acid side chain. A number of extensive resources and guides detailing the bioconjugation chemistries of each modifiable amino acid can be found in the literature.[9-13]
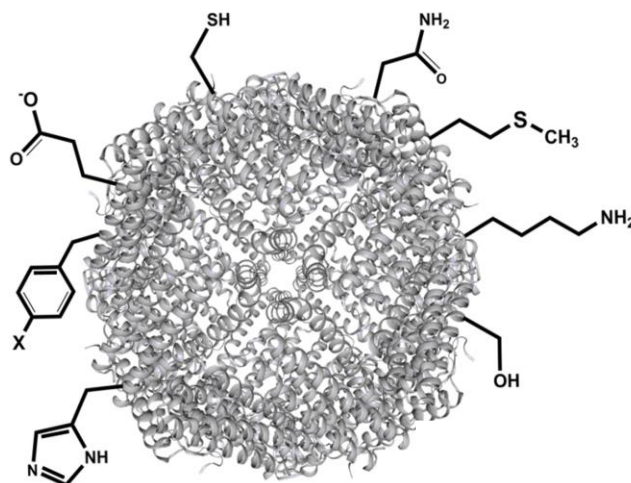
Figure 1.1. Amino acid residues available on the surface of a model protein for modification. (Image credit: Fatima Merza).

Proteins can be genetically engineered to express amino acids at certain positions within the sequence, which could aid in the use of specific and targeted bioconjugation techniques.[11,14] Non-canonical amino acids can also be engineered at a specific position along a protein backbone. The site-specific modification of proteins is one of the major challenges associated with protein bioconjugation chemistry. Depending on the amino acid selected, heterogeneous mixtures of bioconjugates can arise. These mixtures are typically inseparable. For example, lysine is one of the most naturally abundant amino acids whereas cysteine is one of the less commonly occurring residues.[11,14] Designing a protein nanoparticle with conjugation occurring at a specific location on the protein could require cysteine modification or non-canonical amino acids in the bioconjugation strategy. However, if a greater extent of modification is desired, using strategies that employ lysine residues is a good choice.[11]

The second major challenge with bioconjugation strategies involves the use of mild reaction conditions. The practical utility of a specific nucleophilic amino acid side chain is affected by the reaction media, and its reactivity towards a given electrophile. [15] Proteins can be sensitive to changes in temperature, pH, and organic solvents. Typically, aqueous buffers are used and the reactions are conducted at low temperatures (≤ 37 °C).[13] Although chemically robust proteins can tolerate harsher reaction conditions, care must be taken so that the bioconjugation strategy does not result in the loss of protein functionality or three-dimensional structure. In practice, most bioconjugation reactions are conducted at biologically relevant conditions (around neutral pH) in order to preserve the structural integrity of the protein. The pKa of the ε-amine of lysine is ~10.[10,13,15] However, this pKa can vary depending on the surrounding chemical environment, allowing for the modification of lysines at physiological pH.[16,17] In comparison, the guanidinyl group of arginine has a pKa of >12. [10,15] This amino acid would be a poor choice for bioconjugation at relatively neutral pHs, as the majority of these residues will be protonated and unable to participate in most reactions.[15] Therefore, when designing a novel bioconjugation strategy, the reaction conditions must be accounted for in order to obtain novel conjugates that still retain their function. The choice of the chemical handle must be carefully selected depending on its intrinsic nucleophilicity and the degree of specificity desired.

While several bioconjugation guides exist in the literature, the research described in this thesis only focuses on a small subset of these reactions: the non-specific modification of lysine, and the chemoenzymatic modification of glutamine residues. In this chapter, bioconjugation chemistries that are relevant to the techniques utilized throughout this thesis will be presented. The chemistry of the two most frequently modified amino acids, lysine and cysteine will be discussed. A brief discussion on the most common synthetic polymer used for bioconjugation, particularily

for drug delivery applications, is included. Chemoenzymatic bioconjugation approaches will also be discussed, along with the most pertinent bioconjugation applications: the design of molecular probes, ADCs, protein therapeutics and the immobilization of proteins onto solid surfaces.

1.1. PEGylation of Proteins

An important synthetic polymer that is frequently used in the fabrication of protein conjugates, particularly for biomedical applications, is polyethylene glycol (PEG). PEGylation reagents are powerful and versatile tools for engineering protein nanoparticles and biomaterials. The general structure of PEG is shown in Figure 1.2.
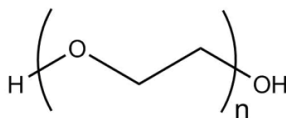
Figure 1.2. Poly(ethylene glycol).

Hydrocarbon linkers are not typically used for protein modification as the chain will undergo a hydrophobic collapse in an aqueous solution. PEG is a flexible and hydrophilic polymer, and these properties are quite useful for protein bioconjugation.[3,18,19] It has been demonstrated that polymer-protein conjugates containing PEG exhibit greater solubility in certain aqueous solvents that the proteins may not normally be soluble in.[19-21] Similarly, attaching a PEG chain to a non-polar synthetic compound increases the aqueous solubility of the compound. This facilitates the conjugation of proteins with water-insoluble moieties. The length of the PEG chain can affect the resulting hydrophilicity of a conjugate. However, longer PEG chains may block a second reagent from attaching to the surface of the protein, if the two potential sites of modification are in close vicinity.[22]

Moreover, PEG polymer-protein conjugates have been used as therapeutic agents since the early 1990s, although studies concerning the fabrication of these conjugates have been known since the 1970s.[18,19] PEG polymers have been approved for their use in protein therapeutics due to their non-toxicity, their ability to mask the protein from the body's immune system, and increasing its circulation time within the body.[14,18,19,22-24] In recent years, alternatives to protein PEGylation for therapeutic purposes have been explored. In some patients, anti-PEG antibodies are produced, leading to an immune response.[25] Depending on the size of the PEG chain attached to the protein, PEG can accumulate in the liver.[25] Regardless of these challenges, PEG is the only synthetic polymer approved by the United States Food and Drug Administration for clinical use.[26]

One example of the fabrication of therapeutic nanoparticles is the synthesis of a polymer-protein conjugate that could potentially be used to detect and target melanoma metastases.[27] Ferritin protein capsules were genetically engineered to express melanocyte-stimulating hormone on their surface, and then decorated with PEG polymer chains.[27] The nanoparticles were subsequently injected into mice having melanoma. The melanocyte-stimulating hormone interacted specifically with receptors found on melanoma metastases. The PEG chains were crucial in increasing the retention time and masking the protein from the immune system.[27]

The synthesis of reactive PEGylation reagents is complicated by the fact that ethylene oxide does not have readily reactive functional groups. Nevertheless, several PEGylation reagents with different lengths, architectures, and reactive groups are commercially available. A procedure for the synthesis of a variety of PEGylation reagents with common chemical functional groups, such as activated esters for the modification of primary amines, alkynes for click chemistry reactions, acrylates, and carboxylic acids has been described by Li et al.[28] PEGylation reagents can be discrete or polydisperse. Discrete PEGylation reagents (termed dPEG) are synthesized

according to a complicated synthetic organic protocol, yielding PEG chains with a known number of ethylene oxide repeating units.[29] Polydisperse PEGylation reagents are synthesized using classic polymerization methods such as the anionic polymerization of ethylene oxide.[30]

The methods described in this thesis primarily involve the use of commercially available discrete PEGylation reagents for protein bioconjugation. The chemical structure of each reagent will be given in the three experimental chapters (Chapters 2-4). An array of reagents with different lengths and functional groups were utilized, depending on the bioconjugation method studied.

1.2. Protein Bioconjugation with the Michael Addition Reaction

The Michael addition reaction of thiols and alkenes is one of the most common methods for cysteine bioconjugation. Site-specific modification of proteins can be achieved with this chemistry as cysteine is one of the least abundant naturally occurring amino acids.[31] The cysteine thiol has a pK$_a$ of ~ 8.5, making it one of the most nucleophilic side chain residues of the twenty canonical amino acids.[10,32] This technique can be classed as a "click chemistry" reaction, since the resulting products are typically regio- and stereospecific, high yields can be obtained, the production of side products is limited or absent, and the reaction conditions are mild (physiological pH and temperature).[9,33] Thiol-ene click chemistry is particularly important in the development of antibody-drug conjugates (ADCs), but also in the formation of complex nanomaterials.[31,33-35] In particular, the reaction of maleimides (MAL) with thiols is a well-known bioconjugation strategy (Scheme 1.1). Maleimides have been reported to be more reactive than other Michael acceptors, such as acrylates or vinyl sulfones.[33] However, the hydrolysis of maleimides is a major disadvantage for this type of chemistry. The subsequent alkene-containing compound is unable to further react with thiols (Scheme 1.1). If the thiol-MAL complex has already been formed, the hydrolytic conversion in an aqueous solution can still occur, affecting the stability of ADCs *in*

vivo.[36] For biologically relevant reaction conditions, this type of hydrolysis is mediated by the pH of the reaction medium. Ring opening hydrolysis increases with increasing pH.[9] Furthermore, thiol-MAL complexes are susceptible to thiol exchange reactions, further decreasing the stability of ADCs.[37] The retro-Michael reaction has also been reported for these complexes, resulting in deconjugation.[37] Due to these unfavourable side reactions, the search for stable alternatives is underway. Costa et al. used computational methods to study the thiol-Michael addition reaction with maleimide and over forty electrophilic alternatives.[38] However, they reported that a number of the electrophilic substitutes were still prone to unfavourable side reactions, along with slower reaction kinetics compared to maleimide.
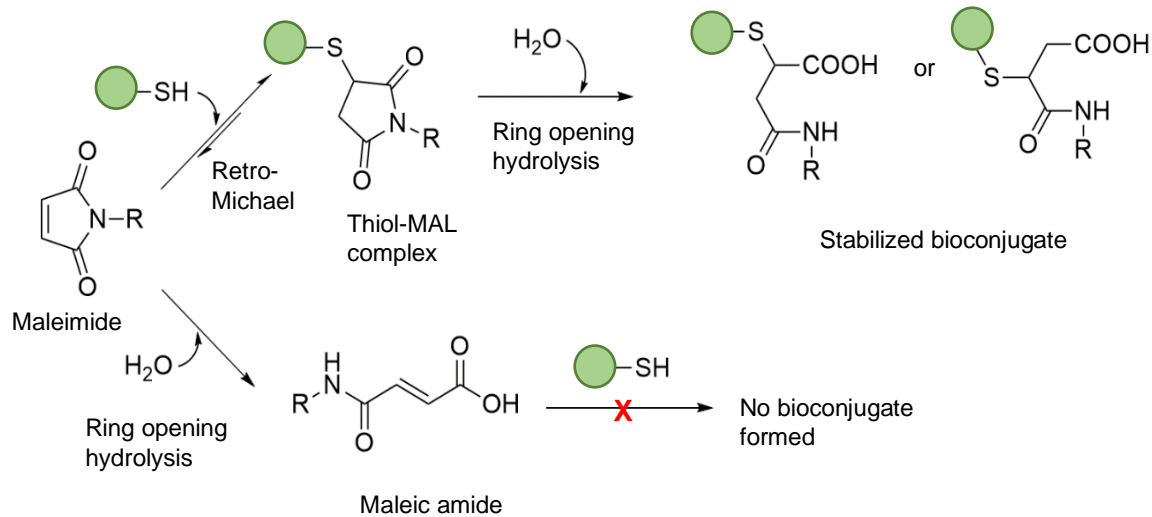
Scheme 1.1. General reaction scheme for the thiol-maleimide Michael addition and hydrolysis pathways. R represents any chemical moiety that can be used to modify a protein (green circle).

The phospha-Michael addition reaction has gained recent interest as a new bioconjugation technique.[39] This chemistry has already been well-described in organic synthesis reactions.[40] The reaction proceeds as the nucleophilic phosphine (Michael donor) reacts with the electrophile (Michael acceptor) (Scheme 1.2). As with the thiol-Michael addition reaction, maleimides are common Michael acceptors for this chemistry. When the electrophile is the same, phospha-Michael addition reactions are kinetically favoured compared to the analogous thiol-Michael reaction.[39,41,42] Nucleophilic phosphines are not naturally found in the side chains of the twenty canonical amino acid residues. Therefore, an electrophilic entity or the phosphine itself must be installed on the protein prior to bioconjugation.
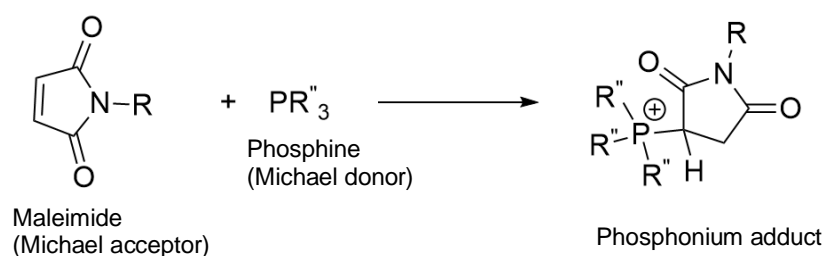
Scheme 1.2. General reaction scheme for the phospha-Michael addition. R represents any chemical moiety that can be used to modify or attach to the surface of a protein. R" represents the chemical moieties on a triphosphine (alkyl or aryl groups).

Kantner and Watts discovered that tris(2-carboxyethyl)phosphine (TCEP) and maleimides react to form phosphonium adducts.[43] The reaction scheme of the TCEP-MAL adduct formation and the role of TCEP in bioconjugation reactions is given in Chapter 2 of this thesis. The investigation reported by Kantner and Watts in 2016 was influential in the use of the phospha-Michael addition for protein modification. Researchers began to exploit the phospha-Michael chemistry with TCEP to probe electrophilic moieties on proteins. TCEP is a water-soluble trialkyl

phosphine containing three carboxylic acid functional groups which serve as a point-of-derivatization in the synthesis of TCEP analogues. Other phosphines, such as triphenylphosphine (TPP) are not water-soluble and do not have facile procedures for analogue synthesis.

Vinyl ketones and amides are electrophilic moieties that are not naturally present in the side chain residues of the twenty amino acids. However, certain post-translational modifications of lysine found on histone proteins, such as crotonylation, result in the formation of chemical groups containing these types of functionalities.[44] These electrophilic moieties serve as epigenetic markers in the regulation of gene expression.[44] Recently, the phospha-Michael addition chemistry has been utilized to probe these post-translational modifications. [39,41,42,45] A typical procedure involves the synthesis of TCEP with a fluorophore, such as dansylcadaverine, or biotin (Scheme 1.3).
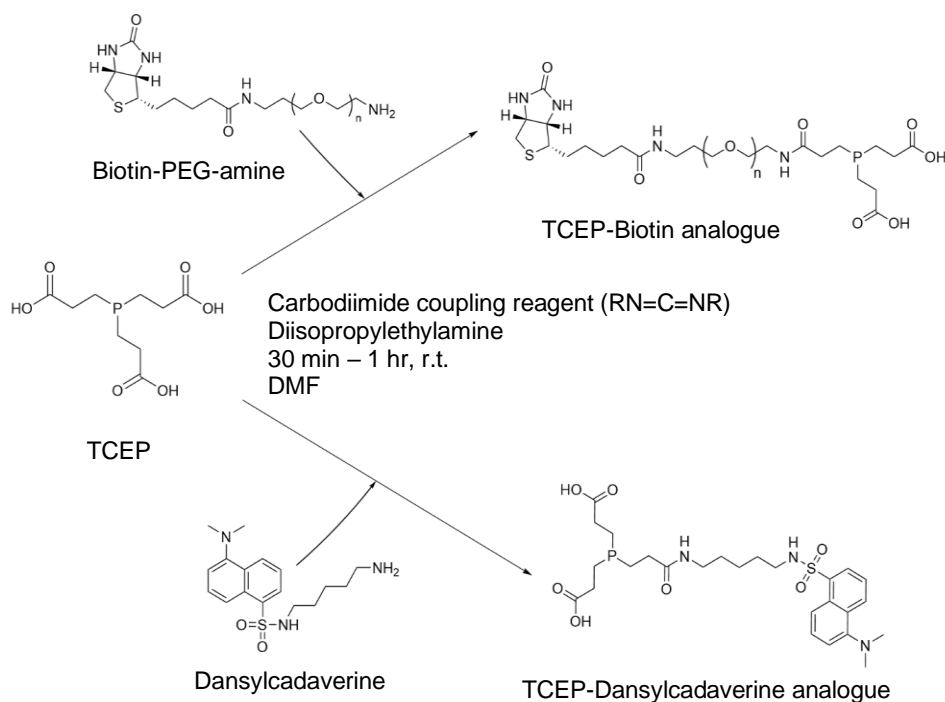
Scheme 1.3. General reaction scheme for the synthesis of TCEP analogues. Procedure adapted from Bos and Muir, 2018.[45]

9

The carboxylic acid groups are activated with a carbodiimide coupling reagent. The activated carboxylic acid reacts with a nucleophilic compound in order to obtain the TCEP analogues. Dansylcadaverine contains a primary amine functional group in its chemical structure. A heterobifunctional PEG reagent with a biotin moiety and a primary amine can be commercially purchased. Biotin and avidin interact strongly to form non-covalent complexes. Avidin, from chicken egg white, is a tetrameric biotin-binding protein with four binding sites. Given that the dissociation constant (K_d) equals 10^{-15} M for the biotin-avidin system, it is one of the strongest known non-covalent interactions.[46,47] Therefore, it is a good choice to use in the design of a molecular probe. In this way, proteins that are modified with a TCEP-biotin analogue can be easily detected and captured when biotin interacts with avidin.

One example of the phospha-Michael click modification reaction was reported by Lee et al.[41] An unnatural amino acid containing an acrylamide moiety was installed on the surface of the protein and subsequently reacted with a dansylcadaverine-labelled TCEP (Scheme 1.4). The fluorescence signal given by dansylcadaverine is readily detected.
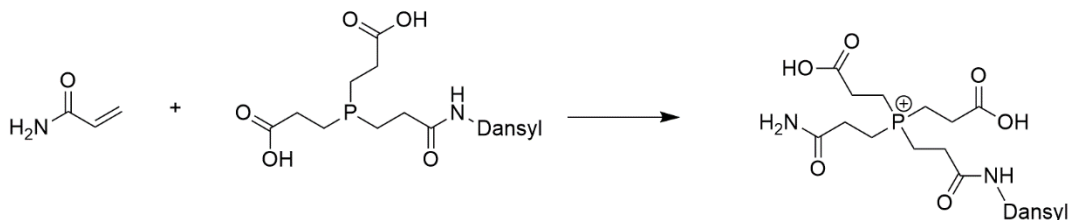
Scheme 1.4. General reaction scheme for the reaction of acrylamide with a TCEP-dansylcadaverine probe. Adapted from Lee et al.[41]

Lysine crotonylation, an important post-translational modification of histone proteins, was studied by Bos and Muir using the phospha-Michael reaction with a TCEP-biotin analogue (Scheme 1.5).[45] Bos and Muir attempted to explain the formation of the cationic Michael addition product, which was also observed by Lee et al. They proposed that the negative charge on the

carboxyl acid group, which would be present at the pH used in the reaction conditions (pH = 8), would stabilize the cationic species.
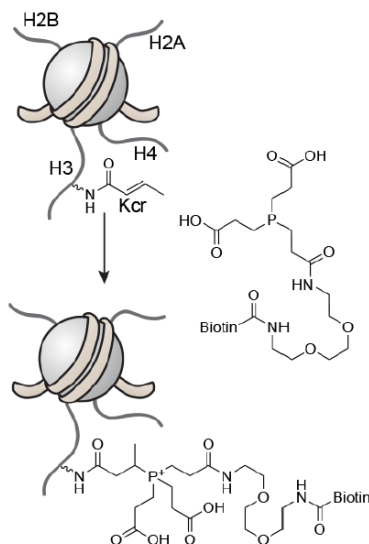
Scheme 1.5. General reaction scheme for the reaction of a lysine crotonyl group on a histone protein with a TCEP-biotin probe. Reprinted with permission from Bos and Muir, copyright 2018 © American Chemical Society.[45]

The phospha-Michael addition shows promising utility in bioconjugation reactions. The work presented in this thesis aims to develop a novel phosphorous-based bioconjugation approach utilizing the phospha-Michael addition for the generation of phosphonium adducts. These adducts will be further reacted with aldehydes in a Wittig reaction for the formation of protein-based conjugates. The Wittig reaction mechanism has been described in Chapter 2, and further work involving solid-supported phosphines has been described in Chapter 3.

1.3. Lysine Modification with Activated Ester Reagents

The acylation of lysine residues using activated esters is a classic bioconjugation tool for the non-specific derivatization of proteins.[9] PEGylation reagents containing reactive ester end groups, such as *N*-hydroxysuccinimide (NHS) or 2,3,5,6-tetrafluorophenol (TFP) are commonly used to modify the surface of proteins via an amide bond linkage with lysine. While it is a quick and reliable method to modify a target protein at physiological pH, its general non-specificity and lack of control over the number of modifications obtained is disadvantageous for some applications.[9,31] Depending on the size of the molecule that is being attached, steric hindrance may result in decreased modification yields due to the random orientation and position of lysine residues on a protein.[48] Shown below is an outline of the general reaction of a primary amine with an NHS or TFP ester reagent (Scheme 1.6).
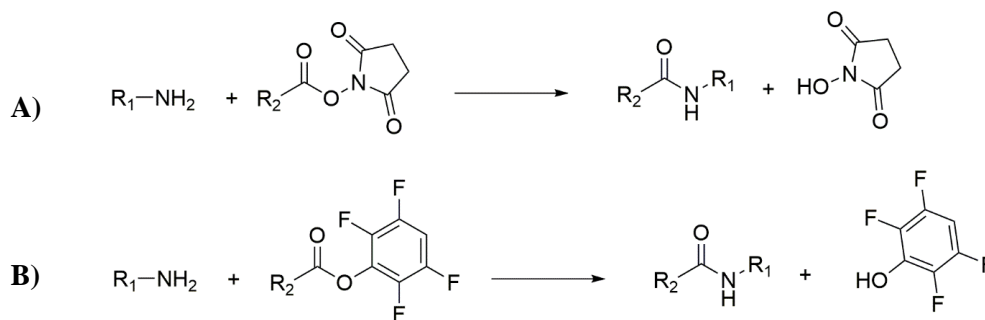
Scheme 1.6. General reaction of amines with NHS or TFP esters for bioconjugation techniques. **A)** Reaction of an amine with an NHS ester. **B)** Reaction of an amine with a TFP ester. R_1 denotes a biomolecule, such as the side chain of lysine. R_2 denotes any chemical moiety that is to be displayed from the biomolecule, such as PEG_n-biotin.

A large excess of the NHS ester is typically required because these esters hydrolyze readily in aqueous solutions. The half-life of the NHS ester decreases rapidly as the pH increases, which limits their use in experiments requiring basic conditions. [10,49] Lockett et al. studied the hydrolysis rates of NHS and TFP esters at different pH conditions.[49] Both esters showed a decrease in half-

life as the pH increased from pH 7.0 to 10.0.[49] However, at these pH conditions, the TFP ester had a longer half-life compared to the NHS ester.[49]

Although TFP esters are less susceptible to hydrolysis, the NHS ester is still the more popular choice for experiments involving the formation of bioconjugates through primary amine groups. This is likely because techniques using NHS esters have been well-established, and a wider variety of reagents containing the NHS ester are commercially available, circumventing the need to synthesize the reagents in the laboratory.

Researchers studying bioconjugation methodologies have been challenged by the ubiquitous nature of lysine residues in protein sequences. The indiscriminatory modification of proteins with activated ester reagents can lead to loss of function. Matos et al. attempted to exploit subtle differences in pKa values between neighbouring lysine residues for the targeted modification of a specific lysine residue within a protein.[50] Computational methods were used to identify suitable electrophiles that would selectively target lysine residues.[50] They were able to demonstrate the regioselective modification of lysine residues with the sulfonyl acrylate reagents that were computationally identified. However, a review by Shadish and DeForest cautions that this method would not be applicable for a large number of proteins.[51] In the report presented by Matos et al., lysines associated with the lowest pKa values were modified. Depending on the protein being studied, these lysine residues may be inaccessible or essential for protein function.[51]

The research in the Honek laboratory focused on the use of heterobifunctional PEGylation reagents with an NHS or TFP-activated ester functional group for modifying lysine residues of proteins. The second functional group on these reagents was maleimide. This NHS/TFP-PEG$_n$-MAL reagent was a starting point for our studies involving the phospha-Michael addition and

subsequent Wittig reactions. The chemical structures of the reagents and experimental details are described in Chapter 2 and 3 of this thesis.

1.4. Bioconjugation Chemistry of Aldehydes

This thesis focuses on the development of a novel method for the modification of proteins with aldehydes using maleimide and phosphorous-based chemistry. The alkylation of lysine residues with aldehydes in the presence of sodium borohydride is an existing classic bioconjugation technique.[52] When the ε-amine of lysine is deprotonated, it acts as a nucleophile attacking the electrophilic carbon of the aldehyde compound, resulting in the loss of one equivalent of water. A Schiff base is formed, and sodium borohydride is used in the subsequent reduction step (Scheme 1.7).

Scheme 1.7. Mechanism for the reductive alkylation of a lysine residue with an aldehyde and sodium borohydride. R represents any chemical moiety used to modify the protein.

Bootorabi et al. found that the modification of bovine carbonic anhydrase with acetaldehyde using sodium borohydride resulted in a marked decrease of enzymatic activity.[53] They also determined that the isoelectric point (pI) of the protein was decreased, even when relatively low concentrations of acetaldehyde were used in the reaction. The pI of the unmodified enzyme was approximately 7.9, whereas the pI of the enzyme after modification with 100 μM of acetaldehyde was found to be approximately 6.8.[53] As illustrated by this example, bioconjugation methods readily affect the properties of a protein. Care must be taken to ensure that the bioconjugation method does not alter the function of the protein, if its retention is essential.

Changing the pH of the reaction medium can be used to strategically control the selectivity of the bioconjugation reaction while maintaining the activity of the protein. The pKa of the N-terminal α-amine is ~7.6-8.[10] The selective modification of the N-terminal α-amine can be achieved due to the difference in pKa values between this amine and the ε-amine of lysine (pKa ~ 10).[54-56] Chen et al. used reductive alkylation to modify human insulin with a variety of benzaldehyde derivatives at pH = 6.1.[54] At slightly acidic pH conditions, the majority of the ε-amine of lysine is protonated and will not behave as a nucleophile. Chen et al. reported excellent selectivity for this reaction with 99% of the N-terminal α-amine derivatized.[54] Compared to acylation of the N-terminus, they reported that reductive alkylation with an aldehyde moiety and a reducing agent resulted in a 5-fold increase in the bioactivity of the protein.[54] These findings are significant in a pharmacokinetic context as it is essential to maintain the function of therapeutic proteins and peptides.

Without the inclusion of sodium borohydride in the reduction step, one of the major disadvantages of this reaction is that the C=N bond of the resulting Schiff base is susceptible to hydrolysis. Bioconjugation reactions with poor hydrolytic stability are not useful or practical as nearly all manipulations with proteins will occur in aqueous media. The half-life of these conjugates vary dramatically with changes in pH.[57] Generally, the reduction step is necessary to prevent deconjugation. However, the use of aldehydes as chemical handles on proteins is another method that can result in stable bioconjugates. Hydrazide- and hydrazine-containing compounds are commonly used as nucleophilic entities (Figure 1.3). The reaction mechanism between an aldehyde and a hydrazine is given in Chapter 3.

Acyl hydrazide   **Sulfonyl hydrazide**   **Hydrazine**
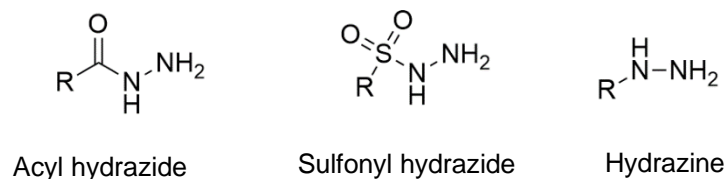
Figure 1.3. Chemical structures of common nucleophilic compounds reacting with aldehydes. R represents any chemical group or tag that can be used to modify a protein.

Aldehydes that are installed on the N-terminus of proteins and peptides act as non-canonical amino acids for site-specific bioconjugation.[52,55,58] For example, N-terminal serine or threonine residues can be rapidly transformed into aldehyde functionalities in the presence of sodium periodate (Scheme 1.8).[58,59] The major drawback of this method is that sulfur-containing amino acid residues, such as cysteine and methionine, can also be oxidized. To mitigate this unwanted side-reaction, excess methionine can be added to the reaction mixture.

R = H or CH$_3$
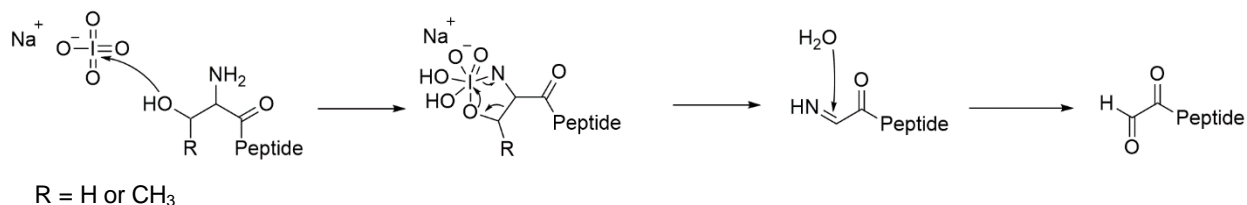
Scheme 1.8. Mechanism for the conversion of serine or threonine residues into aldehydes with sodium periodate.

A nucleophilic entity can be reacted with the aldehyde-derivatized peptide shown in Scheme 1.8. Geoghegan and Stroh oxidized the N-terminal serine residue of recombinant interleukin-1α to obtain an aldehyde chemical handle.[60] Using biotin and a fluorophore containing a hydrazide functional group, they were able to perform the bioconjugation reaction.

In another example, Hartmann et al. reported the oxidation of an N-terminal serine with sodium periodate for the formation of an aldehyde-tagged protein.[61] The aldehyde functional group was subsequently reacted in an aqueous Wittig reaction with a MAL-TPP adduct. Further exploration into aqueous Wittig reactions will be described in Chapter 2. Nevertheless, this example demonstrates the utility of aldehyde bioconjugate chemistry in conjunction with the phospha-Michael addition reaction.

1.5. Chemoenzymatic Bioconjugation

The catalytic power of enzymes can be harnessed for bioconjugation techniques. In nature, the post-translational modifications of proteins are often mediated by specific enzymes. The selectivity of these enzymes is exploited in the site-specific modification of proteins. This technique has been reported in the fabrication of ADCs, polymer-protein drug therapeutics, immobilized proteins, protein-based nanoparticles, and biomaterials.[62-65] For example, ligation reactions are commonly facilitated by sortases, transglutaminases, peroxidases, and tyrosinases.[9,63,66] In this thesis, the transglutaminase mediated ligation of PEG-based Wittig products to proteins was also explored. Details involving the structure and mechanistic action of transglutaminase are given in Chapter 4.

An advantage of chemoenzymatic bioconjugation methods is that typical reactions occur at physiological conditions. Temperatures commonly range from 4-37 °C, and the pH of the reaction medium is biologically relevant.[9,63,66] However, chemoenzymatic bioconjugation can be complicated if the enzyme requires a cofactor for its activity. For example, mammalian transglutaminases require calcium for enzymatic activity. Without the correct concentration of the cofactor, the reaction kinetics can be slowed down. The presence of cofactors can complicate the purification of the final desired product or affect the function of the protein substrate.

Antibodies are often conjugated with cytotoxic compounds for targeted drug delivery. This minimizes the potential side effects, which are particularly worrisome in cancer treatments, and increases the effectiveness of the drug.[67] Chemoenzymatic ligation is a good strategy for the design of these types of bioconjugates owing to its inherent site-specificity. Dennler et al. designed an ADC with a toxic payload using a combination of transglutaminase mediated ligation and azide/alkyne click chemistry (Scheme 1.9).[68] Transglutaminase acts on the glutamine residues of an antibody to attach an amine and azide-functionalized heterobifunctional linker. A toxic drug compound, trastuzumab, was synthesized with a dibenzocyclooctyne group. The strain-promoted azide-alkyne click chemistry reaction attached the drug to the antibody, allowing for targeted delivery of the toxic compound.
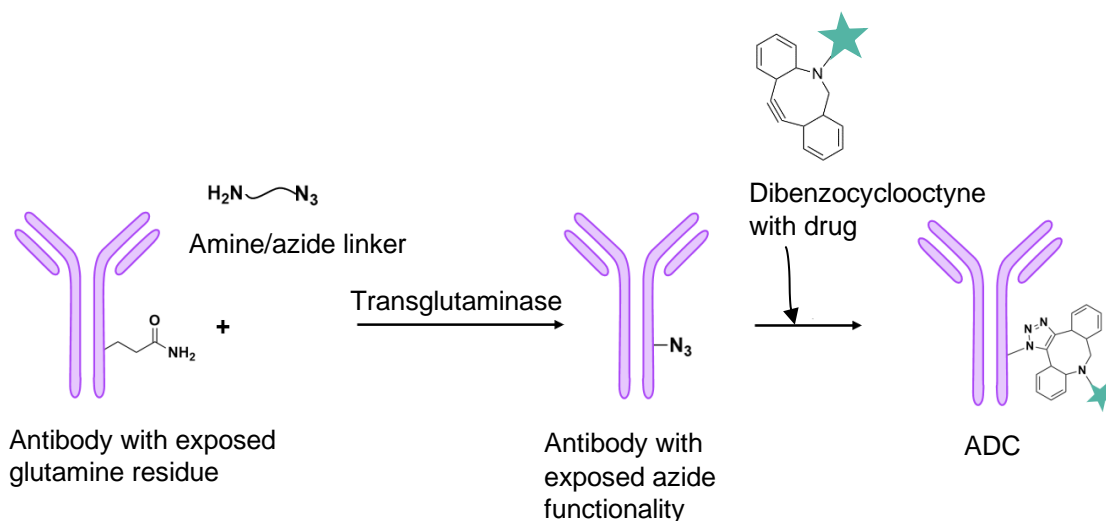
Scheme 1.9. Design of an ADC with enzyme mediated and click chemistry bioconjugation strategies. Adapted from Dennler et al.[68]

The design of novel protein-based networks can also be undertaken with chemoenzymatic bioconjugation. One example is the design of a streptavidin-based scaffold described by Matsumoto et al, as shown in Figure 1.4. [62] Streptavidin is a biotin-binding protein similar to avidin. Unlike avidin, streptavidin does not contain carbohydrate residues on its surface, which

contribute to non-specific binding of proteins and other exogenous molecules. Streptavidin is derived from the bacterium *Streptomyces avidinii*.
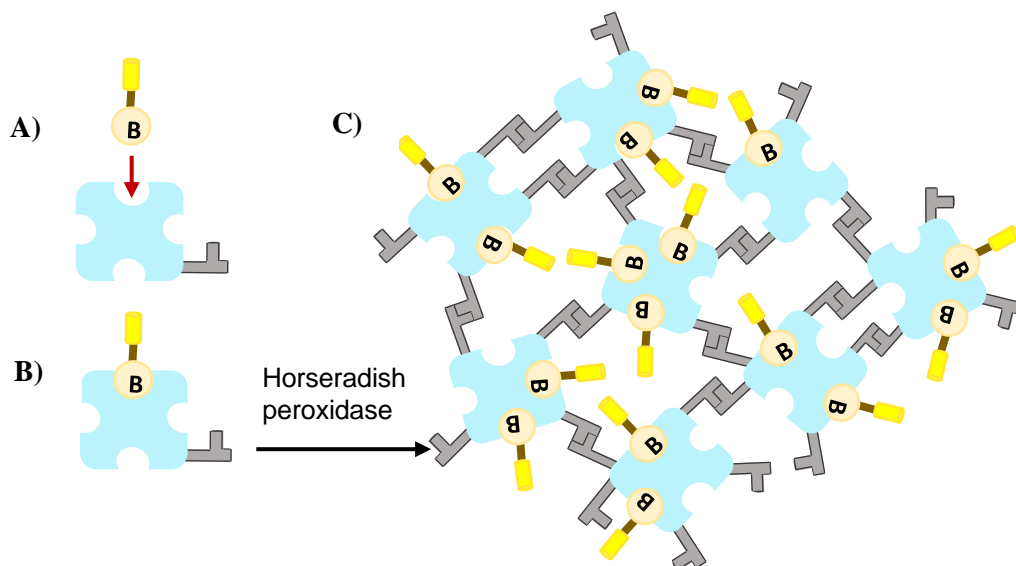
Figure 1.4. A streptavidin protein scaffold. **A)** The addition of a biotinylated fluorophore (yellow) to streptavidin (blue) with tyrosine-containing peptide residues (grey). B depicts the biotin moiety. **B)** The enzyme mediated polymerization of the streptavidin scaffold. **C)** The resulting streptavidin scaffold functionalized with fluorophores. Adapted from Matsumoto et al.[62]

Biotinylated fluorescent proteins were non-covalently attached to the biotin-binding pockets on streptavidin.[62] The scaffold was formed by the horseradish peroxidase-catalyzed crosslinking of tyrosine-containing peptide residues.[62] Horseradish peroxidase oxidizes two tyrosine residues when one molecule of hydrogen peroxide is reduced to form a tyrosyl radical.[69] The free radical found on the aromatic ring quickly reacts with a second tyrosyl radical to form stable dimers. This chemoenzymatic bioconjugation method formed the covalent crosslinks of the protein network. In another example reported from the same researchers, sortase A was the enzyme used for chemoenzymatic crosslinking.[70] Polystyrene beads functionalized with biotin residues were non-covalently attached to streptavidin proteins containing a sortase recognition sequence. In this recognition sequence, threonine and glycine are found next to each other. Sortase A cleaves

the peptide bond between these two amino acid residues, and can subsequently link the threonine carboxylic acid group with the N-terminal glycine amine.[71] A fluorophore containing a glycine-oligomer tag was conjugated to streptavidin in this fashion. A second biotinylated fluorophore was added to the empty biotin-binding sites of streptavidin. The result was a fluorophore-functionalized polystyrene particle. Both of the examples presented here by Matsumoto et al. can be expanded if two unique enzymes, instead of fluorophores, were added to the streptavidin-based materials. This would provide the networks or particles with a specific biological function. The fabrication of multi-enzyme complexes requires different bioconjugation strategies for their specific attachment or immobilization onto the protein/polymer networks.

1.6. Immobilization of Proteins

Proteins may be immobilized on the surface of different solid particles or on polymer-supported resins, particularly in the design of biosensors for diagnostic applications.[72,73] Bioconjugation plays a key role in the fabrication of biosensors. The substrate-specific element, such as an antibody or enzyme, needs to be immobilized on a solid surface. This can be achieved through either covalent or non-covalent attachments. A classic example of a biosensor is the immobilization of glucose oxidase onto solid-supports, such as gold or silver nanoparticles, magnetic nanoparticles, or polymeric films.[74,75] Glucose oxidase is an enzyme that catalyzes the conversion of β-D-glucose to D-glucono-δ-lactone and hydrogen peroxide. Biosensors with glucose oxidase are important for testing the glucose levels in food and blood sugar monitoring in diabetic patients.[76] Glutaraldehyde, a homobifunctional alkane with two aldehyde groups, is often used to crosslink proteins or immobilize enzymes, such as glucose oxidase, onto solid-supports.[75] Both the solid supports and the proteins have primary amine functional groups that react with glutaraldehyde for immobilization.[75]

The immobilization of enzymes is especially practical in chemical and manufacturing processes.[73, 78] It is expected that enzymes would exhibit improved stability when attached to a solid-support.[78] Immobilization allows for the enzymes to be re-used, and for facile separation from the resulting products.[78] As the density of immobilized proteins or enzymes increases, arrays or networks may be formed. When this occurs, the proximity of enzymes within an immobilized array possess enhanced enzymatic activity due to substrate channeling.[79] The sophistication of these arrays can be further improved by the addition of synthetic molecules, or small peptides, enzymes, and fluorescent proteins. This is useful in the design of biosensors and enzymatic assays. Fluorescent entities, or enzymes capable of catalyzing small chromogenic compounds can be attached to the network in order to obtain a detectable signal. Small proteins or enzymes that are immobilized to a polymer-protein scaffold will functionalize a scaffold that may otherwise be biologically inactive.

In order to covalently attach proteins onto solid surfaces or polymer-supported resins, the supports can be modified to display compounds that react with specific functional groups of amino acid residues.[72,73] For non-covalent linkages, the use of biotin-avidin complexes have been studied.[72,73] For example, molecules that contain biotin moieties can be non-covalently attached onto avidin-coated solid supports in order to further functionalize the material.[72,73] Lu et al. reported the immobilization of streptavidin proteins onto biotinylated polymer fibres as a starting point for the fabrication of more complex, bioactive materials.[80] Since streptavidin has four biotin-binding sites, additional proteins, antibodies, and enzymes conjugated with biotin can be attached to create a novel functionalized material. In this manner, streptavidin acts as the crosslinker. For example, if a biotinylated antibody was linked to this material, then specific

antigen capture can occur.[80] The entire complex can easily be separated and purified from the remainder of the mixture.

Immobilization strategies often combine bioconjugation techniques. Zimmerman et al. used a linear heterobifunctional PEG polymer containing an NHS activated ester functional group on one end, and maleimide on the other end to immobilize peptides onto solid surfaces (Scheme 1.10).[81] Amine-functionalized glass slides were first incubated with NHS-PEG$_n$-MAL. Using thiol-Michael addition chemistry, site-specific attachment of the peptides through a cysteine residue onto the maleimide-functionalized solid surface was achieved.
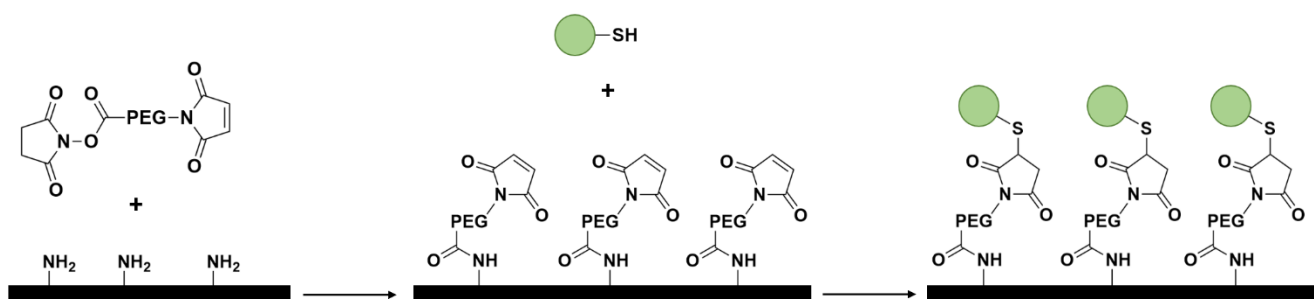
Scheme 1.10. Thiol-Michael addition mediated immobilization of proteins or peptides (green circle) onto maleimide-functionalized solid surfaces. Adapted from Zimmermann et al.[81]

1.7. Research Objectives

The bioconjugation toolkit is constantly expanding. As protein engineering becomes more complex, new bioconjugation techniques are required. The overall objective of the research presented in this thesis is to expand the diversity of approaches for the phospha-Michael addition. Starting with maleimide as the electrophile, three different approaches will be studied (Figure 1.5). Chapter 2 will discuss the aqueous Wittig reaction of maleimide-based phosphonium adducts with a water-soluble benzaldehyde on the surface of proteins. Chapter 3 will discuss the solid phase

organic synthesis of activated ester-functionalized Wittig products for protein bioconjugation. Finally, Chapter 4 will discuss the chemoenzymatic bioconjugation of amine-functionalized Wittig products with microbial transglutaminase. While the bioconjugation methodology in Chapters 2 and 3 involve the non-specific modification of lysine residues with activated ester functional groups, Chapter 4 describes the potential application of our methodology for the site-specific derivatization of proteins. It is anticipated that the phosphorous-based chemistry presented herein can be used for the immobilization of enzymes on solid supports, or for the modification of proteins with synthetic molecules (polymers, drug molecules, fluorophores).
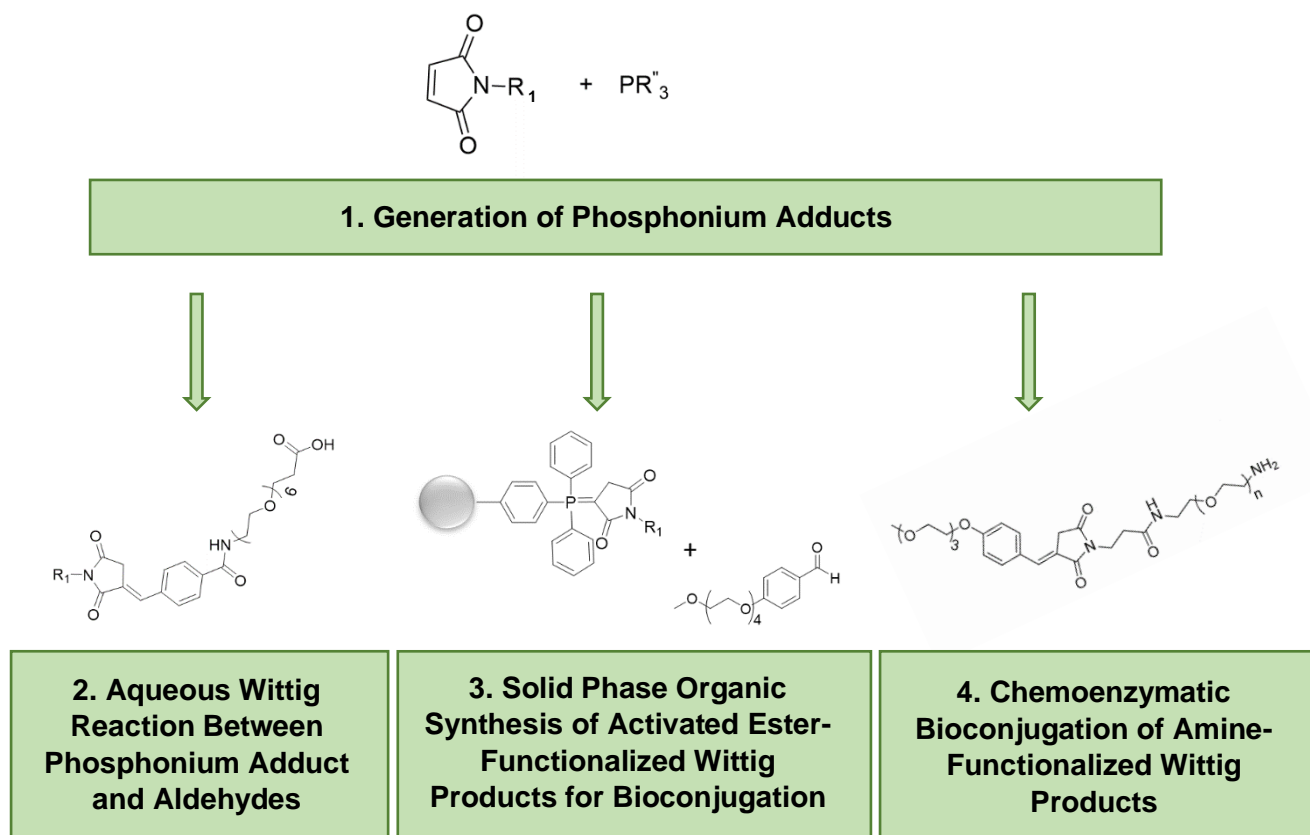
Figure 1.5. An overview of the experimental approaches investigated in this thesis for the development of a phosphorous-based bioconjugation method. R_1 represents a chemical functional group, such as NHS/TFP-PEG_n for attachment to lysine residues. $R^{''}$ represents the alkyl or aryl groups of the phosphine used.

Chapter 2.0. The Development of a Novel Phosphorous-Based Bioconjugation Method

2.1. Introduction

Bioconjugation methods involving maleimide (MAL) are typically used to modify the cysteine residues of proteins.[31,33] Cysteine residues can be present as disulfide bridges (cystine) in a protein. It is necessary to first reduce the cystine to the cysteine form so that it may react with maleimide. For this reduction step, the addition of a thiol, such as beta-mercaptoethanol, or tris(2-carboxyethyl)phosphine (TCEP) are commonly used reagents (Figure 2.1).[31,43]
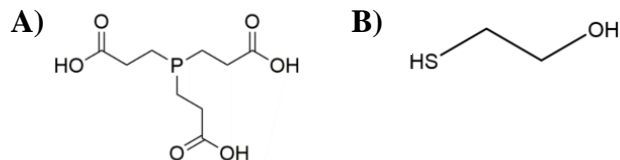
Figure 2.1. The structures of disulfide reducing agents. **A)** TCEP. **B)** Beta-mercaptoethanol.

However, unlike reactions with sulfur-containing reducing agents, reactions involving TCEP are odourless and irreversible.[43] Scheme 2.1 shows the reaction schemes for the reduction of cystines with both the TCEP and beta-mercaptoethanol reducing agents.
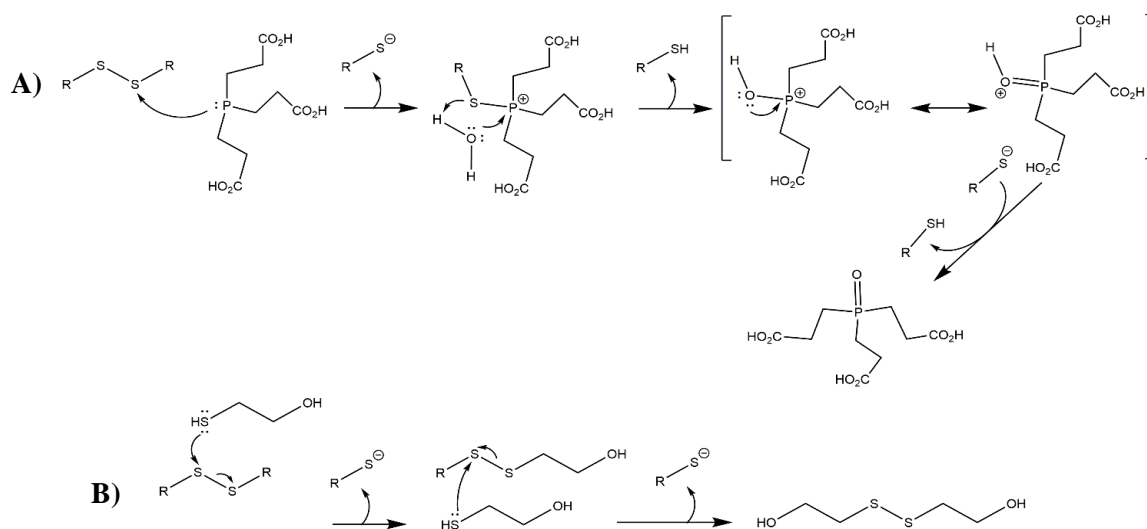
Scheme 2.1. Reduction of cystine residues with **A)** TCEP and **B)** beta-mercaptoethanol. The structure "R-S-S-R" depicts the disulfide bridge found in a protein structure. R-SH depicts the reduced sulfhydryl group.

24

A major disadvantage in the use of maleimide and TCEP reagents for cysteine modification is that if TCEP is not completely removed prior to the addition of maleimide, the formation of MAL-TCEP adducts can lower bioconjugation yields.[43,82] Kantner and Watts found that the reaction of maleimide functional groups with TCEP formed a MAL-TCEP ylene, resulting in a dead-end reaction.[43,83] No further reaction with cysteine would be possible.[43] Our research group hypothesized that this ylene could in fact be developed into a novel set of bioconjugation reactions employing lysine residues if the lysine side chain could be functionalized so that it displays a maleimide. Furthermore, our research group hypothesized that the ylene might be utilized in a possible Wittig reaction on a protein surface. This involves the reaction of an aldehyde or ketone with a phosphorous ylene for the formation of alkenes. The side product is phosphine oxide. The reaction involves the formation of a cyclic oxaphosphenate intermediate (Scheme 2.2).
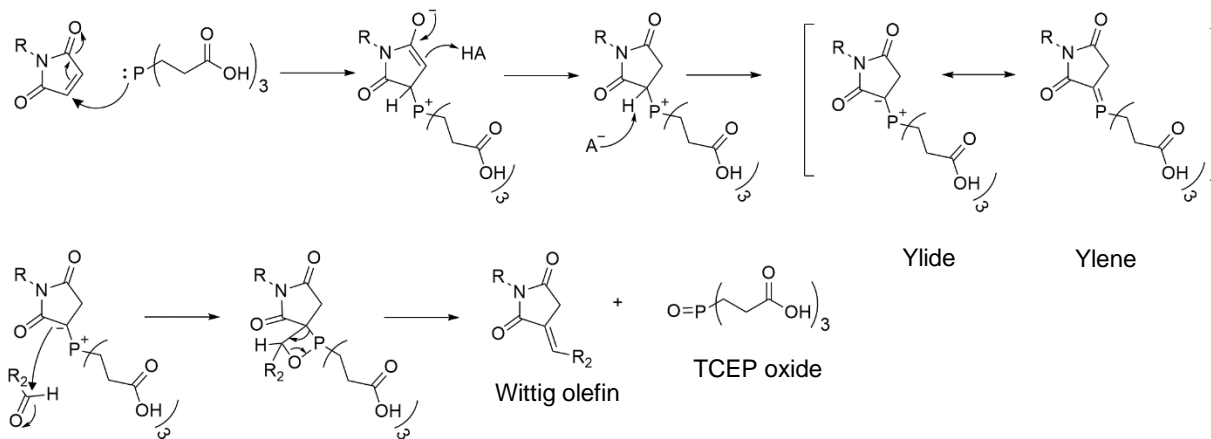
Scheme 2.2. Ylene formation and Wittig reaction mechanism. R represents a functional group that may be used to attach the maleimide to the surface of a protein. R_2 represents any tag that may be used to modify a protein.

This proposed novel bioconjugation method might be used to target proteins in order to display synthetic molecules on their surfaces. A survey of maleimide-phosphorus ylenes in the organic literature appeared to support our hypothesis, at least for small organic molecules.[83-85] Previous synthetic organic studies involved the reaction of a maleimide-phosphorous Wittig

reagent with aldehydes to produce a range of drug molecules[86-96] or, in a few reports, the Wittig reaction of aldehydes on a polymer-supported resin containing the ylene.[97,98] Although small molecule Wittig reactions are often conducted in organic solvents, examples of phosphorous-based aqueous Wittig reactions can be found in the literature.[61,99-102] In the context of protein bioconjugation, there is precedence for aqueous Wittig reactions.[61,99,100] For this bioconjugation technique, the N-terminus of a peptide or protein is transformed into an aldehyde by the addition of sodium periodate. A phosphorous-based Wittig reagent with a specific tag, such as a fluorophore, or an alkene functional group, is added to the aldehyde-functionalized peptide or protein (Figure 2.2).
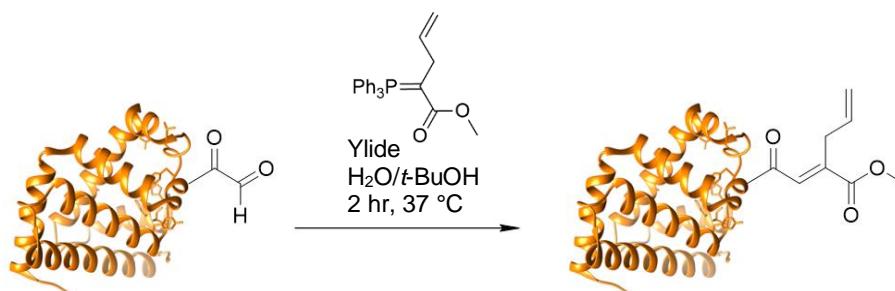
Figure 2.2. Bioconjugation of myoglobin containing an N-terminal aldehyde with stabilized ylide. Adapted from Han et al. [100]

Bergdahl's group reported the aqueous Wittig reaction with a triphenylphosphine (TPP) and α-bromoester stabilized ylide.[101] Although Bergdahl's group did not use maleimide and TCEP, TPP can also be used in aqueous Wittig reactions, if it is conjugated with a water-soluble molecule. Similarily, Janda's group reported the use of a PEG-supported TPP reagent for the aqueous synthesis of Wittig olefins.[103] Instead of maleimide, Janda's group utilized benzyl bromide for the synthesis of the stabilized ylide. Both of the ylides synthesized by Bergdahl's and Janda's groups were reported to be stable in water. [101,103] In this chapter, a study of the stability of MAL-TCEP and MAL-TPP adducts was undertaken. In order for the Wittig reaction to proceed on the protein surface, the Wittig reagents must be stable in an aqueous solution.

One of the model proteins used in our study of the phosphorous-based bioconjugation method was a ferritin from the thermophilic archaeon *Pyrococcus furiosus* (PfFtn). PfFtn is an example of a capsule protein and part of the ferritin protein superfamily. Ferritins, like most capsule proteins, are chemically and thermally robust, allowing for the use of harsher experimental conditions. The thermostability of PfFtn allows it to be heated in a reaction mixture for several hours at 50-60 °C.[104,105] PfFtn is able to withstand temperatures as high as 120 °C.[106]

The second model protein used in our experiments outlined in this chapter is bovine carbonic anhydrase (BCA). Carbonic anhydrases, such as BCA, are enzymes that catalyze the conversion of carbon dioxide into bicarbonate ions and play a key role in regulating body pH.[107,108] BCA is a monomeric protein with a molecular weight of 30 kDa.[108] As a metalloenzyme, the active site and catalytic activity of BCA involves a zinc ion which is coordinated with three histidine residues and water.[107,108] While BCA is not nearly as thermostable as PfFtn, its optimum temperature is 60 °C.[107,109] Between 60 and 65 °C, BCA shows a rapid decrease in catalytic activity, and above 65 °C, no activity could be discerned.[107] Variants of carbonic anhydrase that tolerate higher temperatures have been discovered, but they are not commercially available. One example includes the bacterial carbonic anhydrase from *Sulfurihydrogenibium yellowstonense*.[109] The enzymes found from this source are stable up to 100 °C.[109] Unlike PfFtn, the activity of BCA can be tested to measure if the bioconjugation method has had any effect on its activity. It has been observed by Pocker et al. that esters of *p*-nitrophenyl, such as *p*-nitrophenyl acetate and propionate, as well as pyruvate esters, can function as substrates for BCA.[110,111] The activity of BCA can be tested by using one of these esters.[110,111]

As the thiol-maleimide addition is a common reaction, it was important to choose proteins that do not contain cysteines so that these amino acid residues do not interfere with our

experiments. The amino acid sequences of PfFtn and BCA do not contain cysteine residues (Figure 2.3B&D). These two proteins have several lysine residues available on their surface, allowing for the attachment of a heterobifunctional PEG-MAL chain using an activated ester, such as NHS or TFP (Figure 2.3A&C). BCA contains 18 lysine residues, whereas PfFtn has 15 lysine residues per subunit, although not all residues are available for modification. To our knowledge, the exact number of lysine residues and their positions on the surface of a PfFtn subunit have not been specifically characterized yet.
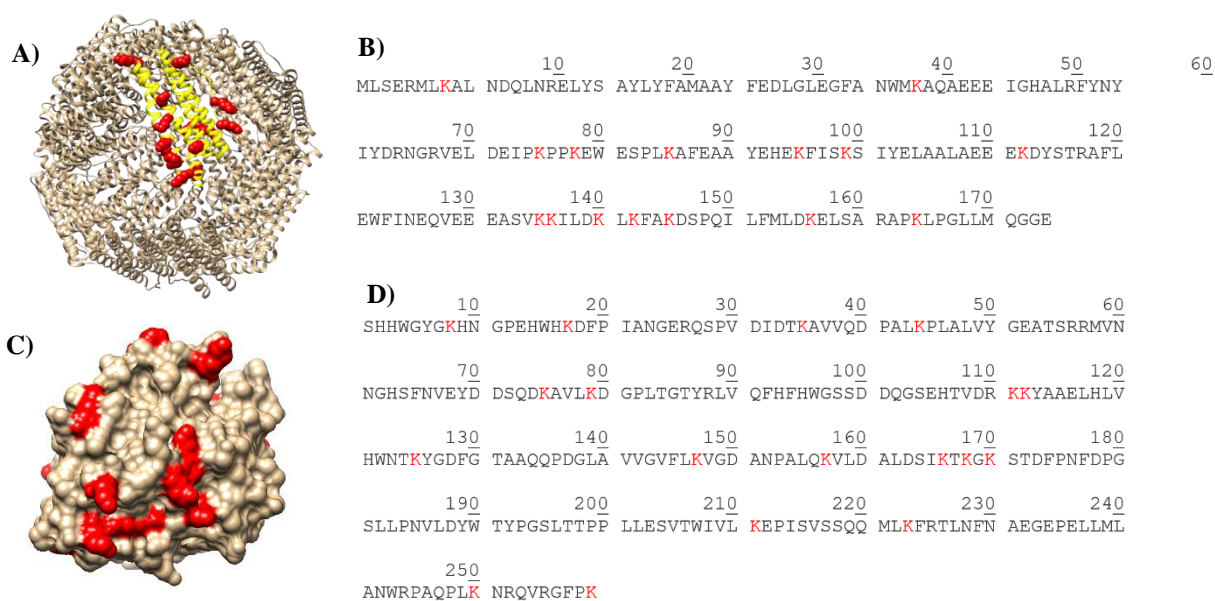
Figure 2.3. Structural representations of PfFtn and BCA. **A)** Reactive lysines on the surface of PfFtn (single subunit) (PDB: 2JD7). **B)** Amino acid sequence of PfFtn (PDB: 2JD7). Lysine residues (K) in red. **C)** Reactive lysines on the surface of BCA II (PDB: 1V9E). **D)** Amino acid sequence of BCA II (PDB: 1V9E). Lysine residues (K) in red.

Initially, TCEP was chosen as the water-soluble phosphine reagent for the formation of a MAL-TCEP ylene on the surface of a protein with an installed maleimide on its lysine residue. A second approach to the bioconjugation method involves the organic synthesis of an ylene with the water-insoluble TPP and a heterobifunctional PEG chain containing a maleimide on one end and an activated ester functional group (TFP or NHS) for lysine modification. Examples of synthetic

organic studies involving MAL-TPP Wittig reagents are often conducted in an organic solvent, such as acetone, and with refluxing.[88-91] In this approach, the Wittig reagent can be directly installed onto the surface of the protein (Scheme 2.3). The Honek laboratory initially studied the first approach involving TCEP. Experiments involving the second approach were undertaken and further described in this chapter.
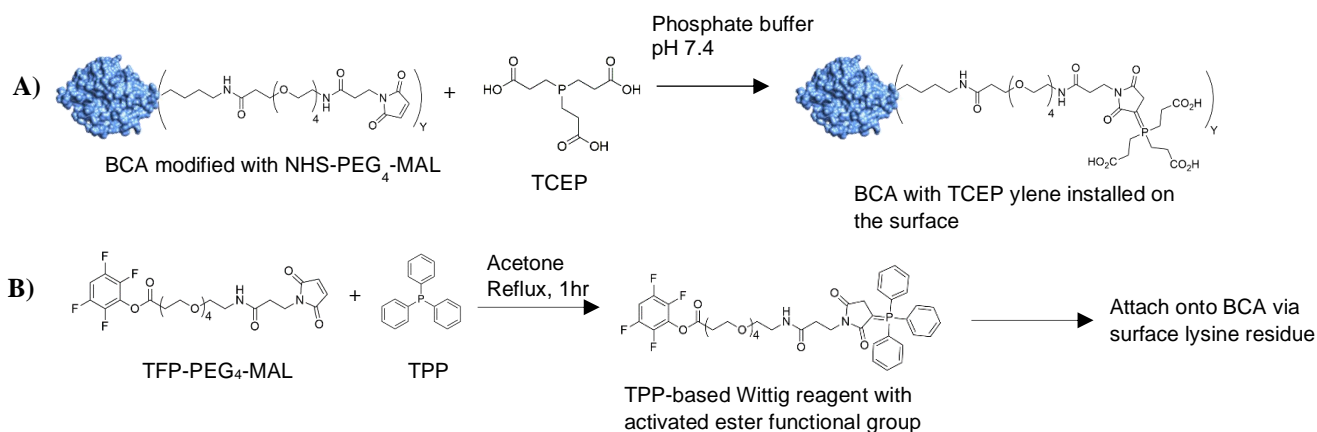
Scheme 2.3. Two approaches for modifying a protein with a Wittig reagent. **A)** TCEP addition with maleimide on BCA protein (blue) in an aqueous solution. **B)** An activated ester-PEG-TPP ylene synthesized in organic conditions.

If either approach described was further used to modify the surface of proteins with various compounds containing an aldehyde group, new types of protein-based nanoparticles or networks may be formed. An assortment of aldehydes exists and may be reacted with a protein containing the phosphorous-based reagent. In this way, libraries of modified proteins could be constructed for applications in biomaterials science or for the synthesis of therapeutic protein nanoparticles.

2.2. Objectives

This chapter outlines the development and optimization of a novel multi-step phosphorous-based bioconjugation method for protein modification. This approach involves both small molecule and protein studies. *N*-Ethylmaleimide (NEM), NHS-PEG$_4$-MAL, TFP-PEG$_4$-MAL,

TCEP, and water-soluble aldehyde reagents such as methoxy-PEG$_4$-benzaldehyde (mPEG$_4$BA) and AldPhPEG$_6$COOH will be used for these studies (Figure 2.4). An array of water-soluble TPP-based phosphines, along with TPP itself, were also studied for their potential application in the novel bioconjugation method, replacing TCEP as the phosphine (Figure 2.4).
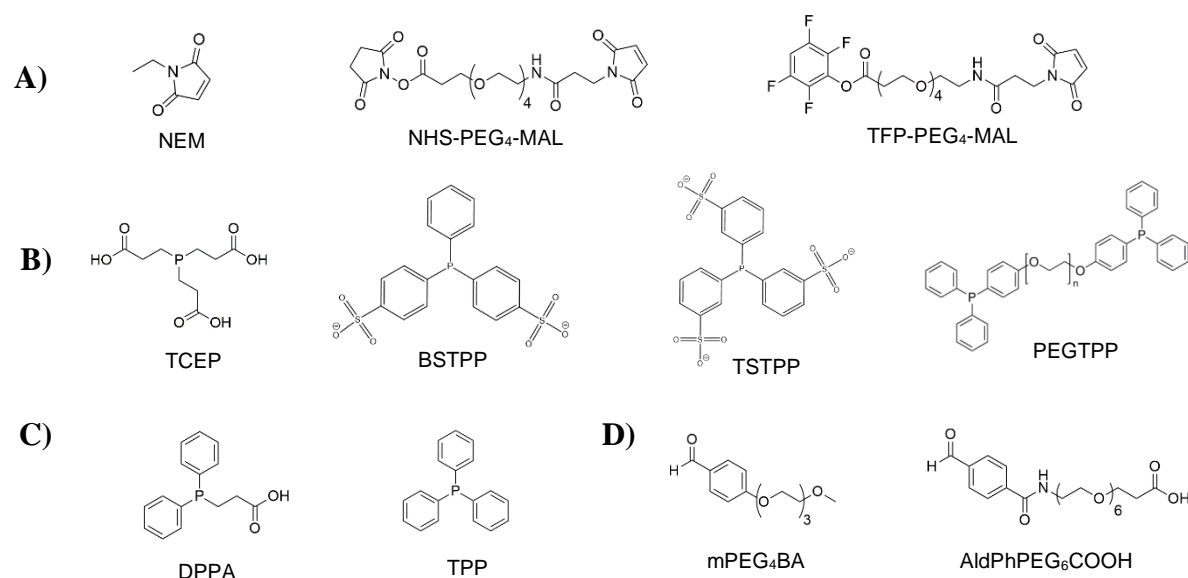
Figure 2.4. Reagents used in development of the novel bioconjugation method. **A)** Maleimide reagents. **B)** Water-soluble phosphines. **C)** Water-insoluble phosphines. **D)** Water-soluble aldehydes.

The protein studies require the modification of PfFtn and BCA with the NHS-PEG$_4$-MAL reagent through their lysine residues, to which the reducing agent TCEP will be added. The Wittig reaction of an aldehyde and phosphorous ylene will subsequently modify the surface of PfFtn and BCA (Scheme 2.4). As the modifications are of a low molecular weight, the electrospray ionization mass spectrometry (ESI MS) technique will be used in order to characterize the conjugates. As PfFtn is not commercially available, BCA was chosen as the model protein for optimization studies. BCA is easily obtained from commercial sources and is readily detected by ESI MS.
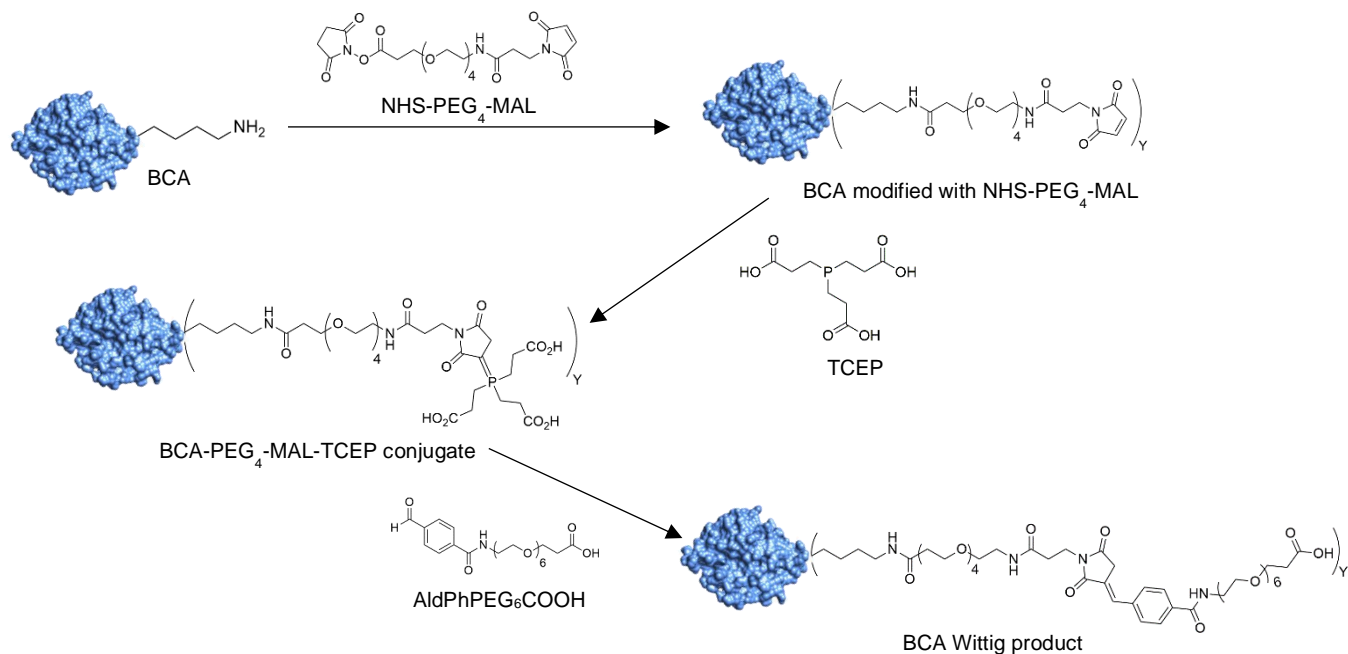
Scheme 2.4. Proposed phosphorous-based bioconjugation method on BCA.

If it is shown that BCA can be modified with the two model aldehyde reagents, an expanded set of aldehydes will be employed for the attachment of new functional groups. The goal of this approach is to develop a mild bioconjugation method that can be used to target a wide array of proteins in order to display synthetic molecules on their surfaces. Several reaction conditions were studied, including varying the temperature of the reaction and determining if the presence of a strong base is required for the aqueous Wittig reaction. If heating and addition of base is not required, then it may be possible to extend this bioconjugation strategy to non-thermally stable proteins.

2.3. Materials and Methods

Proteins: Ferritin from *Pyrococcus furiosus* (PfFtn) is not commercially available. PfFtn was obtained from a previous student (Dr. Hawa Gyamfi) in the Honek laboratory, who prepared and purified the protein according to the method outlined in her thesis.[112] Bovine carbonic anhydrase

II (BCA) was purchased commercially from Sigma Aldrich, Canada. Centrifugal filters (0.5 mL) with a molecular weight cut-off (MWCO) of 10 kDa were purchased from Amicon® Ultra (Millipore Sigma, Burlington, MA, United States).

PEG reagents: mPEG$_4$BA (95%; MW = 268.3 Da) and AldPhPEG$_6$COOH (99%; MW = 485.5 Da) were purchased from Broadpharm, San Diego, CA, USA. NHS-dPEG$_4$-MAL (>90%; MW = 513.5 Da) and TFP-dPEG$_4$-MAL (>90%; MW = 564.5 Da) were purchased from Quanta BioDesign Ltd (Plain City, OH, USA).

Maleimide and phosphines: *N*-ethylmaleimide (NEM; MW = 125.1 Da) was purchased from J.T. Baker Chemical Co. NJ, USA. *Tris*(2-carboxyethyl)phosphine hydrochloride (TCEP-HCl; ≥98%; MW = 250.2 Da), triphenylphosphine (TPP; 99%; MW = 262.3 Da), bis(*p*-sulfonatophenyl) phenylphosphine dihydrate dipotassium salt (BSTPP; 97%; MW = 534.6 Da), polyethylene glycol triphenylphosphine (PEGTPP; MW = 3500 Da), and 3-(diphenylphosphino) propionic acid (DPPA; 97%; MW = 258.3 Da) were purchased from Sigma Aldrich, Canada. Tris(3-sulfophenyl)phosphine trisodium salt (TSTPP; 85%; MW = 568.4 Da) was purchased from Toronto Research Chemicals, ON, Canada.

Resins: Polystyrene-supported *p*-toluenesulfonyl hydrazide PS-Ts-NHNH$_2$ (loading capacity: 3.06 mmol/g) was purchased from Biotage (Uppsala, Sweden).

Solvents, buffers and bases: Dimethylsulfoxide (DMSO; ≥99.9%), *N,N*-dimethylformamide (DMF) Sure/Seal™ Sigma Aldrich, anhydrous tetrahydrofuran (THF) (≥99.0 %), methanol (MeOH) (≥99.9%), acetone (≥99.9%), and sodium hydroxide (NaOH) were purchased from Sigma Aldrich, Canada. Ethyl acetate and anhydrous ethanol (EtOH) were purchased directly from ChemStores (University of Waterloo, Canada). 4-(2-hydroxyethyl)-1-piperazineethanesulfonic

acid (HEPES), boric acid, and potassium phosphate (KP) were purchased from BioShop Canada Inc. (Burlington, ON, Canada). For experiments involving phosphines, solvents were degassed by flushing with argon gas.

Instrumentation: The masses of all protein samples were analyzed with electrospray ionization mass spectrometry (ESI MS) using a high resolution Thermo Scientific™ Q-Exactive (Thermo QE) Hybrid Quadrupole-Orbitrap mass spectrometer, 10 µL/min injection rate, positive mode, with 1:1 MeOH:H_2O+0.1% formic acid (FA), as the solvent. The masses of all small molecule compounds described in this chapter were analyzed with ESI MS using either the high resolution Thermo QE instrument (positive mode, 10 µL/min injection rate, 1:1 MeOH:H_2O+0.1% FA) or the low resolution Thermo Scientific™ Linear Ion Trap (Thermo LTQ) mass spectrometer (positive mode, 20 µL/min injection rate, 1:1 MeOH:H_2O+0.1% FA).

Phosphine adducts were characterized by Phosphorous Nuclear Magnetic Resonance (^{31}P NMR) using a 500 MHz high resolution UltraShield™ Bruker Spectrometer (^{31}P frequency of 202.46 MHz). The reference standard used was phosphoric acid (H_3PO_4). The pulse program used was zgpg30 with a pulse delay of 3 seconds. The chemical shifts were reported in parts per million (ppm).

2.3.1. Wittig Modification of PfFtn with mPEG₄BA

Synthesis of PfFtn-MAL conjugates: PfFtn (0.076 mg, 0.0036 µmol, 1.0 eq) from a 0.8 mg/mL in 50 mM, pH 7.4 HEPES stock (obtained from Dr. Hawa Gyamfi) and NHS-dPEG₄-MAL (0.37 mg, 0.7113 µmol, 200.0 eq) from a 0.016 mg/mL in DMSO stock were incubated overnight at 4 °C. Next, the sample was prepared for analysis with ESI MS. The sample containing the HEPES buffer and DMSO solvent was exchanged with ddH₂O using Amicon® Ultra centrifugal filters with an MWCO of 10 kDa and five cycles of centrifugation at 10 000 x *g* (10 minutes per cycle).

Characterization of PfFtn-MAL conjugates: The PfFtn-MAL conjugates were subsequently diluted with the solvent containing 1:1 MeOH:ddH$_2$O+0.1% FA. The solvent (90 µL) was added to 10 µL of the diluted PfFtn-MAL solution. These conjugates were characterized using ESI MS (Thermo QE). The final concentration of the PfFtn-MAL conjugate solution that was injected was 0.03 µM. The resulting spectrum was deconvoluted with the Thermo Scientific BioPharma Finder (version 3.0) software. All subsequent ESI mass spectra concerning PfFtn conjugates were analyzed using this software. All of the following samples containing PfFtn conjugates were prepared for and characterized with ESI MS using this procedure and diluted to 0.03 µM.

Synthesis of PfFtn-MAL-TCEP conjugates: A solution of 0.045 mg/mL TCEP in degassed ddH$_2$O (10 µL) was added to 440 µL of a 0.3 µM PfFtn-MAL conjugate solution in degassed doubly distilled water (ddH$_2$O). The reaction mixture was incubated overnight at 4 °C. The conjugates were characterized with ESI MS using the procedure described above.

Synthesis of PfFtn-mPEG$_4$BA Wittig conjugates: mPEG$_4$BA was weighed out so that a 1:1 molar ratio of the 0.3 µM PfFtn-ylene solution to mPEG$_4$BA was reacted. One equivalent of 2 M sodium hydroxide (NaOH) was added. This reaction mixture was heated for 4 hours at 50 °C. A solution of the PfFtn-MAL-mPEG$_4$BA conjugates were characterized with ESI MS using the procedure outlined above.

2.3.2. Wittig Modification of BCA with mPEG$_4$BA

Synthesis of BCA-MAL conjugates: BCA (2.0 mg, 6.897x10^{-5} mmol, 1.0 eq) from a 20.0 mg/mL in 0.15 M pH 7.4 KP buffer stock and NHS-dPEG$_4$-MAL (0.0708 mg, 1.379x10^{-5} mmol, 2.0 eq) from an 8.5 mg/mL stock in DMSO were incubated in 0.15 M pH 7.4 KP buffer overnight at 4 °C in a 200 µL total reaction volume. Next, the sample was prepared for analysis with ESI MS. The sample containing the KP buffer and DMSO solvent was exchanged with ddH$_2$O using centrifugal

filters with an MWCO of 10 kDa and five cycles of centrifugation at 10 000 x g (10 minutes per cycle). The BCA-MAL conjugates were subsequently diluted with the 1:1 MeOH:ddH$_2$O+0.1% FA solvent until the concentration of the sample was in the range of 1-10 μM and then characterized with ESI MS (Thermo QE). The resulting spectrum was deconvoluted with the Thermo Scientific BioPharma Finder software (version 3.0). All subsequent ESI mass spectra concerning BCA conjugates were analyzed using this software. All of the following samples containing BCA conjugates were prepared for and characterized with ESI MS using this procedure.

Synthesis of BCA-MAL-TCEP conjugates: BCA-MAL in ddH$_2$O (1.48 mg, 5.103x10^{-5} mmol, 1.0 eq of BCA protein in the reaction) and TCEP (0.7315 mg, 0.002551 mmol, 50.0 eq) from 6.4 mg/mL in degassed ddH$_2$O were reacted together in 214.3 μL degassed ddH$_2$O (total reaction volume). Unreacted TCEP was removed from the reaction mixture using centrifugal filters with an MWCO of 10 kDa as previously described. The BCA-MAL-TCEP conjugates were subsequently characterized with ESI MS as previously described.

Synthesis of BCA-mPEG$_4$BA Wittig conjugates: The solution containing the BCA-MAL-TCEP ylene was reacted with mPEG$_4$BA using four different reaction conditions:

Reaction 1a: BCA-MAL-TCEP (100 μL, 0.0067 μmol, 1.0 eq of BCA protein in the reaction), mPEG$_4$BA (0.1347 mg, 0.5025 μmol, 75.0 eq) from a 0.67 mg/mL stock in DMSO, and 1 mM NaOH (0.0067 μmol, 1.0 eq) were reacted together in 307.7 μL ddH$_2$O (total reaction volume) at 50-60 °C for 4 hours.

Reaction 1b: BCA-MAL-TCEP (100 μL, 0.0067 μmol, 1.0 eq of BCA protein in the reaction), and mPEG$_4$BA (0.1347 mg, 0.5025 μmol, 75.0 eq) from a 0.67 mg/mL stock in DMSO were reacted in 207.7 μL ddH$_2$O (total reaction volume) at 50-60 °C for 4 hours.

Reaction 2a: BCA-MAL-TCEP (100 μL, 0.0067 μmol, 1.0 eq of BCA protein in the reaction), mPEG$_4$BA (0.1347 mg, 0.5025 μmol, 75.0 eq) from a 0.67 mg/mL stock in DMSO, and 1 mM NaOH (0.0067 μmol, 1.0 eq) were reacted in 307.7 μL ddH$_2$O (total reaction volume) at room temperature for 24 hours.

Reaction 2b: BCA-MAL-TCEP (100 μL, 0.0067 μmol, 1.0 eq of BCA protein in the reaction), and mPEG$_4$BA (0.1347 mg, 0.5025 μmol, 75.0 eq) from 0.67 mg/mL in DMSO were reacted in 207.7 μL ddH$_2$O (total reaction volume) at room temperature for 24 hours.

BCA-mPEG$_4$BA Wittig conjugates obtained in reactions **1a, 1b** and **2a, 2b** were prepared for analysis and subsequently characterized by ESI MS as previously described.

2.3.3. Wittig Modification of BCA with AldPhPEG$_6$COOH

Synthesis of BCA-MAL conjugates: The BCA-MAL conjugates were prepared according to the procedure outlined in Section 2.3.2, using double the amounts listed.

Synthesis of BCA-MAL-TCEP conjugates: To the solution containing BCA-MAL conjugates, TCEP (2.8 mg, 0.009767 mmol, 70.8 eq) in 100 μL degassed ddH$_2$O was added. The reaction proceeded at room temperature for 2 hours. The amount of TCEP to be added was calculated assuming 100% of the initial amount of BCA was retained in the reaction mixture to ensure that this reagent was in excess. After reaction completion, unreacted TCEP was separated from the reaction mixture using MWCO 10 kDa centrifugal filters as previously described.

Synthesis of BCA-AldPhPEG$_6$COOH Wittig conjugates: The addition of AldPhPEG$_6$COOH is described according to the following three reactions. All amounts were calculated assuming 100% of the initial amount of BCA was retained in the reaction mixture to ensure that AldPhPEG$_6$COOH was in excess:

Reaction 3a: AldPhPEG₆COOH (6.7 mg, 0.0138 mmol, 100.0 eq) was added to the solution containing BCA-MAL-TCEP conjugates. The reaction was incubated at room temperature for 24 hours in 700 µL ddH₂O.

Reaction 3b: AldPhPEG₆COOH (6.7 mg, 0.0138 mmol, 100.0 eq) was added to the solution containing BCA-MAL-TCEP conjugates. The reaction was incubated overnight at 40 °C in pH 8.3 0.15 M tricine buffer in a total volume of 700 µL.

Reaction 3c: AldPhPEG₆COOH (6.7 mg, 0.0138 mmol, 100.0 eq) was added to the solution containing the BCA-MAL-TCEP conjugates. The reaction was incubated overnight at room temperature in pH 9.0 0.15 M borate buffer with a total volume of 1.0 mL.

The final BCA-AldPhPEG₆COOH conjugates from reactions **3a-c** were prepared for and analyzed by ESI MS as previously described.

2.3.4. Optimization of the Wittig Reaction using NEM and mPEG₄BA as Model Compounds
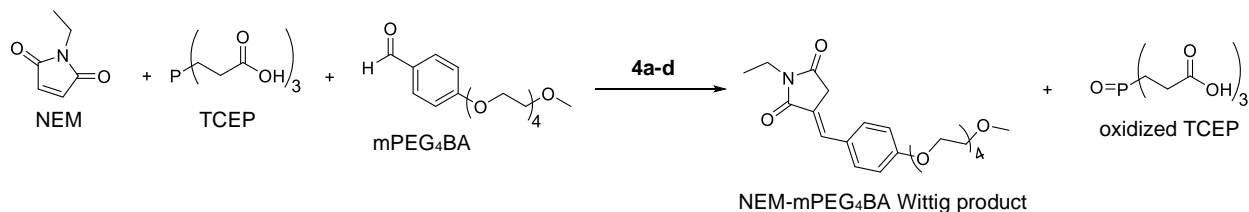
Scheme 2.5. Wittig reaction with NEM, TCEP, and mPEG₄BA as model compounds.

Reaction 4a: NEM (0.8730 mg, 0.0070 mmol, 1.0 eq) from 13.4 mg/mL in degassed ddH₂O, TCEP (2.0 mg, 0.0070 mmol, 1.0 eq) from 21 mg/mL in degassed ddH₂O, mPEG₄BA (9.4 mg, 0.0349 mmol, 5.0 eq) from 19.7 mg/mL in degassed ddH₂O, and 1 M NaOH (0.0349 mmol, 5.0 eq) were reacted together overnight at room temperature. The amounts of reagents and reaction conditions for reaction **4b** were identical to those described for reaction **4a**, except that 1 M NaOH was

excluded. The reaction mixtures were not purified prior to characterization with ESI MS. High resolution ESI MS (Thermo QE) was used to characterize the reaction mixture.

Reaction 4c: NEM (0.8730 mg, 0.0070 mmol, 1.0 eq) from 13.4 mg/mL in degassed ddH$_2$O, TCEP (2.0 mg, 0.0070 mmol, 1.0 eq) from 21 mg/mL in degassed ddH$_2$O were reacted in a 0.15 M pH 7.4 KP buffer for 1 hour at room temperature in 224 µL total reaction volume. After 1 hour, 476 µL of 19.7 mg/mL mPEG$_4$BA in degassed ddH$_2$O was added to 224 µL containing the NEM-TCEP conjugates. This solution (350 µL) was removed and reacted at room temperature overnight. The remaining 350 µL was reacted for 4 hours at 50-60 °C (reaction **4d**). Extraction with ethyl acetate was used to separate the product from the buffer in order to prepare the compound for characterization with ESI MS. Reactions **4c** and **4d** were rinsed with ethyl acetate (3 x 1 mL), and the ethyl acetate fractions were pooled in a round bottom flask. The ethyl acetate was removed with rotary evaporation under vacuum. The resulting compounds were characterized with high resolution ESI MS (Thermo QE).

2.3.5. Computational Determination of pKas for Phosphonium Adducts
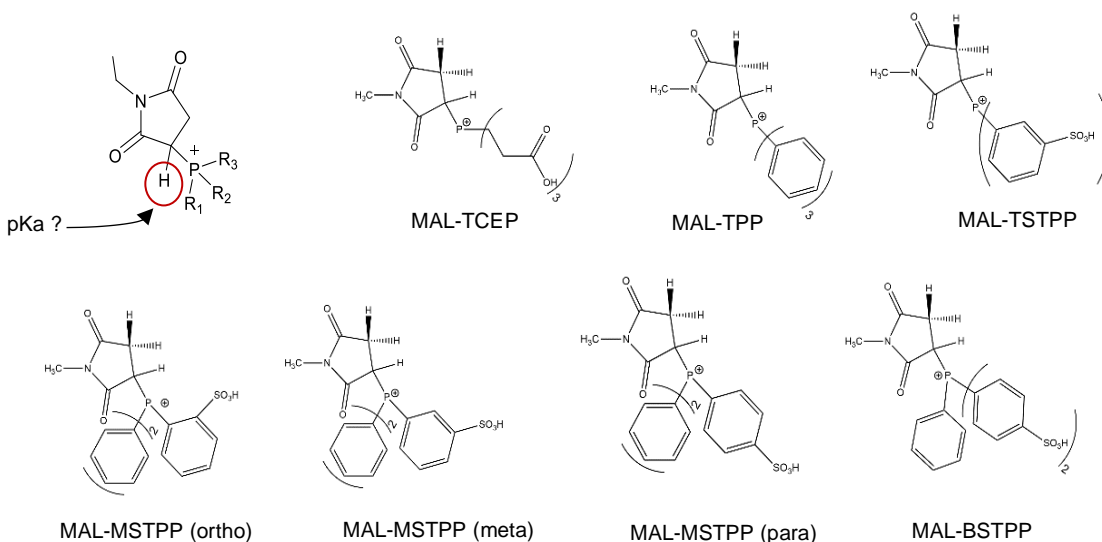
Figure 2.5. Chemical structures of phosphonium adducts for pKa calculations.

The structures shown in Figure 2.5 were drawn in Maestro (Schrodinger LLC) and minimized using the default OPLS4 forcefield. The pKa values were calculated using the Jaguar pKa Module (Schrodinger LLC) using default settings. The sulfonate groups were protonated for these calculations. The MSTPP label refers to the 3-(diphenylphosphino) monobenzenesulfonic acid compound.

2.3.6. Water-Soluble TPP-Based Ylene Formation with NEM
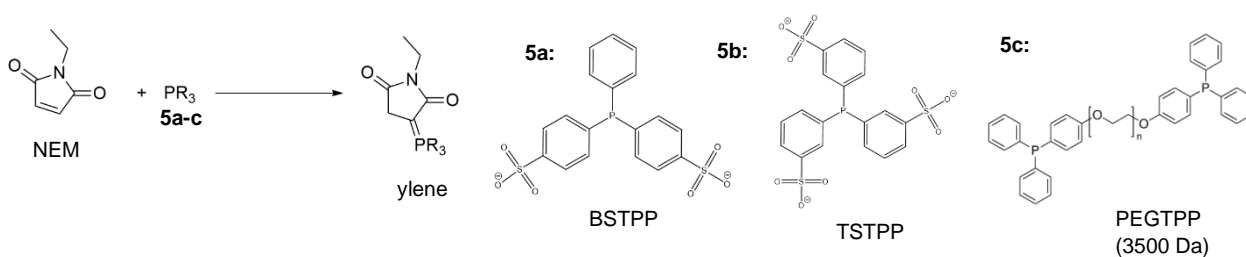
Scheme 2.6. Ylene formation with NEM and water-soluble TPP-based phosphines.

Reaction 5a: NEM (1.0 mg, 0.0080 mmol, 1.0 eq) from 13.4 mg/mL in degassed ddH$_2$O and BSTPP (7.4 mg, 0.014 mmol, 1.7 eq) were reacted overnight at room temperature in 625 μL of degassed ddH$_2$O.

Reaction 5b: NEM (1.0 mg, 0.0080 mmol, 1.0 eq) from 13.4 mg/mL in degassed ddH$_2$O and TSTPP (8.02 mg, 0.012 mmol, 1.5 eq) were reacted overnight at room temperature in 625 μL of degassed ddH$_2$O.

Reaction 5c: NEM (0.25 mg, 0.0020 mmol, 1.0 eq) from 13.4 mg/mL in degassed ddH$_2$O and PEGTPP (3500 g/mol) (10.5 mg, 0.0030 mmol, 1.5 eq) were reacted overnight at room temperature in 900 μL of degassed ddH$_2$O.

Characterization of reactions 5a-c with ESI MS: High resolution ESI MS (Thermo QE) was used to characterize the reaction mixture for reactions **5a-b** without any purification. Reaction **5c** could

not be successfully characterized by high resolution ESI MS due to the molecular weight dispersity of the PEGTPP compound.

*Characterization of reactions **5a-c** with ^{31}P NMR*: Small amounts of BSTPP, TSTPP, PEGTPP, NEM-BSTPP (**5a**), NEM-TSTPP (**5b**), and NEM-PEGTPP (**5c**) were dissolved in degassed ddH$_2$O and then characterized using ^{31}P NMR (202 MHz).

2.3.7. Water-Insoluble TPP Ylene Formation with NEM
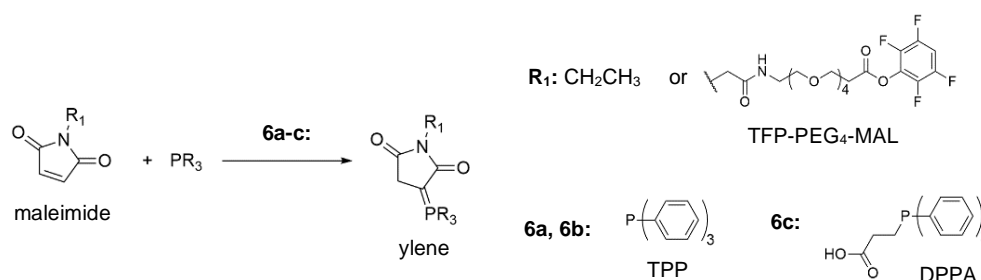
Scheme 2.7. Ylene formation with NEM and water-insoluble TPP-based phosphines.

Reactions **6a-c** were all conducted in degassed HPLC-grade acetone, with refluxing for 1 hour. The experimental conditions for the MAL-TPP ylene synthesis were obtained from Jung et al., Kaur et al., Luo et al., and Brackman et al.[88-91]

*Reaction **6a***: NEM (15.3 mg, 0.1222 mmol, 1.0 eq) and TPP (29.3 mg, 0.1117 mmol, 0.9 eq) were weighed out under argon in a 5 mL round bottom flask and dissolved in 2 mL degassed HPLC-grade acetone and refluxed at 50 °C for 1 hour. After 1 hour, acetone was removed with rotary evaporation to concentrate the solution.

*Reaction **6b***: TFP-dPEG$_4$-MAL (24.2 mg, 0.0923 mmol, 1.0 eq) and TPP (52.6 mg, 0.0932 mmol, 1.0 eq) were weighed out under argon in a 5 mL round bottom flask and dissolved in 2 mL degassed HPLC-grade acetone and refluxed at 50 °C for 1 hour. After 1 hour, acetone was removed with rotary evaporation to concentrate the solution.

Reaction 6c: TFP-dPEG$_4$-MAL (18.6 mg, 0.0330 mmol, 1.0 eq) and DPPA (9.4 mg, 0.0364 mmol, 1.1 eq) were weighed out under argon in a 25 mL round bottom flask and dissolved in 1 mL degassed HPLC-grade acetone and refluxed at 50 °C for 1 hour. After 1 hour, acetone was removed with rotary evaporation to concentrate the solution.

Characterization of reactions 6a-6c with ESI MS: Reaction **6a** was characterized with high resolution ESI MS (Thermo QE). Reactions **6b, 6c** were characterized by low resolution ESI MS (Thermo LTQ).

2.3.8. Determining the Stability of TCEP and TPP Ylenes in Water

Stability of NEM-TCEP in aqueous solution: TCEP-HCl was dissolved in degassed ddH$_2$O and immediately analyzed with ^{31}P NMR (202 MHz). NEM-TCEP was prepared as follows: NEM (22.2 mg, 0.1774 mmol, 1.0 eq) and TCEP (50.8 mg, 0.1774 mmol, 1.0 eq) were dissolved in 2 mL degassed ddH$_2$O and the reaction mixture was kept at room temperature. After 2, 4, 6, 24 hours and one week (five time points total) of the NEM-TCEP reaction, a small sample at each of these time points was analyzed by ^{31}P NMR in degassed ddH$_2$O as the solvent and low resolution ESI MS (LTQ).

Stability of TPP-based ylenes in aqueous solution: Unreacted TPP, along with NEM-TPP and TFP-dPEG$_4$-MAL-TPP (as prepared in Section 2.3.7, reactions **6a** and **6b**, respectively) were dissolved in degassed anhydrous DMF for analysis with ^{31}P NMR (202 MHz). TFP-dPEG$_4$-MAL-TPP was dissolved in 5% anhydrous DMF in ddH$_2$O and the mixture was left on the bench for 2 hours at room temperature. A sample of this mixture was analyzed with ^{31}P NMR after 2 hours and the remainder of the sample was left on the bench for 24 hours. After 24 hours, the sample was analyzed again with ^{31}P NMR.

2.4. Results and Discussion

2.4.1. Wittig Modification of PfFtn with mPEG₄BA

This project has focused on developing a new bioconjugation method for the lysine residues of proteins using maleimide, TCEP, and an aldehyde. Previous efforts by a graduate student (Fatima Merza) in the Honek laboratory to analyze the commercially available horse spleen ferritin protein using ESI MS were unsuccessful.[113] However, PfFtn is able to be analyzed using this technique. First, a control spectrum of the PfFtn protein subunit was obtained (Figure 2.6). In order to obtain the mass of the unmodified subunit, the resulting spectrum was deconvoluted with the Thermo Scientific BioPharma Finder software (version 3.0). All other mass spectra for protein modification presented in this section were analyzed with this software.
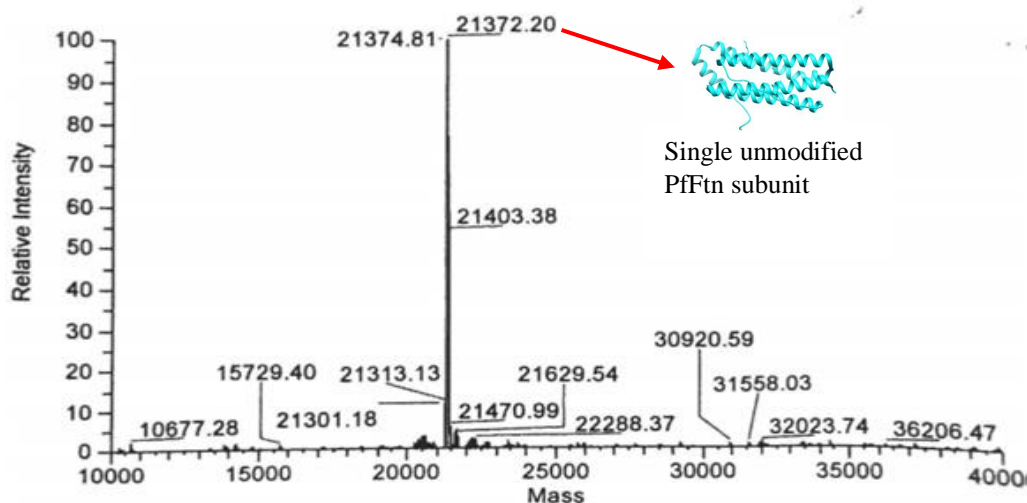
Figure 2.6. ESI MS of an unmodified subunit of PfFtn (scanned image). Subunit in turquoise.

The molas mass of a PfFtn subunit is 21372 Da. The mass of the unmodified PfFtn subunit will be used to determine if modifications occurred in the following steps. The first step was to modify PfFtn so that it displays a maleimide group. The molar mass of the resulting modification with the NHS-PEG₄-MAL reagent equals 399.5 Da.

42
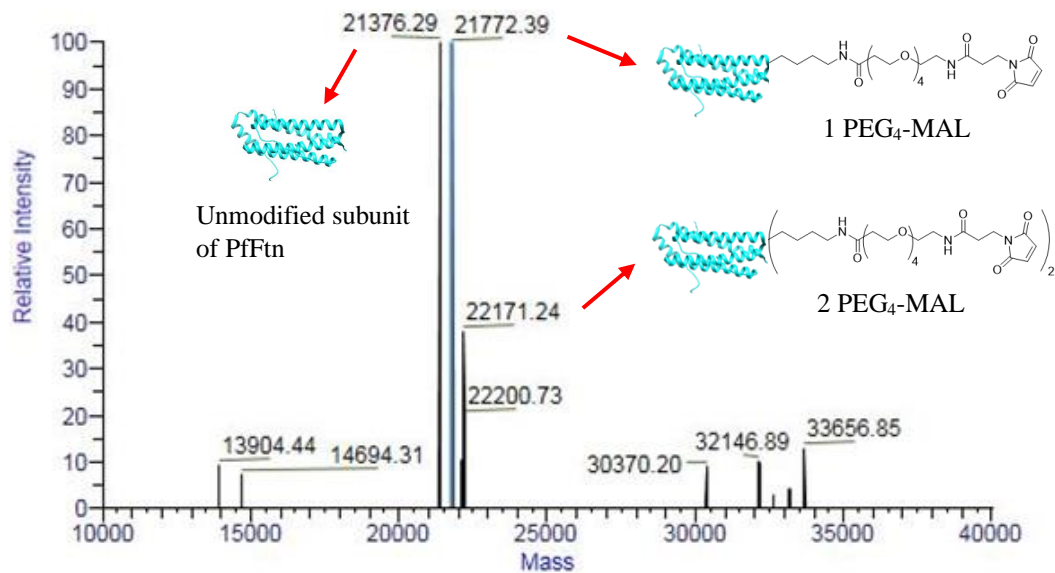
Figure 2.7. ESI MS of a PfFtn subunit modified with NHS-PEG$_4$-MAL.

Figure 2.7 shows the modification of a PfFtn subunit with the maleimide analogue. The masses of a single subunit modified with one and two maleimides are 21772 Da and 22171 Da, respectively. There also exists a mass peak at 21376 Da, which also corresponds to an unmodified PfFtn subunit. Next, the PfFtn-MAL adduct was reacted with TCEP to form the ylene. The results of this reaction are shown in the following mass spectrum (Figure 2.8).
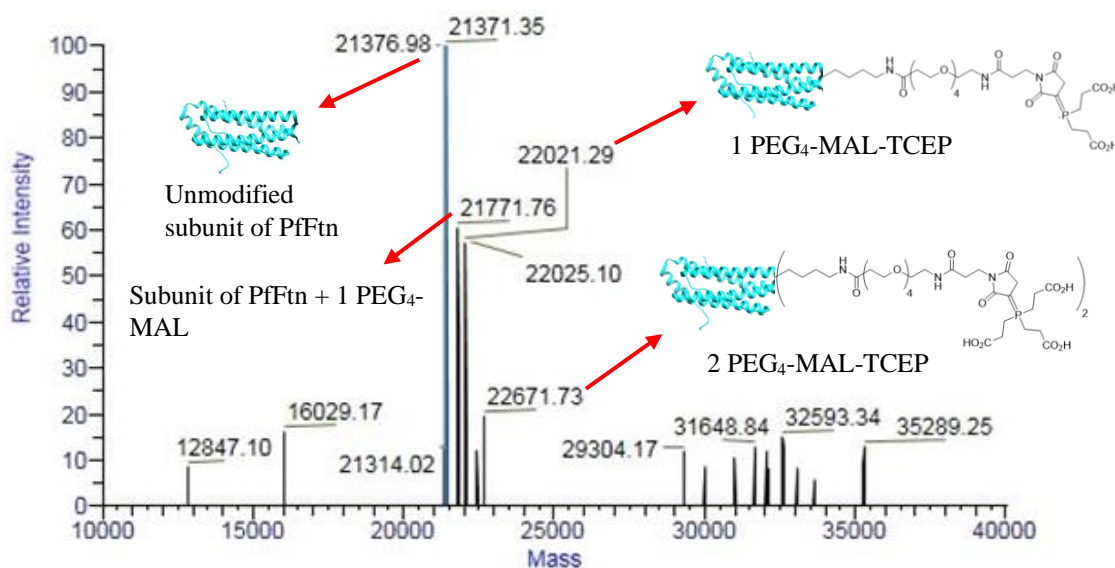
Figure 2.8. ESI MS of a PfFtn subunit modified with NHS-PEG₄-MAL-TCEP.

The molecular weight of this modification equals 649.7 Da. The mass at 22021 Da corresponds to one modification of a subunit of PfFtn. Another mass, found at 22671 Da, corresponds to two modifications of the PfFtn subunit. Some of the PfFtn-MAL adduct did not react with TCEP, and this peak is shown in Figure 2.8 with a molecular weight of 21771 Da.

Lastly, the PfFtn-MAL-TCEP ylene was reacted with mPEG₄BA. The final molar mass of a single modification with the aldehyde equals 667.3 Da. The results of this modification are shown in Figure 2.9.
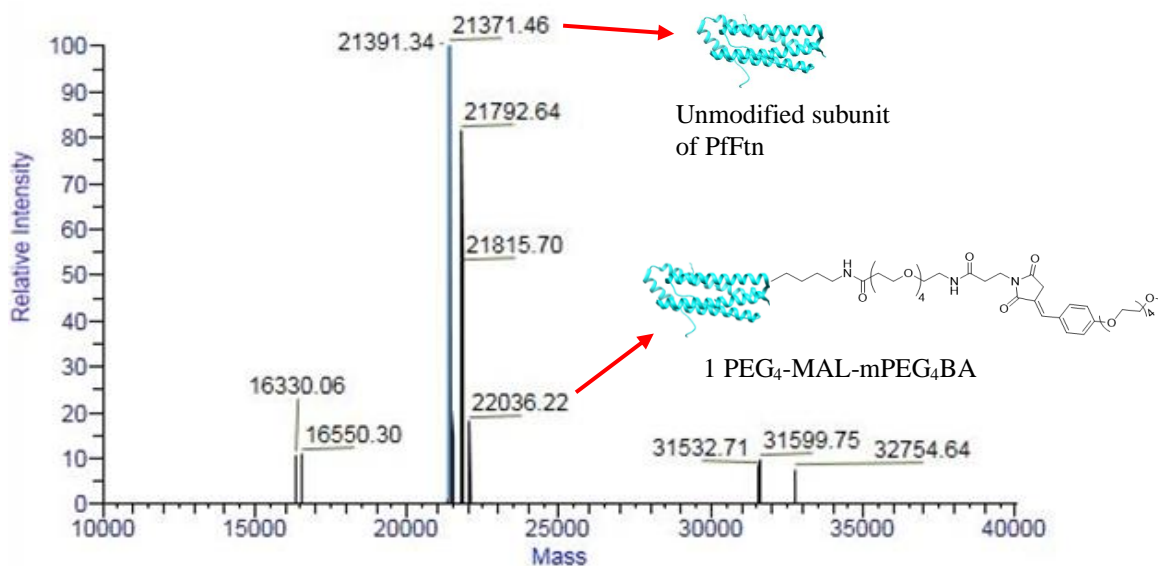
Figure 2.9. ESI MS of a PfFtn subunit modified with NHS-PEG$_4$-MAL and mPEG$_4$BA.

The two main mass peaks in Figure 2.9 are located at 21371 Da and 22036 Da. The first of these two mass peaks corresponds to an unmodified subunit of PfFtn. Mass peaks corresponding to unmodified subunits are expected to be found in all of the mass spectra presented because the full extent of modification was never attempted with the NHS-dPEG$_4$-MAL reagent. The second mass peak at 22036 Da corresponds to the mass of a subunit with one modification with the aldehyde. Using the ESI MS technique, it was shown that this novel bioconjugation method is a promising new strategy that could be used to modify PfFtn. However, PfFtn is not a commercially available protein. Therefore, BCA was used as a model protein for studying the novel bioconjugation strategy as it is commercially available and it is also able to withstand higher temperatures, although not to the extent that PfFtn can tolerate.

2.4.2. Wittig Modification of BCA with mPEG$_4$BA

The protein BCA was used for subsequent studies of the novel bioconjugation method. As with PfFtn, BCA was first modified with NHS-dPEG$_4$-MAL and then TCEP to form the ylene conjugate on its surface (Figure 2.10A & B, respectively).

45

A)

B)
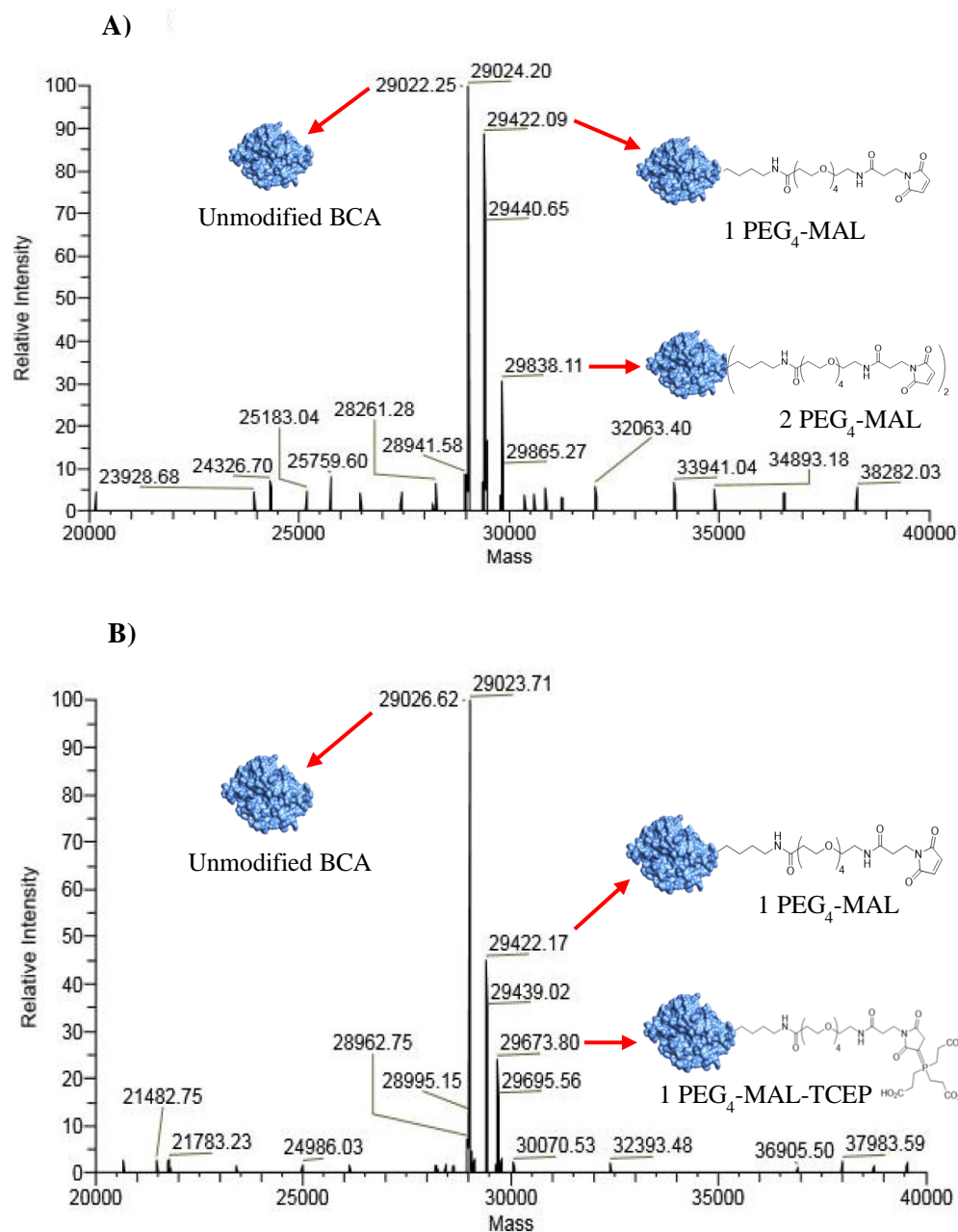
Figure 2.10. ESI mass spectra of BCA modified with **A)** NHS-PEG$_4$-MAL and **B)** PEG$_4$-MAL-TCEP. BCA in blue.

In Figure 2.10B, BCA with one PEG$_4$-MAL-TCEP conjugate can be observed. Since this ylene could be characterized by ESI MS, the next step was to conduct the Wittig reaction with mPEG$_4$BA as the water-soluble aldehyde on the surface of the BCA protein. Four different conditions were attempted for this modification step. Reaction **1** refers to the Wittig reaction with

BCA- PEG$_4$-MAL-TCEP conjugates and mPEG$_4$BA at 50 – 60 °C for 4 hours with reactions **1a** and **1b** referring to the reaction with and without a base, respectively. Reaction **2** refers to the Wittig reaction with BCA-PEG$_4$-MAL-TCEP conjugates and mPEG$_4$BA at room temperature for 24 hours, with reactions **2a** and **2b** referring to the reaction with and without a base, respectively. A 75-fold molar excess of mPEG$_4$BA to the amount of BCA was used for all four reactions. NaOH (1 mM) was used for the base reactions. The spectra for reactions **1a-b, 2a-b**, and the chemical structure of the modified BCA are shown in Figure 2.11A-E, respectively.

C)

D)

E)
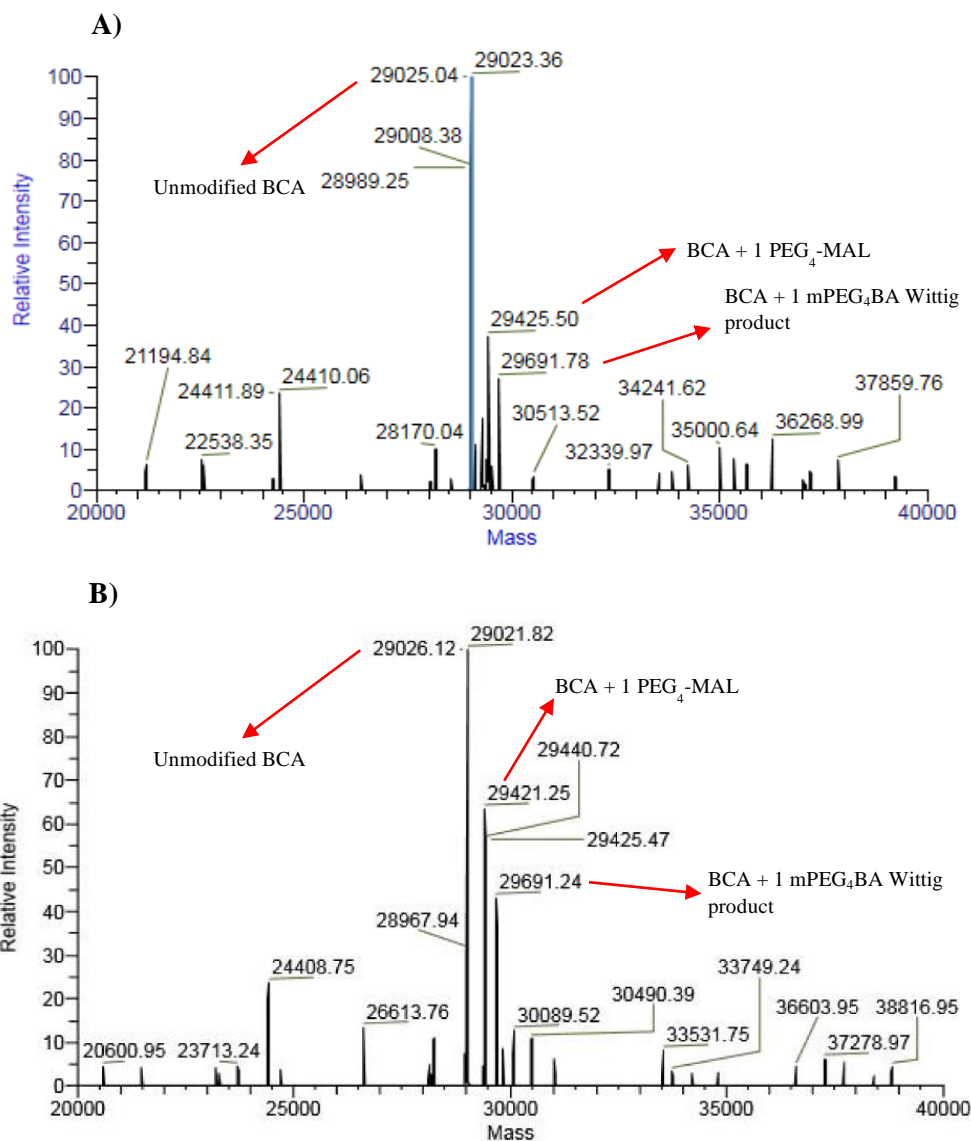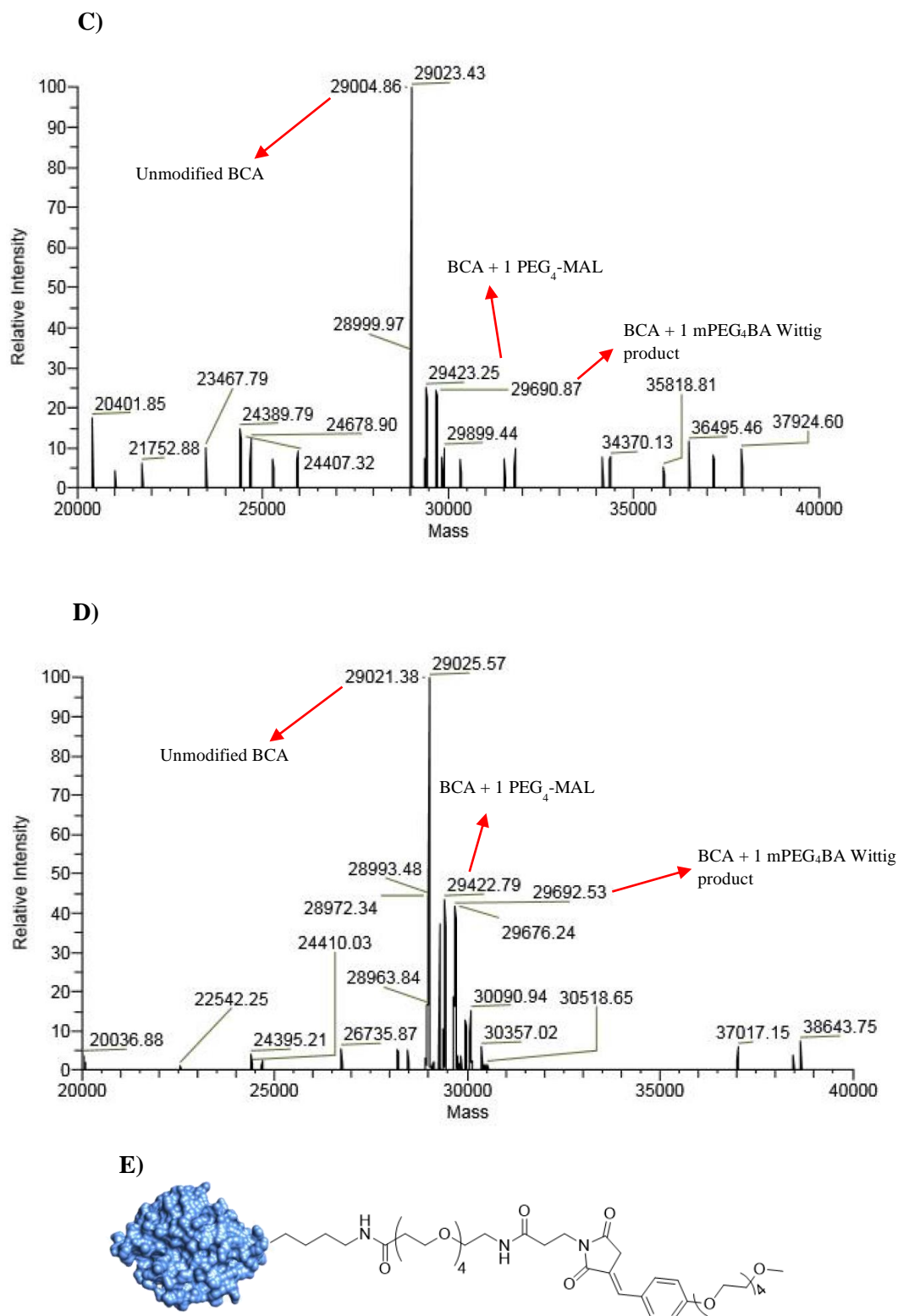
Figure 2.11. ESI MS of BCA modified with mPEG$_4$BA. **A)** Reaction **1a**. **B)** Reaction **1b**. **C)** Reaction **2a**. **D)** Reaction **2b**. **E)** Structure of BCA modified with AldPhPEG$_6$COOH.

The expected molar mass of a single modification of BCA with mPEG$_4$BA is 667.3 Da. In each spectrum shown Figure 2.11A-D, the peak that appears to correspond to the modification with this aldehyde is seen at 29693 Da (±1.5 Da). These results would indicate that the Wittig reaction may proceed in an aqueous solution either at room temperature for 24 hours, or at 50-60 °C for 4 hours, with or without base since all four spectra are identical. Although a base may be added in many organic Wittig reactions, it was not known if the addition of one equivalent of 1 mM NaOH would have any affect on the aqueous Wittig reaction. The amount of NaOH added (1 mM) is quite low, since 0.067 μmol of BCA was present in the reaction mixture. BCA has many ionizable amino acid side chain groups on its surface, and it would be likely that the small amount of base would react with some of these side chain groups instead of contributing to the Wittig reaction. Based on these experiments, it would appear that the Wittig reaction may proceed under mild (i.e. no heat or base) aqueous conditions.

It is important to note that the spectra shown in Figure 2.11 cannot conclusively confirm if the Wittig reaction proceeds in aqueous conditions on the surface of BCA. The expected molar mass of a single modification of BCA with PEG$_4$-MAL-TCEP equals 649.7 Da. A sodium adduct of this conjugate would have an expected molar mass change of 649.7 + 23 = 672.7 Da. This is approximately 5 Da different from the expected change with the mPEG$_4$BA reagent (667.3 Da). Given that the resolution of ESI MS for protein characterization is typically not high enough to differentiate between such low molecular weight differences, it is possible that the Wittig product peaks in Figure 2.11 correspond to BCA + PEG$_4$-MAL-TCEP + Na$^+$ adducts. Samples are commonly ionized with protons, sodium, and potassium ions for detection with ESI MS. The next section (2.4.3) describes the modification of BCA with a new water-soluble aldehyde: AldPhPEG$_6$COOH. This reagent is larger than mPEG$_4$BA (MW = 485.5 Da versus MW = 268.3

Da, respectively). Experiments with AldPhPEG$_6$COOH will help determine the reproducibility of the aqueous Wittig reaction. The modification of BCA with this reagent will not overlap with the observed mass of the BCA + PEG$_4$-MAL-TCEP + Na$^+$ adduct.

2.4.3. Wittig Modification of BCA with AldPhPEG$_6$COOH

BCA was modified first with NHS-PEG$_4$-MAL, and then TCEP was added, as described in Section 2.3.3. The mass spectra obtained for each modification step are identical to the spectra shown in Figure 2.10 in Section 2.4.2. As it was confirmed by ESI MS that the Wittig reagent was displayed on the surface of BCA, the AldPhPEG$_6$COOH reagent was reacted with the BCA-TCEP conjugates in ddH$_2$O, at room temperature for 24 hours, without base (reaction **3a**). This reaction was meant to replicate the reaction conditions of the BCA-PEG$_4$-MAL-TCEP conjugates with mPEG$_4$BA. ESI MS analysis lead to the conclusion that the Wittig modification did not occur with this reagent under these conditions (data not shown). The next reaction (**3b**) was conducted at pH 8.3, 40 °C, overnight to test if milder temperatures (comparing to 50-60 °C tested with mPEG$_4$BA) would result in a successful Wittig reaction on BCA (Figure 2.12A).
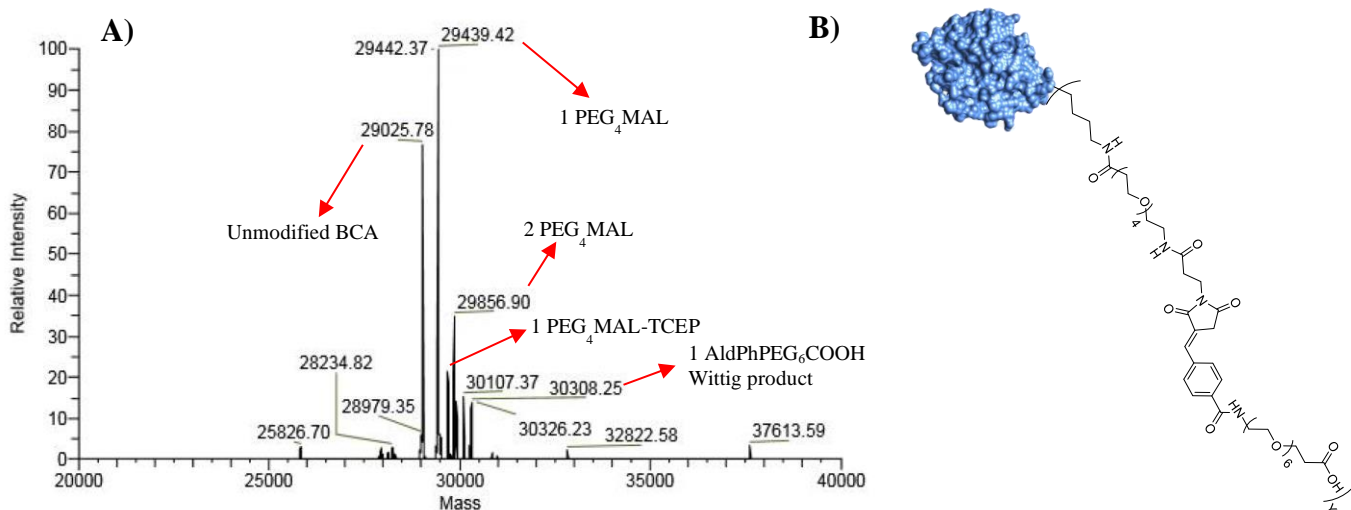
Figure 2.12. ESI spectra of BCA modification with AldPhPEG$_6$COOH. **A)** Wittig reaction at 40 °C overnight at pH 8.3. **B)** Structure of the BCA-AldPhPEG$_6$COOH Wittig product conjugate.

The expected molar mass change for the modification of BCA with AldPhPEG$_6$COOH is 868 Da. The mass difference between 29025 Da and 30308 Da in Figure 2.12A is in agreement with this expected modification. Since the reaction conditions for **3b** (40 °C, overnight) may be harsh for many proteins, resulting in the loss of their structure or function, this bioconjugation method is not necessarily applicable for many proteins. This is particularly concerning for the synthesis of protein therapeutic agents, as the bioconjugation method may impact the protein structure and render it ineffectual for drug delivery applications. It was therefore necessary to optimize the Wittig reaction so that a variety of proteins may be modified with aldehydes using this chemistry. The next reaction with BCA-ylene conjugates and AldPhPEG$_6$COOH was therefore conducted at pH 9.0, overnight, at room temperature (reaction **3c**). The modification of BCA with the AldPhPEG$_6$COOH reagent was not observed with ESI MS (data not shown). In order to further study optimal conditions for this bioconjugation method, small molecule experiments with NEM and mPEG$_4$BA were undertaken. NEM is a less expensive reagent than NHS-dPEG$_4$-MAL, making the use of small molecule reactions ideal for the optimization studies. The next sections describe these experiments and their results.

2.4.4. Optimization of the Wittig Reaction using NEM and mPEG$_4$BA as Model Compounds

Small molecule model reactions with the inclusion or absence of base were attempted in order to test if a base is required for the reaction to proceed. Reactions **4a** and **4b** were one-pot reactions where NEM, TCEP, and mPEG$_4$BA were reacted together at room temperature in degassed water. Reaction **4a** had five equivalents of NaOH relative to the equivalents of NEM in the reaction, whereas reaction **4b** did not include the base. The resulting mass spectra are shown in Figure 2.13A-B. Both reactions **4c** and **4d** were tested in a potassium phosphate buffer solution (pH 7.4) to mimic a protein reaction. Reactions **4c** and **4d** were conducted at room temperature

overnight and at 50-60 °C for four hours, respectively. These reactions were conducted to determine if heating is required for the reaction to proceed in a buffer solution at pH 7.4. The resulting mass spectra are shown in Figure 2.13C-D. Prior to ESI MS analysis, the buffer was removed with washes of ethyl acetate, where the organic fractions were pooled together and evaporated. It was anticipated that the product would be extracted in the organic phase. The aqueous phase was saved for each of these two reactions and pooled together in case further analysis was required.

A)

B)
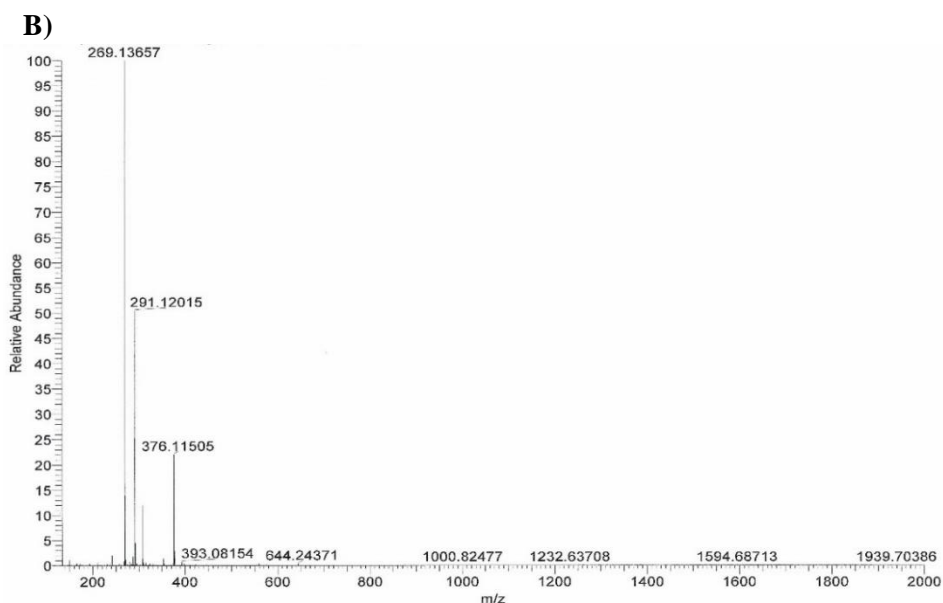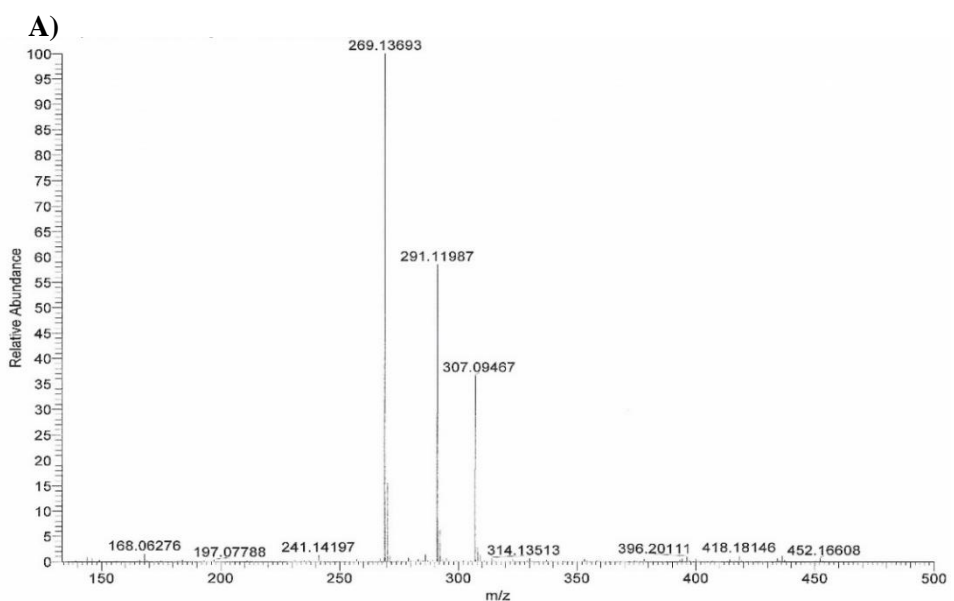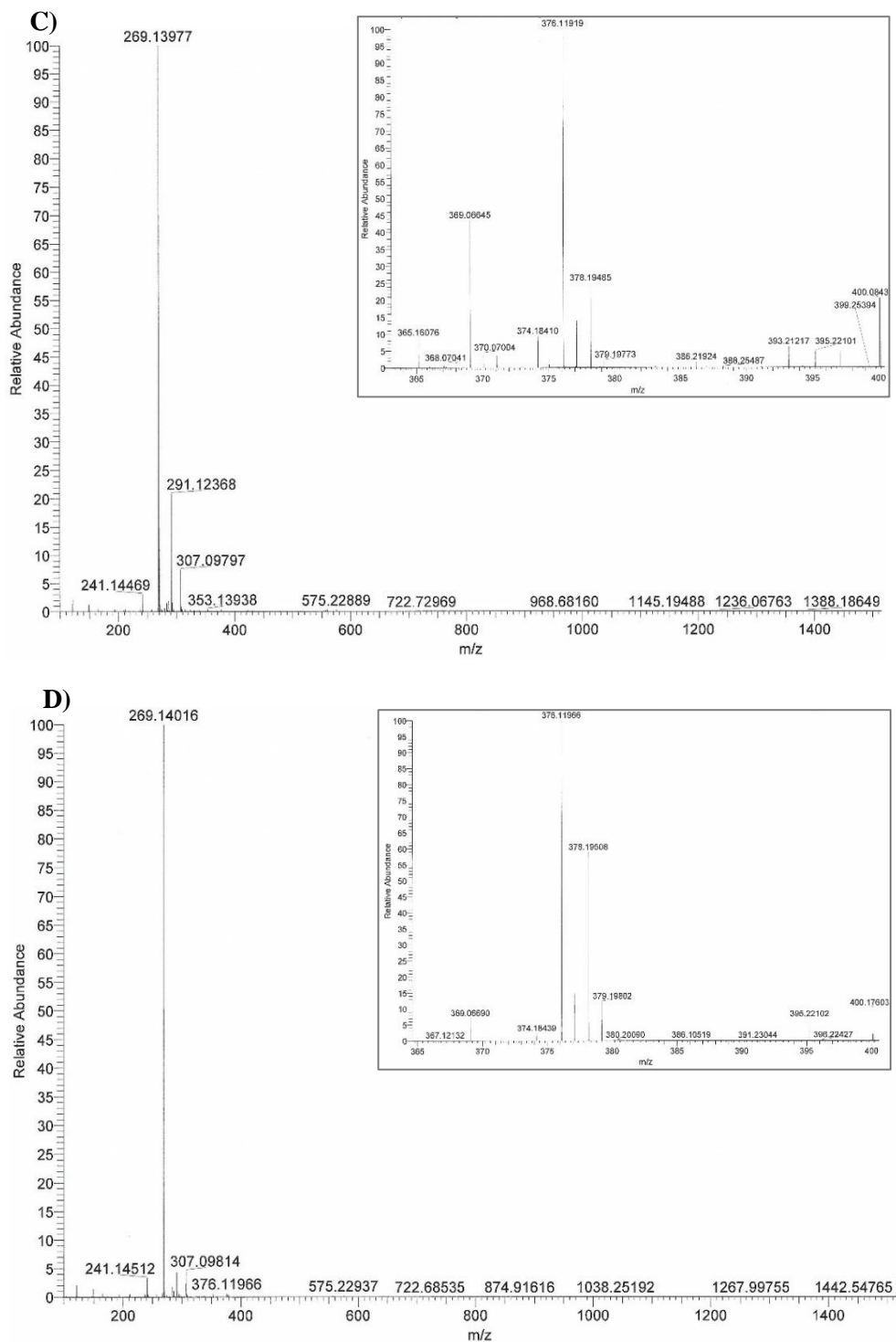
Figure 2.13. ESI MS of NEM, TCEP, and mPEG$_4$BA small molecule reactions. **A)** Reaction in ddH$_2$O at room temperature with 5 equivalents of NaOH (**4a**). **B)** Reaction in ddH$_2$O at room without base (**4b**). **C)** Reaction in KP buffer, pH 7.4, room temperature (**4c**). Insert: mass spectrum obtained from m/z = 365 – 400 Da. **D)** Reaction in KP buffer, pH 7.4, 50-60 °C. (**4d**). Insert: mass spectrum obtained from m/z = 365 – 400 Da.

In all four spectra shown in Figure 2.13, the predominant peak is unreacted mPEG$_4$BA (269 Da) along with the sodium and potassium adducts of this molecule (291 Da and 307 Da, respectively). In Figure 2.13B, the NEM-TCEP ylene adduct is observed at 376 Da. One of the disadvantages of utilizing ESI MS is that ion suppression of analytes can occur in complex mixtures containing more than one unique analyte. Comparison of peak intensities cannot be used to determine if a reaction was successful, or if one analyte is present in a greater proportion than another. One possibility is that the unreacted mPEG$_4$BA compound is suppressing the Wittig product when analyzed with ESI MS. With this taken into consideration, each reaction **4a-d** was analyzed with ESI MS when the scan range was changed to m/z = 365-400 Da in order to exclude the unreacted mPEG$_4$BA adducts. The two reactions **4c** and **4d** produced the NEM- mPEG$_4$BA compound as the peak at 378 Da corresponding to this Wittig product was observed (MS inserts seen on Figure 2.13C-D). This suggests that if the mPEG$_4$BA compound was removed entirely from the reaction mixtures prior to analysis with ESI MS, the desired product would likely be observed. Another possibility concerning reactions **4c** and **4d** is that the majority of the desired product was retained in the aqueous phase during the ethyl acetate rinses. In an attempt to mitigate these two problems, a polystyrene-supported aldehyde scavenging resin (*p*-toluenesulfonyl hydrazide bound on polystyrene beads) was applied to the samples corresponding to reactions **4c** and **4d**. The saved aqueous fractions for these two samples were also analyzed.

A three-fold excess of the resin was added assuming that 100% of the mPEG$_4$BA reagent was unreacted to ensure aldehyde removal. After 1.5 hours of reaction time with the resin, the resin was washed with dichloromethane and the fractions were collected and evaporated. ESI MS analysis was conducted, and the removal was not completely successful as the unreacted aldehyde was still observed by mass spectrometry (data not shown). The aqueous fractions from reactions

4c and **4d** were evaporated separately to obtain the solid containing the buffer and possible Wittig product. This solid was rinsed three times with ethyl acetate, and the organic phase was extracted, pooled together, and the solvent was removed with rotary evaporation. It was anticipated that, if no water was present, the product would be soluble in ethyl acetate, while the buffer salts would remain as an insoluble solid and would not enter the organic phase. The two samples were analyzed with ESI MS, but the peak corresponding to the product was not observed, and the 376 Da peak corresponding to the NEM-TCEP ylene was the predominant peak (data not shown).

The challenge with small molecule systems for the Wittig reaction optimization versus using BCA is that it is difficult to separate the buffer and unreacted materials from the final product other than by employing a method such as chromatography. As BCA is much larger than the buffer salts and unreacted small molecule components, they can easily be separated by size-exclusion filtration. Temperature changes (room temperature versus heating at 50-60 °C), and the addition or exclusion of a base were studied for the reaction of BCA with mPEG$_4$BA and AldPhPEG$_6$COOH. The reactions were unsuccessful under mild conditions (room temperature and no base) for AldPhPEG$_6$COOH as the aldehyde. The presence of unreacted mPEG$_4$BA and NEM-TCEP in the small molecule reactions suggests that there is a low conversion to the Wittig product. The next step was to determine if TCEP is an appropriate phosphine to use in the Wittig reactions.

2.4.5. Computational Determination of pKas for Phosphonium Adducts

The second step shown in the Wittig mechanism in Scheme 2.2, Section 2.1, shows that the following compound needs to be deprotonated in order for the Wittig reaction to proceed:
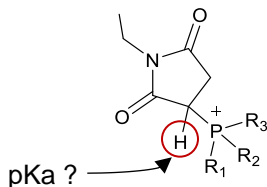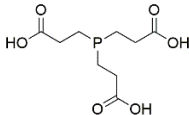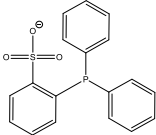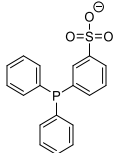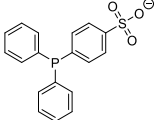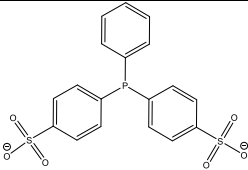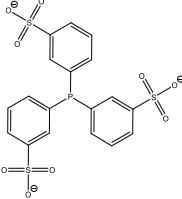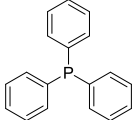
Figure 2.14. Wittig reaction intermediate structure.

55

Depending on which ligands are present on the phosphine (R_1, R_2, and R_3), the pKa of the circled proton will vary. A number of different phosphines were chosen to be studied for their effects on this pKa value (Table 2.1 below). The compounds were drawn in Maestro (Schrodinger LLC), and after minimization with the OPLS4 forcefield to obtain the lowest energy compounds, the theoretical pKas were calculated using the Jaguar pKa module (Schrodinger LLC).

Table 2.1. Theoretical pKa values for various phosphines and their chemical structures.

Phosphine Name	Phosphine Structure	Theoretical pKa (±1 pKa unit)	Notes
TCEP		9.95	Commercially available, water-soluble
MSTPP (ortho)		5.12	Commercially available, water-soluble
MSTPP (meta)		6.53	Not commercially available, water-soluble
MSTPP (para)		7.69	Commercially available, water-soluble
BSTPP		6.42	Commercially available, water-soluble
TSTPP		5.58	Commercially available, water-soluble
TPP		5.12	Commercially available, water-insoluble

Although the theoretical method does not provide the exact pKa of the compound, it is expected to provide information on the trend in the pKa change with molecular structure. The calculations indicated that the structure with NEM and TCEP would yield the highest pKa value. Taking into account the inherent error of the computational calculations ($\pm$ 1 pKa unit), the use of TCEP as the phosphine still results in the highest pKa value. It is possible that without the addition of an excess of strong base and/or high temperatures, the Wittig reaction would not proceed with TCEP as the phosphine in an aqueous solution with maleimide. This is consistent with the previous studies outlined in this chapter. The overall goal is to develop a bioconjugation method that is amenable to a variety of proteins. High temperatures and strong bases may denature proteins. If TCEP is not an appropriate phosphine for this bioconjugation strategy, then other phosphines are available.

The remainder of the structures have lower theoretical pKa values. These are all aryl phosphines. It should be noted that for the water-soluble sulfonated phosphines, the sulfate groups had to be protonated for the computational calculation to proceed. In an aqueous solution, these sulfate groups would be deprotonated. Therefore, the experimental pKa would likely be different than the computational pKa values obtained, and there is an inherent error in the calculation.

TPP and MSTPP (ortho) have the lowest calculated pKa values (pKa = 5.12). However, TPP is completely water-insoluble, and not a suitable phosphine for an aqueous Wittig reaction, unless attached to a water-soluble component, such as PEG. The two phosphines BSTPP and TSTPP are water-soluble aryl phosphines with pKas lower than TCEP. They were the two phosphines from Table 2.1 that were purchased commercially. The next section describes the reactions of NEM and these water-soluble phosphines.

2.4.6. Water-Soluble TPP Ylene Formation with NEM

Before the Wittig reaction can proceed with an aldehyde, it is imperative to determine that a Wittig reagent is being formed. NEM was reacted with three different water-soluble phosphines: BSTPP, TSTPP, and PEGTPP (reactions **5a-c**, respectively). The high resolution ESI mass spectra are shown in Figure 2.15.
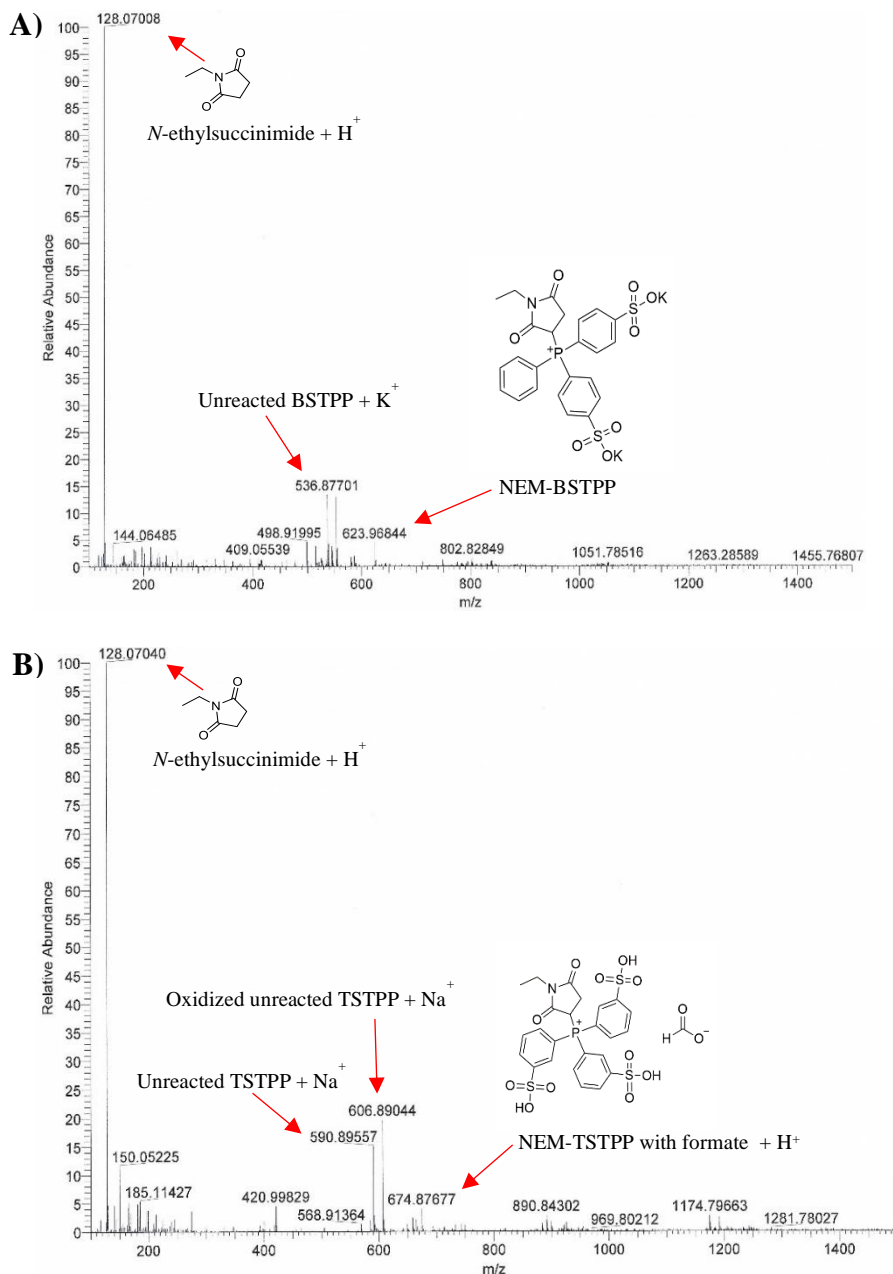
Figure 2.15. ESI MS of NEM and water-soluble phosphine adducts. **A)** Reaction of NEM with BSTPP. **B)** Reaction of NEM with TSTPP.

It should be noted that NEM-PEGTPP (**5c**) could not be successfully characterized by high resolution ESI MS due to the molecular weight dispersity of the PEGTPP compound. For both the NEM-BSTPP (**5a**) and NEM-TSTPP (**5b**) reactions, the adducts of both compounds were observed at 623 Da and 674 Da, respectively. Specifically, the mass at 674 Da corresponds to the NEM-TSTPP adduct with a formate counterion, which is contributed by the formic acid in the solvent used for ESI MS. The mass at 128 Da is common to both spectra. It corresponds to *N*-ethylsuccinimide, the reduced form of NEM. The presence of this compound could potentially indicate the instability of the NEM-BSTPP and NEM-TSTPP adducts in an aqueous solution.

Given that high resolution ESI MS poses challenges, such as ion suppression, and difficulties with determining the presence of an NEM-PEGTPP adduct, another technique used to characterize these compounds was ^{31}P NMR. This analytical technique was used to determine if the phosphorous-based compounds are unreacted, oxidized, or bound to a carbon, depending on the chemical shift of the phosphorous. The samples were dissolved in degassed ddH$_2$O and immediately analyzed with ^{31}P NMR. The ^{31}P NMR spectra are given in Appendix A. A summary of the chemical shifts is given in Table 2.2.

Table 2.2. ^{31}P NMR chemical shifts for the unreacted TPP analogues and the NEM-TPP phosphonium adducts.

Label	Chemical Structure	Chemical shift δ (ppm)
BSTPP		-7.11
NEM-BSTPP		-6.49 -6.13 28.21 36.10 36.34
TSTPP		-5.8082 -34.4316
NEM-TSTPP		-3.49 36.73
PEGTPP		35.78 35.962 36.140
NEM-PEGTPP		37.93 38.08 38.85

The ^{31}P NMR chemical shifts for the NEM-PEGTPP adduct and unreacted PEGTPP suggests that the NEM-PEGTPP adduct was not formed as the chemical shifts for this compound are identical to the shifts for the unreacted phosphine compound (δ = 37.93-38.85 ppm). It cannot be conclusively said if this chemical shift corresponds to oxidized PEGTPP or not. For NEM-BSTPP, the unreacted BSTPP chemical shift (δ = -7.11 ppm) is still present in the ylene sample, indicating that the phosphine has not fully reacted to form the adduct. There are two other peaks

present in the NEM-BSTPP sample at $\delta = 28.21$ ppm and $\delta = 36.10$-36.34 ppm. It is likely that the oxidized BSTPP corresponds to the highest chemical shift. Similarily, unreacted TSTPP ($\delta = -3.49$ ppm) was observed for the NEM-TSTPP sample. The second chemical shift observed ($\delta = 36.73$ ppm) is similar to the oxidized BSTPP chemical shift, and similar to the unreacted PEGTPP chemical shift, although it cannot be conclusively stated if this corresponds to oxidized TSTPP or the NEM-TSTPP adduct.

By ESI MS, both NEM-BSTPP and NEM-TSTPP form adducts, while the NEM-PEGTPP mass could not be determined. By ^{31}P NMR, the NEM-BSTPP adduct is seen, whereas the NEM-PEGTPP adduct is not formed, and the formation of NEM-TSTPP is inconclusive. Based on these experiments, the best water-soluble aryl phosphine to use for future Wittig reactions would be BSTPP.

2.4.7. Water-Insoluble TPP Ylene Formation with NEM

The two water-insoluble phosphines, TPP and DPPA were also studied for their potential use in the Wittig reaction for protein bioconjugation. Although these two phosphines are insoluble in an aqueous solution, it is possible to first form the ylene with organic conditions using a heterobifunctional PEG reagent containing an activated ester on one end and a maleimide on the opposite end. The phosphine will be more water-soluble due to the PEG group and the ylene can be attached directly onto the protein lysine residues through the activated ester. Three reactions were done (**6a-c**) with one equivalent of the maleimide-containing compound and roughly equivalent molar amounts (0.9-1.1 eq) of the phosphine were mixed together in acetone at 50 °C for 1 hour. Acetone was chosen as the solvent as all the compounds were soluble in it. Acetone will not hydrolyze the activated ester group and it is easily removed with rotary evaporation. The resulting mass spectra are shown in Figure 2.16.
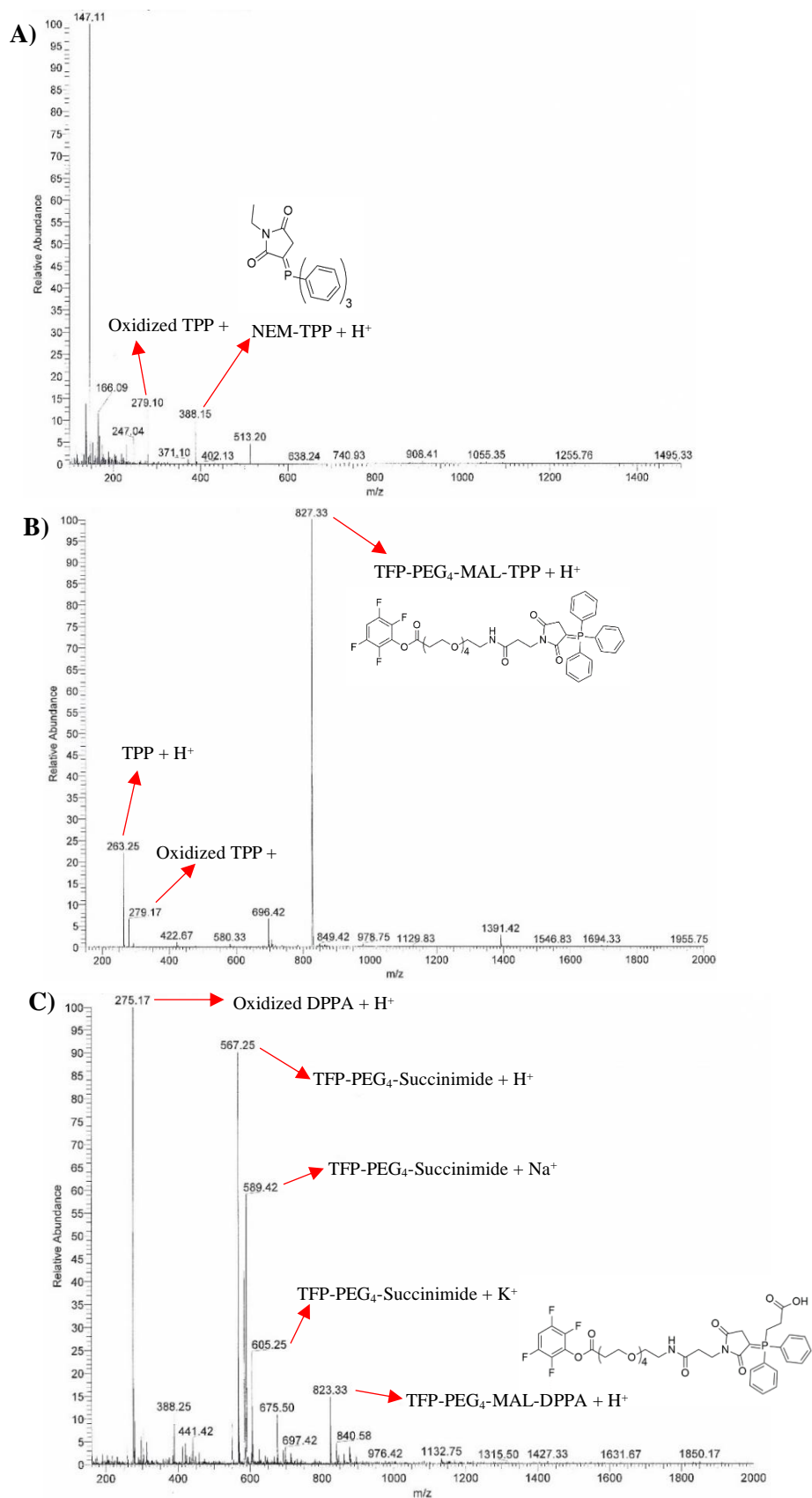
Figure 2.16. ESI MS of TPP and DPPA ylenes. **A)** NEM-TPP (**6a**). **B)** TFP-PEG₄-MAL-TPP (**6b**). **C)** TFP-PEG₄-MAL-DPPA (**6c**).

The molecular weights of the products from reactions **6a-c** are 388 Da, 827 Da, and 823 Da, respectively. In Figure 2.16C, a mass of 567 Da was also observed, corresponding to the reduced maleimide (succinimide) structure of the unreacted TFP-PEG$_4$-MAL reagent. A mass corresponding to *N*-ethylsuccinimide was also observed by ESI MS for the NEM-BSTPP and NEM-TSTPP compounds described in Section 2.4.6. The presence of the succinimide compounds suggests that hydrolysis is occurring. The reduction of maleimide to succinimide is irreversible and phosphines cannot further react with these compounds. The resulting oxidation of the phosphines is also irreversible.

Conjugation of both the TFP-PEG$_4$-MAL-TPP and TFP-PEG$_4$-MAL-DPPA adducts with BCA using a similar procedure as outlined in Section 2.3.2 was attempted. The resulting mass spectra obtained with ESI MS are identical to the mass spectrum shown in Figure 2.10A. The TPP or DPPA-based ylenes were not conjugated to the surface of BCA successfully. Only the masses of unmodified BCA and BCA modified with TFP-PEG$_4$-MAL were seen (data not shown). The reduction of maleimide to succinimide results in a mass difference of 2 Da. Unfortunately, low resolution ESI MS used for protein characterization does not have a high enough resolution to distinguish between these two species.

The stability of ylene adducts in an aqueous solution is an important question to answer before proceeding with the Wittig reaction. If the ylenes are not stable in an aqueous solution, then the Wittig reaction with an aldehyde cannot proceed as we have hypothesized.

2.4.8. Determining the Stability of TCEP and TPP Ylenes in Water

The stability of the NEM-TCEP and NEM-TPP compounds in water was studied with ^{31}P NMR. A sample of NEM-TCEP was prepared in degassed ddH$_2$O and the reaction was conducted at room temperature. The ESI MS and ^{31}P NMR spectra were acquired at 2, 4, 6, 24 hours, and

one week after the reaction was started. A ^{31}P NMR spectrum of unreacted TCEP in degassed ddH$_2$O was also obtained (Appendix A). The low resolution mass spectrum of the NEM-TCEP compound after one week in water is shown in Figure 2.17 below. The peak corresponding to the NEM-TCEP adduct (376 Da) is present after one week. The spectra obtained at 2, 4, 6, and 24 hours are identical to the spectrum shown in Figure 2.17 and are given in Appendix A. Furthermore, the ^{31}P NMR spectra obtained show that this adduct is still stable in water and present at each of these time points. The ^{31}P NMR spectra are given in Appendix A. The chemical shifts obtained from the ^{31}P NMR spectra are recorded in Table 2.3.
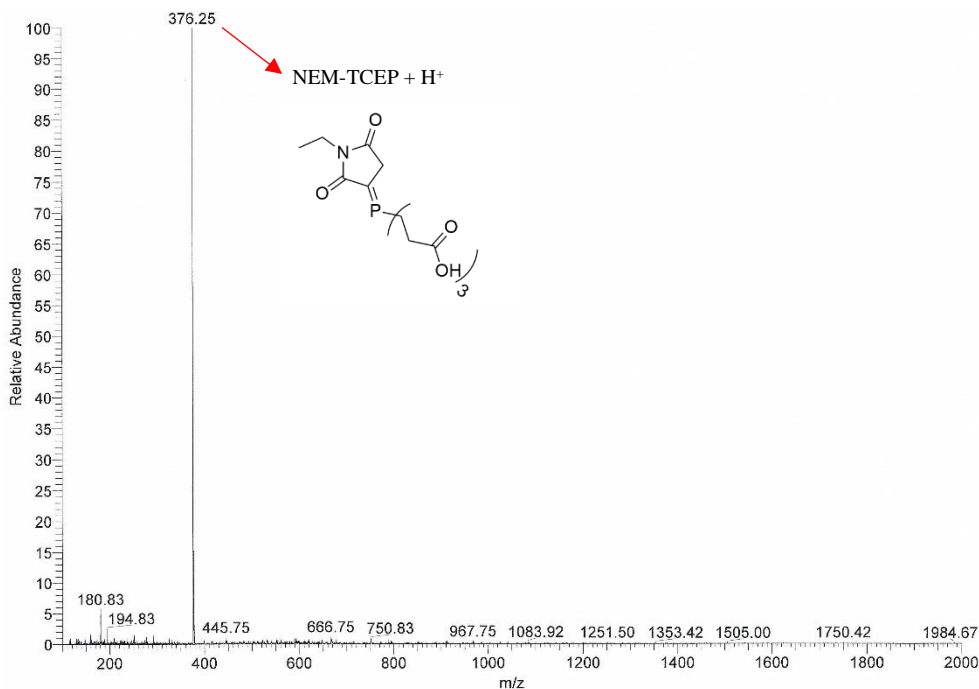
Figure 2.17. ESI MS of the NEM-TCEP ylene after one week in ddH$_2$O.

64

Table 2.3. ^{31}P NMR chemical shifts for unreacted TCEP, and NEM-TCEP after 2, 4, 6, 24 (hours) and 1 week in ddH$_2$O.

Label	Time after reaction start (hr)	Chemical shift δ (ppm)
TCEP	0	16.47
NEM-TCEP	2	17.86 36.00 40.61
	4	16.61 39.12 39.33 39.53
	6	16.60 39.11 39.33 39.53 56.83
	24	16.60 39.12 39.33 39.53 56.83
	1 week	39.10 39.31 39.51 56.81 57.07

The chemical shift of unreacted TCEP was δ = 16.47 ppm and it was present at all the time points except for one week after the reaction started. At this point, all of the unreacted TCEP has fully oxidized (δ = 56.81 ppm). The chemical shifts corresponding to the NEM-TCEP adduct (δ = 39.10-39.51 ppm) were present at all the time points, indicating that this compound is stable even after one week in water. The signal corresponding to the NEM-TCEP adduct is consistent with the ^{31}P NMR data reported by Kantner et al.[43]

The stability of TFP-PEG$_4$-MAL-TPP in ddH$_2$O was determined by ^{31}P NMR at 2 and 24 hours. Initial ^{31}P NMR measurements of unreacted TPP, NEM-TPP, and TFP-PEG$_4$-MAL-TPP in

degassed, anhydrous DMF were conducted. The measurements obtained in DMF were used to compare the chemical shifts obtained once the compounds were dissolved in water (with 5% DMF to ensure solubility) as it is not expected that DMF would hydrolyze the ylene. The ^{31}P NMR spectra corresponding to each of these samples are given in Appendix A, and the chemical shifts are summarized in Table 2.4.

Table 2.4. ^{31}P NMR chemical shifts for unreacted TPP, NEM-TPP, and TFP-PEG$_4$-MAL-TPP in DMF and ddH$_2$O.

Label	Solvent	Time point (hr)	Chemical shift δ (ppm)
TPP	DMF	0	-5.59
NEM-TPP	DMF	0	-5.58 9.98 11.58 11.78 25.49
TFP-PEG$_4$-MAL-TPP	DMF	0	-5.57 11.68 13.00
TFP-PEG$_4$-MAL-TPP	ddH$_2$O	2	-6.16 35.35
	ddH$_2$O	24	-6.16 35.35

The signal corresponding to unreacted TPP was δ = -5.59 ppm and this signal was seen in each of the samples studied. The NEM-TPP adduct has a chemical shift at δ = 11.58-11.78 ppm, which is identical to the signal for the TFP-PEG$_4$-MAL-TPP sample in DMF (δ = 11.68-13.00 ppm). However, even after 2 hours of TFP-PEG$_4$-MAL-TPP in ddH$_2$O, the signals corresponding to this adduct completely disappear, and only the unreacted TPP and oxidized TPP (δ = 35.35 ppm) signals were observed. The signal for oxidized TPP is in agreement with the signal reported by Pal et al.[114] Therefore, as demonstrated by the ^{31}P NMR experiments, this compound is not stable in

water. TPP and the aryl phosphines cannot be used to modify proteins in the novel bioconjugation method.

The stability of the maleimide and phosphorous-based ylenes for an alkyl phosphine in an aqueous solution has been previously reported by Kantner et al.[43] They studied the stability of the NEM-TCEP adduct and the reaction of NEM-tris(hydroxypropyl) phosphine (THPP) in water. Our data on the NEM-TCEP adduct is in agreement with Kantner et al. They did not observe hydrolysis for this compound, but they did observe the reduction of NEM to *N*-ethylsuccinimide for the NEM-THPP reaction.[43]

The DPPA phosphine studied in Section 2.4.7 was chosen as it contains two aryl ligands and one ligand that is identical to the TCEP structure. We hypothesized that a MAL-DPPA adduct would be more resistant to hydrolysis than the other TPP-based phosphines because the NEM-TCEP compound is stable in an aqueous solution, while maintaining the low pKa that the other aryl phosphines provide (Section 2.4.5). However, this compound appears to be susceptible to hydrolysis as well by ESI MS (Figure 2.16C). To our knowledge, studies on the stability of NEM and various aryl phosphines in water have not been published. Pal et al. describe the TPP promoted conversion of maleimides to succinimide in methanol with refluxing.[114] The proposed mechanism for the hydrolysis of the NEM-TPP adduct in methanol is shown in Scheme 2.8.
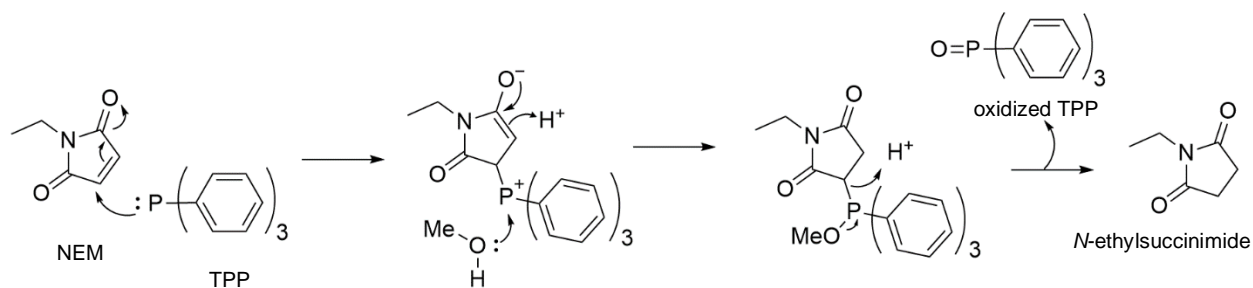
Scheme 2.8. Proposed mechanism for the hydrolysis of an NEM-TPP compound in a protic solvent (methanol). Adapted from Pal et al.[114]

Furthermore, Pal et al. postulated that any protic solvent, such as methanol, contributes to hydrolysis via the proposed mechanism.[114] Pal et al. reported that the MAL-TPP compounds are stable in aprotic solvents, which is in agreement with our observations when dissolving the compounds in DMF.

2.5. Conclusions

The objective of our studies was to develop and optimize a simple phosphorous-based bioconjugation method involving a Wittig reaction for the modification of proteins with aldehydes. NHS-PEG$_4$-MAL was used to modify the lysine residues of PfFtn and BCA so that these proteins display a maleimide on their surface. Most protein studies were conducted with BCA as it is commercially available, unlike PfFtn, and is readily characterized by ESI MS, which was the technique used to characterize the protein conjugates. These proteins were chosen due to their stability at elevated temperatures (up to 120 °C for PfFtn and 60 °C for BCA). TCEP was the phosphine used and mPEG$_4$BA was the water-soluble model aldehyde for the Wittig reaction. Initially, it appeared that the Wittig reaction on the surface of these two proteins was successful, when the reaction mixture was heated at 50-60 °C for four hours at pH 7.4. Further studies with BCA, NHS-PEG$_4$-MAL, TCEP, and mPEG$_4$BA were undertaken to determine if heating and the addition of a base was necessary for our proposed Wittig bioconjugation method. Attempts to replicate these reactions and to obtain a BCA-Wittig product conjugate in this fashion with AldPhPEG$_6$COOH as the aldehyde were unsuccessful, except for the reaction at 40 °C and pH 8.3. As many proteins may be thermosensitive, and sensitive to additions of strong bases, small molecule studies involving NEM, TCEP, and mPEG$_4$BA were undertaken to determine the most optimal reaction conditions. The reactions at room temperature and without the addition of a strong base were unsuccessful for this small molecule system. However the TCEP-based Wittig reaction

under basic conditions might find use for non-protein molecules in the future and could possibly be employed in materials research.

The pKa of various phosphonium adducts were calculated computationally. The pKa of NEM-TCEP was 9.95, which was significantly greater than the pKa for different NEM-TPP-based structures (pKa = 5.12-7.69). It was decided to proceed with water-soluble aryl phosphines (BSTPP, TSTPP, and PEGTPP), along with water-insoluble aryl phosphines (TPP and DPPA) and NEM or TFP-PEG$_4$-MAL. These compounds (except for NEM-PEGTPP) were successfully characterized with high resolution ESI MS. Masses corresponding to *N*-ethylsuccinimide were also observed. ^{31}P NMR was used to characterize the phosphine-based compounds. When TFP-PEG$_4$-MAL-TPP was dissolved in 5% DMF in ddH$_2$O for 2 to 24 hours, the signal corresponding to this adduct disappeared. Instead, signals corresponding to unreacted and oxidized TPP were observed.

Although NEM-TCEP is stable in water (as characterized by ESI MS and ^{31}P NMR for up to one week), NEM and aryl phosphines are not stable in an aqueous solution. Therefore, based on our experiments, the aryl phosphines studied are not appropriate for our proposed phosphorous-based bioconjugation method. The ylene would hydrolyze rapidly on the surface of the protein and the Wittig reaction with an aldehyde would not proceed. Since the NEM-TCEP ylene structure has a high pKa (calculated computationally), our experiments suggest that the Wittig reaction will not proceed unless heated at 40-60 °C. This is not amenable for thermosensitive proteins, especially if they are to be used in the design of protein therapeutics. Retaining the structure and function of the protein is important for this type of application. Chapter 3.0 will discuss a new approach to the phosphorous-based bioconjugation method involving the resin-based synthesis and purification of Wittig olefin products.

Chapter 3.0. Solid Phase Organic Synthesis and Purification of Wittig Olefins for Protein Bioconjugation

3.1. Introduction

Solid phase organic synthesis (SPOS) is used for the high-throughput generation of small molecule products. SPOS is particularly useful in the pharmaceutical industry, where large numbers of chemical libraries need to be produced.[115-119] This technique involves the use of solid supports, or resins, which are functionalized with reactive chemical groups for facilitating synthetic organic reactions. Polystyrene-supported (PS) resins are the most commonly used solid supports for SPOS as polystyrene is chemically inert and easily functionalized.[115,120] Other types of solid supports, such as cellulose, or hydrophilic PEG-based resins have been reported.[120] In this chapter, a methodology describing the SPOS of Wittig olefins will employ PS resins.

Polystyrene-supported triphenylphosphine (PS-TPP) is an example of a resin-bound reagent used in the SPOS of various reactions and chemical transformations.[98,121] Previously reported applications of the PS-TPP reagent include its use in Wittig reactions, Mitsunobu reactions, Staudinger reactions, and halogenation reactions.[97,98,121-125] A number of procedures for the preparation of the PS-TPP resin have been reported.[98,121,126] The polystyrene supports are typically prepared by the free radical copolymerization of styrene and divinylbenzene as the crosslinker.[124,126] The molar ratio of the monomer and crosslinker will affect the degree of crosslinking, which will influence the porosity of the resin and the availability of the chemical functional groups as a function of the type of organic solvent employed. The lithiation of a 4-bromopolystyrene solid support, followed by the reaction of chlorodiphenylphosphine yields the PS-TPP resin.[98,121,126] Fortunately, the PS-TPP resin is commercially available, and typically does not need to be prepared in the laboratory.

A procedure for the one-pot synthesis of Wittig olefins using a commercially available PS-TPP resin, TFP-PEG4-MAL, and various aldehydes will be described in this chapter. Using the PS-TPP resin bypasses the need for the removal of oxidized TPP, which is often difficult to separate from reaction mixtures.[97,125] The maleimide starting material (TFP-PEG4-MAL) will be captured by the PS-TPP resin, forming the solid-bound Wittig reagent. It is hypothesized that a Wittig olefin product will form and will be released from the resin when an aldehyde reacts with the solid-bound phosphorous ylene (Scheme 3.1).
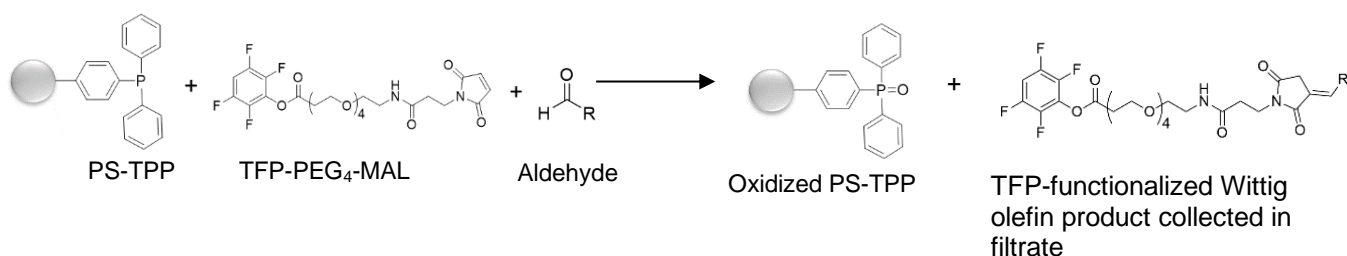
Scheme 3.1. One-pot synthesis of a TFP-functionalized Wittig olefin product using the PS-TPP resin.

Furthermore, it is anticipated that the desired product will be easily separated from the resin by filtration, avoiding tedious and time-consuming chromatographic methods. The filtrate containing the desired product will be collected and the solvent evaporated to obtain the solid crude product. The product will have an activated ester functional group (TFP), which is expected to modify the surface lysine residues of proteins such as BCA (Scheme 3.2).
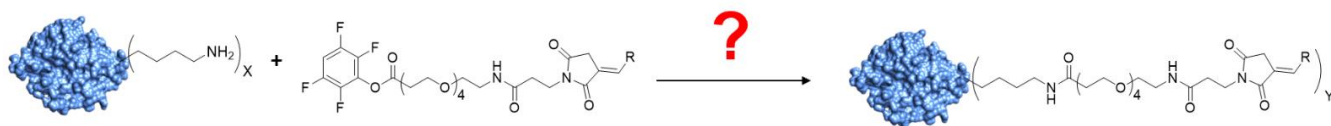
Scheme 3.2. Expected BCA bioconjugation reaction with surface lysine residues and a TFP-functionalized Wittig olefin product. BCA in blue. R represents any chemical moiety or tag that is used to modify the protein.

Previous studies by Bayat et al. report the use of a PS-TPP resin for the synthesis of Wittig olefins using maleimides and a variety of aldehydes in good yields.[97] Sieber et al. reported the procedure for the fabrication of a PEG-based TPP resin in order to facilitate Wittig reactions in aqueous media.[103] Otherwise, polystyrene-supported resins, such as PS-TPP, require a non-polar solvent like toluene or dichloromethane to swell the resin, ensuring that the chemical functional groups are available for reaction.[120] Tetrahydrofuran (THF) can also be used as the solvent.[127] Our procedure for the synthesis of a TFP-functionalized Wittig olefin will utilize ethanol (EtOH) and THF in equal parts as the solvent. Yan et al. have previously reported that an aqueous one-pot Wittig reaction involving TPP (free reagent) and maleimides can be conducted in ethanol.[128] Although the MAL-TPP ylenes studied in Chapter 2 were determined to be unstable in water, Yan et al. suggest that a protic solvent, such as ethanol, is necessary for the proton shift in the MAL-TPP ylene formation mechanism to occur without heating or a strong base.[128] Our methodology avoids the use of a strong base because it may catalyze the reaction of ethanol with the TFP ester, forming the ethyl ester of the bioconjugation reagent. If this were to occur, the Wittig olefin could not be attached to the surface of BCA via its lysine residues.

Furthermore, this chapter discusses the development of a chromatography-free method to purify the TFP-functionalized Wittig olefin products using PS resins. There is precedence for the use of solid-bound reagents in the purification protocols of peptide and small molecule products.[116,124,129-132] These reagents are often used in the "Catch-and-Release" technique, where the desired product is captured on the resin.[116] The resin is rinsed to remove unwanted compounds. Next, the product is subsequently released from the resin and collected in the filtrate. The same reagents may also be used as scavenger resins. A scavenger resin consists of a polymer-bound functional group that is capable of selectively reacting with by-products, impurities, or

unreacted materials. An undesired compound is sequestered by the scavenger resin. The desired product is obtained in the filtrate when the reaction mixture containing the resin is filtered (Scheme 3.3).

A)

Solution containing unwanted compounds and functionalized resin that can "catch" the desired compound

Solution only contains resin with "caught" desired compound

Filter resin and obtain desired compound

B)

Solution containing desired compound and functionalized resin that can scavenge unwanted compound

Desired compound is collected in the filtrate
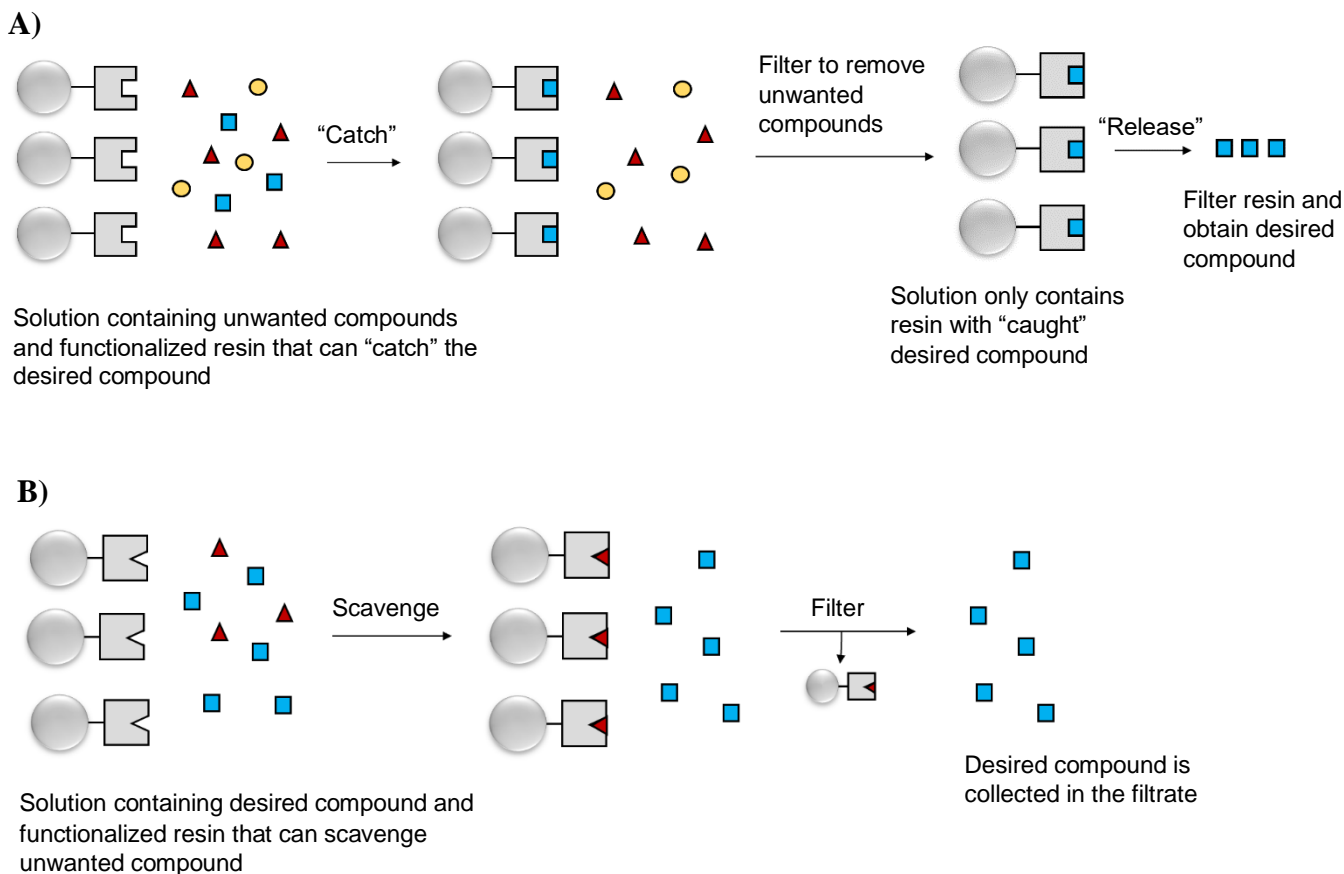
Scheme 3.3. Functionalized resins in purification protocols. **A)** "Catch-and-Release" technique. **B)** Scavenger resin technique. The functionalized PS resin (grey circle and grey linker), desired compound (blue square) and undesired compounds (red triangle, yellow circle) are depicted.

Several examples involving the use of scavenger resins exist. Egusa et al. reported the use of a PS-TPP reagent for the removal of small molecule products containing an azide functional group.[131] Musonda et al. utilized a polystyrene-supported *p*-toluenesulfonic acid (PS-TsOH) reagent to remove amine containing compounds as a part of their purification protocol for the design of an antimalarial drug.[133] Porcheddu et al. described the use of a polystyrene-supported

isocyanate resin (PS-Isocyanate) for the simple removal of secondary amines in the assembly of a chemical library of formamidines, an important class of inhibitors used in the pharmaceutical industry.[134]
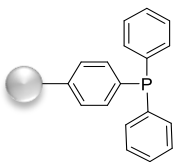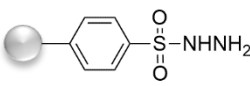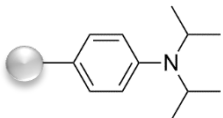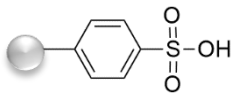
Another example of a scavenger resin is a polymer-bound hydrazine resin that can be used to remove aromatic aldehydes.[135,136] An example of this resin that is commercially available is the polystyrene-supported p-toluenesulfonyl hydrazide (PS-Ts-NHNH$_2$). The major unreacted component of the phosphorous-based Wittig reaction described in this chapter is the aldehyde reagent. In this section, the use of a PS-Ts-NHNH$_2$ resin in the purification of TFP-functionalized Wittig olefin products will be described. The reaction mechanism of a hydrazine functional group with an aldehyde is shown in Scheme 3.4.
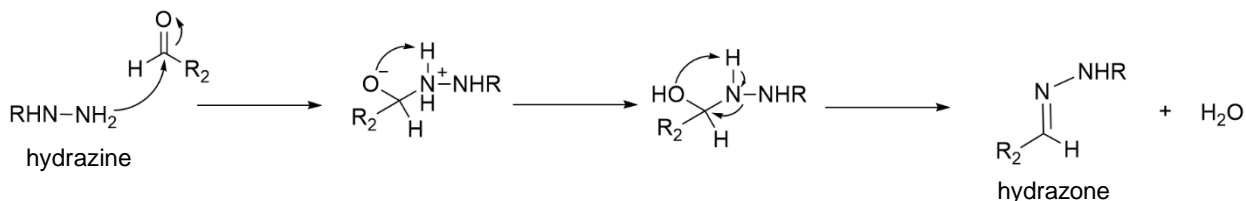
Scheme 3.4. General reaction scheme of a hydrazine scavenging an aldehyde. R represents the resin.

Table 3.1 lists each polystyrene-supported resin used in this chapter. The resins that are denoted with "MP" refer to resins that are on a macroporous polystyrene solid support. These resins typically have a high degree of crosslinking, and are highly porous, compared to the resins that are denoted with "PS", which have a lower degree of crosslinking. The MP resins can maintain their porosity in the presence of a wider range of organic solvents than the PS resins. However not all scavenger or reagent resins are available in both "PS" and "MP" forms.

Table 3.1. Chemical structures and functions of polymer-supported resins utilized in Chapter 3.

Full Resin Name	Commercial Name	Structure	Functionality
Polystyrene triphenylphosphine	PS-TPP		Wittig reaction Removal of unreacted maleimide-containing compounds
Polystyrene *p*-toluenesulfonyl hydrazide	PS-Ts-NHNH$_2$		Electrophile scavenger: removal of unreacted aldehydes
Polystyrene diisopropylethylamine	PS-DIEA		Tertiary amine base used in procedure for synthesis of dansylcadaverine-based aldehydes
Macroporous *p*-toluenesulfonic acid	MP-TsOH		Nucleophile scavenger: removal of unreacted amines

3.1.1. Microwave-Assisted Organic Synthesis

The synthesis of the TFP-functionalized Wittig olefins using a microwave synthesis reactor with the PS-TPP resin and free TPP was explored in this chapter. The first reported use of microwave-assisted organic reactions was in 1986 by Gedye et al.[137] Recently, microwave synthesis reactors have been popular for green chemistry methodology.[138-141] Microwave-assisted organic synthesis is more energy efficient compared to conventional conduction or convection heating methods, allowing for the acceleration of chemical reactions. A microwave synthesis reactor is available in the Honek laboratory (Figure 3.1).
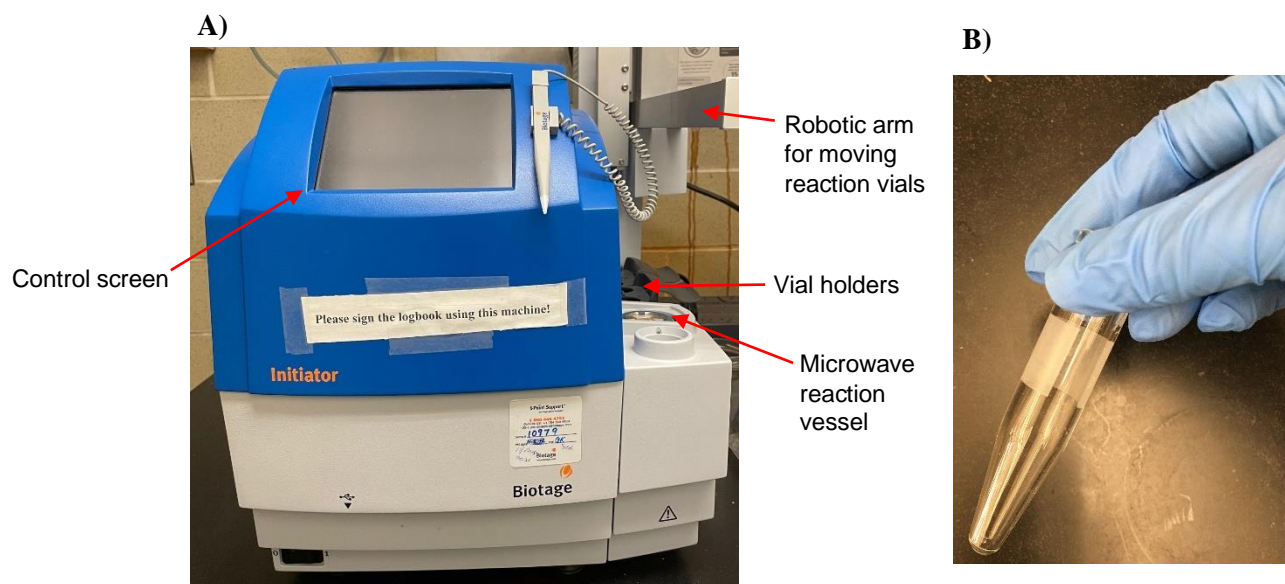
Figure 3.1. The Biotage Initiator+ Inc. microwave synthesis reactor in the Honek laboratory. **A)** Microwave synthesis reactor with labelled components. **B)** Reaction container: glass microwave vial (0.5-2.0 mL). Image credit: Amanda Rose Ratto.

The basic principle of microwave reactors involves the dielectric heating of polar molecules which are able to absorb microwave energy.[141] The absorption of microwave energy by polar molecules induces molecular rotations, influencing the subsequent motions of neighbouring molecules.[141] The rotation of one polar molecule results in the rapid dispersion of energy to the neighbouring molecules, therefore generating heat inside the reaction vessel.[141] In comparison, conventional heating methods in the laboratory, such as using a Bunsen burner, hot plate, and water or oil baths, will also heat the reaction vessel. The use of a microwave reactor is advantageous because of a faster increase in temperature for the reaction mixture compared with conventional heating methods. The boiling point of the solvent used for the reaction can be elevated by increasing the pressure in the microwave vessel. Higher temperatures allow for an increase in the rate of chemical reactions. Unsurprisingly, the time for reaction cooling is also quicker for microwave-assisted organic syntheses (Figure 3.2).
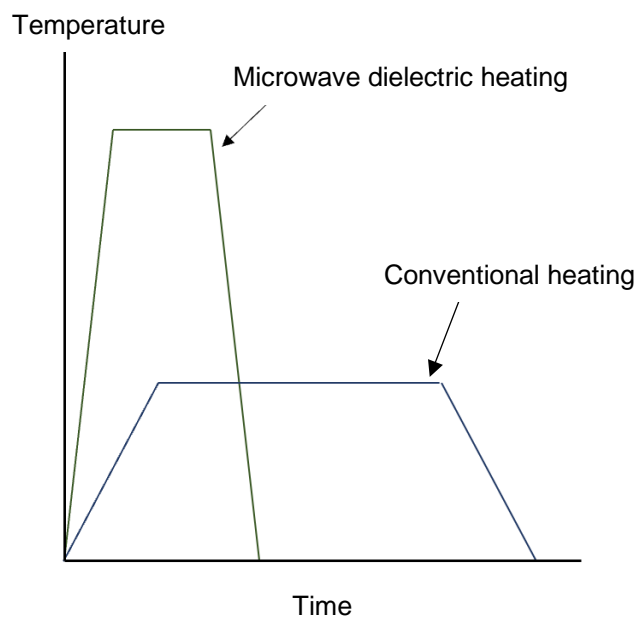
Figure 3.2. Representation of the differences in the temperature-time profiles for microwave dielectric and conventional heating (green and blue lines, respectively). Adapted from Tierney et al.[141]

Westman reported a protocol for the one-pot microwave-assisted organic synthesis of Wittig olefins using a PS-TPP resin.[123] Westman used a variety of aldehydes to synthesize Wittig olefins in DMF at 180 °C for five minutes with a microwave synthesis reactor.[123] The polar solvents used in our Wittig reaction studies were DMF, methanol (MeOH), and acetonitrile (ACN). Our reactions were conducted at temperatures ranging from 70 °C to 180 °C, with reaction times ranging from 20 minutes to three hours. Under atmospheric pressure, these solvents have a boiling point of 153 °C, 64.6 °C, and 81.6 °C respectively.[142] The microwave synthesis reactor will allow for reaction temperatures to exceed the given boiling points of these solvents.

Although a portion of this chapter is dedicated to testing the synthesis of Wittig olefins using the microwave synthesis reactor at higher temperatures, the remainder of the chapter will discuss this chemistry using SPOS and purification of Wittig olefins without the use of this instrument.

3.2. Objectives

This chapter outlines the procedure for the SPOS and purification of novel TFP-functionalized Wittig olefins as bioconjugation reagents. We anticipate that these compounds can be synthesized in a one-pot reaction using the PS-TPP resin, TFP-PEG$_4$-MAL, and several aldehydes. The purification of these compounds will also be undertaken using the scavenger resin PS-Ts-NHNH$_2$. If successful, this methodology would present a new and facile method to prepare bioconjugation reagents that can be employed to modify proteins with an aldehyde containing chemical tag (Scheme 3.5).
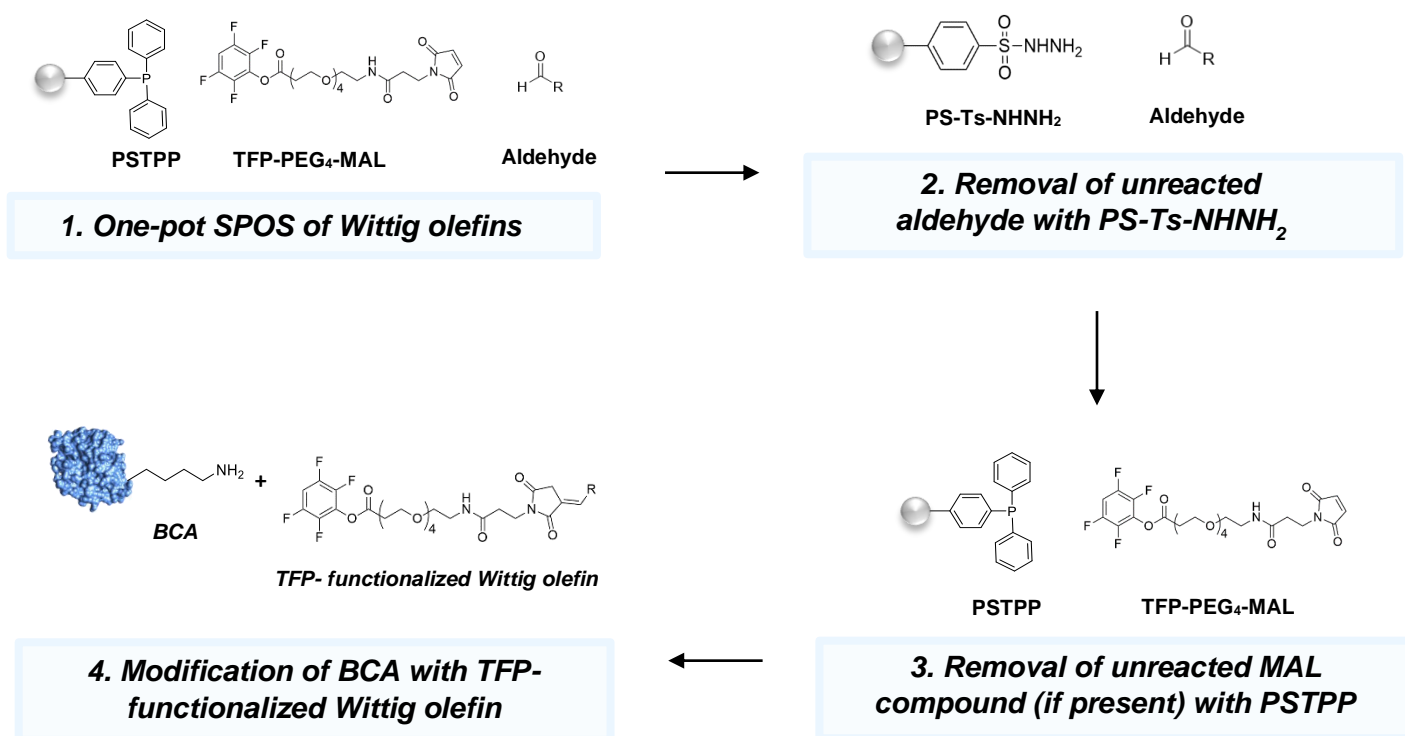
Scheme 3.5. Summary of the SPOS of the TFP-functionalized Wittig olefin. R represents any chemical moiety or tag that can be used to modify a protein.

A number of different reaction conditions for the SPOS of Wittig products were studied. Initially, a microwave synthesis reactor was utilized to determine if higher temperatures are required for our maleimide and phosphorous-based Wittig reaction. Microwave-assisted synthesis reactions were undertaken with both PS-TPP and with free TPP using DMF, MeOH, and ACN as solvents. As microwave synthesis reactors are not present in many research laboratories, our focus was shifted to developing a procedure that does not involve this equipment. This would permit an expanded number of research laboratories to employ our strategies even if they lacked microwave synthesis instruments.

The chemical structures of the aldehydes used in the synthesis of the TFP-functionalized Wittig olefins are shown in Figure 3.3. The dansylcadaverine- and biotin-based benzaldehydes are not commercially available and had to be synthesized in the laboratory.

Dansylcadaverine-PEG$_2$-Ph-Aldehyde

Biotin-PEG$_5$-Ph-Aldehyde

mPEG$_4$BA

mPEG$_8$-Aldehyde

p-Anisaldehyde
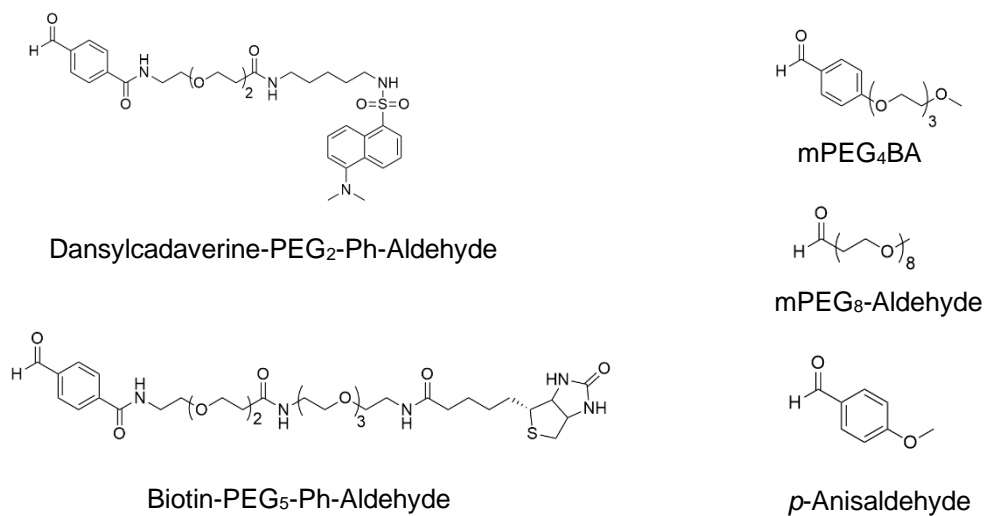
Figure 3.3. A palette of aldehydes used in the SPOS of TFP-functionalized Wittig olefins.

The resulting Wittig olefin synthesized from each of the five aldehydes shown above will be characterized with high resolution ESI MS and ^{1}H NMR analytical techniques. Fluorophores,

such as dansylcadaverine, and biotin moieties are commonly used to modify proteins in protein bioconjugation reactions. This is why these two aldehyde compounds were synthesized for our bioconjugation studies. The modification of BCA with the five TFP-functionalized Wittig olefins will demonstrate that the solid phase Wittig reaction and purification of a variety of TFP-based compounds may be used to derivatize proteins in the proposed manner.

3.3. Materials and Methods

Proteins: Bovine carbonic anhydrase II (BCA) was purchased commercially from Sigma Aldrich, Canada. Centrifugal filters (0.5 mL) with a molecular weight cut-off (MWCO) of 10 kDa were purchased from Amicon® Ultra (Millipore Sigma, Burlington, MA, USA).

PEG reagents and aldehydes: mPEG$_4$BA (95%; MW = 268.3 Da), mPEG$_8$Ald (95%; MW = 396.5 Da), and AldPhPEG$_2$NHS (95%; MW = 406.4 Da) were purchased from Broadpharm (San Diego, CA, USA). TFP-PEG$_4$-MAL (MW = 564.5 Da), and biotin-PEG$_3$-NH$_3^+$TFA$^-$ (MW = 560.63 Da) were purchased from Quanta BioDesign Ltd (Plain City, OH, USA). *p*-Anisaldehyde (98%; MW = 136.15 Da) was purchased from Sigma Aldrich, Canada.

Maleimide and dansylcadaverine: *N*-Ethylmaleimide (NEM; MW = 125.1 Da) was purchased from J.T. Baker Chemical Co. NJ, USA. Dansylcadaverine (≥97%; MW = 335.5 Da) was purchased from Sigma Aldrich, Canada.

Resins: PS-TPP (loading capacity: 3.0 mmol/g) and polymer-bound *p*-toluenesulfonic acid (MP-TsOH; loading capacity: 2.0-3.0 mmol/g) were purchased from Sigma Aldrich, Canada. PS-DIEA (loading capacity: 4.06 mmol/g), and PS-Ts-NHNH$_2$ (loading capacity: 3.06 mmol/g) were purchased from Biotage (Uppsala, Sweden).

Solvents, buffers and bases: Potassium phosphate (KP) was purchased from BioShop Canada, Inc. (Burlington, ON, Canada). Anhydrous *N,N*-dimethylformamide (DMF) Sure/Seal^{TM} ($\geq$99.0 %), anhydrous tetrahydrofuran (THF) ($\geq$99.0 %), anhydrous dichloromethane (DCM) ($\geq$99.8%), HPLC-grade methanol (MeOH) ($\geq$99.9%), HPLC-grade acetonitrile ($\geq$99.9%), and triethylamine (TEA) ($\geq$99.5%) were purchased from Sigma Aldrich, Canada. Anhydrous ethanol (EtOH) and ethyl acetate were purchased directly from ChemStores (University of Waterloo, ON, Canada). Solvents were degassed by flushing with argon gas when used for phosphine-containing reactions.

Chromatography: Thin layer chromatography (TLC) Silica gel 60 F$_{254}$ 20x20 cm aluminum sheets were purchased from Millipore Sigma (Burlington, MA, USA). Flash chromatography: Biotage Flash+ chromatography system connected to the REACH Devices Chromatography Detector Model: RD2 280-250 (Boulder, CO, USA). The Biotage Isolera One Flash Purification (Biotage, Uppsala, Sweden) instrument was used for reverse-phase high performance liquid chromatography (RP-HPLC). SiliaSep^{TM} Silica Gel Cartridge (4 grams, size 230-400 mesh 40-63 μm) and SiliaSep^{TM} Premium Flash Cartridge (C18, 25 μm, 4 grams) were purchased from SiliCycle (Quebec City, QC, Canada).

Instrumentation: The masses of all protein samples were analyzed with ESI MS using a high resolution Thermo Scientific^{TM} Q-Exactive (Thermo QE) Hybrid Quadrupole-Orbitrap mass spectrometer, 10 μL/min injection rate, positive mode, with 1:1 MeOH:H$_2$O+0.1% FA as the solvent. The masses of all small molecule compounds described in this chapter were analyzed with ESI MS using either the high resolution Thermo QE instrument (positive mode, 10 μL/min injection rate, 1:1 MeOH:H$_2$O+0.1% FA) or the low resolution Thermo Scientific^{TM} Linear Ion Trap (Thermo LTQ) mass spectrometer (positive mode, 20 μL/min injection rate, 1:1 MeOH:H$_2$O+0.1% FA).

Small molecule compounds were characterized by ^{1}H NMR using a 300 MHz high resolution UltraShield^{TM} Bruker Spectrometer. The pulse program used was zgpg30 with a pulse delay of 3 seconds. The solvent used was deuterated chloroform (CDCl$_3$, Sigma Aldrich Canada), whose reference chemical shift is δ = 7.26 ppm. The chemical shifts were reported in parts per million (ppm).

3.3.1. Microwave-Assisted Organic Wittig Reactions with TPP and PS-TPP

The Biotage Initiator+ Fourth Generation Microwave System (Uppsala, Sweden) was used to test varying temperatures for the Wittig reaction with NEM, mPEG$_4$BA, and TPP or PS-TPP. Reaction temperatures that exceed the atmospheric boiling points of the solvents used (DMF, MeOH, or ACN) without solvent evaporation can be achieved with a microwave reactor. These experiments were undertaken with a CHEM 494 student, Amanda Rose Ratto.

Two-step microwave reactions with TPP as the phosphine: NEM (67.7 mg, 0.5355 mmol, 1.0 eq) and TPP (125.8 mg, 0.4823 mmol, 0.9 eq) were dissolved in 3 mL degassed acetone and refluxed for 1 hour at 50 °C. After one hour, the reaction solution was cloudy and white. The solvent was removed using rotary evaporation under vacuum. A pink oil (201 mg) containing the NEM-TPP ylene was obtained and further split into three vials to run three additional reactions. Note that the following amounts given were calculated assuming that 100% of the crude mass is the NEM-TPP ylene:

Reaction 1a: NEM-TPP crude product (53.7 mg, 0.1421 mmol, 1.0 eq) and mPEG$_4$BA (22.7 mg, 0.0846 mmol, 0.6 eq) were dissolved in 1 mL anhydrous DMF in a 0.5-2 mL glass microwave vial and reacted in the microwave synthesis reactor for 20 minutes at 160 °C. The solvent was removed with rotary evaporation under vacuum. The resulting product was a sticky red oil.

Reaction 1b: NEM-TPP crude product (54.5 mg, 0.1442 mmol, 1.0 eq) and mPEG$_4$BA (24.4 mg, 0.0910 mmol, 0.6 eq) were dissolved in 1 mL MeOH in a 0.5-2 mL glass microwave vial and reacted in the microwave synthesis reactor for 1 hour at 70 °C. The solvent was removed with rotary evaporation under vacuum. The resulting product was a sticky red oil.

Reaction 1c: NEM-TPP crude product (51.2 mg, 0.1354 mmol, 1.0 eq) and mPEG$_4$BA (17.3 mg, 0.0646 mmol, 0.5 eq) were dissolved in 1 mL anhydrous ACN in a 0.5-2 mL glass microwave vial and reacted in the microwave synthesis reactor for 1 hour at 70 °C. The solvent was removed with rotary evaporation under vacuum. The resulting product was a sticky red oil.

Reactions **1a-c** were analyzed by TLC (silica plates, mobile phase: 10:0.4 DCM:MeOH, visualization: ultraviolet (UV) lamp with wavelength = 254 nm) and characterized by low resolution ESI MS (Thermo LTQ). Each subsequent reaction in this section (3.3.1) was tested with these TLC conditions to qualitatively determine the extent of reaction using the conditions described here.

Two-step microwave reaction with PS-TPP as the phosphine: NEM (20.0 mg, 0.1598 mmol, 1.0 eq) and PS-TPP (72.0 mg, 0.2160 mmol, 1.4 eq of TPP) were reacted together in 1.2 mL degassed anhydrous DMF in a 0.5-2 mL glass microwave vial. The reaction proceeded for 20 minutes at 120 °C using the microwave synthesis reactor. The next step was the addition of the mPEG$_4$BA reagent. Note that the amounts given were calculated assuming that 100% of the crude mass is the NEM-TPP compound:

Reaction 1d: mPEG$_4$BA (31.4 mg, 0.1170 mmol, 0.7 eq) was first dissolved in 300 μL degassed, anhydrous DMF and added directly to the 0.5-2 mL glass microwave vial containing 1.2 mL of the NEM and PS-TPP mixture. The reaction proceeded for 30 minutes at 180 °C using the

microwave synthesis reactor. The resulting solution had a dark red-brown colour. Next, the resin was filtered using a pipette filter. The pipette filter was made by inserting a small piece of a Kimwipe (Kimberly-Clark Professional™) in a glass Pasteur pipette. The reaction mixture containing PS-TPP was rinsed and filtered with DMF until the rinses were clear (approximately 3 x 9 mL). Each subsequent reaction containing PS-TPP was filtered using the pipette filter described above. The DMF filtrate was pooled in a round bottom flask and the solvent was removed with rotary evaporation under vacuum. The resulting product was a dark red-brown sticky oil. Reaction **1d** was evaluated by TLC using the conditions described above and characterized by low resolution ESI MS (Thermo LTQ).

One-pot microwave-assisted reactions with PS-TPP: The following reactions with DMF as the solvent and PS-TPP as the phosphine were undertaken at two different temperatures:

Reaction 1e: NEM (21.7 mg, 0.1737 mmol, 1.0 eq), PS-TPP (82.2 mg, 0.2466 mmol, 1.4 eq of TPP), and mPEG$_4$BA (41.1 mg, 0.1532 mmol, 0.9 eq) were reacted together in 0.8 mL degassed anhydrous DMF in a 0.5-2 mL glass microwave vial. The reaction proceeded for 2 hours at 180 °C using the microwave synthesis reactor.

Reaction 1f: NEM (21.0 mg, 0.1679 mmol, 1.0 eq), PS-TPP (101.0 mg, 0.3030 mmol, 1.8 eq of TPP), and mPEG$_4$BA (40.6 mg, 0.1513 mmol, 0.9 eq) were reacted together in 0.8 mL degassed anhydrous DMF in a 0.5-2 mL glass microwave vial. The reaction proceeded for 3 hours at 90 °C using the microwave synthesis reactor.

PS-TPP was removed from reactions **1e-f** using a pipette filter and DMF rinses (3 x 9 mL) as described previously. The DMF filtrate was collected in a round bottom flask. The solvent was removed with rotary evaporation under vacuum. The resulting product was a dark red-brown sticky

oil. Reactions **1e-f** were subsequently evaluated by TLC using the conditions described previously and characterized by low resolution ESI MS (Thermo LTQ).

3.3.2. Synthesis of the NEM and mPEG$_4$BA Wittig Olefin using PS-TPP

Synthesis of NEM-mPEG$_4$BA: NEM (22.6 mg, 0.1807 mmol, 1.0 eq), mPEG$_4$BA (50.2 mg, 0.1871 mmol, 1.1 eq), and PS-TPP (87.2 mg, 0.2610 mmol, 1.5 eq of TPP) were reacted together in degassed, anhydrous 1:1 THF:EtOH (800 μL total reaction volume) with gentle stirring for 48 hours at room temperature. After 48 hours, the reaction solution had a pale-yellow appearance. Next the PS-TPP resin was rinsed and filtered using a pipette filter as described earlier with anhydrous EtOH (3 x 6 mL). The collected filtrate was transparent and pale-yellow in appearance. EtOH was removed with rotary evaporation under vacuum. The mass of the crude product obtained was 78.1 mg. The crude product was analyzed by low resolution ESI MS (Thermo LTQ).

Purification of crude NEM-mPEG$_4$BA: The crude product (78.1 mg) was added to the PS-Ts-NHNH$_2$ resin (108.6 mg, 0.2987 mmol, 1.6 eq of hydrazide). These amounts were calculated using 100% of the initial molar amount of mPEG$_4$BA in the reaction, ensuring that the resin is in excess to unreacted mPEG$_4$BA. The crude product and the PS-Ts-NHNH$_2$ resin were solubilized in 800 μL of anhydrous DCM and reacted at room temperature with gentle stirring. After one hour, the reaction progression was checked with TLC using silica plates (mobile phase: 10:0.2 DCM:MeOH, visualization: UV lamp with wavelength = 254 nm). It was qualitatively determined by TLC that mPEG$_4$BA was removed after 2 hours. Next, the PS-Ts-NHNH$_2$ resin was filtered using a pipette filter with anhydrous DCM (3 x 6 mL). The clear DCM filtrate was collected and the solvent was removed with rotary evaporation under vacuum. The resulting NEM-mPEG$_4$BA product (62 mg) was obtained. The product was a thick yellow oil.

Characterization of NEM-mPEG4BA: ^{1}H NMR (300 MHz, in CDCl$_3$): δ 7.51 (d, 2H), 7.29 (s, 1H), 7.00 (d, 2H), 4.13 (q, 2H), 3.85 (t, 2H), 3.75–3.47 (m, 10H), 3.40 (s, 3H), 1.81 (s, 2H), 1.22 (t, 3H). High resolution ESI-MS: calculated for C$_{20}$H$_{28}$O$_6$N [M+H]$^+$: 378.1911 Da, found 378.1914 Da. Yield: 83%.

3.3.3. Synthesis of Dansylcadaverine and Biotin-Labelled Benzaldehydes
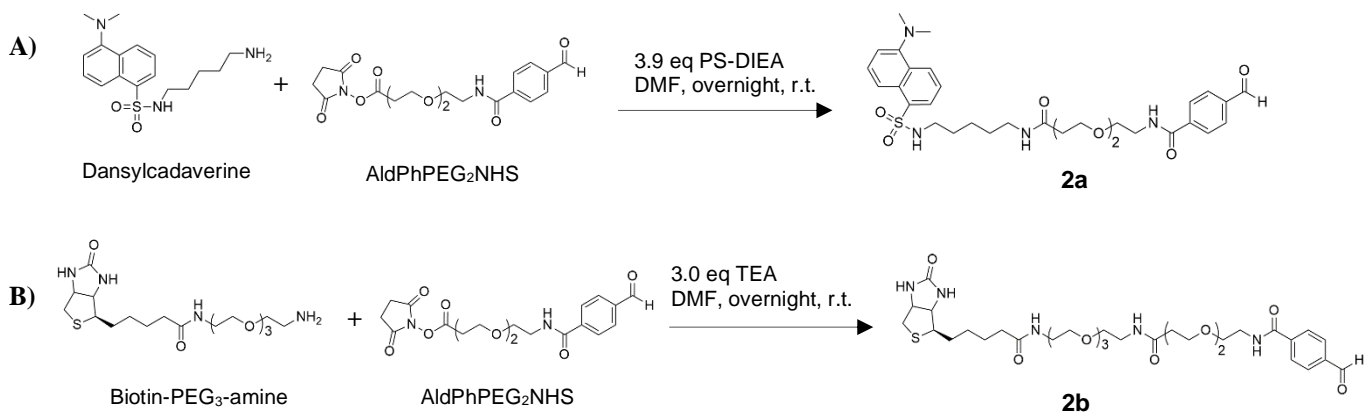
Scheme 3.6. Synthesis of dansylcadaverine and biotin-labelled benzaldehydes. **A)** Dansylcadaverine-labelled benzaldehyde (**2a**). **B)** Biotin-labelled benzaldehyde (**2b**).

The following reactions and their purifications were undertaken with Julian Marlyn and Ethan Solomon, two CHEM 494 undergraduate students in the Honek research group.

Reaction 2a: AldPhPEG$_2$NHS (93.0 mg, 0.229 mmol, 1.0 eq), dansylcadaverine (99.8 mg, 0.297 mmol, 1.3 eq), and PS-DIEA (219.8 mg, 0.892 mmol, 3.9 eq of DIEA) were reacted together in 2 mL anhydrous DMF. The 20 mL glass scintillation vial containing the reaction mixture was covered with aluminum foil. The reaction proceeded overnight at room temperature with gentle stirring. The PS-DIEA resin was filtered using a pipette filter (previously described) with three rinses of DCM (3 x 6 mL). The filtrate was pooled and the solvent containing DMF and DCM was removed with rotary evaporation under vacuum. The crude product (235.3 mg) was obtained as a

thick yellow-orange oil. TLC (mobile phase: 10:0.5 DCM:MeOH, visualization: UV lamp with wavelength = 254 nm and an I_2 stain) was used to qualitatively determine the extent of reaction for the crude product mixture.

Purification of 2a: The crude product was purified with normal-phase flash chromatography using the Biotage Flash+ Chromatography system connected to the REACH Devices chromatography detector set at monitoring the 280 nm wavelength. The column used was the SiliaSep™ Silica Gel Cartridge (4 grams). The mobile phase was 3% EtOH in ethyl acetate. Fractions were analyzed with TLC using the conditions described above for product **2a** and the relevant fractions were pooled together. The solvent was removed with rotary evaporation under vacuum. The product (25 mg) was obtained as a clear pale-yellow oil. This product was used for the next step (Wittig reaction) described in Section 3.3.4 (reaction **2f**).

Characterization of 2a: ^{1}H NMR (300 MHz, in CDCl$_3$): δ 10.04 (s, 1H), 8.56 (d, 1H), 8.32 (m, 2H), 8.20 (d, 4H), 7.91 (d, 2H), 7.70 (s, 2H), 7.51 (t, 2H), 4.15 (t, 2H), 3.78-3.66 (m, 10H), 3.14 (t, 2H), 2.89 (s, 6H), 2.67 (t, 2H), 1.45-1.28 (m, 6H). High resolution ESI-MS: calculated for $C_{32}H_{43}O_7N_4S$ [M+H]$^+$: 627.2828 Da, found 627.2847 Da. Yield: 17.5%.

Reaction 2b: AldPhPEG$_2$NHS (22.4 mg, 0.055 mmol, 1.0 eq), biotin-PEG$_3$-amine (TFA salt) (37.0 mg, 0.066 mmol, 1.2 eq) and TEA (16.7 mg, 0.165 mmol, 3.0 eq) were reacted together in 400 μL anhydrous DMF with gentle stirring overnight at room temperature. Next, DMF and TEA were removed with rotary evaporation under vacuum. The crude product (102 mg) was obtained as a thick yellow-orange oil. TLC (mobile phase: 0.9% MeOH in DCM, visualization: UV lamp with wavelength = 254 nm and an I_2 stain) was used qualitatively to check the crude product mixture.

Purification of 2b: The crude product was purified using the Biotage Isolera One Flash Purification instrument for RP-HPLC. The column used was a SiliaSep™ Premium Flash Cartridge (C18, 25 μm, 4 grams). The gradient for the mobile phase was 0-80% acetonitrile in water and the detection wavelengths were 205 nm and 248 nm. The fractions of interest were pooled together and the solvent was removed with rotary evaporation under vacuum. The total mass of the recovered product was 19.4 mg.

Characterization of 2b: Low resolution ESI MS (Thermo LTQ) was used to obtain the molecular weight of **2b**. The mass for the compound $C_{35}H_{56}N_5O_{10}S$ $[M+H]^+$: 738.42 Da. The product was used without further characterization for the next step (Wittig reaction) described in Section 3.3.4 (reaction **2g**).

3.3.4. The SPOS and Purification of TFP-Functionalized Wittig Olefin Products with Various Aldehydes
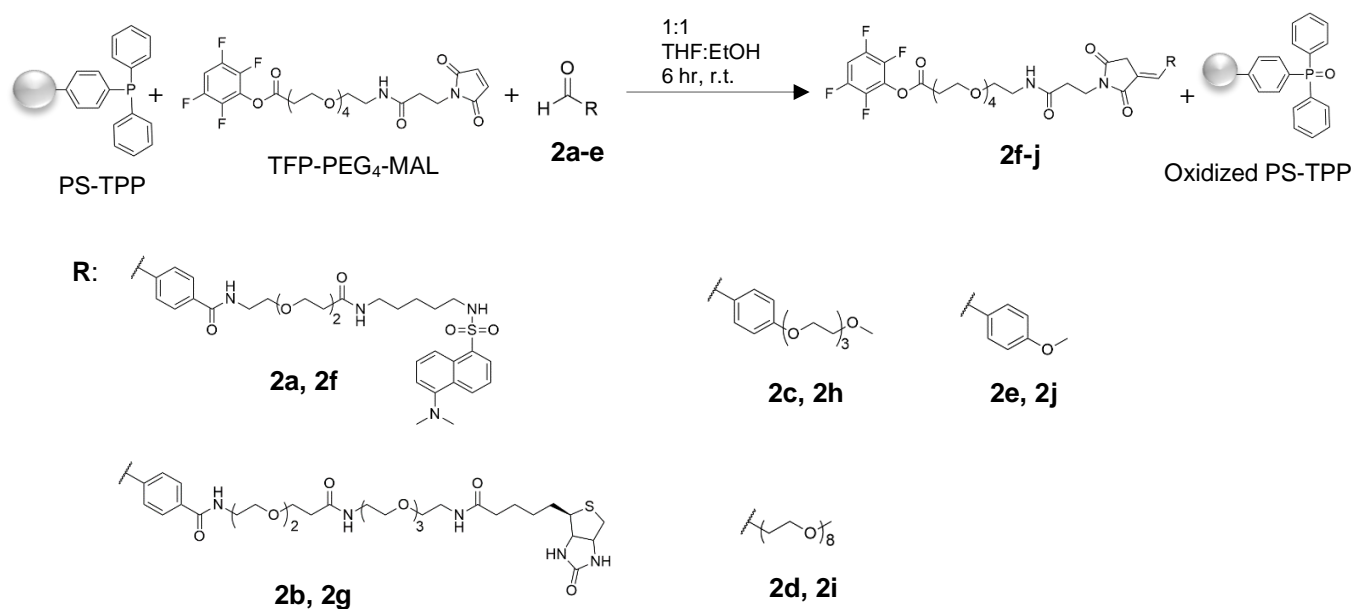
Scheme 3.7. Synthesis of five TFP-functionalized Wittig olefin products for protein modification.

Reaction 2f: TFP-PEG$_4$-MAL (18.6 mg, 0.0334 mmol, 1.0 eq), PS-TPP (15.6 mg, 0.0468 mmol, 1.4 eq of TPP), and **2a** (25.1 mg, 0.0401 mmol, 1.2 eq) were reacted together in 800 μL of 1:1 THF:EtOH (degassed, anhydrous) for 6 hours at room temperature with stirring. After six hours, the PS-TPP resin was rinsed and filtered using a pipette filter as previously described with DCM (3 x 6 mL). The solvent was removed from the collected filtrate with rotary evaporation under vacuum. The crude product obtained (43.5 mg, **2f**) was a pale yellow and sticky oil.

Purification of 2f: The following amounts were calculated using 100% of the initial amount of **2a** in the reaction in order to ensure complete removal of the aldehyde reagent (**2a**). PS-Ts-NHNH$_2$ (40.5 mg, 0.1239 mmol, 3.1 eq of hydrazide) was added directly to 43.5 mg of crude **2f** and solubilized in 800 μL DCM. The reaction was checked with TLC in one hour increments (mobile phase: 10:0.7 DCM:MeOH, visualization: UV lamp with wavelength = 254 nm). After four hours, it was qualitatively determined by TLC that unreacted **2a** was removed. The PS-Ts-NHNH$_2$ resin was filtered using a pipette filter and rinsed with DCM (3 x 6 mL). The crude product obtained (28.6 mg, **2f**) was a pale yellow and sticky oil. Next, unreacted TFP-PEG$_4$-MAL was removed with the PS-TPP resin. The following amounts were calculated using 100% of the initial amount of TFP-PEG$_4$-MAL in the reaction in order to ensure complete removal of this reagent. PS-TPP (33.4 mg, 0.1002 mmol, 3.0 eq of TPP) was added to 28.6 mg of crude **2f** and solubilized in 600 μL DCM. The reaction was periodically checked with TLC using the same conditions described above. The reaction was left overnight at room temperature with gentle stirring. The complete removal of TFP-PEG$_4$-MAL was qualitatively determined with TLC using the same conditions described above. The final product obtained (20.8 mg, **2f**) was a pale yellow and sticky oil.

Characterization of 2f: ^{1}H NMR (300 MHz, in CDCl$_3$): δ 8.50 (d, 1H), 8.22 (d, 1H), 8.20 (d, 1H), 8.01 (s, 1H), 7.93 (d, 1H), 7.55 (m, 5H), 7.28 (d, 2H), 7.12 (s, 3H), 6.25 (s, 1H), 4.00 (d, 2H), 3.97-

3.43 (m, 26H), 3.12 (t, 4H), 2.98 (t, 4H), 2.87 (s, 6H), 3.70 (s, 2H), 2.59 (t, 2H), 2.44 (t, 2H), 1.45 (m, 6H). High resolution ESI-MS: calculated for $C_{56}H_{71}O_{15}N_6F_4S$ [M+H]$^+$: 1175.4588 Da, found 1175.4629 Da. Yield: 53.1%

Synthesis of 2g: TFP-PEG$_4$-MAL (12.4 mg, 0.0219 mmol, 1.0 eq), PS-TPP (10.2 mg, 0.0307 mmol, 1.4 eq of TPP), and **2b** (19.4 mg, 0.0263 mmol, 1.2 eq) were reacted together in 800 μL of 1:1 THF:EtOH (degassed, anhydrous) for 6 hours at room temperature with stirring. After six hours, the PS-TPP resin was rinsed and filtered using a pipette filter with DCM (3 x 6 mL). The filtrate was collected and the solvents were evaporated with rotary evaporation under vacuum. The crude product obtained (27.7 mg, **2g**) was a pale pink and sticky oil.

Purification of 2g: The following amounts were calculated using 100% of the initial amount of **2b** in the reaction in order to ensure complete removal of the aldehyde reagent (**2b**). PS-Ts-NHNH$_2$ (25.8 mg, 0.0790 mmol, 3.0 eq of hydrazide) was added directly to 27.7 mg of crude **2g** and solubilized in 600 μL DCM. The reaction was checked with TLC (mobile phase: 10:0.7 DCM:MeOH, visualization: UV lamp with wavelength = 254 nm and I$_2$ stain) in one hour increments. After five hours, it was qualitatively determined by TLC that unreacted **2b** was removed. The PS-Ts-NHNH$_2$ resin was filtered using a pipette filter and rinsed with DCM (3 x 6 mL). The crude product obtained (19 mg, **2g**) was a pale pink, sticky oil. Next, unreacted TFP-PEG$_4$-MAL was removed with the PS-TPP resin. The following amounts were calculated assuming that 100% of TFP-PEG$_4$-MAL was unreacted in order to ensure complete removal of this reagent. PS-TPP (21.9 mg, 0.0658 mmol, 3.0 eq of TPP) was added to 19 mg of crude **2g** and solubilized in 600 μL DCM. The reaction was periodically checked with TLC using the same conditions described above. The reaction was left overnight at room temperature with gentle stirring. The complete removal of TFP-PEG$_4$-MAL was qualitatively determined with TLC using

the same conditions described above. The final product obtained (16.3 mg, **2g**) was a pale yellow and sticky oil.

Characterization of 2g: ^{1}H NMR (300 MHz, in CDCl$_3$): δ 7.97 (d, 1H), 7.61-.745 (m, 5H), 7.28 (m, 2H), 6.70 (t, 1H), 6.55 (m, 2H), 5.92 (s, 1H), 4.50 (d, 1H), 4.30 (d, 1H), 3.97 (t, 4H), 3.917-3.325 (m, 36H), 3.20-3.10 (m, 4H), 2.98 (m, 3H), 2.97-2.19 (m, 12H), 1.90-1.24 (m, 8H), 0.89 (dd, 2H). High resolution ESI-MS: calculated for C$_{59}$H$_{84}$O$_{18}$N$_7$F$_4$S [M+H]$^+$: 1286.5595 Da, found 1286.5524 Da. Yield: 57.7%.

Synthesis of 2h-j: Three separate one-pot reactions were conducted. TFP-PEG$_4$-MAL (50.0 mg, 0.0886 mmol, 1.0 eq) and PS-TPP (41.8 mg, 0.1251 mmol, 1.4 eq of TPP) were reacted with one of **2c** (28.0 mg, 0.1063 mmol, 1.2 eq), **2d** (42.1 mg, 0.1063 mmol, 1.2 eq), or **2e** (14.5 mg, 0.1064 mmol, 1.2 eq) in 800 μL of 1:1 THF:EtOH (degassed, anhydrous) for 6 hours at room temperature with stirring. After 6 hours, the PS-TPP resin was rinsed and filtered with three rinses of DCM (3 x 6 mL). The filtrate containing the solvents were pooled together and removed with rotary evaporation under vacuum. The three crude products obtained (73.1 mg **2h**; 98.6 mg **2i**; 86.2 mg **2j**) were pale yellow and sticky oils.

Purification of 2h-j: The following describes a chromatography-free, resin-based purification method for the **2h-j** Wittig products. The following amounts were calculated using 100% of **2c-e** and TFP-PEG$_4$-MAL that was initially present in the reaction in order to ensure complete removal of the aldehyde reagent (**2c-e**) and the TFP-PEG$_4$-MAL reagent:

PS-Ts-NHNH$_2$, the aldehyde-scavenging resin, was added so that there was at least a 3-fold molar excess of the hydrazide functional group to the unreacted aldehyde (calculated by assuming that 100% of the aldehyde is unreacted). Therefore the hydrazide functional group on

the resin is in a far greater excess to reagents **2c-e**. The specific masses added to crude **2h**, **2i**, and **2j** were 123.9 mg, 178.6 mg, and 115.8 mg, respectively. The reactions were solubilized in 1 mL of DCM for 2-4 hours. Each reaction was checked at intervals of 1 hour to determine when the unreacted aldehyde had been completely removed. The following conditions were used for TLC: **2h** 10:0.3 DCM:MeOH, **2i** 10:0.8 DCM:MeOH, and **2j** 10:0.6 DCM:MeOH. The visualization method used for each reaction was a UV lamp with wavelength = 254 nm. Reaction **2i** required an additional I_2 stain for visualization. After aldehyde-removal, the PS- Ts-NHNH$_2$ resin was filtered with a pipette filter (previously described) and rinsed with DCM (3 x 6 mL). The filtrates for each reaction were collected separately and the solvent was removed with rotary evaporation under vacuum. For each crude **2h-j**, a pale yellow, sticky oil was obtained. Then, PS-TPP (88.6 mg, 0.2643 mmol, 3.0 eq) was added directly to each vial containing **2h**, **2i**, or **2j**. This is the TFP-PEG$_4$-MAL removal step. These reactions were conducted overnight at room temperature with gentle stirring. The removal of TFP-PEG$_4$-MAL was qualitatively determined with TLC, using the conditions described above for each product **2h-j**. The PS-TPP resin was rinsed and filtered with DCM (3 x 6 mL) as previously described. The final masses obtained for **2h**, **2i**, and **2j** were 33.7 mg, 56.0 mg, and 60.7 mg, respectively.

Characterization of 2h-j: **2h**: ^{1}H NMR (300 MHz, in CDCl$_3$): δ 8.01 (s, 1H), 7.58 (s, 1H), 7.43 (d, 2H), 6.98 (d, 2H), 6.50 (s, 1H), 4.21 (t, 2H), 3.94-9.46 (m, 30H), 3.40 (s, 3H), 2.94 (t, 2H), 2.29 (s, 2H), 1.79 (d, 2H). High resolution ESI-MS: calculated for $C_{38}H_{49}O_{13}N_2F_4$ $[M+H]^+$: 817.3165 Da, found 817.3176 Da. Yield: 46.6%. **2i**: ^{1}H NMR (300 MHz, in CDCl$_3$): δ 8.02 (s, 1H), 6.50 (s, 1H), 6.80 (t, 1H), 3.91 (t, 2H), 3.87-3.25 (m, 48H), 2.94 (s, 3H), 2.89 (s, 2H), 2.59-2.43 (t, 4H), 1.44 (d, 2H). High resolution ESI-MS: calculated for $C_{42}H_{65}O_{17}N_2F_4$ $[M+H]^+$: 945.4214 Da, found 945.3998 Da. Yield: 66.8%. **2j**: ^{1}H NMR (300 MHz, in CDCl$_3$): δ 8.01 (s, 1H), 7.53 (s, 1H), 7.42

(d, 2H), 6.92 (d, 2H), 6.40 (s, 1H), 5.26 (s, 3H), 3.93-3.47 (m, 18H), 2.93 (t, 2H), 3.37 (s, 2H), 2.56 (t, 4H). High resolution ESI-MS: calculated for $C_{32}H_{37}O_{10}N_2F_4$ $[M+H]^+$: 685.2379 Da, found 685.2394 Da. Yield: 77.1%.

3.3.5. Modification of BCA with TFP-Functionalized Wittig Olefin Products

BCA obtained from Sigma Aldrich, Canada was first dissolved in ddH_2O and the buffer salts were exchanged with 0.15 M pH 7.4 KP buffer using centrifugal filters with an MWCO of 10 kDa and five cycles of centrifugation at 10 000 x g (10 minutes per cycle). A 20 mg/mL stock in 0.15 M pH 7.4 KP buffer was prepared from this solution.

BCA from 20.0 mg/mL in 0.15 M pH 7.4 KP buffer stock (2.0 mg, 6.897×10^{-5} mmol, 1.0 eq) and one of **2f-j** (6.897×10^{-2} mmol, 10.0 eq) were reacted together in 0.15 M pH 7.4 KP buffer for 2 hours at room temperature (five separate reactions). The products **2f-j** were previously dissolved in DMF and the volume of DMF in each of the protein modification reactions was <5% of the total reaction volume. Additionally, the BCA reaction with **2j** was conducted for 2, 4, 6, and 24 hours to determine if the reaction time would affect the extent of modification. After each reaction, the samples containing the KP buffer and DMF solvent were exchanged with ddH_2O using centrifugal filters with an MWCO of 10 kDa and five cycles of centrifugation at 10 000 x g (10 minutes per cycle). The BCA-Wittig olefin product conjugates were then subsequently diluted with the 1:1 MeOH:ddH_2O+0.1% FA solvent until the concentration of the sample was in the range of 1-10 μM and then characterized with ESI MS (Thermo QE). The resulting spectrum was deconvoluted with the Thermo Scientific BioPharma Finder software (Version 3.0).

3.4. Results and Discussion

3.4.1. Microwave-Assisted Organic Wittig Reactions with TPP and PS-TPP

The NEM and mPEG$_4$BA reagents were chosen as model compounds for testing the feasibility of the Wittig reaction with PS-TPP or free TPP as the phosphines. The model compounds were used to optimize the Wittig reaction conditions with less expensive, readily available reagents so that the comparatively more expensive TFP-PEG$_4$-MAL reagent may be used to synthesize the TFP-functionalized Wittig olefin products for surface modification of proteins. The temperature of the Wittig reaction and the solvent are two parameters that were explored. Reactions involving the microwave synthesis system were undertaken in DMF, MeOH, or ACN. The microwave synthesis system allowed us to study the Wittig reaction at temperatures higher than the boiling points of the solvents used. In addition, the robotic arm of the Biotage instrument could allow for up to eight Wittig reactions to occur in an automated and unattended fashion if the microwave-assisted reactions were successful. Reactions **1a-f** all yielded the NEM-mPEG$_4$BA product, as characterized by low resolution ESI MS ([M+H]$^+$ = 378 Da) and qualitatively determined by TLC. This desired product mass was observed, regardless of whether the reaction was done in a two-step fashion (NEM-TPP ylene synthesized prior to Wittig reaction) or in a one-pot reaction. This was also observed with TPP or PS-TPP as the phosphine. Given that many laboratories might not be equipped with a microwave synthesis system, this method of synthesizing Wittig products for protein modification might not be applicable or approachable for many researchers. Since we did not observe any particular advantage of increasing temperatures for this reaction, and there was a concern regarding the degradation of chemical functional groups at these high temperatures, the microwave synthesis system was not utilized in further studies.

Nevertheless these scouting reactions indicate that microwave-assisted Wittig reactions to prepare new bioconjugation reagents could be practical and efficient for an individual laboratory.

3.4.2. The SPOS and Purification of TFP-Functionalized Wittig Olefin Products with Various Aldehydes

Previous work by Yan et al. found that a one-pot aqueous Wittig reaction with EtOH as the solvent resulted in the best yield for Wittig reactions involving maleimides and TPP.[128] Yan et al. hypothesized that the use of a protic solvent, such as EtOH, would allow the proton shift in the MAL-TPP reaction to occur without heating.[128] Since EtOH is not a good solvent for the non-polar polystyrene resin, THF was chosen to be the co-solvent in order to swell the PS-TPP resin so that the TPP functional groups would be available for reaction. THF has been previously reported as a solvent that can be used for swelling polystyrene-based resins.[127] Therefore, our next experiment was to study a one-pot reaction involving NEM, mPEG$_4$BA, and PS-TPP with equal parts EtOH/THF as the solvent at room temperature. The use of PS-TPP in the Wittig reaction bypasses the tedious chromatographic or crystallization methods required to remove the TPP oxide side product. Unreacted mPEG$_4$BA was qualitatively observed by low resolution ESI MS (Thermo LTQ) and TLC (data not shown). The commercially available PS-Ts-NHNH$_2$ resin was used to scavenge the unreacted aldehyde.[135] The high resolution ESI mass spectrum and ^{1}H NMR spectrum of the purified NEM-mPEG$_4$BA product is given in Appendix A. By ^{1}H NMR, unreacted mPEG$_4$BA was completely removed because the chemical shift for the aldehyde proton ($\delta = 9.69$ ppm) was absent. The ^{1}H NMR spectra for the NEM and mPEG$_4$BA starting materials are also given in Appendix A.

After mPEG$_4$BA removal with the PS-Ts-NHNH$_2$ resin, the NEM-mPEG$_4$BA Wittig product was obtained in an 83% yield. This was satisfactory, and it was decided to pursue the

synthesis of several TFP-functionalized Wittig olefin products with TFP-PEG$_4$-MAL and various aldehydes using these reaction conditions. The model Wittig reaction with NEM was allowed to proceed for 48 hours. The TFP-PEG$_4$-MAL reagent contains an activated tetrafluorophenyl ester functional group. It is possible that the EtOH solvent may react with the ester, lowering the amount of available Wittig product for protein modification. Therefore, the procedure was altered so that the Wittig reaction proceeded for 6 hours, instead of 48 hours. The TFP-PEG$_4$-MAL reagent was chosen over the NHS-PEG$_4$-MAL reagent because TFP esters are known to be more stable to hydrolysis than NHS esters over a longer period of time.[49]

Five different aldehydes were used to synthesize the Wittig products **2f-j** using PS-TPP as the phosphine at room temperature and in 1:1 THF:EtOH. Two of the aldehydes, namely **2a** and **2b**, were synthesized according to the procedure described in Section 3.3.3. Aldehyde **2a** was characterized with high resolution ESI MS and ^{1}H NMR (spectra given in Appendix A) and aldehyde **2b** was characterized with low resolution ESI MS (Appendix A). A resin-based purification protocol with MP-TsOH was previously attempted for the removal of unreacted dansylcadaverine and biotin-PEG$_3$-amine (reactions **2a** and **2b**, respectively). While this resin was capable of removing the amine-containing compounds, the presence of unreacted AldPhPEG$_2$NHS was still detected with low resolution ESI MS. If this reagent is still present in the aldehyde products, then it will also undergo a Wittig reaction to yield the Wittig product shown in Figure 3.4. This side product has the capability of modifying BCA because it has the TFP ester functional group. A conjugate of BCA with the Wittig side product shown in Figure 3.4 was observed by ESI MS when BCA was reacted with **2a** that was purified with MP-TsOH (data not shown). The molecular weight of this compound is 858 Da, and the expected molecular weight change on BCA is 693 Da, when TFP is the leaving group. Resins targeting the aldehyde functional group will also

scavenge the desired product. Therefore, it was decided to employ chromatographic methods to purify **2a** and **2b**.
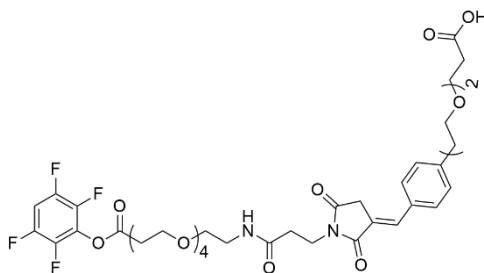
Figure 3.4. Chemical structure of the TFP-PEG$_4$-MAL and AldPhPEG$_2$NHS side product. The NHS is hydrolyzed in an aqueous solution to yield the carboxylic acid functional group.

A resin-based purification protocol was employed to remove unreacted starting materials from the crude TFP-functionalized Wittig olefin products (**2f-j**). As with the NEM-mPEG$_4$BA model reaction, the PS-Ts-NHNH$_2$ resin was used to scavenge the unreacted aldehydes. Since the reaction time was shorter, unreacted TFP-PEG$_4$-MAL was qualitatively observed with low resolution ESI MS and TLC for each of the five reactions. The reintroduction of PS-TPP to the crude product in DCM removed the remaining maleimide reagent. By qualitatively checking the extent of reaction with TLC, it was determined that the reaction needed to proceed overnight in order to completely remove the maleimide reagent. Each purified Wittig product was subsequently characterized with high resolution ESI MS and ^{1}H NMR (spectra shown in Appendix A). The ^{1}H NMR spectrum of the unreacted TFP-PEG$_4$-MAL and biotin-PEG$_3$-amine starting materials are also given in Appendix A. Due to the effects of ion suppression in ESI MS, this characterization method should not be used to definitively determine the absence of specific analytes. By ^{1}H NMR, it was observed that the aldehydes used in the Wittig reactions (**2a-e**) were removed by the PS-Ts-NHNH$_2$ resins as the characteristic aldehyde proton shift usually found at $\delta = 10.0$-9.5 ppm was absent. Using a combination of TLC, high resolution ESI MS, and ^{1}H NMR analytical methods,

we concluded that our resin-based purification approach was sufficient to purify the Wittig products **2f-j**, if they were to be used for protein modification reactions. Table 3.2 summarizes the percent conversion obtained for each reaction and their chemical structures. Although the yields are lower than what was obtained with the model NEM-mPEG$_4$BA reaction, the amounts of the synthesized Wittig products obtained were sufficient for modification of BCA.

Table 3.2. Summary of the percent conversion obtained in the synthesis and purification of **2f-j** along with their chemical structures.

Label	Wittig Olefin Structure	% Yield
NEM-mPEG$_4$BA		83%
2f		53.1
2g		57.7
2h		46.6
2i		66.8
2j		77.1

3.4.3. Modification of BCA with TFP-Functionalized Wittig Olefin Products

The reaction of BCA with **2j** was analyzed at four different time points (2, 4, 6, and 24 hours) in order to determine the optimal reaction time required to modify BCA with the TFP-functionalized Wittig olefin product, if the amount of Wittig product (**2j**) is kept constant relative to the amount of BCA in the reaction. In this case, **2j** was in a 10-fold molar excess to the moles of BCA initially present in the reaction mixture. The reaction was conducted at pH 7.4 in a 0.15 M potassium phosphate buffer. Figure 3.5A depicts a chemical representation of this conjugate, and Figure 3.5B shows the mass spectra obtained after 2 hours of reaction time. The spectra obtained for the remaining time points were identical to the spectrum shown in Figure 3.5B.
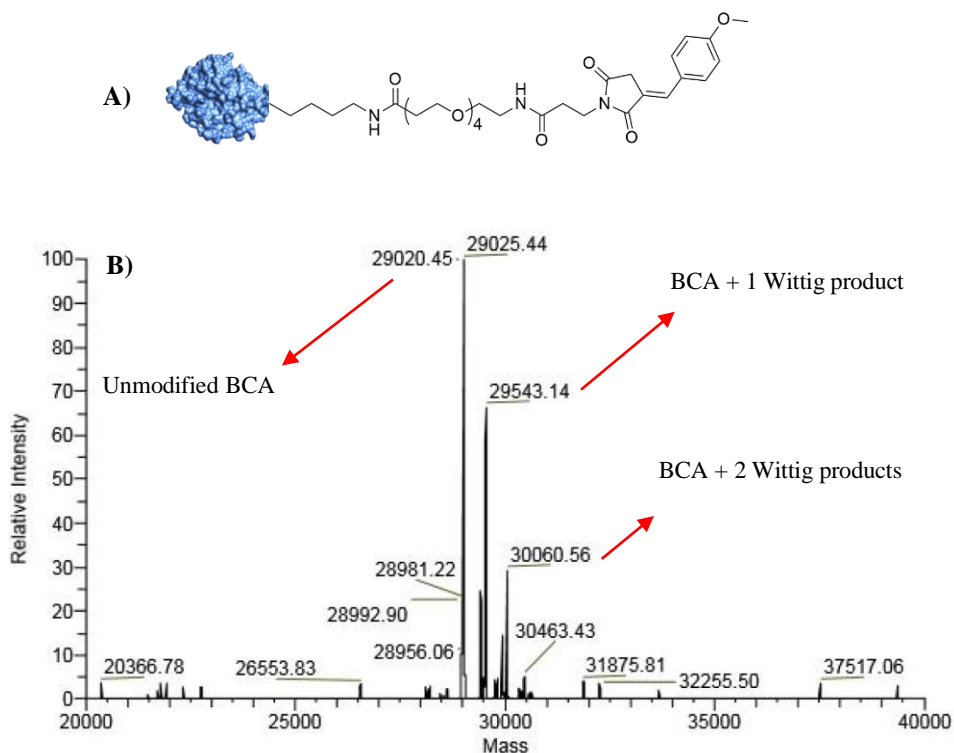
Figure 3.5. ESI MS of BCA modified with Wittig olefin **2j**. **A)** BCA-**2j** Wittig product conjugate. **B)** Spectrum after 2 hours reaction time.

The expected mass change on BCA is 520 Da when **2j** is the Wittig olefin product used to modify BCA. On the spectrum shown in Figure 3.5B, up to two modifications on BCA can be observed. Up to two modifications were also observed for the remaining time points (data not shown). Based on these experiments, a reaction time of 2-4 hours is sufficient for modifying BCA with a TFP-activated ester-based reagent at room temperature. The remaining Wittig products, **2f-i** were used to modify BCA in a 10-fold molar excess to BCA for 2 hours. The reaction was conducted at pH 7.4 in 0.15 M potassium phosphate buffer. The spectra corresponding to BCA modifications are shown in Figure 3.6 and a depiction of the conjugates are shown in Figure 3.7
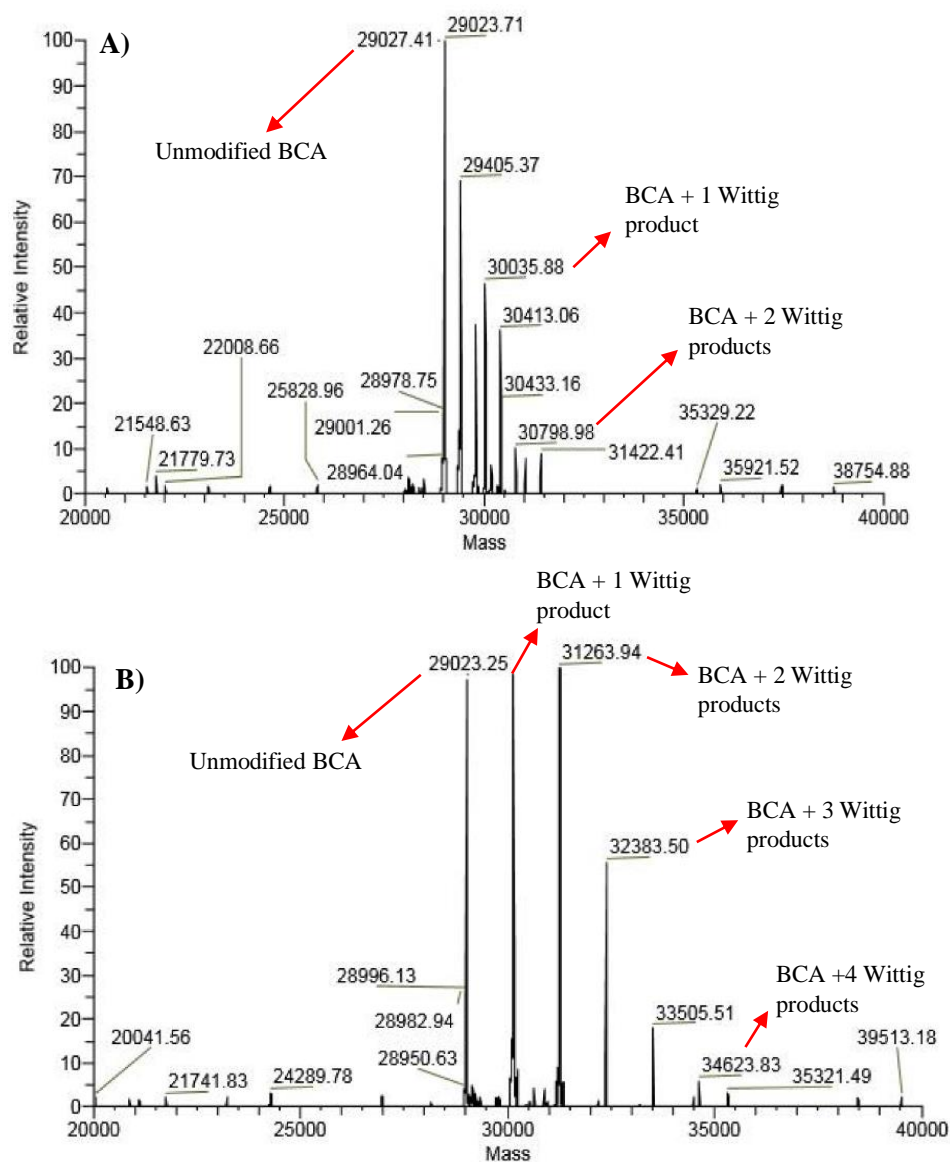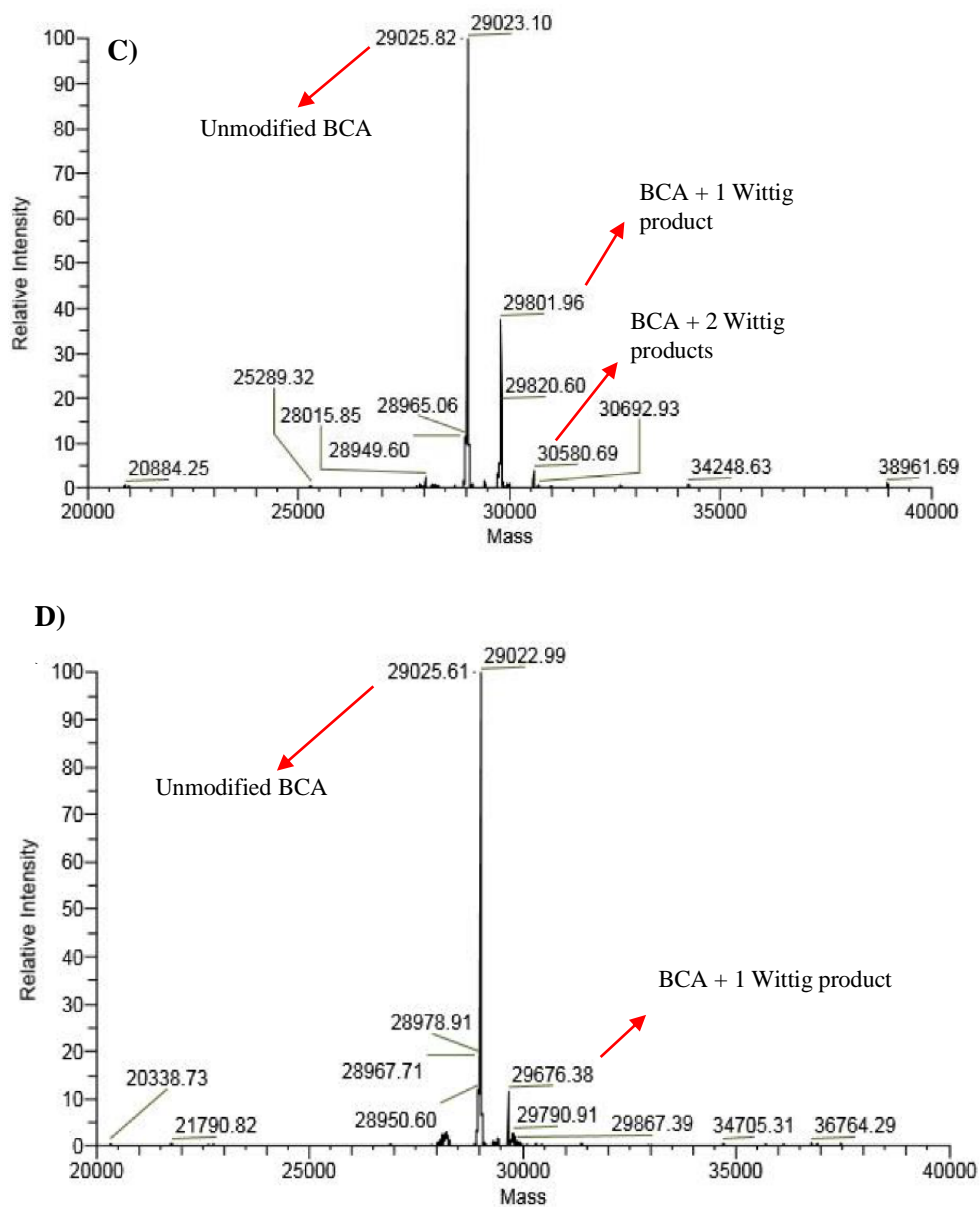
Figure 3.6. ESI MS of BCA modified with Wittig olefins **2f-i**. **A)** ESI MS of BCA and **2f** Wittig product conjugate. **B)** ESI MS of BCA and **2g** Wittig product conjugate. **C)** ESI MS of BCA and **2h** Wittig product conjugate. **D)** ESI MS of BCA and **2i** Wittig product conjugate.
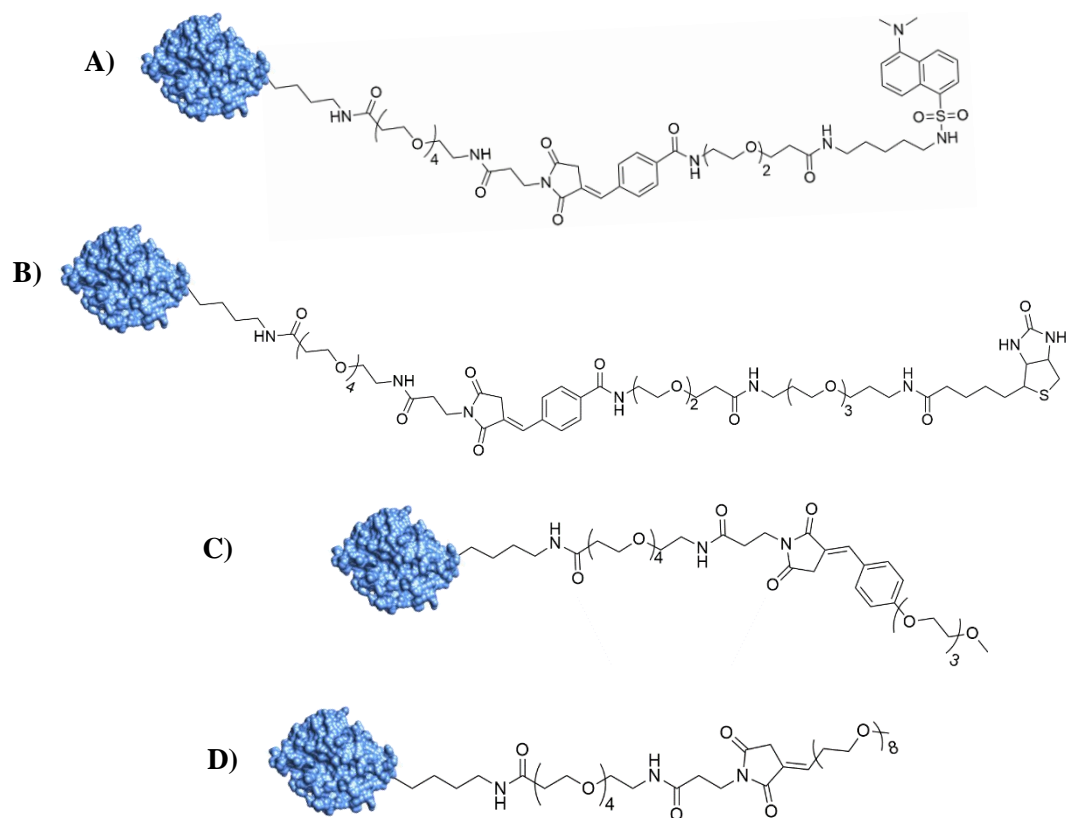
Figure 3.7. Chemical structures of BCA modified with Wittig olefins **2f-i**. **A)** BCA and **2f** Wittig product conjugate. **B)** BCA and **2g** Wittig product conjugate. **C)** BCA and **2h** Wittig product conjugate. **D)** BCA and **2i** Wittig product conjugate.

The expected mass changes for the modification of BCA with **2f-i** is 1009 Da, 1120 Da, 652 Da, and 779 Da, respectively. Based on the mass spectra presented in Figure 3.6A-D, the modification of BCA with each Wittig olefin was successful, with each reaction resulting in 1-4 modifications of the BCA protein. The modification of BCA with **2g** (biotin-based Wittig olefin product) yielded up to four modifications on BCA. The mass spectrum shown in Figure 3.6A shows additional mass peaks that do not correspond to modifications with **2f** (dansylcadaverine-based Wittig olefin product). The peak at m/z = 29784 Da corresponds to one of the two side products shown in Figure 3.8 below. Both of these species would result in a modification of 736

Da on BCA. The TFP group of the chemical structure shown in Figure 3.8A would react with the lysine residues of BCA to modify the protein. The chemical structure shown in Figure 3.8B has a reactive maleimide residue, which could react with a free primary amine on the protein (for example, with the N-terminus). Without further isolation of this side product and obtaining ^{1}H NMR and ^{13}C NMR spectra, the identity of this species was not conclusively determined solely by mass spectrometry. The other extraneous peaks could not be identified.
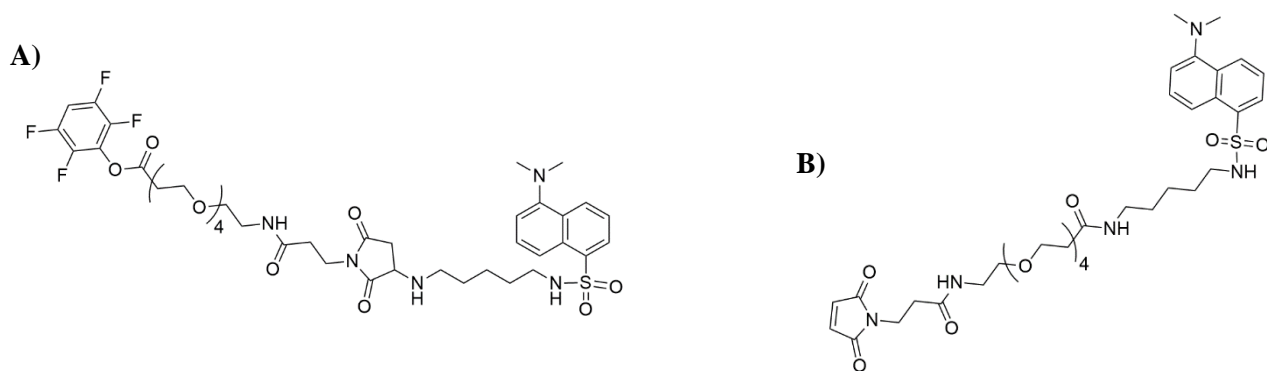
Figure 3.8. Chemical structures of side products associated with Wittig olefin product **2f**. **A)** Side product with TFP-activated ester reactive group. **B)** Side product with maleimide reactive group.

The extent of modification cannot be conclusively determined using ESI MS in this manner. For example, the spectrum in Figure 3.6D for the modification of BCA with **2i** shows that only one BCA-**2i** conjugate was formed using a 10-fold molar excess of **2i** to BCA. It is possible that the mass of unreacted BCA can supress further BCA-**2i** Wittig olefin conjugates with more modifications. Although in Figure 3.6B, up to four modifications of BCA with **2g** are shown, the peak intensities cannot be used to conclude that each of these species are present in equal proportion in a heterogeneous solution containing unreacted BCA and its conjugates. For each of the BCA conjugates shown above, the amounts of each conjugate obtained cannot be known. Therefore, the ESI MS analytical technique is only used to observe if the mass of a particular BCA-

Wittig olefin conjugate can be detected, but the absence of a molecular weight corresponding to a specific conjugate does not necessarily mean that the reaction was unsuccessful.

Overall, the SPOS of the Wittig olefins **2f-j** were successful. The BCA protein could be modified with each TFP-functionalized Wittig olefin **2f-j**. Along with the aromatic aldehydes **2a-c** and **2e**, it was demonstrated that a non-aromatic aldehyde (**2d**) could also be employed in the Wittig reaction, further extending the palette of potential bioconjugation reagents that can be synthesized in this manner. This methodology involving polystyrene-supported functionalized resins for synthesis and purification should be accessible for researchers to utilize in their experiments. Our experiments suggest that a variety of aldehydes can be synthesized and purified using the procedure described herein to contain an activated ester functional group, which can modify the surface of a protein containing an exposed lysine residue or an N-terminal amino group.

3.5. Conclusions

The microwave-assisted organic synthesis of an NEM-mPEG$_4$BA Wittig olefin using DMF, MeOH, and ACN as the solvents was tested at temperatures ranging from 70 °C to 180 °C, with reaction times ranging from twenty minutes to three hours. Both free TPP and PS-TPP were used as the phosphines in these experiments. Although each reaction tested (reactions **1a-f**) resulted in the NEM-mPEG$_4$BA Wittig olefin ([M+H]$^+$ = 378 Da), as detected by low resolution ESI MS, the microwave-assisted organic synthesis was not further pursued in our studies as not every research group would have access to this instrument. The objective of this chapter was to develop a simple procedure for the synthesis and purification of TFP-functionalized Wittig olefins that can be conducted by many researchers.

Five different TFP-functionalized Wittig olefin products were synthesized using PS-TPP. The unreacted aldehyde reagents were removed with PS-Ts-NHNH$_2$, and any remaining TFP-PEG$_4$-MAL was sequestered by the reintroduction of PS-TPP to the crude product. The yields obtained ranged from 46% to 77%. Each compound was characterized with high resolution ESI MS and ^{1}H NMR. The absence of the aldehyde proton chemical shift (δ = 10.0-9.5 ppm) in the ^{1}H NMR spectra of each TFP-functionalized Wittig olefin product **2f-j** suggests that the unreacted aldehyde reagent can be completely sequestered by the PS-Ts-NHNH$_2$ resin.

There were challenges associated with utilizing a solid phase approach for purification. For example, in the synthesis of the dansylcadaverine-based and biotin-based benzaldehydes (**2a-b**), the unreacted AldPhPEG$_2$NHS starting material was not able to be sequestered using the PS-Ts-NHNH$_2$ resin, otherwise the desired product would also be lost. If this starting material is retained for the Wittig reaction using PS-TPP, then its Wittig olefin with TFP-PEG$_4$-MAL can be formed (Figure 3.4 in Section 3.4.2). Any resin capable of sequestering this product would likely also remove the desired TFP-functionalized Wittig olefin product. Therefore, it was more prudent to employ chromatography for the purification of aldehyde reagents **2a-b**.

Each of the compounds **2f-j** were able to modify BCA. By ESI MS, 1-4 modifications of BCA were observed. For the reaction of BCA with the dansylcadaverine-based benzaldehyde (**2f**), an additional mass peak at m/z = 29784 Da was observed, indicating that another side product was present which could not be removed with our given protocol involving functionalized resins. Two proposed structures for these side products were given in Figure 3.8. This example further highlights the challenges associated with a resin-based purification approach. Although the MAL-functionalized chemical structure shown in Figure 3.8B could hypothetically be removed with the PS-TPP resin, the TFP-functionalized chemical structure (Figure 3.8A) cannot be removed using

a functionalized resin. Regardless, the SPOS and purification was successful for Wittig olefins **2g-j**. The reaction of BCA with Wittig olefin **2j** was analyzed with ESI MS at 2, 4, 6, and 24 hours to determine if the bioconjugation reaction was affected by time. For this reaction, it was observed that two hours was sufficient to modify the BCA protein. As the reaction time progresses, it is likely that the TFP-activated ester is being hydrolyzed in the aqueous solution, and the resulting compound cannot modify BCA. This is why the subsequent reactions of BCA with **2h-i** were conducted for 2 hours.

The results presented in this chapter suggest that several TFP-functionalized Wittig olefin products can be synthesized and purified with polystyrene-supported functionalized resins. Given that the resin and maleimide reagents are commercially available, it is expected that the procedure reported herein should be amenable to researchers outside synthetic organic chemistry laboratories. A number of bioconjugation reagents can be synthesized concurrently using different aldehyde compounds with the one-pot Wittig reaction involving the PS-TPP resin. The procedure has been shown to work with five different aldehydes, including a non-aromatic aldehyde. It is expected that a greater number of aldehydes can be used in this fashion to modify the surface of proteins through their lysine residues.

Chapter 4.0. Chemoenzymatic Bioconjugation of Amine-Functionalized Wittig Olefins with Microbial Transglutaminase

4.1. Introduction

Transglutaminases (TGase) (EC 2.3.2.13) are an extracellular class of enzymes that catalyze the acyl transfer reaction between amides (glutamine residues) and primary amines (lysine residues), resulting in an isopeptide bond formation and one equivalent of ammonia released.[143-145] The general mechanism of TGase mediated peptide crosslinking is shown in Scheme 4.1.
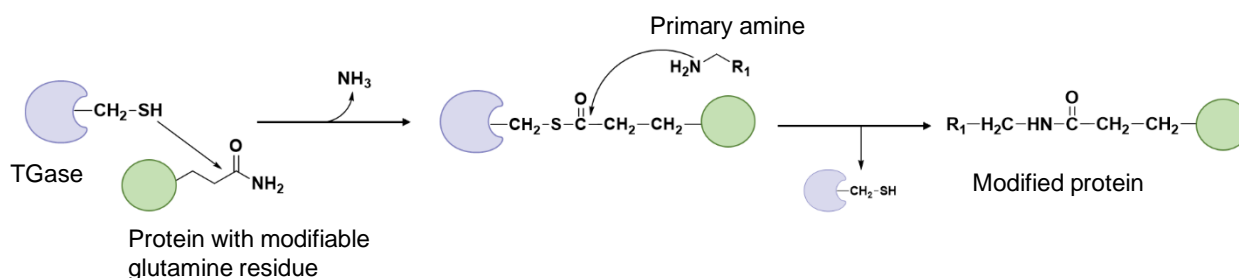
Scheme 4.1. General mechanism for the chemoenzymatic bioconjugation of a protein (green) having a modifiable glutamine residue and a primary amine by TGase (purple). R_1 may represent a second protein, or any chemical moiety that is used to modify a protein.

TGases have been found in mammalian, amphibian, avian, plant, invertebrate, and microbial sources.[145] Microbial transglutaminase (MTGase) is a versatile enzyme commonly used for biotechnological applications to mediate protein bioconjugations in the food, agricultural, and pharmaceutical industries.[143,146-151] These applications are summarized in Figure 4.1. MTGase is most commonly derived from the microbe *Streptomyces mobaraenes*. Other bacterial sources of MTGases have been reported, however, they are not commercially available.[152] MTGase exhibits optimal enzymatic activity at 55 °C and pH 6.0.[148, 153] Unlike mammalian TGase, the activity of MTGase is not dependent on Ca^{2+} or guanosine-5-triphosphate for substrate binding.[143,146-148] For these reasons, the use of *S. mobaraenes*-derived MTGase is advantageous for biotechnological applications, along with its relatively inexpensive cost.[148]
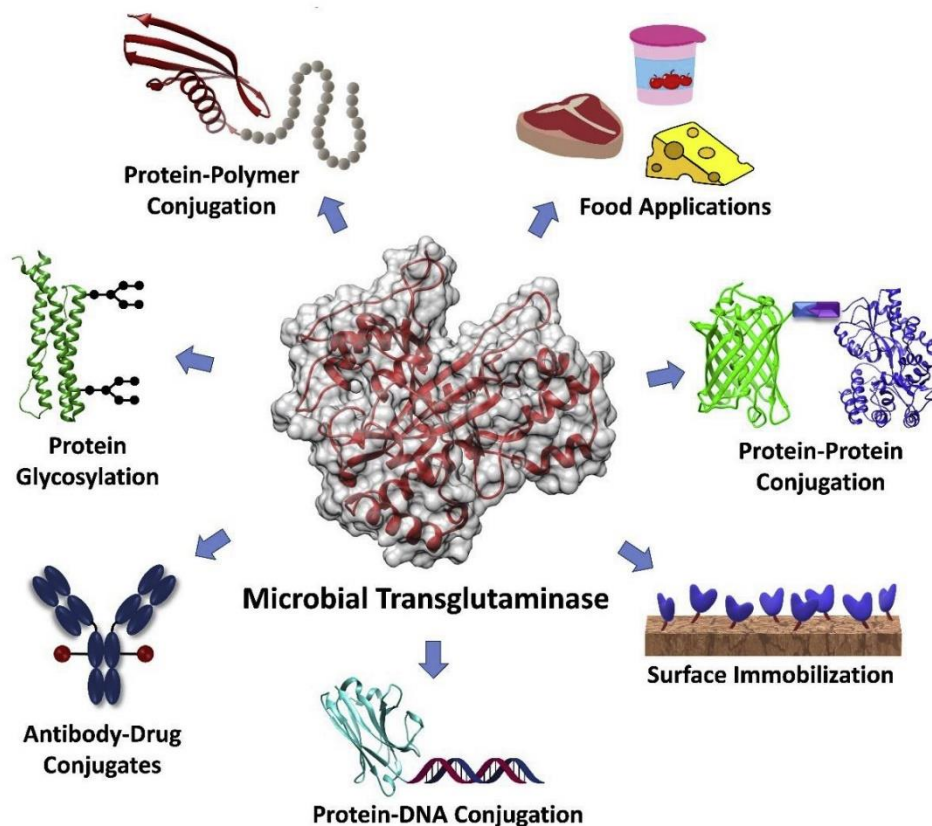
Figure 4.1. Summary of biotechnological and industrial applications of MTGase. Reproduced with permission under CC license from Schneider et al.[151]

In the food industry, MTGase is used to crosslink proteins, forming stable protein networks or gels, thereby improving the texture and consistency of meats, breads, and dairy products.[143,146] For pharmaceutical applications, there exists literature precedence for the use of MTGases in the PEGylation of proteins.[144,154-157] The site-specific modification of therapeutic proteins is essential for developing homogeneous conjugates. Non-specific PEGylation of therapeutic proteins can lead to protein inactivity, therefore decreasing the efficacy of the drug.[158] Grigoletto et al. demonstrated the effectiveness of immobilized MTGases for the rapid synthesis of PEG-protein conjugates.[157] MTGase was immobilized on an agarose gel, stabilising the enzyme and allowing it to retain its enzymatic activity as it was reused in subsequent conjugation reactions.[157] MTGase

is also used in the site-specific modification of antibodies with polymers, such as PEG, or with fluorescent moieties for detection purposes.[151,159-161] MTGase is therefore an extremely versatile and useful bioconjugation tool.

The amino acid sequence and crystal structure of MTGase from *S. mobaraenes* has been well characterized.[162] This monomeric enzyme has a molecular weight of 37.9 kDa and contains 331 amino acids.[162] The active site of MTGase contains a Cys64-His274-Asp255 triad, where Cys64 is the predominant amino acid residue in the enzymatic mechanism.[144,162] The three-dimensional structure and active site catalytic triad are shown in Figure 4.2.
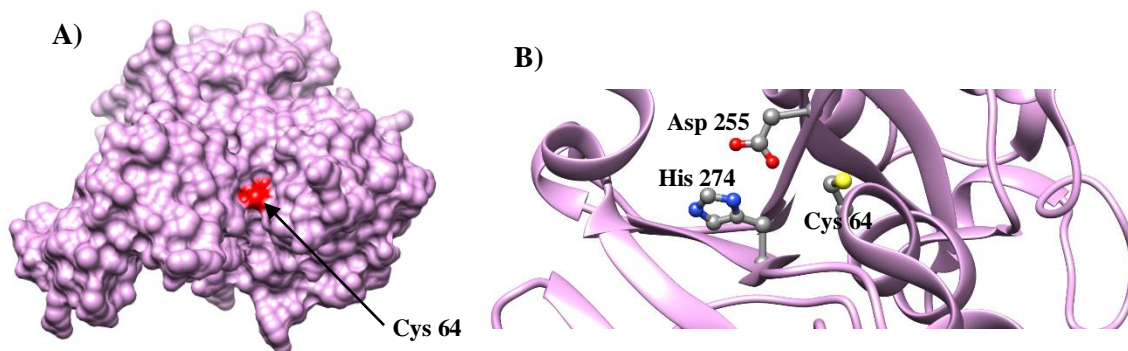
Figure 4.2. Three-dimensional representation of MTGase from *Streptomyces mobaraenses*. **A)** Space-filled MTGase depicting the active site cysteine (red). **B)** Zoomed in active site depicting the catalytic triad. PDB: 1IU4.

A number of protein substrates for MTGase have been reported, including avidin, α-lactalbumin, interferon, interleukin-2, and myoglobin.[147,154,163-165] A recent review by Giosafatto et al. discusses the use of MTGase in the preparation of bioplastics fabricated from various protein sources such as whey, soy, and casein.[166] The inherent specificity of the enzyme allows for controlled polymerization of the protein networks. Subsequently, the degree of crosslinking within the network affects the properties of the biomaterial. Information on the specific protein substrates

of MTGases, and several other types of TGases, can be found in the Transdab Wiki, a free online source compiled of peer-reviewed transglutaminase research articles.[167]

The protein substrate chosen for our bioconjugation studies is myoglobin (Scheme 4.2). Myoglobin proteins contain a heme group that reversibly binds to oxygen. This protein is found in muscle tissues. Myoglobin without the heme group is termed apomyoglobin (ApoMb). Equine skeletal myoglobin is a monomeric protein comprised of 153 amino acids with a molecular weight of 16950 Da.[168,169]
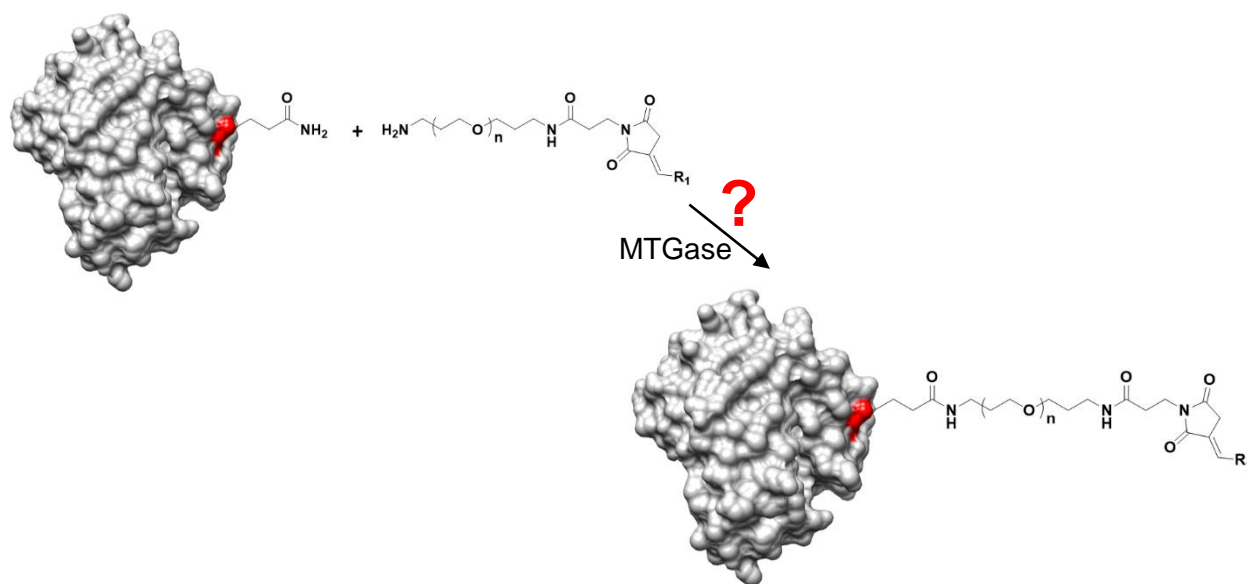
Scheme 4.2. MTGase mediated chemoenzymatic bioconjugation on the glutamine residue of equine skeletal ApoMb (grey) with an amine-functionalized Wittig olefin. R$_1$ may represent any chemical moiety that is used to modify a protein. Red on the protein represents the modifiable glutamine residue. PDB: 5ZZE.

Spolaore et al. have reported the site-specific derivatization of equine skeletal ApoMb with MTGase.[163] The residue that is used as a substrate by MTGase is Gln91.[163] It is found in the locally unfolded helix F region on equine skeletal ApoMb.[163] The other amino acid residues that can be modified by MTGase on this protein are Lys96 and Lys98.[163] Although Gln152 is also

present on the C-terminal end of this chain, it is not modifiable by MTGase.[163] This allows for the derivatization of ApoMb by MTGase to be site-specific. Spolaore et al. hypothesize that Gln152 cannot be modified in this fashion due to its proximity to negatively-charged residues, most notably the carboxylate group of the C-terminus, leading to unfavourable interactions with the MTGase active site.[163] The three-dimensional structure and specific modifiable residue of equine skeletal ApoMb is shown in Figure 4.3.
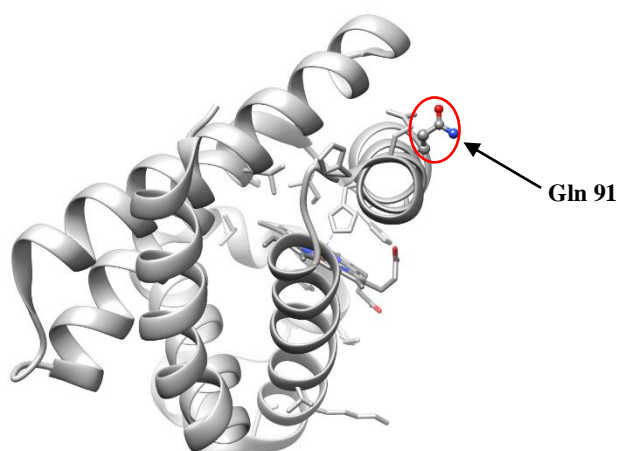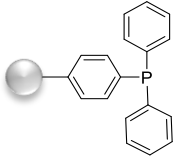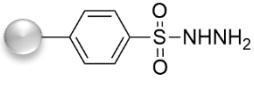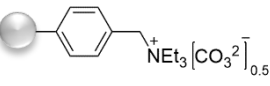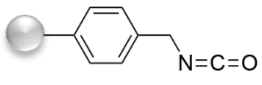
Gln 91

Figure 4.3. Three-dimensional representation of myoglobin (with heme) from equine skeletal muscle with Gln91 on helix F. <u>PDB: 5ZZE</u>.

Spolaore et al. have reported that the modification of the Gln91 residue with dansylcadaverine, a fluorophore with a primary amine functional group, was successfully undertaken with MTGase.[163] Our group hypothesized that equine skeletal ApoMb could be modified using MTGase with amine-functionalized Wittig olefins in a similar manner described by Spolaore et al. In this fashion, a novel method for the site-specific modification of proteins with functionalized aldehydes may be achieved.

4.2. Objectives

Bioconjugation reagents that are capable of selectively modifying the surface of proteins are particularly important in the pharmaceutical industry. The methodology for the SPOS and purification of activated ester-functionalized Wittig olefins described in Chapter 3 will be used to synthesize novel amine-functionalized Wittig olefins. These products will be used in the site-specific modification of the ApoMb Gln91 residue using MTGase in a chemoenzymatic bioconjugation approach. Each polystyrene-supported functionalized resin used in the synthesis and purification of the new Wittig olefins is listed in Table 4.1.

Table 4.1. Chemical structures and functions of polymer-supported resins utilized in Chapter 4.

Full Resin Name	Commercial Name	Structure	Functionality
Polystyrene triphenylphosphine	PS-TPP		Wittig reaction Removal of unreacted maleimide-containing compounds
Polystyrene *p*-toluenesulfonyl hydrazide	PS-Ts-NHNH$_2$		Electrophile scavenger: removal of unreacted aldehydes
Macroporous tetraalkylammonium carbonate	MP-Carbonate		Tertiary amine base: used as a scavenger of acidic molecules such as carboxylic acids or acidic phenols (such as NHS)
Macroporous isocyanate	MP-Isocyanate		Nucleophile scavenger: removal of unreacted primary and secondary amines

The model aldehyde used for the Wittig reaction is mPEG$_4$BA. The 1:1 EtOH:THF solvent system described in Chapter 3 will be used for the Wittig reactions involving PS-TPP, mPEG$_4$BA and a t-Boc-amido-PEG$_3$-MAL compound. Since this compound does not contain an activated

ester functional group, the reaction will be allowed to proceed overnight at room temperature. A summary of the steps undertaken to synthesize and purify the amine-functionalized Wittig olefin products are shown in Scheme 4.3.
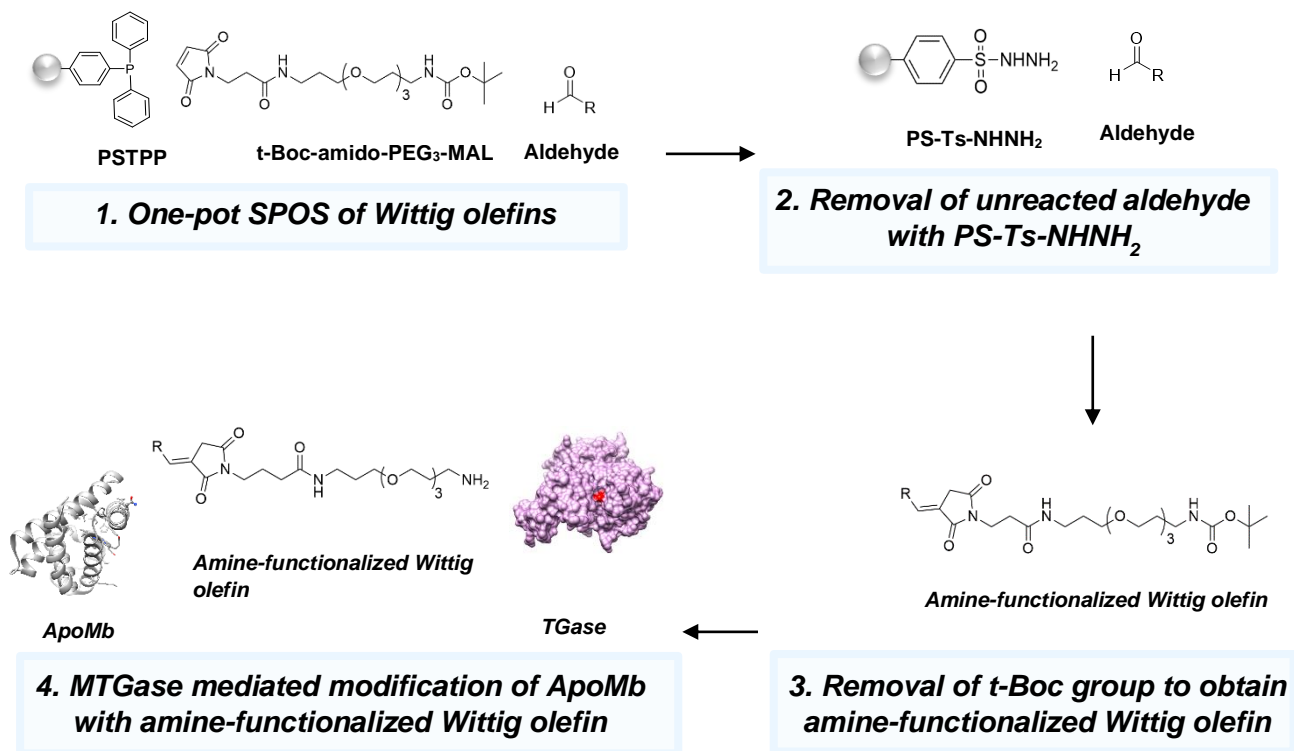
Scheme 4.3. Summary of the SPOS of the amine-functionalized Wittig olefin. R represents any chemical moiety or tag that can be used to modify a protein.

One anticipated challenge in our bioconjugation experiments is that the Wittig olefin may potentially act as an inhibitor of MTGase. Our synthesized olefins may act as Michael acceptors in the Michael addition reaction with the active site cysteine. Zedira, a biopharmaceutical company based in Darmstadt, Germany, has developed Michael acceptor-based peptide inhibitors of TGases, which are sold commercially.[170,171] The Michael-acceptor inhibitors bind irreversibly to the cysteine active site residue.[170] In this chapter, computational studies using the CovDock

module in Maestro (Schrodinger, LLC) with the amine-functionalized Wittig olefin were undertaken to study the binding interactions of this compound to MTGase. Maleimides are also known inhibitors of TGases. [172] This is why it is important that the PS-TPP resin completely captures the maleimide-containing compound. For this reason, the Wittig reaction with PS-TPP was allowed to proceed overnight, instead of six hours (as reported in Chapter 3).

If successful, this approach can be expanded to synthesize a novel set of amine-functionalized bioconjugation reagents using a variety of different aldehydes. The aim of this chapter is to develop bioconjugation reagents that are substrates for MTGase, which can selectively derivatize the surface of ApoMb, or other proteins that are MTGase substrates.

4.3. Materials and Methods

Proteins: Myoglobin from equine skeletal muscle was purchased from Sigma Aldrich, Canada. Microbial transglutaminase (MTGase) from *Streptomyces mobaraensis* was purchased from Zedira (Darmstadt, Germany). Bovine serum albumin was purchased from BioBasic Inc (Markham, ON, Canada). Centrifugal filters (0.5 mL) with a molecular weight cut-off (MWCO) of 10 kDa were purchased from Amicon® Ultra (Millipore Sigma, Canada).

PEG reagents: mPEG$_4$BA (95%; MW = 268.3 Da) was purchased from Broadpharm (San Diego, CA, USA). *Tert*-butyloxycarbonyl-*N*-amido-PEG$_3$-amine (t-Boc-amido-PEG$_3$-amine) (>90%; MW = 320.4 Da) was purchased from Quanta BioDesign Ltd (Plain City, OH, USA).

Maleimide and dansylcadaverine: 3-Maleimidopropionic acid *N*-succinimidyl ester (MPA) (MW = 266.2 Da) was purchased from Toronto Research Chemicals, ON, Canada. Dansylcadaverine (≥97%; MW = 335.5 Da) was purchased from Sigma Aldrich, Canada.

Resins: PS-TPP (loading capacity: 3.0 mmol/g) and MP-Carbonate (loading capacity: 2.5 mmol/g) were purchased from Sigma Aldrich, Canada. PS-Ts-NHNH$_2$ (loading capacity: 2.75 mmol/g) and MP-Isocyanate (loading capacity: 1.18 mmol/g) were purchased from Biotage (Uppsala, Sweden).

Solvents, buffers and bases: Potassium phosphate salt (KP) was purchased from BioShop Canada, Inc. (Burlington, ON, Canada). *N,N*-Dimethylformamide (DMF) Sure/Seal™ (≥99.0%), anhydrous tetrahydrofuran (THF) (≥99.0 %), anhydrous dichloromethane (DCM) (≥99.8%), trifluoroacetic acid (TFA) (99%), and triethylamine (TEA) (≥99.5%) were purchased from Sigma Aldrich, Canada. Anhydrous EtOH was purchased directly from ChemStores (University of Waterloo, Ontario, Canada). Methyl ethyl ketone (MEK) was purchased from Fisher Chemicals (Hampton, NH, USA).

Chromatography: Thin layer chromatography (TLC) Silica gel 60 F$_{254}$ 20x20 cm aluminum sheets were purchased from Millipore Sigma (Burlington, MA, USA).

Instrumentation: The masses of all protein samples were analyzed with ESI MS using a high resolution Thermo Scientific™ Q-Exactive (Thermo QE) Hybrid Quadrupole-Orbitrap mass spectrometer, 10 μL/min injection rate, positive mode, with 1:1 MeOH:H$_2$O+0.1% FA as the solvent. The masses of all small molecule compounds described in this chapter were analyzed with ESI MS using either the high resolution Thermo QE instrument (positive mode, 10 μL/min injection rate, 1:1 MeOH:H$_2$O+0.1% FA) or the low resolution Thermo Scientific™ Linear Ion Trap (Thermo LTQ) mass spectrometer (positive mode, 20 μL/min injection rate, 1:1 MeOH:H$_2$O+0.1% FA).

Small molecule compounds were characterized by ^{1}H NMR using a 300 MHz high resolution UltraShield™ Bruker Spectrometer. The pulse program used was zgpg30 with a pulse

delay of 3 seconds. The solvent used was deuterated chloroform (CDCl₃, Sigma Aldrich Canada), whose reference chemical shift is δ = 7.26 ppm. The chemical shifts were reported in parts per million (ppm).

Absorbance measurements were obtained with a UV-Vis spectrophotometer (SpectraMax 5, Molecular Devices, Sunnyvale, CA, USA). The software used was SoftMax® Pro Enterprise (Molecular Devices, Sunnyvale, CA, USA). Samples were pipetted into a standard transparent polystyrene 96-well plate (Grenier Bio-One, Frickenhausen, Germany).

4.3.1. Synthesis of mPEG₄BA Wittig Product for ApoMb Modification with MTGase
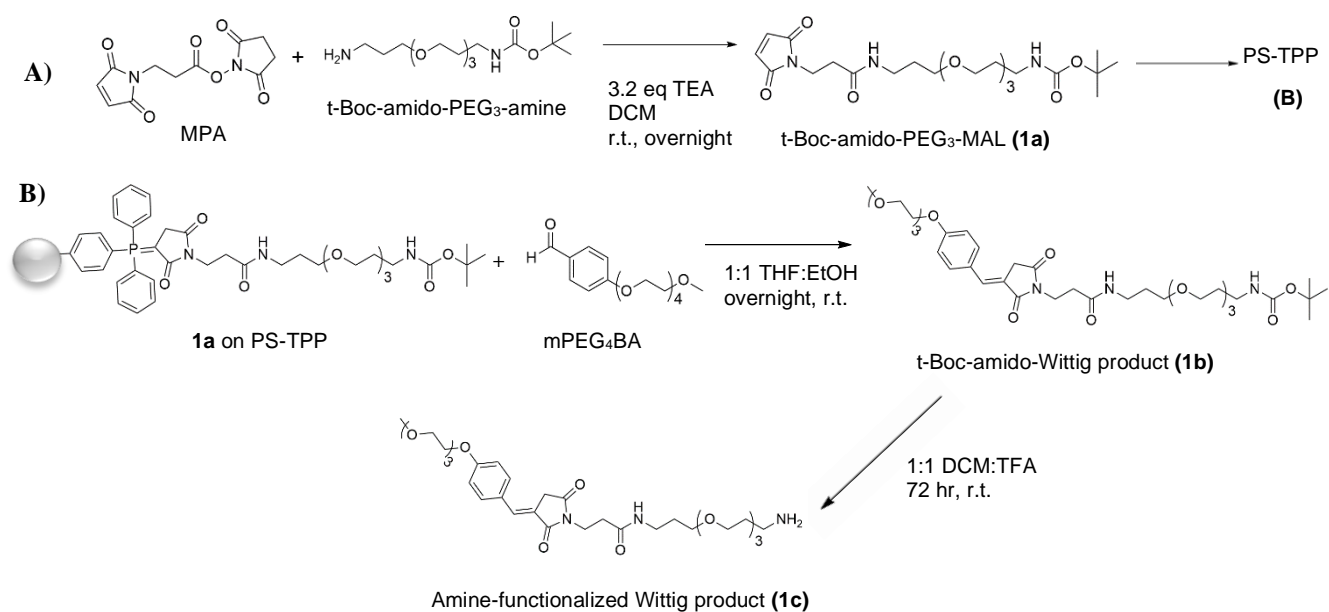
Scheme 4.4. Synthesis of an amine-functionalized Wittig product (**1c**) for ApoMb modification with MTGase. **A)** Synthesis of compound **1a**. **B)** Synthesis of compound **1b** with PS-TPP resin and subsequent deprotection of the t-Boc group yielding compound **1c**.

mPEG$_4$BA was used as a model aldehyde compound to develop and optimize a method for the synthesis of the amine-functionalized Wittig product. These experiments were conducted with CHEM 494 student Amanda Rose Ratto.

*Synthesis of **1a***: MPA (385.3 mg, 1.337 mmol, 1.0 eq), t-Boc-amido-PEG$_3$-amine (709.9 mg, 2.215 mmol, 1.5 eq), and anhydrous TEA (650 µL, 4.689 mmol, 3.2 eq) were dissolved in anhydrous DCM (1.5 mL) and reacted overnight with stirring at room temperature. The reaction was monitored with TLC (solvent system: 10:0.8 DCM:MeOH, visualization: UV lamp with wavelength = 254 nm). The solvent (DCM) was removed with rotary evaporation. The resulting crude (1205.3 mg) was a peach-coloured viscous oil.

*Purification of **1a***: NHS was removed according to the following procedure. MP-Carbonate (1.751 g, 4.377 mmol, 3.3 eq of carbonate with respect to initial mmol of MPA in the reaction) was added to the crude **1a** (1205.3 mg) and solubilized in DCM (4 mL). The reaction was monitored at 2 and 3 hours with TLC (using the same conditions described above). Since the NHS was still present at these time points, the reaction was allowed to proceed overnight at room temperature. Upon checking with TLC again, it was qualitatively determined that NHS was still present so the reaction mixture containing crude **1a** and MP-Carbonate was filtered on a Buchner funnel and washed with DCM (3 x 50 mL). The filtrate was placed under vacuum to evaporate a portion of the DCM and to decrease the volume. To this filtrate, MP-Carbonate (601.3 mg, 1.503 mmol of carbonate functional group) was added. The reaction was stirred at room temperature for 1.5 hours. After checking the reaction mixture with TLC, it was qualitatively determined that the NHS was removed. The resin was filtered on a Buchner funnel and washed with DCM (3 x 50 mL). DCM was removed using rotary evaporation. The crude mass was 926.8 mg. The next step was to remove the unreacted t-Boc-amido-PEG$_3$-amine. To this crude mass, MP-Isocyanate (1.814 g, 2.141

mmol, 1.0 eq isocyanate with respect to the initial mmol of t-Boc-amido-PEG$_3$-amine in the reaction) was added in 8.5 mL DCM. The reaction proceeded for 3 hours at room temperature with stirring. The reaction completion was qualitatively determined with TLC using the conditions described above. The resin was filtered on a Buchner funnel and washed with DCM (3 x 50 mL). DCM was removed with rotary evaporation. The presence of the product (**1a**) was checked with low resolution ESI MS (Thermo LTQ). The mass of **1a** obtained was 734.9 mg.

*Synthesis of **1b***: A portion of synthesized **1a** (105.3 mg) was reacted with PS-TPP (179.9 mg, 0.5379 mmol, 2.4 eq of TPP assuming 100% of crude mass is **1a**) in 800 μL of degassed, anhydrous DCM, with stirring, overnight, at room temperature. The reaction was periodically checked with TLC (using the conditions as previously described) until it was qualitatively determined that **1a** had disappeared from the reaction mixture. The PS-TPP resin bound with **1a** was filtered on a Buchner funnel and washed with DCM (3 x 40 mL). Any impurities remaining with **1a** would be in the filtrate. The solid PS-TPP resin bound with **1a** was dried under vacuum. The solid bound reagent was collected (224.2 mg). mPEG$_4$BA (21.6 mg, 0.0806 mmol, 0.9 eq to **1a** bound on PS-TPP) was added to the solid bound reagent (224.4 mg) and solubilized in 1 mL of degassed, anhydrous 1:1 THF:EtOH. The reaction proceeded overnight at room temperature with stirring. The reaction was checked with TLC (same conditions described previously). The resin was filtered on a Buchner funnel and washed with THF (3 x 5 mL), followed by evaporation of THF under vacuum. Crude **1b** (33.6 mg) was obtained and the viscous oil had a yellow-green appearance.

*Purification of **1b***: To crude **1b** (33.6 mg), PS-Ts-NHNH$_2$ (9.59 mg, 0.26 mmol, 3.3 eq of hydrazide to the initial mmol of mPEG$_4$BA in the reaction) was added and solubilized in 600 μL of anhydrous DCM. The reaction was allowed to proceed with stirring, at room temperature for 3 hours. After 3 hours, the extent of the reaction was qualitatively determined by TLC (solvent

118

system: 10:1 DCM:MeOH, visualization: UV lamp with wavelength = 254 nm) that mPEG$_4$BA was scavenged. The resin was filtered on a Buchner funnel and washed with DCM (3 x 5 mL). DCM was evaporated under vacuum. The resulting product (**1b**) had the appearance of a clear oil, and 21.4 mg (36.7% yield) was obtained.

The remainder of **1a** (629.6 mg) was reacted in the same manner described above for the synthesis of **1b**. Crude **1a** (629.6 mg) was reacted with PS-TPP (1084 mg, 3.252 mmol, 2.4 eq of TPP assuming 100% of crude is **1a**) in 5.2 mL of degassed, anhydrous DCM. The reaction proceeded overnight at room temperature with stirring. The solid bound reagent was filtered as previously described. The solid bound reagent was collected (1124.8 mg). The solid bound reagent (562 mg) was reacted with mPEG$_4$BA (25.5 mg, 0.0950 mmol, 2.3 eq to **1a** bound on PS-TPP) in 2 mL of degassed, anhydrous 1:1 THF:EtOH. The reaction proceeded overnight at room temperature with stirring. After filtering the PS-TPP resin as previously described, the solvent was evaporated under vacuum. The crude mass obtained was 116.4 mg. To this crude mass, PS-Ts-NHNH$_2$ (132.4 mg, 0.3641 mmol, 3.8 eq of hydrazide to the initial mmol of mPEG$_4$BA in the reaction) was added in 1 mL anhydrous DCM. The reaction proceeded under the same conditions described above for aldehyde scavenging. The resin was rinsed and filtered as previously described. **1b** was obtained (25.5 mg; 81.5% yield).

Characterization of 1b: ^{1}H NMR (300 MHz, CDCl$_3$) δ 8.00 (s, 1H), 7.57 (s, 1H), 7.46 (d, 2H), 7.01 (d, 2H), 6.50 (s, 1H), 4.20 (t, 2H), 3.95-3.15 (m, 31H), 2.57 (t, 2H), 2.29 (s, 2H), 1.81 (tt, 4H), 1.45 (s, 9H). High resolution ESI-MS: calculated for C$_{36}$H$_{58}$O$_{12}$N$_3$ [M+H]$^+$: 724.4015 Da, found 724.4022 Da.

Synthesis of 1c: This step was for removal of the t-Boc protecting group, yielding the free amine. Into a vial containing **1b** (25.5 mg), a 400 μL solution of 1:1 TFA:DCM was added and the reaction

proceeded for 2 hours at room temperature. The vial was placed on the rotary evaporator, and once the initial solution was removed, the vial was washed with DCM (4 x 1 mL) and placed on the rotary evaporator. After the solvent was evaporated, the final product (**1c**) was obtained (21.2 mg).

Characterization of 1c: Low resolution ESI MS (Thermo LTQ) was used to obtain the molecular weight of **1c**. The mass for the compound $C_{31}H_{49}N_3O_{10}$ [M+H]$^+$: 624.35 Da. **1c** was used in the experiments involving MTGase (Sections 4.3.2 and 4.3.3.) without further characterization.

4.3.2. MTGase Mediated Modification of ApoMb

A number of bioconjugation reactions with ApoMb and MTGase were undertaken. The bioconjugation of ApoMb with dansylcadaverine and t-Boc-amido-PEG$_3$-amine were conducted as control reactions, to see if the MTGase is capable of modifying ApoMb and if t-Boc-amido-PEG$_3$-amine is a substrate for MTGase. The bioconjugation of ApoMb and **1c** was also attempted. These reactions were undertaken with CHEM 494 student, Amanda Rose Ratto and co-op student, Claire Stoecker.

Heme removal for preparation of ApoMb: The following procedure was obtained from Ascoli et al.[173] Myoglobin from equine skeletal muscle (10 mg) was dissolved in 4 mL of chilled ddH$_2$O. Chilled 0.1 M hydrochloric acid was added dropwise to this solution until pH 2.5 was reached (as tested with pH paper strips). Methyl ethyl ketone (MEK) (4 mL) was added to this solution and swirled gently, then placed in an ice bath for at least 10 minutes. When phase separation was observed, the clear aqueous layer containing ApoMb was removed and transferred to a round bottom flask, where an equal volume of ddH$_2$O was added and placed under high vacuum. Following this step, ddH$_2$O (6 x 8 mL) was added and the solvent was removed with rotary evaporation under vacuum. The final protein concentration was determined using a Bradford assay with bovine serum albumin as the protein standard for the calibration curve.[174] The SpectraMax

120

5 microplate reader was used to obtain absorbance measurements. The final concentration of ApoMb was determined to be 1 mg/mL.

Bioconjugation of ApoMb with dansylcadaverine: MTGase (0.00035 µmol, 1.0 eq), ApoMb (0.0076 µmol, 21.9 eq), and dansylcadaverine (0.379 µmol, 50.0 eq to ApoMb) were reacted in 0.15 M pH 6.0 KP buffer for 6 hours at 40 °C. After the reaction was completed, the sample containing the KP buffer was exchanged with ddH_2O using centrifugal filters with an MWCO of 10 kDa and five cycles of centrifugation at 10 000 x *g* (10 minutes per cycle). The ApoMb-dansylcadaverine product was diluted with the 1:1 MeOH:ddH_2O+0.1% FA solvent until the concentration of the sample was in the range of 1-10 µM and characterized with ESI MS (Thermo QE). The resulting spectrum was deconvoluted with the Thermo Scientific BioPharma Finder software (Version 3.0).

Bioconjugation of ApoMb with t-Boc-amido-PEG$_3$-amine: MTGase (0.00035 µmol, 1.0 eq), ApoMb (0.0076 µmol, 21.9 eq), and t-Boc-amido-PEG$_3$-amine (0.379 µmol, 50.0 eq to ApoMb) were reacted in 0.15 M pH 6.0 KP buffer for 6 hours at 40 °C. After the reaction was completed, the sample containing the KP buffer was exchanged with ddH_2O as previously described. The sample was then subsequently characterized with ESI MS (Thermo QE) as had been done earlier for the ApoMb samples.

*Bioconjugation of ApoMb with **1c***: MTGase (0.00035 µmol, 1.0 eq), ApoMb (0.0076 µmol, 21.9 eq), and **1c** (0.379 µmol, 50.0 eq to ApoMb) were reacted in 0.15 M pH 6.0 KP buffer for 6 hours at 40 °C. After the reaction was completed, the sample containing the KP buffer was exchanged with ddH_2O as previously described. The sample was subsequently characterized with ESI MS (Thermo QE) in the same manner for the ApoMb samples.

4.3.3. Determining the Inhibition of MTGase

As the modification of ApoMb with **1c** was unsuccessful, the next set of experiments focused on determining whether or not **1c** was an inhibitor of MTGase. These reactions were undertaken with CHEM 494 student Amanda Rose Ratto.

Reaction of MTGase with 1c: MTGase (0.001043 μmol, 1.0 eq) and **1c** (0.0522 μmol, 50.0 eq) were incubated together in 0.15 M pH 6.0 KP buffer for 6 hours at 40 °C. After the reaction was completed, the sample containing the KP buffer was exchanged with ddH_2O as previously described. The sample containing MTGase was then subsequently characterized with ESI MS (Thermo QE) using the same conditions as previously described for the ApoMb samples.

Bioconjugation of ApoMb with dansylcadaverine in the presence of the NEM-mPEG₄BA Wittig product: NEM-mPEG₄BA was synthesized according to the procedure outlined in Chapter 3 (Section 3.3.2). MTGase (0.00035 μmol, 1.0 eq) and NEM-mPEG₄BA (2.65 mmol, 7571 eq) were incubated in 0.15 M pH 6.0 KP buffer for 30 minutes at 40 °C. To this solution, ApoMb (0.0079 μmol, 22.5 eq) and dansylcadaverine (0.394 μmol, 50.0 eq to ApoMb) were added and was reacted in 0.15 M pH 6.0 KP buffer for 6 hours at 40 °C. After reaction completion, the sample containing the buffer was exchanged with ddH_2O as done earlier. The sample was then subsequently characterized with ESI MS (Thermo QE) as previously described for ApoMb samples.

4.3.4. Computational Modelling of NEM-mPEG₄BA and *1c* with MTGase

The covalent docking of NEM-mPEG₄BA and **1c** in the active site of MTGase was done with the CovDock module in Maestro (Schrodinger, LLC). The MTGase structure imported was PDB:6GMG. The covalently bound inhibitor peptide analogue found in the X-ray structure with MTGase was removed. The settings used for the docking of the two compounds were the standard CovDock settings. The covalent reaction was set as a 1,4-Michael addition of Cys64 found on

MTGase (active site cysteine) with the exocyclic olefin on NEM-mPEG$_4$BA and **1c**. For the modelling of the hypothetical tetrahedral intermediate with **1c**, the peptide analogue was altered with a glutamine residue into the bound peptide, then reacted with the cysteine thiol to form the tetrahedral intermediate. **1c** was then merged into the workspace and attached to this tetrahedral compound. The resulting structure was minimized using the OPLS4 forcefield in Maestro.

4.4. Results and Discussion

4.4.1. Synthesis of mPEG$_4$BA Wittig Product for ApoMb Modification with MTGase

The procedure for the synthesis of an amine-functionalized Wittig olefin product required several steps. These experiments were conducted with Amanda Rose Ratto, a former CHEM 494 student in the Honek laboratory. Initially, a heterobifunctional alkane reagent containing MAL and NHS (MPA) was reacted with t-Boc-amido-PEG$_3$-amine and triethylamine in DCM at room temperature to obtain **1a** (t-Boc-amido-PEG$_3$-MAL). The purification of this compound was conducted with several polymer-bound scavenger resins. MP-Carbonate was used to sequester unreacted NHS. MP-Isocyanate was used to scavenge the t-Boc-amido-PEG$_3$-amine starting material. Once these species have been removed from the reaction mixture, as qualitatively determined by TLC and low resolution ESI MS, the Wittig product could be synthesized using PS-TPP. The addition of **1a** to PS-TPP served a second function in our synthesis procedure. Any side products that do not contain maleimide and that were not initially removed would be filtered as they could not bind to the PS-TPP resins. The chemical species depicted in Figure 4.4. are undesired side products that were detected by low resolution ESI MS (data not shown).
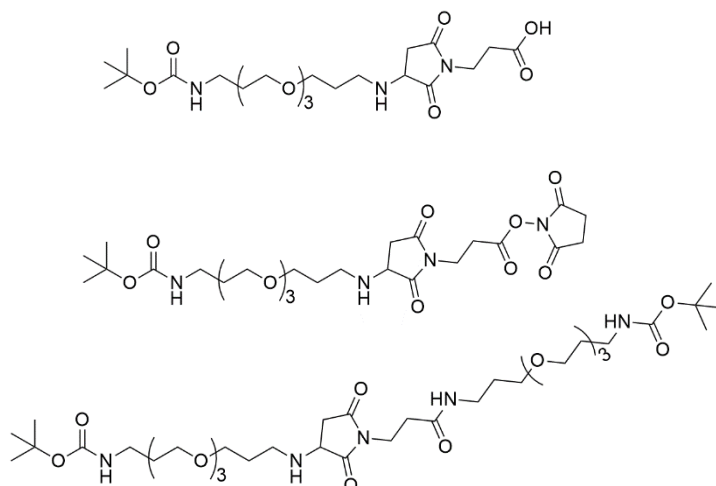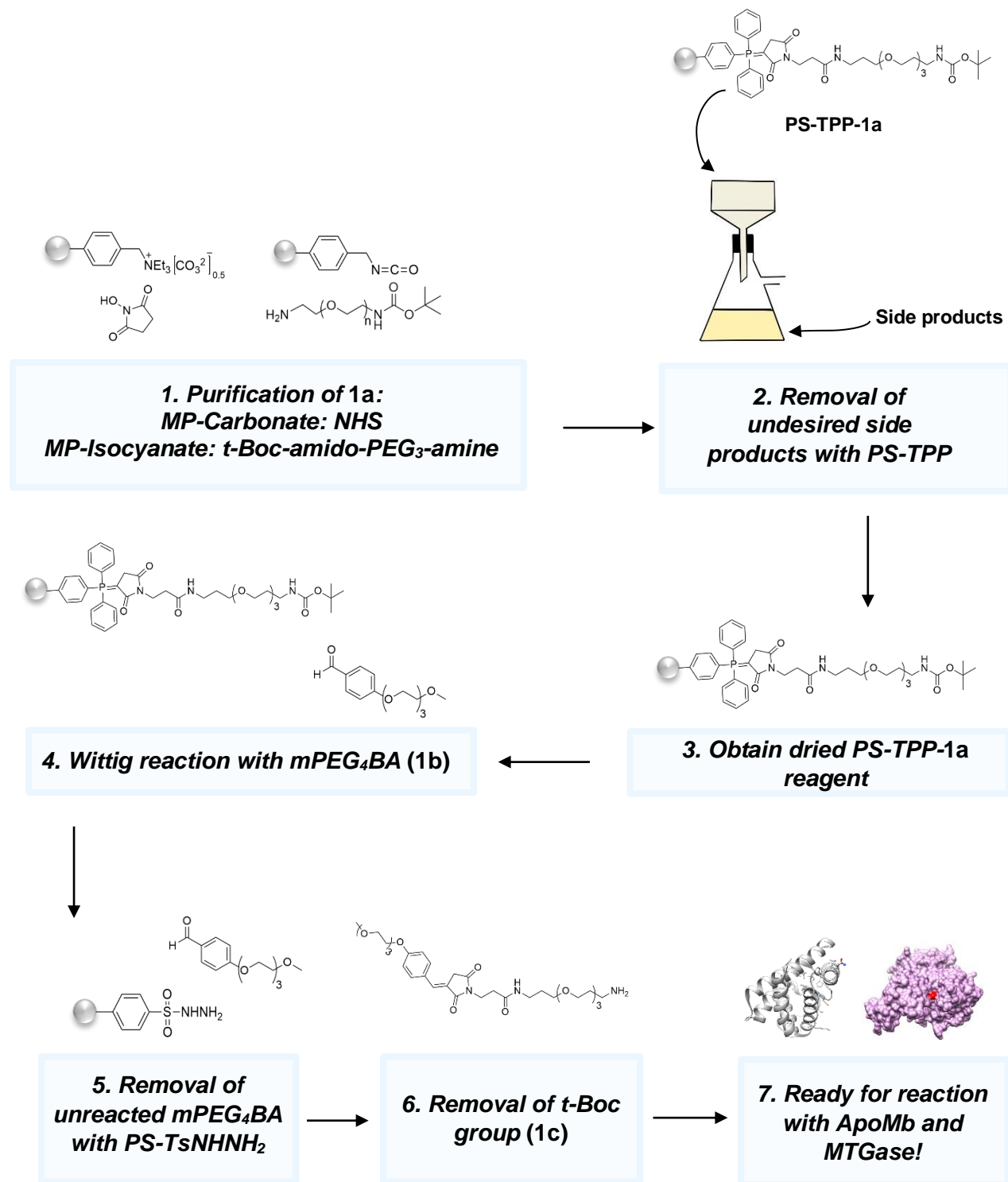
Figure 4.4. Chemical structures of side products after the synthesis of **1a** and **1b** that are filtered from the PS-TPP resin.

These side products were separated from the PS-TPP-**1a** reagent and collected in the filtrate. After several washes of the PS-TPP-**1a** reagent, the reagent was dried under vacuum and subsequently resolubilized in 1:1 THF:EtOH. mPEG$_4$BA was added to the reaction mixture to obtain the Wittig product (**1b**). Unreacted mPEG$_4$BA was removed with PS-Ts-NHNH$_2$. The final step involved the removal of the t-Boc group in order to obtain the final product, the amine-functionalized Wittig olefin (**1c**), which was used in subsequent reactions with MTGase and ApoMb. The overall reaction scheme was given in Scheme 4.4. A summary of the steps involving the polystyrene-supported reagents is given in Scheme 4.5. The high resolution ESI mass spectrum and ^{1}H NMR spectrum of compound **1b** are given in Appendix A. The low resolution ESI mass spectrum of compound **1c** is also given in Appendix A.

PS-TPP-1a

Side products

1. Purification of 1a:
MP-Carbonate: NHS
MP-Isocyanate: t-Boc-amido-PEG₃-amine

2. Removal of undesired side products with PS-TPP

4. Wittig reaction with mPEG₄BA (1b)

3. Obtain dried PS-TPP-1a reagent

5. Removal of unreacted mPEG₄BA with PS-TsNHNH₂

6. Removal of t-Boc group (1c)

7. Ready for reaction with ApoMb and MTGase!

Scheme 4.5. Summary of the procedure for the synthesis and purification of an amine-functionalized Wittig olefin (**1c**).

4.4.2. MTGase Mediated Modification of ApoMb

The heme group of equine spleen myoglobin was removed according to the procedure by Ascoli et al.[173] The concentration of the stock ApoMb used in the subsequent experiments was determined to be 1 mg/mL using a Bradford assay. A control mass spectrum of the ApoMb solution was obtained with ESI MS and subsequent deconvolution of the raw spectral data using the Thermo Scientific BioPharma Finder software (Version 3.0) (Figure 4.5). The mass of unmodified equine skeletal ApoMb is 16950 Da, which is in good agreement with the literature value obtained by Zaia et al.[168]
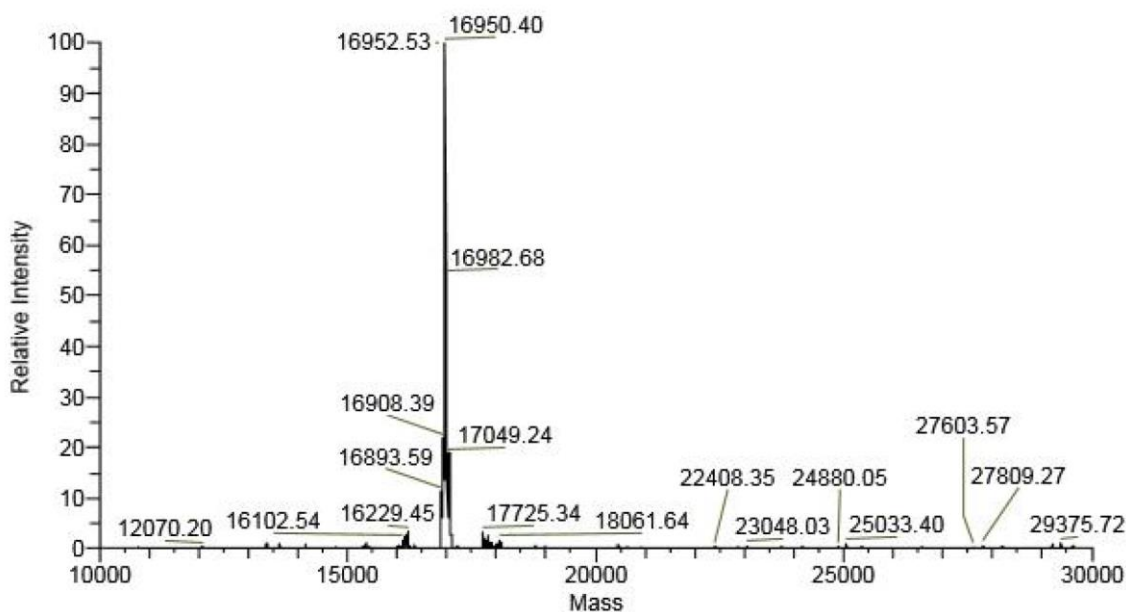
Figure 4.5. ESI MS of unmodified equine skeletal ApoMb.

The bioconjugation of ApoMb and dansylcadaverine using MTGase was undertaken as a control experiment to determine that the prepared ApoMb is modifiable, and that the MTGase enzyme is functional. The Gln91 residue of ApoMb and dansylcadaverine are known substrates of

MTGase.[163] The resulting mass spectrum is shown in Figure 4.6. The expected mass change is 317 Da. The peak corresponding to this mass change was observed at 17268 Da.
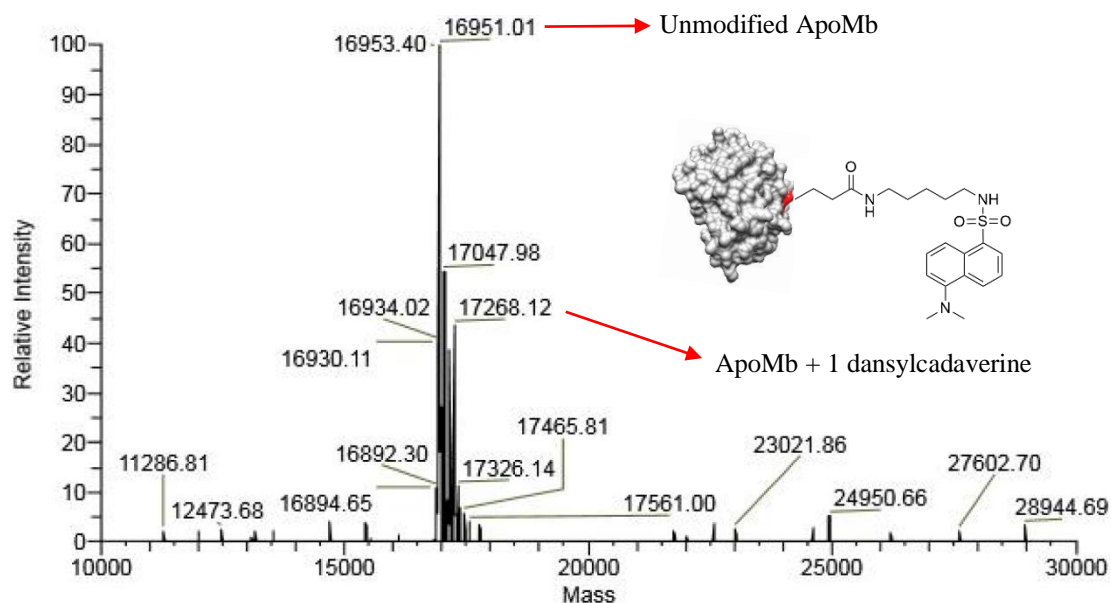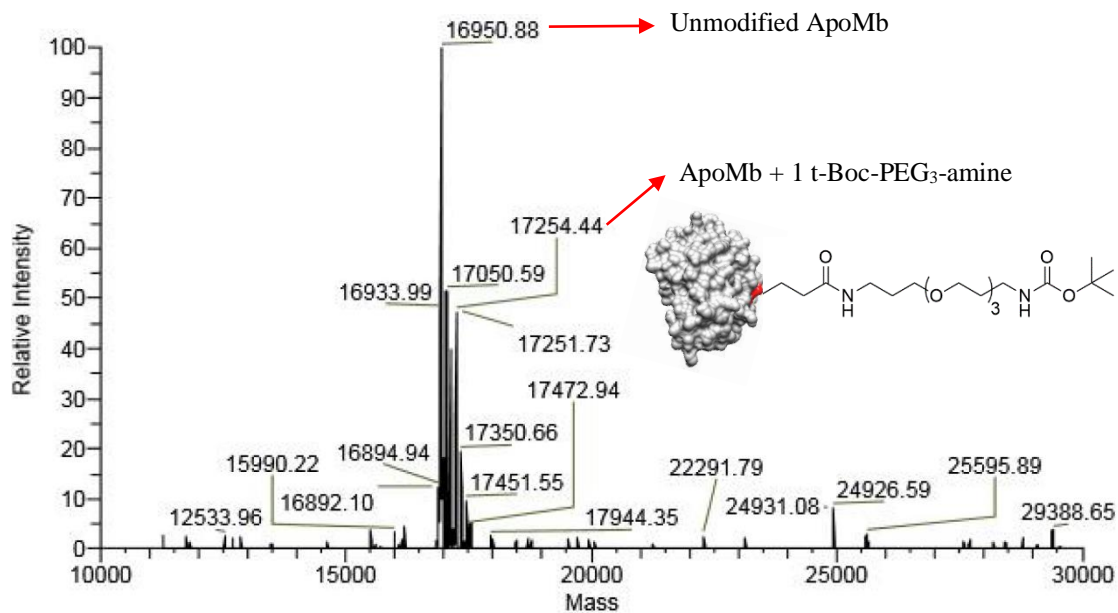

Figure 4.6. ESI MS of equine skeletal ApoMb after MTGase mediated modification with dansylcadaverine.

The second experiment conducted was the reaction of ApoMb with t-Boc-PEG$_3$-amine in order to determine if this compound is a suitable substrate for the MTGase enzyme. The t-Boc-PEG$_3$-amine reagent was used as a starting material in the synthesis of the amine-functionalized Wittig olefin product. The resulting mass spectrum is shown in Figure 4.7. The expected mass change is 304 Da. The peak corresponding to this mass change was observed at 17254 Da.

127

Figure 4.7. ESI MS of equine skeletal ApoMb after MTGase mediated modification with t-Boc-PEG3-amine.

Lastly, MTGase, ApoMb, and **1c** were incubated at 40 °C at pH 6.0 for six hours. The ApoMb-**1c** conjugate was not detected by ESI MS. Only unmodified ApoMb with a molecular weight of 16950 Da was detected (data not shown). It is likely that the compound **1c** was not conjugated to ApoMb. One possibility is that the exocyclic olefin is acting as an inhibitor of MTGase. If this compound is an inhibitor of MTGase, a thiol-Michael addition reaction with the exocyclic olefin of **1c** and the active site thiol of MTGase is proposed. Parmar et al. reported the Michael addition reaction of a free thiol with an exocyclic olefin generated from the Wittig reaction of an aldehyde and the MAL-TPP Wittig reagent.[84] Our next experiments focused on determining if compound **1c** is an inhibitor of MTGase.

4.4.3. Determining the Inhibition of MTGase

MTGase was incubated with a large excess of compound **1c** at 40 °C, pH 6.0 for six hours. The reaction mixture containing MTGase was analyzed with ESI MS to determine if a mass change corresponding to **1c** can be detected. The expected molecular weight change is 623 Da,

corresponding to the molar mass of compound **1c**. By ESI MS, this mass change was not detected for MTGase (data not shown). A second experiment was undertaken where MTGase was incubated with a large excess of the NEM-mPEG$_4$BA Wittig olefin at 40 °C, pH 6.0 for 30 minutes. After this time, ApoMb and dansylcadaverine were added to this solution and incubated using conditions previously described for MTGase experiments. We proposed that if an exocyclic olefin, such as the NEM-mPEG$_4$BA adduct, acts as an inhibitor, then no modification of ApoMb with dansylcadaverine, a known substrate, will occur. However, after analyzing the reaction mixture with ESI MS, the ApoMb-dansylcadaverine conjugate was detected at 17267 Da and the resulting mass spectrum was identical to the one shown in Figure 4.6.

Based on our experiments, it does not appear that **1c** is acting as an inhibitor of MTGase. Therefore, it is likely that the thiol-Michael addition reaction is not occuring. If the compound **1c** is not acting as an inhibitor of MTGase then a second possibility is that it is not a good co-substrate for MTGase. Computational modelling studies were used to gain insight as to how compound **1c** interacts with the active site of MTGase.

4.4.4. Computational Modelling of NEM-mPEG$_4$BA and *1c* with MTGase

The CovDock module in Maestro (Schrodinger LLC) was used to model the binding of NEM-mPEG$_4$BA and **1c** with the active site thiol on MTGase. The results obtained from this computational modelling only depict a hypothetical covalent thiol-Michael adduct, and does not provide enough conclusive data to demonstrate that the compounds bind in this manner. Compound **1c** has two short, yet flexible PEG chains that can have different possible conformations in an aqueous solution, complicating the computational studies. Regardless, some insight on the interaction between the active site residues and the two compounds may be given.

Figure 4.8 depicts the binding interactions of NEM-mPEG$_4$BA in the active site of MTGase, if it forms a thiol-Michael adduct with Cys64. One possibility for the experimentally observed lack of binding is that there are not many hydrogen bonding interactions present between NEM-mPEG$_4$BA and the nearby amino acid residues of MTGase. Only one hydrogen bonding interaction is depicted between the methoxy oxygen of NEM-mPEG$_4$BA and the Arg26 amino acid residue (Figure 4.8A). Water molecules that are present in the active site cavity of MTGase will be hydrogen bonded to nearby amino acid residues. Therefore, the displacement of the water molecules by NEM-mPEG$_4$BA may not be energetically favourable, and the complex will not be formed. Another possibility is that there is a steric clash between the aromatic ring of the NEM-mPEG$_4$BA compound and the side chain of the Val65 residue. If the thiol-Michael addition does not occur, then it is unlikely that the exocyclic olefin of NEM-mPEG$_4$BA will act as an inhibitor of MTGase.
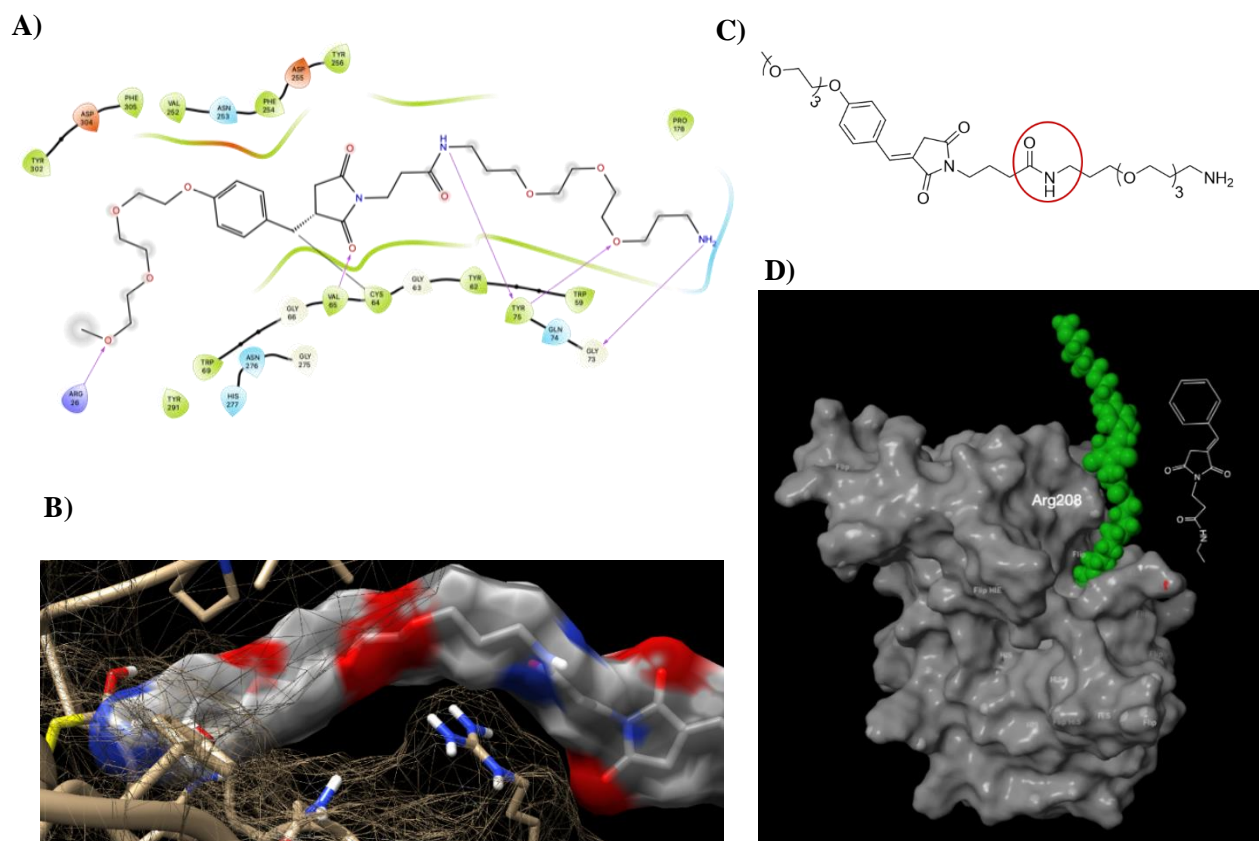
A)

B)
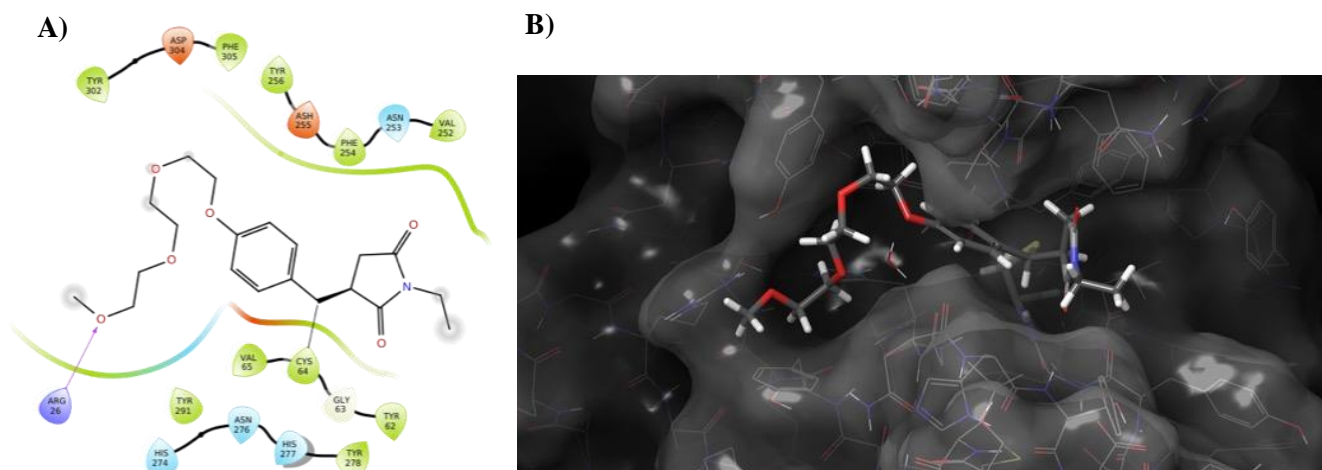
Figure 4.8. Hypothetical docking of NEM-mPEG$_4$BA in the active site of MTGase through the thiol-Michael addition on Cys64. **A)** Potential binding interactions of NEM-mPEG$_4$BA with MTGase active site amino acid residues. **B)** Space-filled structural analysis. PDB: 6GMG

Figure 4.9 depicts the binding interactions of compound **1c** in the active site of MTGase, if it forms a thiol-Michael adduct with Cys64. Based on the computational modelling, there are five potential hydrogen bonding interactions, one of which is on Val65, directly next to the active Cys64 thiol. However, it would appear that there is significant steric interaction between the amide bond on **1c** and Arg208, and the aromatic ring of **1c** and Asn253 in the active site of MTGase, if **1c** were to interact with the active site in this manner. It is possible that because of this problematic steric interaction, **1c** cannot bind to the active site. Then it will not act as an inhibitor or a substrate. If this is the case, then synthesizing **1c** with a longer PEG chain may further displace the amide bond from the Arg208 residue, allowing it to potentially behave as a co-substrate for MTGase.

A)

C)

B)

D)

Figure 4.9. Hypothetical docking of **1c** in the active site of MTGase through the thiol-Michael addition on Cys64. **A)** Potential binding interactions of **1c** with MTGase active site amino acid residues. **B)** Space-filled structural analysis. **C)** Chemical structure of **1c** with circled amide bond (red). **D)** Overview of the space-filled model for the MTGase-**1c** interaction.

131

4.5. Conclusions

An amine-functionalized Wittig product (**1c**) was successfully synthesized and purified using the SPOS methodology that was outlined in Chapter 3. The ApoMb-t-Boc-amido-PEG$_3$-amine and ApoMb-dansylcadaverine conjugates were detected by ESI MS. Although the specific site of conjugation was not confirmed, it is anticipated that the Gln91 residue of ApoMb was selectively modified by MTGase. The MTGase mediated chemoenzymatic bioconjugation of **1c** to ApoMb was unsuccessful. There were two possibilities for the lack of conjugation with **1c**. The first possibility was that the exocyclic olefin of **1c** was acting as an inhibitor, binding to the active site of MTGase via the thiol-Michael addition. The second possibility was that the compound was not a good substrate for the MTGase enzyme. If the compound is not a good substrate, that is, does not favourably interact with the active site, then it is likely not an inhibitor either.

ESI MS was used to determine if a mass change on MTGase corresponding to **1c** could be detected. If this mass change could be detected, it would be likely that the compound forms a covalent linkage with the active site thiol. However, this mass change was not observed on MTGase. In another experiment, the NEM-mPEG$_4$BA Wittig product was first incubated with MTGase for thirty minutes. Next, ApoMb and dansylcadaverine, known MTGase substrates, were added to the reaction mixture. The detection of the ApoMb-dansylcadaverine adduct with ESI MS further supported the possibility that the exocyclic olefins of the two Wittig products do not act as inhibitors in this manner. Finally, computational studies with the NEM-mPEG$_4$BA Wittig product and **1c** were undertaken to determine possible binding interactions with the MTGase active site. Based on these studies, it is likely that the amide component of **1c** could unfavourably interact with the Arg208 residue in the active site. The synthesis of an amine-functionalized Wittig product with a longer PEG chain might overcome this limitation.

Chapter 5.0. Conclusions and Future Research

The primary objective of the research presented in this thesis was to investigate novel phosphorous-based bioconjugation methods for protein derivatization. The approaches that were explored will be summarized in this chapter (Scheme 5.1), along with future research directions. Although not every approach was successful, new information on these types of reactions as it pertains to protein bioconjugation was attained. First reported by Kantner and Watts in 2016,[43] the phospha-Michael addition for protein bioconjugation served as the inspiration for the phosphorous-based approaches studied in this thesis.
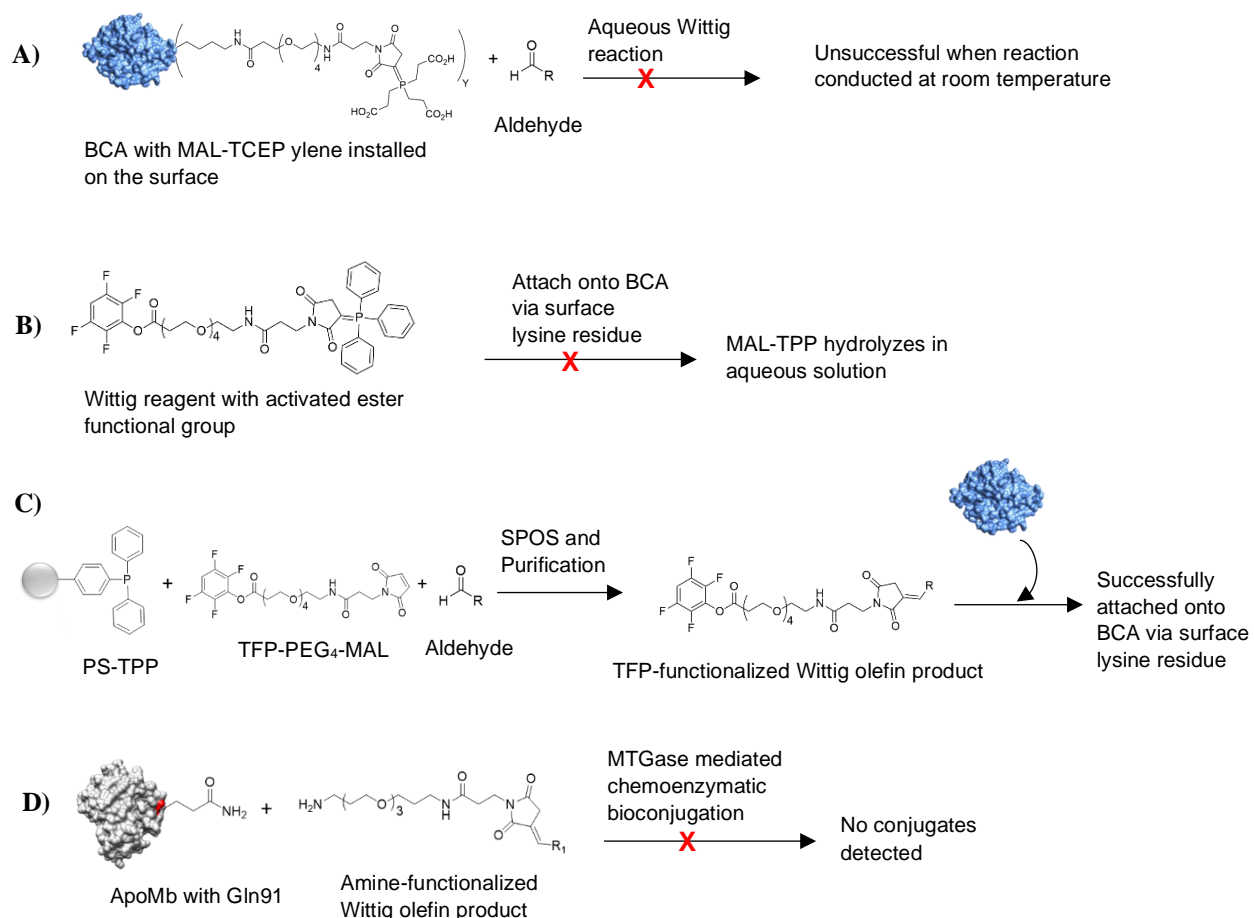
Scheme 5.1. Summary of the four phosphorous-based approaches investigated in this thesis. **A)** Chapter 2: aqueous Wittig reaction on BCA (blue). **B)** Chapter 2: attachment of TFP-PEG$_4$-MAL-TPP ylene on BCA. **C)** Chapter 3: SPOS and purification of activated ester-functionalized Wittig olefin products and subsequent attachment on BCA. **D)** Chapter 4: MTGase mediated chemoenzymatic bioconjugation of amine-functionalized Wittig olefin on ApoMb (grey).

In Chapter 2, the aqueous Wittig reaction was attempted on the surface of the PfFtn and BCA proteins. Initial studies were undertaken at temperatures of 50-60 °C for four hours. At first, the reaction appeared to be successful for both proteins. Further studies involving BCA with the NHS-PEG$_4$-MAL, TCEP, and mPEG$_4$BA compounds were conducted at room temperature, with and without sodium hydroxide. By ESI MS, it appeared that the BCA-Wittig olefin conjugates were detected. However, the BCA-Wittig olefin conjugate had a similar molecular weight to the theoretical BCA-MAL-TCEP + Na$^+$ adduct (about 5 Da difference). The resolution of the mass spectrometry technique for protein characterization is not high enough to distinguish these species. Subsequent investigations using AldPhPEG$_6$COOH as the aldehyde with the same experimental conditions were undertaken. AldPhPEG$_6$COOH is larger than mPEG$_4$BA (MW = 485.5 Da versus MW = 268.3 Da, respectively), which would have allowed for the conclusive identification of conjugates with ESI MS. Unfortunately this BCA-Wittig conjugate was not detected, unless the reaction was heated to 40 °C. Given these relatively harsh conditions, the bioconjugation method would not be expendable to a variety of thermo-sensitive proteins.

One possible explanation for the unsuccessful Wittig olefination on the surface of BCA was that TCEP was not an appropriate phosphine. In order for the Wittig reaction to proceed, the phosphonium adduct needs to be deprotonated (as shown in Scheme 2.2, Chapter 2). Computational studies were undertaken to determine the pKa of a variety of phosphonium adducts involving NEM. It was determined that the NEM-TCEP complex possessed the highest pKa value (pKa = 9.95), even when taking into account the inherent error of calculation ($\pm$1 pKa unit). The structures containing aryl phosphines yielded pKa values of 5.12-7.69. Therefore, these were considered good choices for further optimization of the aqueous Wittig reaction conducted on the surface of a protein.

TPP and DPPA (aryl phosphines) were reacted in acetone with TFP-PEG$_4$-MAL to obtain the ylide. The activated ester group (TFP) would allow for the modification of BCA with this compound. The PEG chain would afford water solubility to the otherwise insoluble TPP. However, this conjugate was not observed with ESI MS. Studies with ^{31}P NMR were conducted to determine the stability of MAL-TPP complexes in water. After two hours in water, a signal corresponding to the TPP oxide compound was detected, and the initial signal corresponding to the MAL-TPP complex disappeared. With these experiments, it was demonstrated that the aqueous Wittig reaction could not be conducted on the surface of a protein with either TCEP or TPP (and its water-soluble analogues).

In Chapter 3, polystyrene-supported resins were used to synthesize and purify activated ester-functionalized Wittig olefins. PS-TPP was used for the synthesis and purification of MAL-containing compounds, and PS-Ts-NHNH$_2$, a hydrazide resin, was used to sequester the excess aldehyde reagent. Five activated ester Wittig olefin products were synthesized and purified with this approach, with yields ranging from 47-77%. Compounds were characterized with high resolution ESI MS and ^{1}H NMR. By ^{1}H NMR, the characteristic signal corresponding to the chemical shift of the aldehyde proton ($\delta = 10.0$-9.5 ppm) disappeared. This indicated that our solid phase purification approach was sufficient for removing unreacted aldehydes. It is anticipated that a larger number of aldehydes can be used to easily modify proteins with this approach.

The experiments conducted in Chapter 4 were undertaken to show the versatility of the phosphorous-based approach involving targeted protein bioconjugation. An amine-functionalized Wittig olefin reagent was synthesized and purified using the solid phase approach described in Chapter 3. It was hypothesized that MTGase could use this compound as a substrate to selectively modify the glutamine residues of proteins. Equine skeletal ApoMb was employed as the co-

135

substrate. Spolaore et al. reported that the Gln91 residue is selectively modified by MTGase.[163] While the amine-functionalized Wittig olefin reagent was successfully synthesized, the conjugate of this compound with ApoMb could not be detected. Further studies with MTGase determined that this compound was not an inhibitor of the enzyme. Subsequent computational studies investigated the binding interactions of this compound with the active site of MTGase. One possibility was that the amide bond found on the reagent had unfavourable interactions with the Arg208 residue found in the active site of MTGase. It was hypothesized that the synthesis of this reagent with a longer PEG chain would avoid these unfavourable interactions.

5.1. Future Research Directions

The next avenue to be explored is the synthesis of an amine-functionalized Wittig olefin with a longer PEG chain. The t-Boc-amido-PEG$_{11}$-amine reagent is sold by Broadpharm (San Diego, CA, USA). The structure of this starting material and the final Wittig olefin product is shown in Figure 5.1. The reagent will be synthesized and purified according to the procedure outlined in Chapter 4, and then incubated with ApoMb and MTGase for six hours at 40 °C, at pH 6.0. It is hypothesized that the longer reagent will behave as an appropriate substrate for MTGase so that ApoMb can be selectively modified. If this approach is successful, then a number of bioconjugation reagents can be synthesized using the t-Boc-amido-PEG$_{11}$-amine as the primary starting material. Aldehydes carrying a specific chemical moiety or tag can be used to synthesize amine-functionalized Wittig olefins for the subsequent site-specific modification of proteins using MTGase.

A)

B)
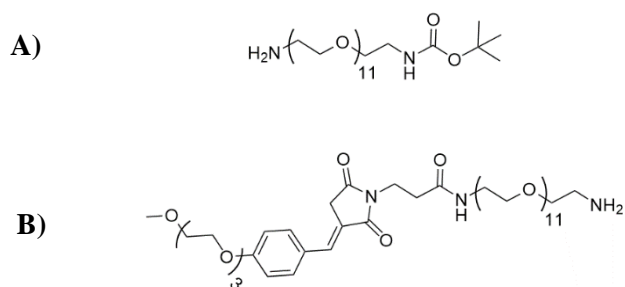
Figure 5.1. Chemical structures of **A)** t-Boc-amido-PEG$_{11}$-amine and **B)** new amine-functionalized Wittig olefin with PEG$_{11}$ chain.

The immobilization of enzymes on a polymer-supported resin will also be undertaken. One such commercially available resin is crosslinked agarose with TCEP moieties displayed. Enzymatic immobilization is important for the fabrication of novel materials for high throughput catalysis. The model protein (BCA) will first be modified with TFP-PEG$_4$-MAL so that the enzyme displays maleimide. The enzyme will be subsequently immobilized onto the resin via the phospha-Michael addition reaction. The enzymatic activity of BCA immobilized on this resin will be measured and compared to the free enzyme activity. It has been previously observed that various esters of *p*-nitrophenol (PNP) can function as substrates for determining the catalytic activity of this enzyme.[110,111] The hydrolysis of a *p*-nitrophenyl ester to PNP results in a yellow-coloured solution that absorbs strongly at 405 nm. This experiment will demonstrate how enzymatic activity for BCA might vary if it is immobilized on a polymer-supported resin (Scheme 5.2).
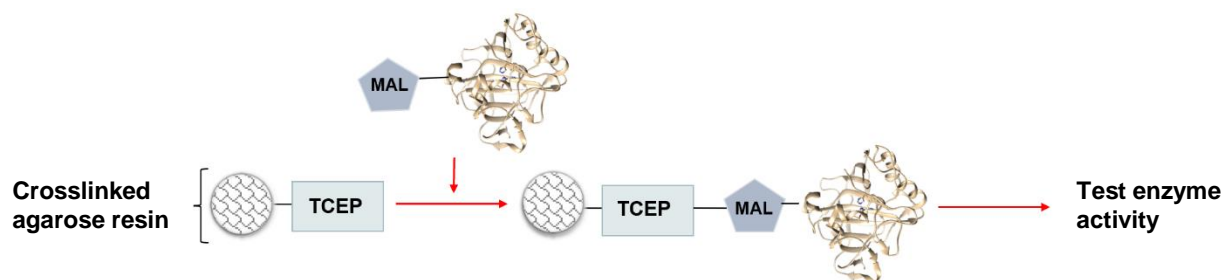
Scheme 5.2. Immobilization of BCA on an agarose-TCEP resin via the phospha-Michael addition reaction.

137

The synthesis of a TCEP analogue containing an activated ester functional group will be pursued. The PS-Carbodiimide resin will be used in the SPOS of the TCEP analogue. This coupling reagent will activate the carboxylic acid group. The compound will then be reacted with a hydroxyl-PEG$_4$-TFP reagent. The activated ester group (TFP) will allow the TCEP analogue to be directly attached onto the surface of proteins through their lysine residues. A second protein, enzyme, or synthetic molecule functionalized with a maleimide can be attached to the protein displaying TCEP. It is anticipated that the phospha-Michael addition reaction will facilitate the formation of new bioconjugates (Scheme 5.3). If successful, this methodology will be another phosphorous-based technique in the bioconjugation toolbox.
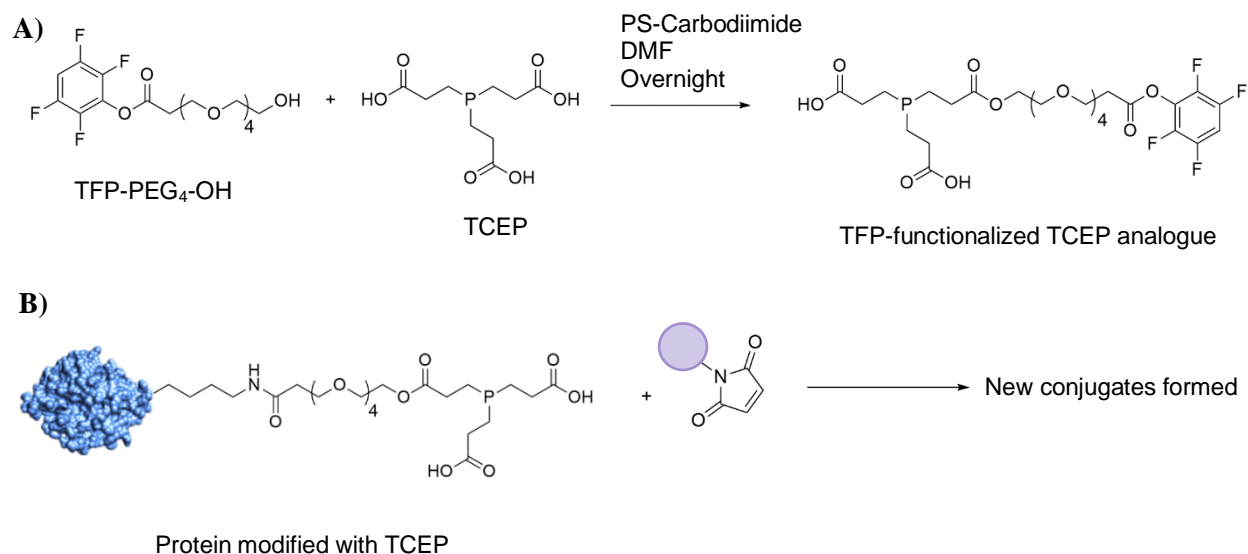
Scheme 5.3. Overview of a new phosphorous-based bioconjugation technique involving TCEP analogues. **A)** General scheme for the synthesis of a TFP-functionalized TCEP analogue. **B)** Attachment of the TCEP analogue onto a model protein, such as BCA (blue) and subsequent reaction with maleimide-modified proteins, enzymes, or synthetic molecules (purple circle).

Letters of Copyright Permission

Copyright use for Scheme 1.5.

CCC RightsLink®

🏠 Home | ❓ Help ⌄ | ✉ Email Support | 👤 Sign in | 👥 Create Account

ACS Publications
Most Trusted. Most Cited. Most Read.

A Chemical Probe for Protein Crotonylation

Author: Jeffrey Bos, Tom W. Muir
Publication: Journal of the American Chemical Society
Publisher: American Chemical Society
Date: Apr 1, 2018

Copyright © 2018, American Chemical Society

PERMISSION/LICENSE IS GRANTED FOR YOUR ORDER AT NO CHARGE

This type of permission/license, instead of the standard Terms and Conditions, is sent to you because no fee is being charged for your order. Please note the following:

- Permission is granted for your request in both print and electronic formats, and translations.
- If figures and/or tables were requested, they may be adapted or used in part.
- Please print this page for your records and send a copy of it to your publisher/graduate school.
- Appropriate credit for the requested material should be given as follows: "Reprinted (adapted) with permission from {COMPLETE REFERENCE CITATION}. Copyright {YEAR} American Chemical Society." Insert appropriate information in place of the capitalized words.
- One-time permission is granted only for the use specified in your RightsLink request. No additional uses are granted (such as derivative works or other editions). For any uses, please submit a new request.

If credit is given to another source for the material you requested from RightsLink, permission must be obtained from that source.

BACK   CLOSE WINDOW

Copyright permission for Figure 4.1.

References

1. Gerrard, J.A. (**2013**). Protein nanotechnology: what is it. In: Gerrard J. (eds) *Protein Nanotechnology. Methods in Molecular Biology (Methods and Protocols)*, vol 996. Human Press: Totowa, NJ, pp 1-15.

2. Abascal, N.C., & Regan, L. The past, present, and future of protein-based materials. *Open Biol*. **2018**, *8*, 180113.

3. Jonker, A.M., Löwik, D.W.P.M., & van Hest, J.C.M. Peptide and protein-based hydrogels. *Chem. Mater*. **2012**, *24*, 759-773.

4. Diaz, D., Care, A., & Sunna, A. Bioengineering strategies for protein-based nanoparticles. *Genes* **2018**, *9*, 370.

5. Verma, D., Gulati, N., Kaul, S., Mukherjee, S., & Nagaich, U. Protein based nanostructures for drug delivery. *Int. J. Pharm*. **2018**, 1-18.

6. Li, F., & Mahato, R.I. Bioconjugate therapeutics: current progress and future perspective. *Mol. Pharmaceutics*. **2017**, *14*, 1321-1324.

7. Kalia, J., & Raines, R.T. Advances in bioconjugation. *Curr. Org. Chem*. **2010**, *14*, 138-147.

8. Geyik, C., Guler, E., Gumus, Z.P., Barlas, F.B., Akbulut, H., Demirkol, D.O., Timur, S., & Yagci, Y. Bioconjugation and applications of amino functional fluorescence polymers. *Macromol. Biosci*. **2017**, *17*, 1600232.

9. Fisher, S.A., Baker, A.E.G., & Stoichet, M.S. Designing peptide and protein modified hydrogels: selecting the optimal conjugation strategy. *J. Am. Chem. Soc*. **2017**, *139*, 7416-7427.

10. Hermanson, G. T. (**1996**). The chemistry of reactive groups. In: *Bioconjugate Techniques*. Elsevier Science: San Diego, California, pp. 137-165.

11. Stephanopoulos, N., & Francis, M.B. Choosing an effective protein bioconjugation strategy. *Nat. Chem. Biol*. **2011**, *7*, 876-884.

12. de Gruyter J.N., Malins, L.R., & Baran, P.S. Residue-specific peptide modification: A chemist's guide. *Biochem*. **2017**, *56*, 3863-3873.

13. Zhang, C., Vinogradova, E.V., Spokoyny, A.M., Buchwald, S.L., & Pentelute, B.L. Arylation chemistry for bioconjugation. *Angew. Chem. Int. Ed*. **2019**, *58*, 4810-4839.

14. Rother, M., Nussbaumer, M. G., Renggli, K., & Bruns, N. Protein cages and synthetic polymers: a fruitful symbiosis for drug delivery applications, bionanotechnology and materials science. *Chem. Soc. Rev*. **2016**, *45*, 6213-6249.

15. Algar, W.R. (**2017**). A brief introduction to traditional bioconjugate chemistry. In: *Chemoselective and Bioorthogonal Ligation Reactions: Concepts and Applications, vol 1*. Wiley-VCH: Weinheim, Germany, pp 1-36.

16. Andre, I., Linse, S., & Mulder, F.A.A. Residue-specific pKa determination of lysine and arginine side chains by indirect ^{15}N and ^{13}C NMR spectroscopy: application to apo calmodulin. *J. Am. Chem. Soc*. **2007**, *129*, 15805-15813.

17. Isom, D.G., Castaneda, C.A., Cannon, B.R., Garcia-Moreno, B. Large shifts in pKa values of lysine residues buried inside a protein. *PNAS*. **2011**, *108*, 5260-5265.

18. Dozier, J.K., & Distefano, M.D. Site-specific PEGylation of therapeautic proteins. *Int. J. Mol. Sci*. **2015**, *16*, 25831-25864.

19. Veronese, F.M., & Mero, A. The impact of PEGylation on biological therapies. *BioDrugs* **2008**, *22*, 315–329.

20. Borchmann, D. E., Carberry, T.P., & Weck, M. "Bio"-macromolecules: polymer-protein conjugates as emerging scaffolds for therapeutics. *Macromol. Rapid Comm*. **2013**, *35*, 27–43.

21. Zeng, Q., Li, T., Cash, B., Li, S., Xie, F., & Wang, Q. Chemoselective derivatization of a bionanoparticle by click reaction and ATRP reaction. *ChemComm*. **2007**, *14*, 1453–1455.

22. Jutz, G., & Böker, A. Bionanoparticles as functional macromolecular building blocks – a new class of nanomaterials. *Polymer* **2011**, *52*, 211–232.

23. Suk, J.S., Xu, Q., Kim, N., Hanes, J., & Ensign, L.M. PEGylation as a strategy for improving nanoparticle-based drug and gene delivery. *Adv. Drug Deliv. Rev*. **2016**, *99*, 28–51.

24. Kiran, P., Khan, A., Neekhra, S., Pallod, S., & Srivastava, R. Nanohybrids as protein-polymer conjugate multimodal therapeutics. *Front. Med. Technol*. **2021**, *3*, 676025.

25. Thi, T.T.H., Pilkington, E.H., Nguyen, D.H., Lee, J.S., Park, K.D., & Truong, N.P. The importance of poly(ethylene glycol) alternatives for overcoming PEG immunogenicity in drug delivery and bioconjugation. *Polymers (Basel)*. **2020**, *12*, 298.

26. Yadav, S., Sharma, A.K., & Kumar, P. Nano-scale self-assembly for therapeutic delivery. *Front. Bioeng. Biotechnol.* **2020**, *8*, 127.

27. Vannucci, L., Falvo, E., Fornara, M., Di Micco, P., Benada, O., Krizan, J., Svoboda, J., Hulikova-Capkova, K., Morea, V., Boffi, A., & Ceci, P. Selective targeting of melanoma by PEG-masked protein-based multifunctional nanoparticles. *Int. J. Nanomed*. **2012**, *7*, 1489–1509.

28. Li, J., & Kao, W.J. Synthesis of polyethylene glycol (PEG) derivatives and PEGylated−peptide biopolymer conjugates. *Biomacromolecules* **2003**, *4*, 1055-1067.

29. Davis, D.P., & Crapps, E.C. Selective and specific preparation of discrete PEG compounds. U.S. Patent 7888536B2, February 13, 2004.

30. Mero, A., Clementi, C., Veronese, F.M., & Pasut, G. Covalent conjugation of poly(ethylene glycol) to proteins and peptides: strategies and methods. *Methods. Mol. Biol.* **2011**, *75*, 95-129.

31. Ravasco, J.M.J.M., Faustino, H., Trindade, A., & Gois, P.M.P. Bioconjugation with maleimides: a useful tool for chemical biology. *Chem. Eur. J.* **2019**, *25*, 43-59.

32. Poole, L.B. The basics of thiols and cysteines in redox biology and chemistry. *Free Radic. Biol. Med.* **2015**, *80*, 148-157.

33. Nair, D.P., Podgorski, M., Chatani, S., Gong, T., Xi, W., Fenoli, C.R., & Bowman, C.N. The thiol-michael addition click reaction: a powerful and widely used tool in materials chemistry. *Chem. Mater.* **2014**, *26*, 724-744.

34. Christie, R.J., Fleming, R., Bezabeh, B., Woods, R., Mao, S., Harper, J., Joseph, A., Wang, Q., Xu, Z.Q., Wu, H., Gao, C., & Dimasi, N. Stabilization of cysteine-linked antibody drug conjugates with N-aryl maleimides. *J. Control. Release.* **2015**, *220*, 660-70.

35. Liu, Y., Hou, W., Sun, H., Cui, C., Zhang, L., Jiang, Y., Wu, Y., Wang, Y., Li, J., Sumerlin, B.S., Liu, Q., & Tan, W. Thiol–ene click chemistry: a biocompatible way for orthogonal bioconjugation of colloidal nanoparticles. *Chem. Sci.* **2017**, *8*, 6182-6187.

36. Lyon, R.P., Setter, J.R., Bovee, T.D., Doronina, S.O., Hunter, J.H., Anderson, M.E., Balasubramanian, C.L., Duniho, S.M., Leiske, C.I., Li, F., & Senter, P.D. Self-hydrolyzing maleimides improve the stability and pharmacological properties of antibody-drug conjugates. *Nat. Biotechnol.* **2014**, *32*, 1059-1062.

37. Fontaine, S.D., Reid, R., Robinson, L., Ashley, G.W., & Santi, D.V. Long-term stabilization of maleimide-thiol conjugates. *Bioconjugate Chem.* **2015**, *26*, 145-152.

38. Costa, A.M., Bosch, L., Petit, E., & Vilarrasa, J. Computational study of the addition of methanethiol to 40+ michael acceptors as a model for the bioconjugation of cysteines. *J. Org. Chem.* **2021**, *86*, 7107-7118.

39. Heiss, T.K., Dorn, R.S., & Prescher, J.A. Bioorthogonal reactions of triarylphosphines and related analogues. *Chem. Rev.* **2021**, *121*, 6802-6849.

40. Enders, D., Saint-Dizier, A., Lannou, M.I., & Lenzem, A. The phospha-michael addition in organic synthesis. *Eur. J. Org. Chem.* **2006**, *1*, 29-49.

41. Lee, Y.J., Kurra, Y., & Liu, W.R. Phospha-michael addition as a new click reaction for protein functionalization. *Chembiochem* **2016**, *17*, 456-461.

42. Chambers, K.A., Abularrage, N.S., Hill, C.J., Khan, I.H., & Scheck, R.A. A chemical probe for dehydrobutyrine. *Angew. Chem. Int. Ed.* **2020**, *59*, 7350-7355.

43. Kantner, T., & Watts, A. G. Characterization of reactions between water-soluble trialkylphosphines and thiol alkylating reagents: implications for protein-conjugation reactions. *Bioconjugate Chem.* **2016**, *27*, 2400-2406.

44. Ntorla, A., & Burgoyne, J.R. The regulation and function of histone crotonylation. *Cell. Dev. Biol.* **2021**, *9*, 624914.

45. Bos, J., & Muir, T.W. A chemical probe for protein crotonylation. *J. Am. Chem. Soc.* **2018**, *140*, 4757-4760.

46. Hiller, Y., Gershoni, J.M., Bayer, E.A., & Wilchek, M. Biotin binding to avidin. Oligosaccharide side chain not required for ligand association. *Biochem. J.* **1987**, *248*, 167-171.

47. Jain, A., & Cheng, K. (2017). The principles and applications of avidin-based nanoparticles in drug delivery and diagnosis. *J. Control. Release*. **2017**, *245*, 27-40.

48. van Moorsel, M.V.A., Urbanus, R.T., Verhoef, S., Koekman, C.A., Vink, M., Vermonden, T., Maas, C., Pasterkamp, G., & Schiffelers, R.M. A head-to-head comparison of conjugation methods for VHHs: random maleimide-thiol coupling versus controlled click chemistry. *Int. J. Pharm*. **2019**, *1*, 10020.

49. Lockett, M.R., Phillips, M.F., Jarecki, J.L., Peelen, D., & Smith, L.M. A tetrafluorophenyl activated ester self-assembled monolayer for the immobilization of amine-modified oligonucleotides. *Langmuir* **2008**, *24*, 69-75.

50. Matos, M.J. Oliveira, B.L., Martínez-Sáez, N., Guerreiro, A., Cal, P.M.S.D., Bertoldo, J., Maneiro, M., Perkins, E., Howard, J., Deery, M.J., Chalker, J.M., Corzana, F., Jiménez-Osés, G., & Bernardes, G.J.L. Chemo- and regioselective lysine modification on native proteins. *J. Am. Chem. Soc*. **2018**, *140*, 4004-4017.

51. Shadish, J.A., & DeForest, C.A. Site-selective protein modification: from functionalized proteins to functional biomaterials. *Matter* **2020**, *2*, 50-77.

52. Spicer, C.D., & Davis, B.G. Selective chemical protein modification. *Nat. Commun*. **2014**, *5*, 4740.

53. Bootorabi, F., Janis, J., Valjakka, J., Isoniemi, S., Vainiotalo, P., Vullo, D., Supuran, C.T., Waheed, A., Sly, W.S., Niemela, O., & Parkkila, S. Modification of carbonic anhydrase II with acetaldehyde, the first metabolite of ethanol, leads to decreased enzyme activity. *BMC Biochem*. **2008**, *9*, 32.

54. Chen, D., Disotuar, M.M., Xiong, X., Wang, Y., & Hung-Chieh Chou, D. Selective N-terminal functionalization of native peptides and proteins. *Chem. Sci*. **2017**, *4*, 2717-2722.

55. De Rosa, L., Di Stasi, R., Romanelli, A., & D'Andrea, L.D. Exploiting protein N-terminus for site-specific bioconjugation. *Molecules* **2021**, *26*, 3521.

56. Sur, S., Qiao, Y., Fries, A., O'Meally, R.N., Cole, R.N., Kinzler, K.W., Vogelstein, B., & Zhou, S. A protein bioconjugation method with exquisite N-terminal specificity. *Sci. Rep*. **2015**, *5*, 18363.

57. Kolmel, D.K., & Kool, E.T. Oximes and hydrazones in bioconjugation: mechanism and catalysis. *Chem. Rev*. **2017**, *117*, 10358-10376.

58. Spears, R.J., & Fascione, M.A. Site-selective incorporation and ligation of protein aldehydes. *Org. Biomol. Chem*. **2016**, *14*, 7622-7638.

59. Trader, D.J., & Carlson, E.E. Chemoselective hydroxyl group transformation: an elusive target. *Mol. Biosyst.* **2012**, *8*, 2484-2493.

60. Geoghegan, K.F., & Stroh, J.G. Site-directed conjugation of nonpeptide groups to peptides and proteins via periodate oxidation of a 2-amino alcohol. Application to modification at N-terminal serine. *Bioconjugate Chem.* **1992**, *3*, 138-146.

61. Hartmann, R.W., Pijnappel, M., Nilvebrant, J., Helgudottir, H.R., Asbjarnarson, A., Traustadottir, G.A., Gudjonsson, T., Nygren, P.A., Lehmann, F., & Odell, L.R. The Wittig bioconjugation of maleimide derived, water soluble phosphonium ylides to aldehyde-tagged proteins. *Org. Biomol. Chem*. **2021**, *19*, 10417-10423.

62. Matsumoto, T., Isogawa, Y., Minamihata, K., Tanaka, T., & Kondo, A. Twigged streptavidin polymer as a scaffold for protein assembly. *J. Biotechnol*. **2016**, *225*, 61-66.

63. Rashidian, M., Dozier, J.L., & Distefano, M.D. Chemoenzymatic labeling of proteins: techniques and approaches. *Bioconjugate Chem*. **2014**, *24*, 1277-1294.

64. Walsh, S.J., Bargh, J.D., Dannheim, F.M., Hanby, A.R., Seki, H., Counsell, A.J., Ou, X., Fowler, E., Ashman, N., Takada, Y., Isidro-Llobet, A., Parker, J.S., Carroll, J.S., & Spring, D.R. Site-selective modification strategies in antibody–drug conjugates. *Chem. Soc. Rev.* **2021**, *50*, 1305-1353.

65. Walper, S.A., Turner, K.B., & Medintz, I.L. Enzymatic bioconjugation of nanoparticles: developing specificity and control. *Curr. Opin. Biotechnol.* **2015**, *34*, 232-241.

66. Milczek, E.M. Commercial applications for enzyme-mediated protein conjugation: new developments in enzymatic processes to deliver functionalized proteins on the commercial scale. *Chem. Rev.* **2018**, *118*, 119-141.

67. Goldmacher, V.S., & Kovtun, Y.V. Antibody–drug conjugates: using monoclonal antibodies for delivery of cytotoxic payloads to cancer cells. *Ther. Deliv.* **2011**, *2*, 397-416.

68. Dennler, P., Chiotellis, A., Fischer, E., Bregon, D., Belmant, C., Gauthier, L., Lhospice, F., Romagne, F., & Schibli, R. Transglutaminase-based chemo-enzymatic conjugation approach yields homogeneous antibody–drug conjugates. *Bioconjugate Chem*. **2014**, *25*, 569-578.

69. Michon, T., Chenu, M., Kellershon, N., Desmadril, M., & Gueguen, J. Horseradish peroxidase oxidation of tyrosine-containing peptides and their subsequent polymerization: a kinetic study. *Biochem*. **1997**, *36*, 8504-8513.

70. Matsumoto, T., Tanaka, T., & Kondo, A. Sortase A-catalyzed site-specific coimmobilization on microparticles via streptavidin. *Langmuir* **2012**, *28*, 3553-3557.

71. Freund, C., & Schwarzer, D. Engineered sortases in peptide and protein chemistry. *Chembiochem* **2021**, *22*, 1347-1356.

72. Faccio, G. From protein features to sensing surfaces. *Sensors (Basel)*. **2018**, *18*, 1204.

73. Wong, L.S., Khan, F., & Micklefield, J. Selective covalent protein immobilization: strategies and applications. *Chem. Rev*. **2009**, *9*, 4025-4053.

74. Hashemifard, N., Mohsenifar, A., Ranjbar, B., Allameh, A., Lotfi, A.S., & Etemadikia, B. Fabrication and kinetic studies of a novel silver nanoparticles-glucose oxidase bioconjugate. *Anal. Chim. Acta.* **2010**, *675*, 181-184.

75. House, J.L., Anderson, E.M., & Ward, W.K. Immobilization techniques to avoid enzyme loss from oxidase-based biosensors: a one-year study. *J. Diabetes Sci. Technol*. **2007**, *1*, 18-27.

76. Yoo, E.H., & Lee, S.Y. Glucose biosensors: an overview of use in clinical practice. *Sensors (Basel)*. **2010**, *10*, 4558-4576.

77. Yushkova, E.D., Nazarova, E.A., Matyuhina, A.V., Noskova, A.O., Shavronskaya, D.O., Vinogradov, V.V., Skvortsova, N.N., Krivoshapkina, E.F. Application of immobilized enzymes in food industry. *J. Agric. Food Chem*. **2019**, *67*, 11553-11567.

78. Lyu, X., Gonzalez, R., Horton, A., & Li, T. Immobilization of enzymes by polymeric materials. *Catalysts* **2021**, *11*, 1211.

79. Xu, K., Chen, X., Zheng, R., & Zheng, Y. Immobilization of multi-enzymes on support materials for efficient biocatalysis. *Bioeng. Biotechnol*. **2020**, *8*, 660.

80. Lu, T., Chen, X., Shi, Q., Wang, Y., Zhang, P., & Jing, X. The immobilization of proteins on biodegradable fibers via biotin-streptavidin bridges. *Acta Biomater*. **2008**, *4*, 1770-1777.

81. Zimmermann, J.L., Nicolaus, T., Neuert, G., & Blank, K. Thiol-based, site-specific and covalent immobilization of biomolecules for single-molecule experiments. *Nat. Protoc*. **2010**, *5*, 875-985.

82. Sanchez, A., Pedroso, E., & Grandas, A. Oligonucleotide cyclization: the thiol-maleimide reaction revisited. *Chem. Commun*. **2013**, *3*, 309-311.

83. Kantner, T., Alkhawaja, B., & Watts, A.G. In situ quenching of trialkylphosphine reducing agents using water-soluble PEG-azides improves maleimide conjugation to proteins. *ACS Omega*. **2017**, *2*, 5785-5791.

84. Parmar, S., Pawar, S. P., Iyer, R., & Kalia, D. Aldehyde-mediated bioconjugation: via in situ generated ylides. *Chem. Commun.* **2019**, *55*, 14926–14929.

85. Kalia, D., Malekar, P.V., & Parthasarathy, M. Exocyclic olefinic maleimides: synthesis and application for stable and thiol-selective bioconjugation. *Angew. Chem. Int. Ed.* **2016**, *55*, 1432-1435.

86. Kim, H., Cho, S.J., Yoo, M., Kang, S.K., Kim, K.R., Lee, H.H., Song, J.S., Rhee, S.D., Jung, W.H., Ahn, J.H., Jung, J.K., & Jung, K.Y. Synthesis and biological evaluation of thiazole derivatives as GPR119 agonists. *Bioorg. Med. Chem. Lett*. **2017**, *27*, 5213-5220.

87. Jiang, S., Tala, S. R., Lu, H., Zou, P., Avan, I., Ibrahim, T.S., Abo-Dya, N.E., Abdelmajeid, A., Debnath, A. K., & Katritzky, A.R. Design, synthesis, and biological activity of a novel series of 2,5-disubstituted furans/pyrroles as HIV-1 fusion inhibitors targeting Gp41. *Bioorganic Med. Chem. Lett.* **2011**, *21*, 6895–6898.

88. Jung, K.Y., Samadani, R., Chauhan, J., Nevels, K., Yap, J.L., Zhang, J., Worlikar, S., Lanning, M.E., Chen, L., Ensey, M., Shukla, S., Salmo, R., Heinzl, G., Gordon, C., Dukes, T., MacKerell, A. D., Shapiro, P., & Fletcher, S. Structural modifications of (Z)-3-(2-aminoethyl)-5-(4-ethoxybenzylidene) thiazolidine-2,4-dione that improve selectivity for inhibiting the proliferation of melanoma cells containing active ERK signaling. *Org. Biomol. Chem.* **2013**, *11*, 3706–3732.

89. Kaur, A., Kaur., M., & Singh, B. One-pot regioselective synthesis of novel 1-*N*-methyl-spiro[2,3′] oxindole-spiro[3,3″]-1″-*N*-arylpyrrolidine-2″,5′-dione-4-arylpyrrolidines through multicomponent 1,3-dipolar cycloaddition reaction of azomethine ylide. *J. Heterocyclic Chem.* **2015**, *46*, 827-833.

90. 11. Luo, Y., Ma, L., Zheng, H., Chen, L., Li, R., He, C., Yang, S., Ye, X., Chen, Z., Li, Z., Gao, Y., Han, J., He, G., Yang, L., & Wei, Y. Discovery of (Z)-5-(4-methoxybenzylidene)thiazolidine-2,4-dione, a readily available and orally active glitazone for the treatment of concanavalin a-induced acute liver injury of BALB/c mice. *J. Med. Chem.* **2010**, *53*, 273–281.

91. Brackman, G., Al Quntar, A.A.A., Enk, C.D., Karalic, I., Nelis, H.J., Van Calenbergh, S., Srebnik, M., & Coenye, T. Synthesis and evaluation of thiazolidinedione and dioxazaborocane analogues as inhibitors of AI-2 quorum sensing in *Vibrio harveyi*. *Bioorganic Med. Chem.* **2013**, *21*, 660-667.

92. Keil, A.M., Frederick, D.M., Jacinto, E.Y., Kennedy, E.L., Zauhar, R.J., West, N.M., Tchao, R., & Harvison, P. J. Cytotoxicity of thiazolidinedione-, oxazolidinedione- and pyrrolidinedione-ring containing compounds in HepG2 cells. *Toxicol. Vitr.* **2015**, *29*, 1887–1896.

93. Zhang, L., Liu, W., Mao, F., Zhu, J., Dong, G., Jiang, H., Sheng, C., Miao, L., Huang, L., & Li, J. Discovery of benzylidene derivatives as potent syk inhibitors: synthesis, SAR analysis, and biological evaluation. *Arch. Pharm. (Weinheim).* **2015**, *348*, 463–474.

94. Spicer, J.A., Huttunen, K.M., Miller, C.K., Denny, W.A., Ciccone, A., Browne, K.A., & Trapani, J.A. Inhibition of the pore-forming protein perforin by a series of aryl-substituted isobenzofuran-1(3H)-ones. *Bioorganic Med. Chem.* **2012**, *20*, 1319–1336.

95. Ha, Y.M., Kim, J. A., Park, Y.J., Park, D., Choi, Y.J., Kim, J.M., Chung, K.W., Han, Y.K., Park, J.Y., Lee, J. Y., Moon, H.R., & Chung, H.Y. Synthesis and biological activity of hydroxybenzylidenyl pyrrolidine-2,5-dione derivatives as new potent inhibitors of tyrosinase. *Med. Chem. Comm.* **2011**, *2*, 542–549.

96. Paternotte, I., Fan, H.J., Scrève, P., Claesen, M., Tulkens, P. M., & Sonveaux, E. Syntheses and hydrolysis of basic and dibasic ampicillin esters tailored for intracellular accumulation. *Bioorganic Med. Chem.* **2001**, *9*, 493–502.

97. Bayat, M., Hosseini, S.R., & Asmari, E. Simple synthesis of (E) and (Z)-2-(arylmethylidene)-n-phenyl succinimides via wittig olefination by using PS-TPP resin. *Phosphorous Sulfur Silicon Relat. Elem.* **2017**, *192*, 98-102.

98. Moussa, Z., Judeh, Z.M.A., & Ahmed, S.A. Polymer-supported triphenylphosphine: application in organic synthesis and organometallic reactions. *RSC Adv.* **2019**, *9*, 35217–35272.

99. Lum, K.M., Xavier, V.J., Onh, M.J.H., Johannes, C.W., & Chan, K.P. Stabilized wittig olefination for bioconjugation. *Chem. Commun.* **2013**, *49*, 11188-11190.

100. Han, M.J., Xiong, D.C., & Ye, X.S. Enabling wittig reaction on site-specific protein modification. *Chem. Commun.* **2012**, *48*, 11079-11081.

101. El-Batta, A., Jiang, C., Zhao, W., Anness, R., Cooksy, A.L., & Bergdahl, M. Wittig reactions in water media employing stabilized ylides with aldehydes. Synthesis of a,B-unsaturated esters from mixing aldehydes, a-bromoesters and Ph_3P in aqueous $NaHCO_3$. *J. Org. Chem.* **2007**, *72*, 5244-5259.

102. Wu, J., Zhang, D., & Wei, S. Wittig reactions of stabilized phosphorous ylides with aldehydes in water. *Synth. Commun.* **2005**, *35*, 1213-1222.

103. Sieber, F., Wentworth, P., Toker, J.D., Wentworth, A.D., Metz, W.A., Reed, N.N., & Janda, K.D. Development and application of a poly(ethylene glycol)-supported triarylphosphine reagent: expanding the sphere of liquid-phase organic synthesis. *J. Org. Chem*. **1999**, *64*, 5188-5192.

104. Flenniken, M.L., Uchida, M., Liepold, L.O., Kang, S., Young, M.J., & Douglas, T. (**2009**). A library of protein cage architectures as nanomaterials. In: *Viruses and Nanotechnology Current Topics in Microbiology and Immunology*. Springer: Berlin, Heidelberg, Germany, pp. 71–93.

105. Jutz, G., Rijn, P.V., Miranda, B. S., & Böker, A. Ferritin: a versatile building block for bionanotechnology. *Chem. Rev.* **2015**, *115*, 1653-1701.

106. Tatur, J., Hagedoorn, P.L., Overeijnder, M.L., & Hagen, W.R. A highly thermostable ferritin from the hyperthermophilic archaeal anaerobe *Pyrococcus furiosus*. *Extremophiles* **2006**, *10*(2), 139-148.

107. Lavecchia, R., & Zugaro, M. Thermal denaturation of erythrocyte carbonic anhydrase. *FEBS Lett.* **1991**, *292*, 162-164.

108. Saito, R., Sato, T., Ikai, A., & Tanaka, N. Structure of bovine carbonic anhydrase II at 1.95 Å resolution. *Acta Cryst.* **2004**, *60*, 792-795.

109. Capasso, C., De Luca, V., Carginale, V., Cannio, R., & Rossi, M. Biochemical properties of a novel and highly thermostable bacterial α-carbonic anhydrase from Sulfurihydrogenibium yellowstonense YO3AOP1. *J. Enzyme Inhib. Med. Chem.* **2012**, *27*, 892-897.

110. Pocker, Y., & Stone, J.T. The catalytic versatility of erythrocyte carbonic anhydrase III. Kinetic studies of the enzyme-catalyzed hydrolysis of p-nitrophenyl acetate. *Biochem.* **1967**, *6*, 668-678.

111. Pocker, Y., Meany, J.E., & Davis, B.C. Alpha-keto esters as substrates of erythrocyte carbonic anhydrase. Kinetic studies of enzyme-catalyzed hydration of methyl and ethyl pyruvate. *Biochem*. **1974**, *13*, 1411-1416.

112. Gyamfi, H. (**2019**). Protein engineering of microbial ferritins. (Doctoral dissertation). Retrieved from: UWSpace*, https://uwspace.uwaterloo.ca/handle/10012/15116

113. Merza, F. (**2020**). Supramolecular assembly of three-dimensional protein networks. (Masters thesis). Retrieved from: UWSpace, https://uwspace.uwaterloo.ca/handle/10012/16233

114. Pal, B., Pradhan, P.K., Jaisankar, P., & Giri, V.S. First triphenylphosphine promoted reduction of maleimides to succinimides. *Synthesis* **2003**, *10*, 1549-1552.

115. Buchmeiser, M.R. (**2003**). Organic synthesis on polymeric supports. In: *Polymeric Materials in Organic Synthesis and Catalysis*. Wiley-VCH: Weinheim, Germany, pp. 137-199.

116. Bhattacharyya, S. Polymer-assisted solution-phase organic synthesis: advances in multi-step synthetic applications. *Indian J. Chem*. **2001**, *40*, 878-890.

117. Abdildinova, A., & Gong, Y.D. Current parallel solid-phase synthesis of drug-like oxadiazole and thiadiazole derivatives for combinatorial chemistry. *ACS Comb. Sci.* **2018**, *20*, 309-329.

118. Vaino, A.R., & Janda, K.D. Solid-phase organic synthesis: a critical understanding of the resin. *J. Comb. Chem*. **2000**, *2*, 579-596.

119. Kaur, N. Solid-phase synthesis of sulfur containing heterocycles. *J. Sulphur. Chem*. **2018**, *39*, 544-577.

120. Tulla-Puche, J., & Albericio, F. (**2008**). The (classic concept of) solid support. In: *The Power of Functional Resins in Organic Synthesis*. Wiley-VCH: Weinheim, Germany, pp. 3-12.

121. Thomas, G.L., Bohner, C., Ladlow, M., & Spring, D.R. Synthesis and utilization of functionalized polystyrene resins. *Tetrahedron* **2005**, *61*, 12153-12159.

122. Charette, A.B., Boezio, A.A., & Janes, M.K. Synthesis of a triphenylphosphine reagent on non-cross-linked polystyrene support: application to the staudinger/aza-wittig reaction. *Org. Lett.* **2000**, *2*, 3777-3779.

123. Westman, J. An efficient combination of microwave dielectric heating and the use of solid-supported triphenylphosphine for wittig reactions. *Org. Lett*. **2001**, *3*, 3745-3747.

124. Buchmeiser, M.R. (**2003**). Supported reagents and scavengers in multi-step organic synthesis. In: *Polymeric Materials in Organic Synthesis and Catalysis*. Wiley-VCH: Weinheim, Germany, pp. 53-136.

125. Tulla-Puche, J., & Albericio, F. (**2008**). Nucleophilic, electrophilic, and radical reactions. In: *The Power of Functional Resins in Organic Synthesis*. Wiley-VCH: Weinheim, Germany, pp. 121-137.

126. Choi, M.K.W., He, H.S., & Toy, P.H. Direct radical polymerization of 4-styryldiphenylphosphine: preparation of cross-linked and non-cross-linked triphenylphosphine-containing polystyrene polymers. *J. Org. Chem*. **2003**, *68*, 9831-9834.

127. Lopez, J., Pletscher, S., Aemissegger, A., Bucher, C., & Gallou, F. X N-Butylpyrrolidinone as alternative solvent for solid-phase peptide synthesis. *Org. Process Res. Dev*. **2018**, *22*, 494-503.

128. Yan, L., Wenguo, Y., Lixin, L., Yang, S., & Zhiyong, J. A One-pot green synthesis of alkylidenesuccinimides. *Chin. J. Chem.* **2011**, *29*, 1906-1910.

129. Zitterbart, R., Berger, N., Reimann, O., Noble, G.T., Ludtke, S., Sarma, D., & Seitz, O. Traceless parallel peptide purification by a first-in-class reductively cleavable linker system featuring a safety-release. *Chem. Sci.* **2021**, *12*, 2389-2396.

130. Kheirabadi, M., Creech, G.S., Qiao, J.X., Nirschl, D.S., Leahy, D.K., Boy, K.M., Carter, P.H., & Eastgate, M.D. Leveraging a "catch–release" logic gate process for the synthesis and nonchromatographic purification of thioether or amine-bridged macrocyclic peptides. *J. Org. Chem.* **2018**, *83*, 4323-4335.

131. Egusa, K., Kusumoto, S., & Fukase, K. A new catch-and-release purification method using a 4-azido-3-chlorobenzyl group. *Synlett*. **2001**, *6*, 777-780.

132. Ley, S.V., & Baxendale, I.R. New tools and concepts for modern organic synthesis. *Nat. Rev. Drug Discov*. **2002**, *1*, 573-586.

133. Musonda, C.C., Gut, J., Rosenthal, P.J., Yardley, V., Carvalho de Souza, R.C., & Chibale, K. Application of multicomponent reactions to antimalarial drug discovery. Part 2: New antiplasmodial and antitrypanosomal 4-aminoquinoline γ- and δ-lactams via a 'catch and release' protocol. *Bioorg. Med. Chem*. **2006**, *14*, 5605-5615.

134. Porcheddu, A., Giacomelli, G., & Piredda, I. Parallel synthesis of trisubstituted formamidines: a facile and versatile procedure. *J. Comb. Chem.* **2009**, *11*, 126-130.

135. Emerson, D.W., Emerson, R.R., Joshi, S.C., Sorensen, E.M., & Turek, J.E. Polymer-bound sulfonylhydrazine functionality. Preparation, characterization, and reactions of copoly(styrene-divinylbenzenesulfonylhydrazine). *J. Org. Chem*. **1979**, *44*, 4634-4640.

136. Zhu, M., Ruijter, E., & Wessjohann, L.A. New scavenger resin for the reversible linking and monoprotection of functionalized aromatic aldehydes. *Org. Lett*. **2004**, *6*, 3921-3024.

137. Gedye, R., Smith, F., Westaway, K., Ali, H., Baldisera, L., Laberge, L., & Rousell, J. The use of microwave ovens for rapid organic synthesis. *Tetrahedron Lett*. **1986**, *3*, 279-282.

138. Stefanidis, G., & Stankiewicz, A. (**2016**). Microwave-assisted green organic synthesis. In: *Alternative Energy Sources for Green Chemistry*. The Royal Society of Chemistry: Cambridge, United Kingdom, pp. 1-33.

139. Gawande, M.B., Shelke, S.N., Zboril, R., & Varma, R.S. Microwave-assisted chemistry: synthetic applications for rapid assembly of nanomaterials and organics. *Acc. Chem. Res*. **2014**, *7*, 1338-1348.

140. Sharma, N., Sharma, U.K., & Van der Eycken, E.V. (**2018**). Microwave-assisted organic synthesis: overview of recent applications. In: *Green Techniques for Organic Synthesis and Medicinal Chemistry, Second Edition*. John Wiley & Sons, Ltd: Chichester, United Kingdom, pp. 441-468.

141. Tierney, J.P., & Lidstrom, P. (**2005**). Theoretical aspects of microwave dielectric heating. In: *Microwave Assisted Organic Synthesis*. Blackwell Publishing CRC Press: Oxford, United Kingdom, pp. 1-21.

142. Lide, D.R. (**2003**). Physical constants of organic compounds. In: *CRC Handbook of Chemistry and Physics, 84ᵗʰ Ed*. CRC Press: Oxford, United Kingdom, pp. 3-1 – 3-573.

143. Kieliszek, M. & Misiewicz, A. Microbial transglutaminase and its application in the food industry. A review. *Folia Microbiol*. **2014**, *59*, 241-250.

144. Fontana, A., Spolaore, B., Mero, A., & Veronese, F.M. Site-specific modification and PEGylation of pharmaceutical proteins mediated by transglutaminase. *Adv. Drug Deliv. Rev*. **2008**, *60*, 13-28.

145. Griffin, M., Casadio, R., & Bergamini, C. Transglutaminases: nature's biological glues. *Biochem. J*. **2002**, *368*, 377-396.

146. Camolezi Gaspar, A.L., & Pedroso de Goes-Favoni, S. Action of microbial transglutaminase (MTGase) in the modification of food proteins: a review. *Food Chem.* **2015**, *171*, 315-322.

147. Nieuwenhuizen, W., Dekker, H.L., de Koning, L.J., Groneveld, T., de Koster, C.G., & de Jong, J.A.H. Modification of glutamine and lysine residues in holo and apo alpha-lactalbumin with microbial transglutaminase. *J. Agric. Food Chem.* **2003**, *51*, 132-139.

148. Strop, P. Versatility of microbial transglutaminase. *Bioconjugate Chem*. **2014**, *25*, 855-862.

149. Oteng-Pabi, S.K., Pardin, C., Stoica, M., & Keillor, J.W. Site-specific protein labelling and immobilization mediated by microbial transglutaminase. *Chem. Commun*. **2014**, *50*, 6604-6606.

150. Rachel, N.M., Toulouse, J.L., & Pelletier, J.N. Transglutaminase-catalyzed bioconjugation using one-pot metal-free bioorthogonal chemistry. *Bioconjugate Chem.* **2017**, *28*, 2518-2523.

151. Schneider, H., Deweid, L., Avrutina, O., & Kolmar, H. Recent progress in transglutaminase-mediated assembly of antibody-drug conjugates. *Anal. Biochem.* **2020**, *595*, 113615.

152. Steffen, W., Ko, F.C., Patel, J., Lyamichev, V., Albert, T.J., Benz, J., Rudolph, M.G., Bergmann, F., Streidl, T., Kratzsch, P., Boenitz-Dulat, M., Oelschlaegel, T., & Schraeml, M. Discovery of a microbial transglutaminase enabling highly site-specific labeling of proteins. *J. Biol. Chem*. **2017**, *292*, 15622-15635.

153. Zhang, L., Zhang, L., Yi, H., Du, M., Han, X., Feng, Z., Jiao, Y., & Zhang, Y. Enzymatic characterization of transglutaminase from Streptomyces mobaraensis DSM 40587 in high salt and effect of enzymatic cross-linking of yak milk proteins on functional properties of stirred yogurt. *J. Dairy Sci*. **2012**, *95*, 3559-3568.

154. Fontana, A., Spolaore, B., Mero, A., & Veronese, F.M. (**2009**). The site-specific TGase-mediated PEGylation of proteins occurs at flexible sites. In: *PEGylated Protein Drugs: Basic Science and Clinical Applications*. Birkhauser, Springer: Basel, Switzerland, pp. 89-112.

155. Mero, A., Spolaore, B., Veronese, F.M., & Fontana, A. Transglutaminase-mediated PEGylation of proteins: direct identification of the sites of protein modification by mass spectrometry using a novel monodisperse PEG. *Bioconjugate Chem*. **2009**, *20*, 384-389.

156. Herrera Belen, L., de Oliviera Rangel-Yagui, C., Lissabet, J.F.B., Effer, B., Lee-Estevez, M., Pessoa, A., Castillo, R.L., & Farias, J.G. From synthesis to characterization of site-selective PEGylated proteins. *Front. Pharmacol.* **2019**, *10*, 1450.

157. Grigoletto, A., Mero, A., Yoshioka, H., Schiavon, O., & Pasut, G. Covalent immobilisation of transglutaminase: stability and applications in protein PEGylation. *J. Drug Target.* **2017**, *25*, 856-864.

158. Ko, J.H., & Maynard, H.D. A guide to maximizing the therapeutic potential of protein-polymer conjugates by rational design. *Chem. Soc. Rev.* **2018**, *47*, 8998-9014.

159. Ebenig, A., Juettner, N.E., Deweid, L., Avrutina, O., Fuchsbauer, H.L., & Kolmar, H. Efficient site-specific antibody–drug conjugation by engineering a nature-derived recognition tag for microbial transglutaminase. *ChemBioChem* **2019**, *20*, 2411-2419.

160. Agarwal, P., & Bertozzi, C.R. Site-specific antibody–drug conjugates: the nexus of bioorthogonal chemistry, protein engineering, and drug development. *Bioconjugate Chem.* **2015**, *26*, 176-192.

161. Yamakazi, C.M., Yamaguchi, A., Anami, Y., Xiong, W., Otani, Y., Lee, J., Ueno, N.T., Zhang, N., An, Z., & Tsuchikama, K. Antibody-drug conjugates with dual payloads for combating breast tumor heterogeneity and drug resistance. *Nat. Commun.* **2021**, *12*, 3528.

162. Kashiwagi, T., Yokoyama, K., Ishikawa, K., Ono, K., Ejima, D., Matsui, H., Suzuki, E. Crystal structure of microbial transglutaminase from *Streptoverticillium mobaraense*. *J. Biol. Chem.* **2002**, *277*, 44252-44260.

163. Spolaore, B., Raboni, S., Molina, A.R., Satwekar, A.A., Damiano, N., & Fontana, A. Local unfolding is required for the site-specific protein modification by transglutaminase. *Biochem.* **2012**, *51*, 8679-8689.

164. Spolaore, B., Damiano, N., Raboni, S., & Fontana, A. Site-specific derivatization of avidin using microbial transglutaminase. *Bioconjugate Chem.* **2014**, *25*, 470-480.

165. Spolaore, B., Raboni, S., Satwekar, A.A., Grigoletto, A., Mero, A., Montagner, I.M., Rosato, A., Pasut, G., & Fontana, A. Site-specific transglutaminase-mediated conjugation of interferon α-2b at glutamine or lysine residues. *Bioconjugate Chem.* **2016**, *27*, 2695-2706.

166. Giosafatto, C.V.L., Fusco, A., Al-Asmar, A., & Mariniello, L. Microbial transglutaminase as a tool to improve the features of hydrocolloid-based bioplastics. *Int. J. Mol. Sci.* **2020**, *21*, 3656.

167. Csosz, E., Mesko, B., & Fesus, L. Transdab wiki: the interactive transglutaminase substrate database on web 2.0 surface. *Amino Acids* **2009**, *36*, 615-617.

168. Zaia, J., Annan, R.S., & Biemann, K. The correct molecular weight of myoglobin, a common calibrant for mass spectrometry. *Rapid Commun. Mass Spectrom.* **1992**, *1*, 32-36.

169. Fontana, A., Zambonin, A., Polverino de Laureto, P., de Filippis, V., Clementi, A., & Scaramella, E. Probing the conformational state of apomyoglobin by limited proteolysis. *J. Mol. Biol*. **1997**, *266*, 223-230.

170. Keillor, J.W., Apperley, K.Y.P., & Akbar, A. Inhibitors of tissue transglutaminase. *Trends Pharmacol. Sci*. **2015**, *36*, 32-40.

171. Oertel, K. Michael systems as transglutaminases inhibitors. U.S. Patent 8471,063 B2, May 15th, 2008.

172. Ando, H., Adachi, M., Umeda, K., Matsuura, A., Nonaka, M., Uchio, R., Tanaka, H., & Motoki, M. Purification and characteristics of a novel transglutaminase derived from microorganisms. *Agric. Biol. Chem*. **1989**, *53*, 2613-2617.

173. Ascoli, F., Rossi Fanelli, M.R., & Antonini, E. Preparation and properties of apohemoglobin and reconstituted hemoglobins. *Methods. Enzymol*. **1981**, *76*, 72–87.

174. Bradford, M. A rapid and sensitive method for the quantitation of microgram quantities of protein utilizing the principle of protein-dye binding. *Anal. Biochem*. **1976**, *72*, 248-254.

Appendix A: ^{31}P NMR, ^{1}H NMR, and ESI MS Spectra

bis(p-sulfonatophenyl) phenyl phosphine
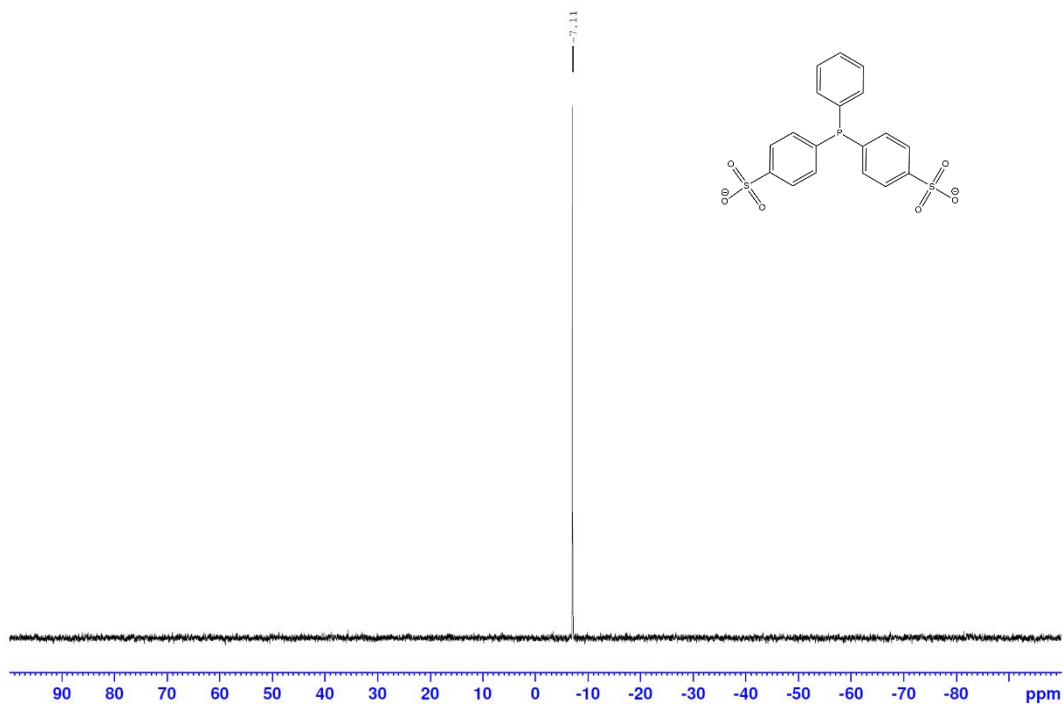
Figure A.1. ^{31}P NMR spectrum of BSTPP (solvent: ddH$_2$O).

BS-TPP:NEM
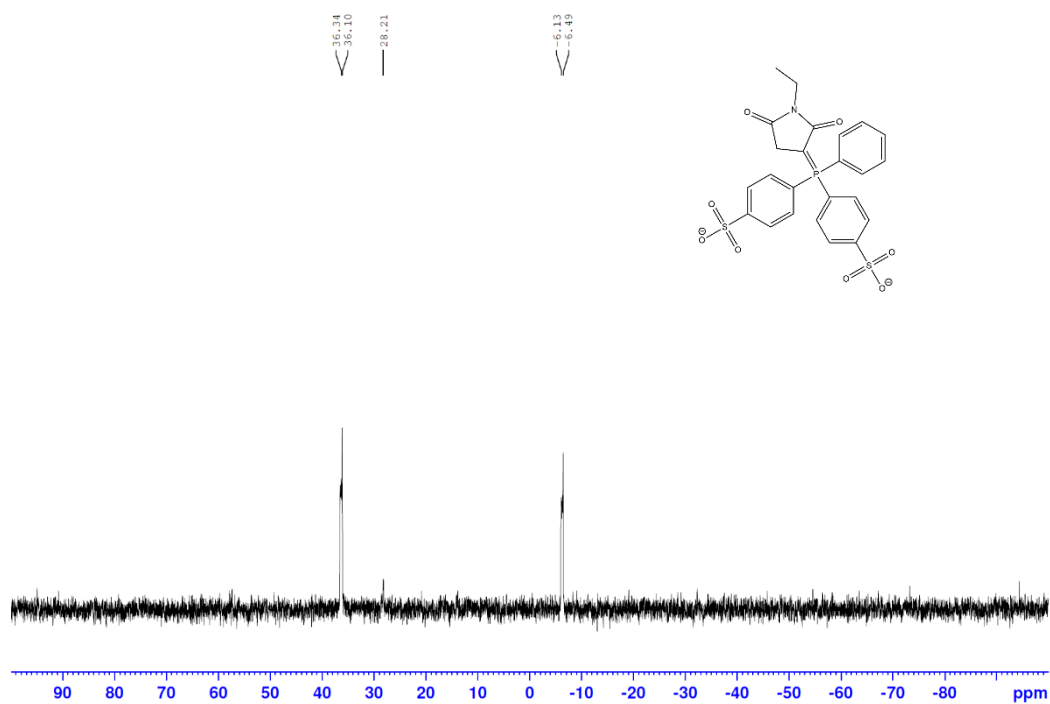
Figure A.2. ^{31}P NMR spectrum of NEM-BSTPP (solvent: ddH$_2$O).

154
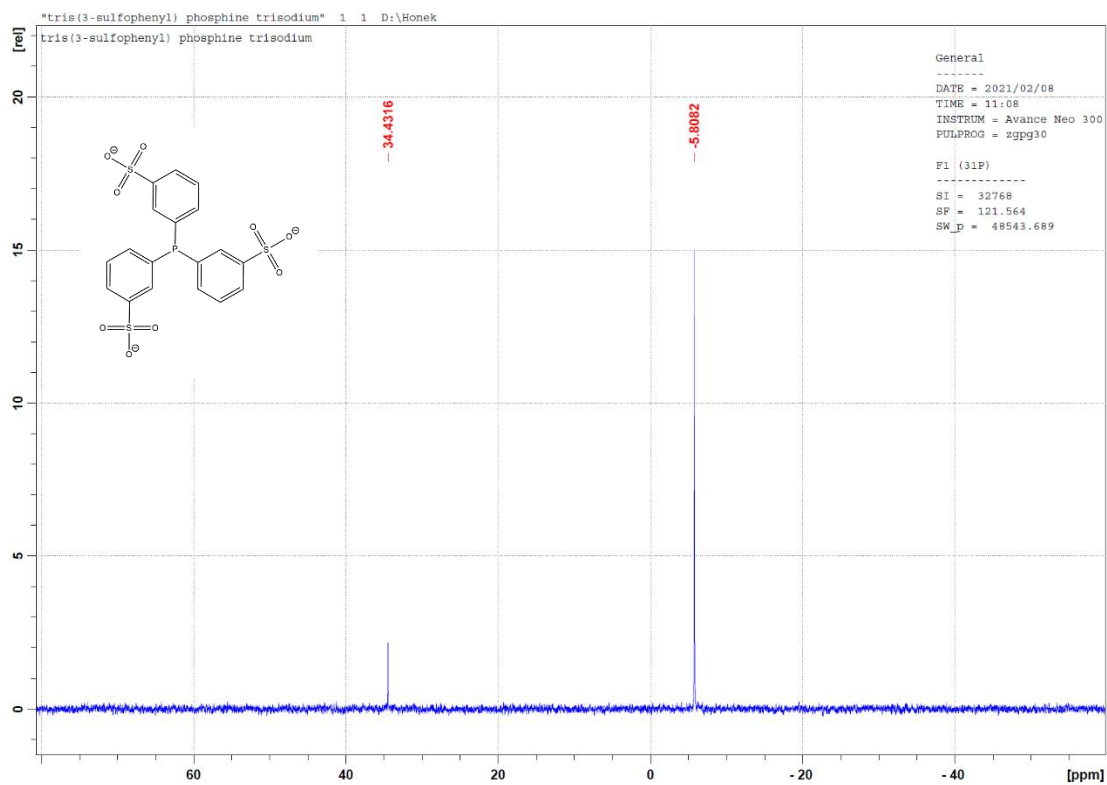
Figure A.3. ^{31}P NMR spectrum of TSTPP (solvent: ddH$_2$O).
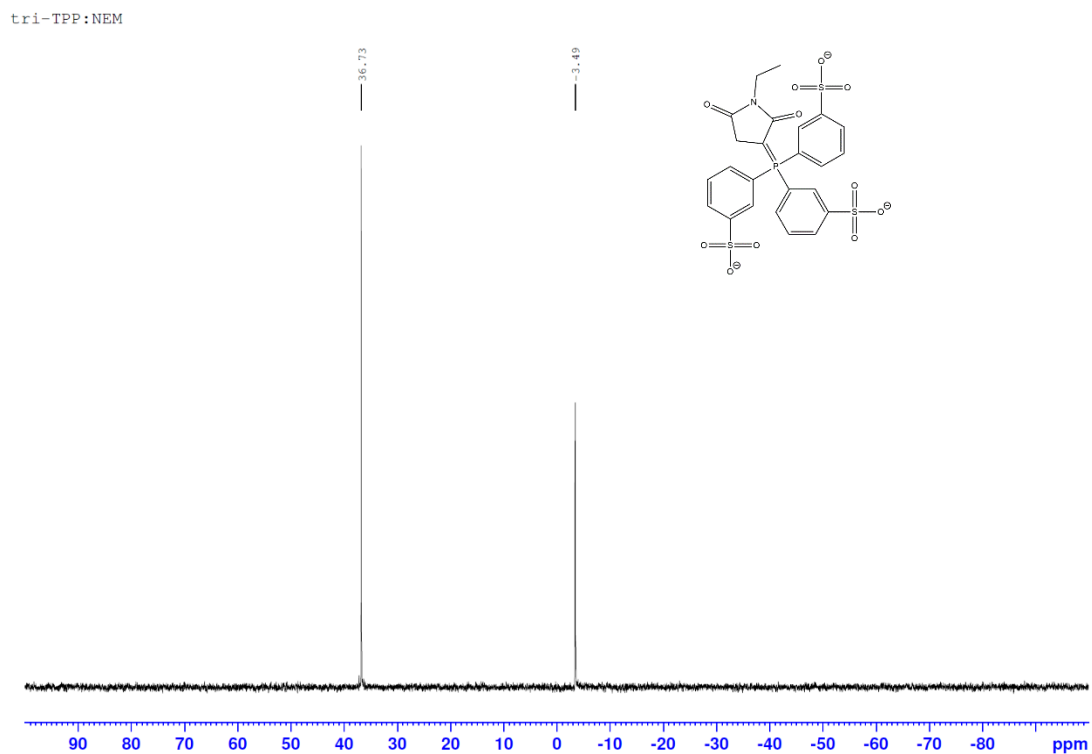
Figure A.4. ^{31}P NMR spectrum of NEM-TSTPP (solvent: ddH$_2$O).

Figure A.5. ^{31}P NMR spectrum of PEGTPP (solvent: ddH$_2$O).

Figure A.6. ^{31}P NMR spectrum of NEM-PEGTPP (solvent: ddH$_2$O).

tris (2-carboxyethylphosphine) (TCEP)
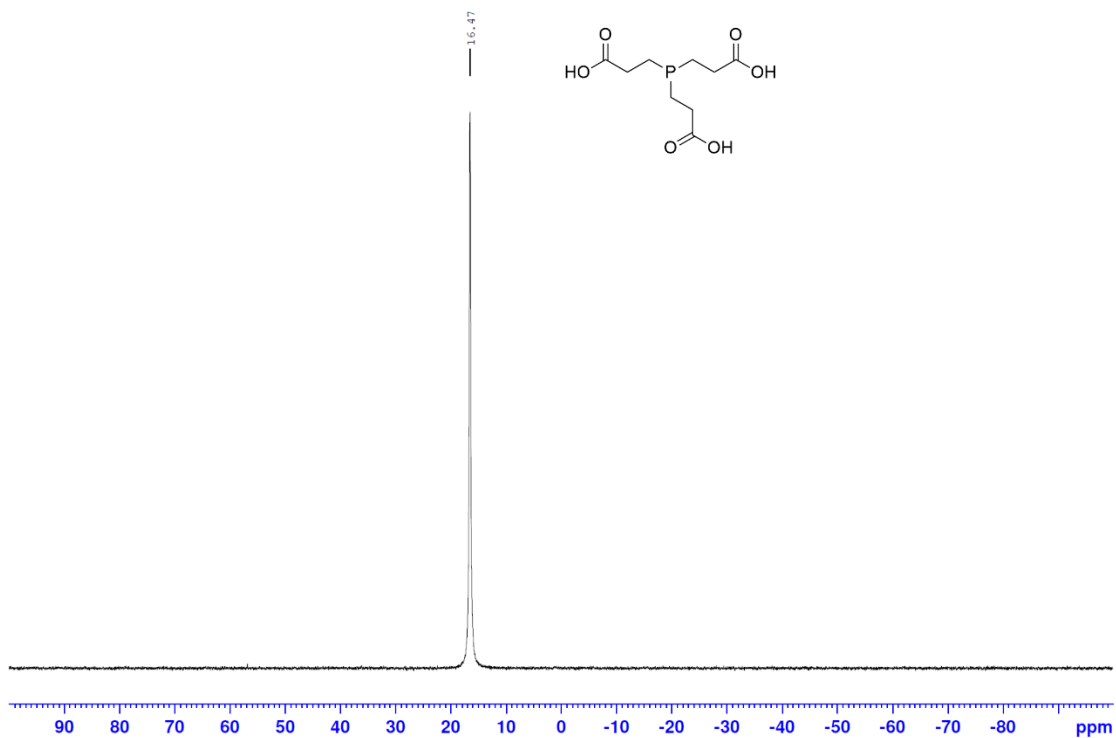
Figure A.7. ^{31}P NMR spectrum of TCEP (solvent: ddH$_2$O).
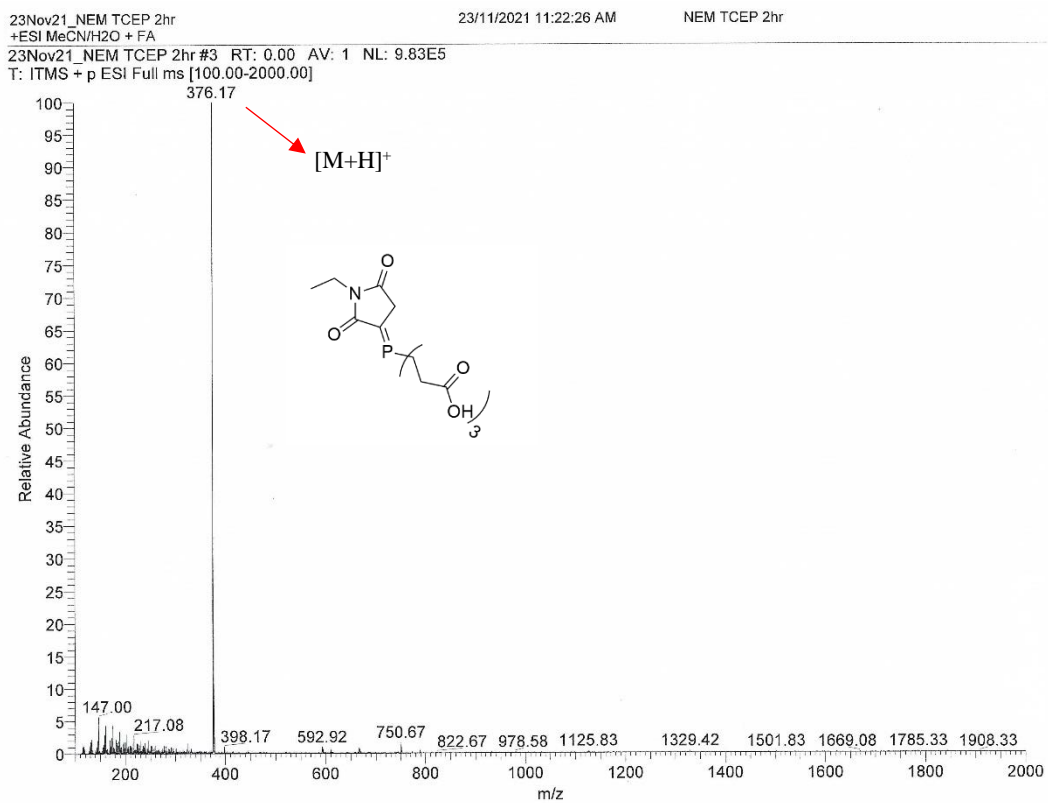
Figure A.8. Low resolution ESI MS of NEM-TCEP (2 hours).
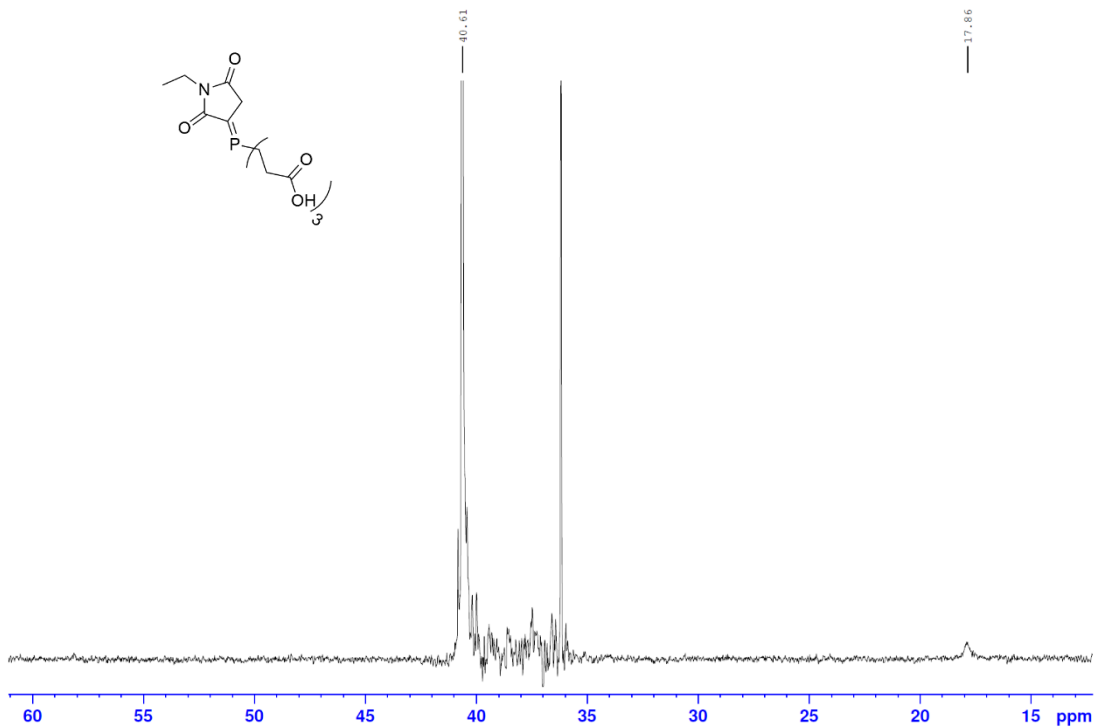
Figure A.9. ^{31}P NMR spectrum of NEM-TCEP (2 hours) (solvent: ddH$_2$O).
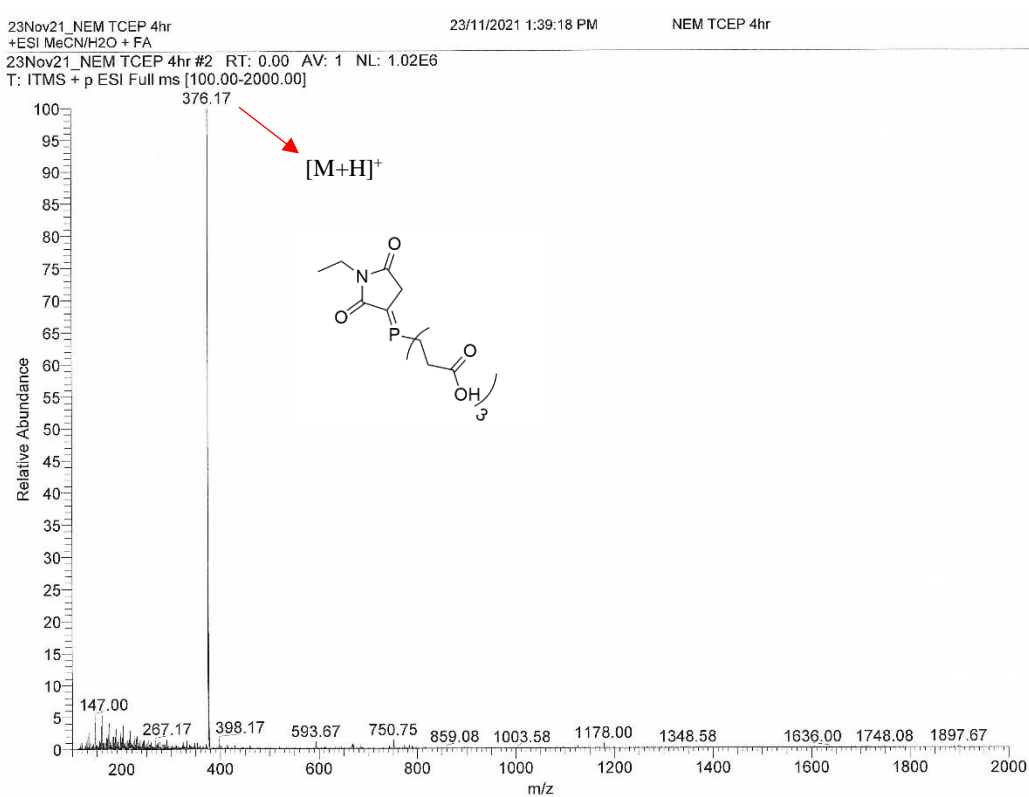
Figure A.10. Low resolution ESI MS of NEM-TCEP (4 hours).
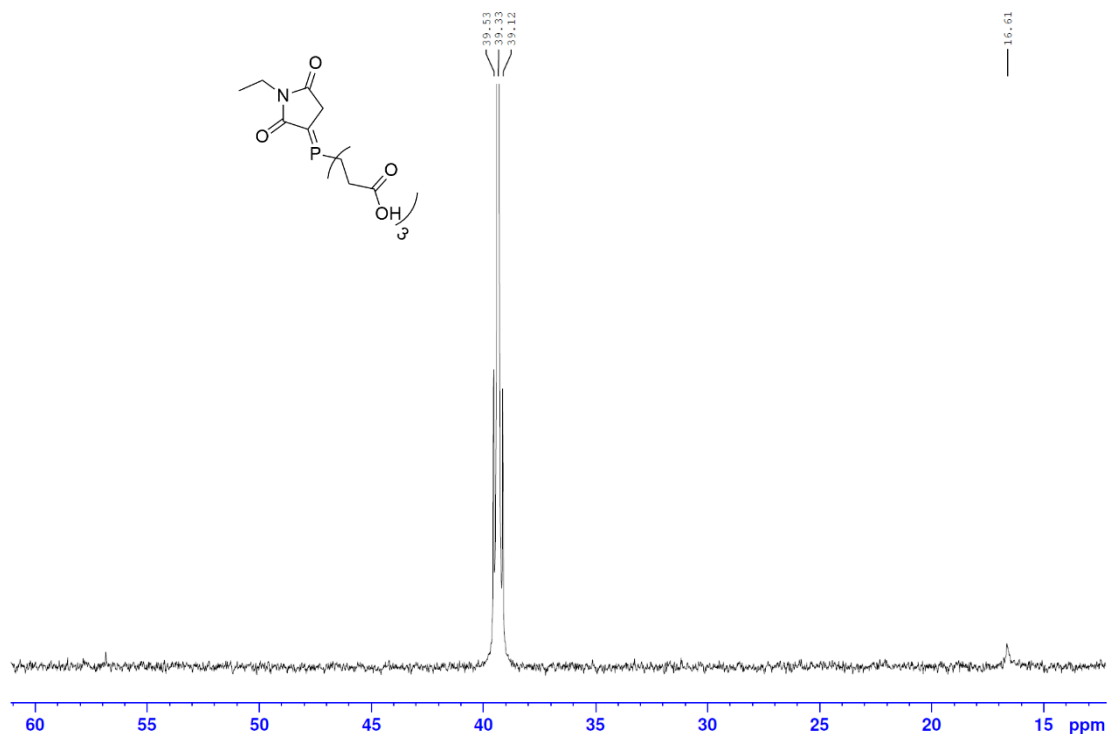
Figure A.11. ^{31}P NMR spectrum of NEM-TCEP (4 hours) (solvent: ddH$_2$O).
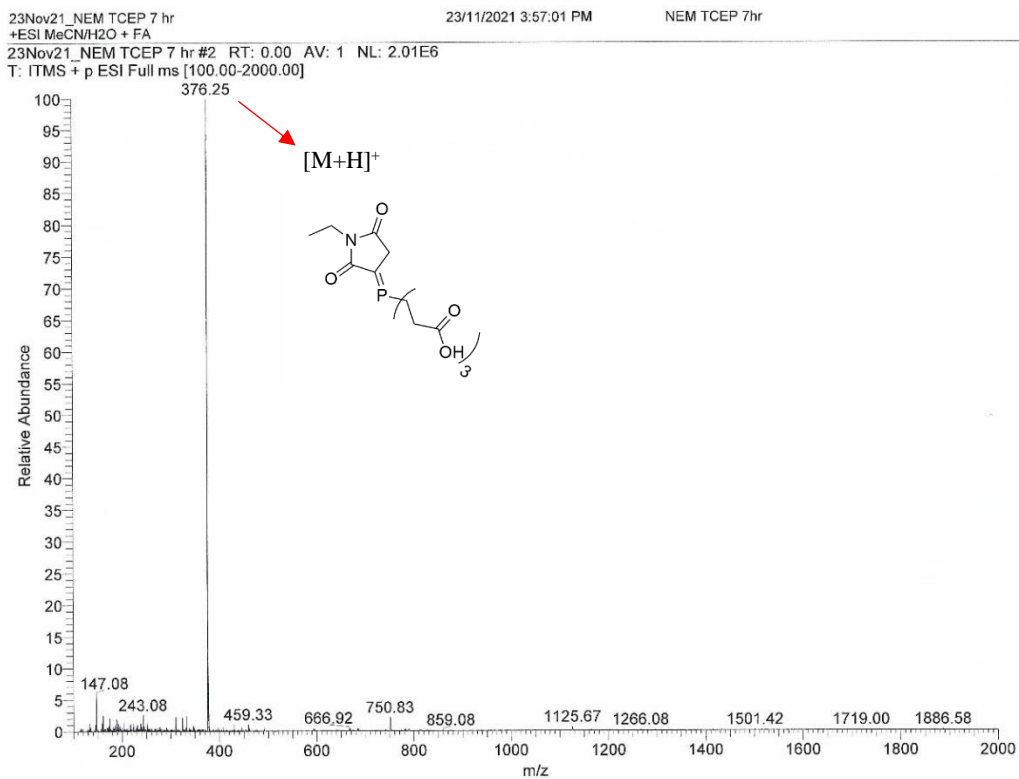
Figure A.12. Low resolution ESI MS of NEM-TCEP (6 hours).

159
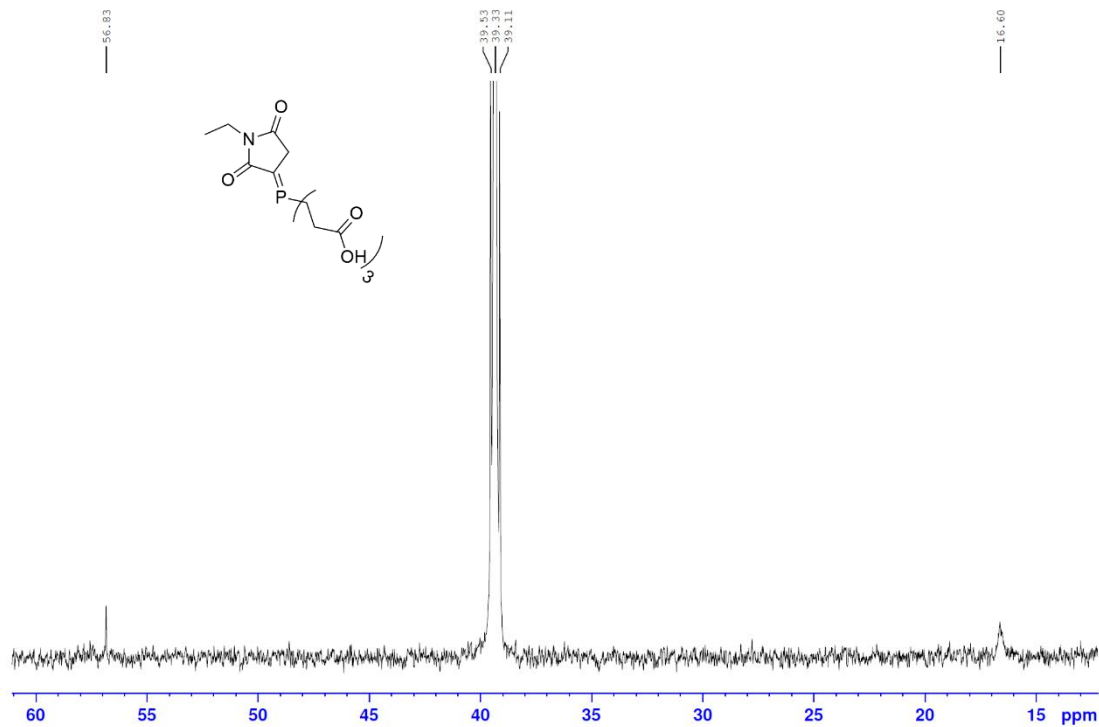
Figure A.13. ^{31}P NMR spectrum of NEM-TCEP (6 hours) (solvent: ddH$_2$O).
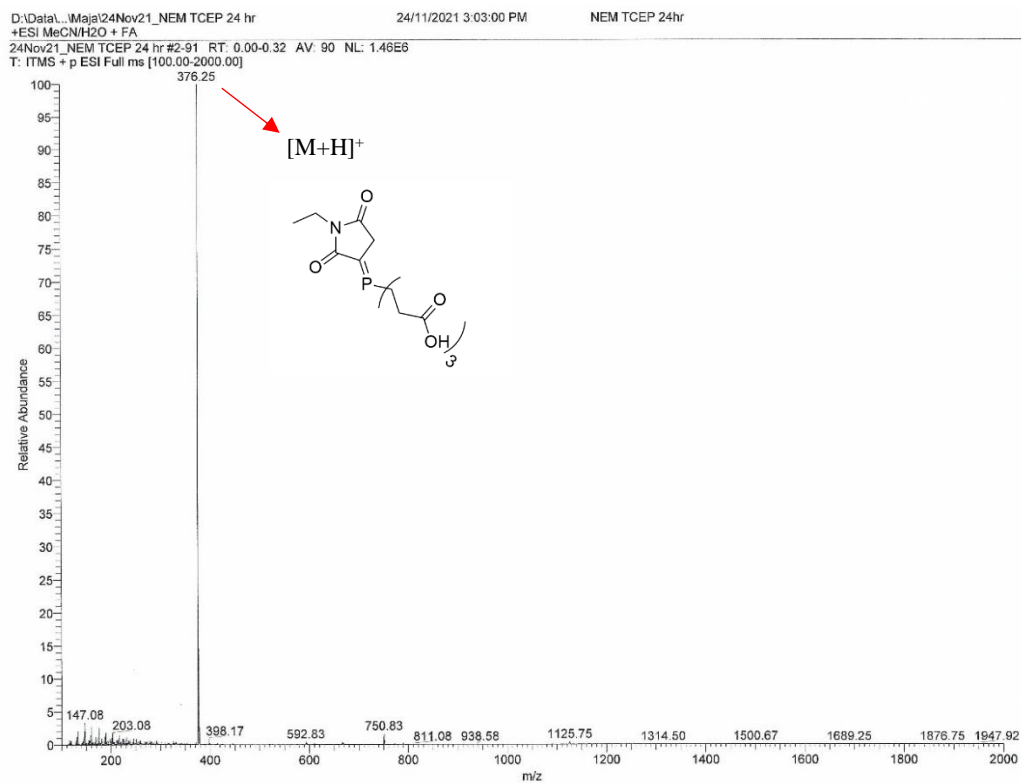
Figure A.14. Low resolution ESI MS of NEM-TCEP (24 hours).
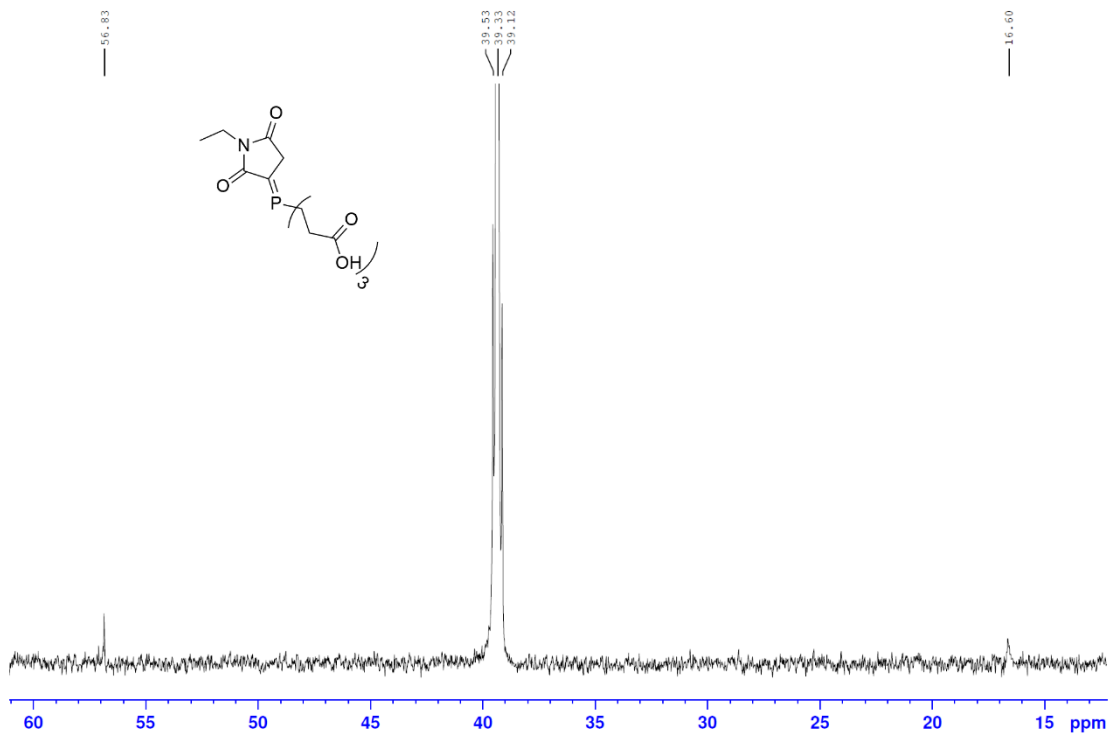
Figure A.15. ^{31}P NMR spectrum of NEM-TCEP (24 hours) (solvent: ddH$_2$O).
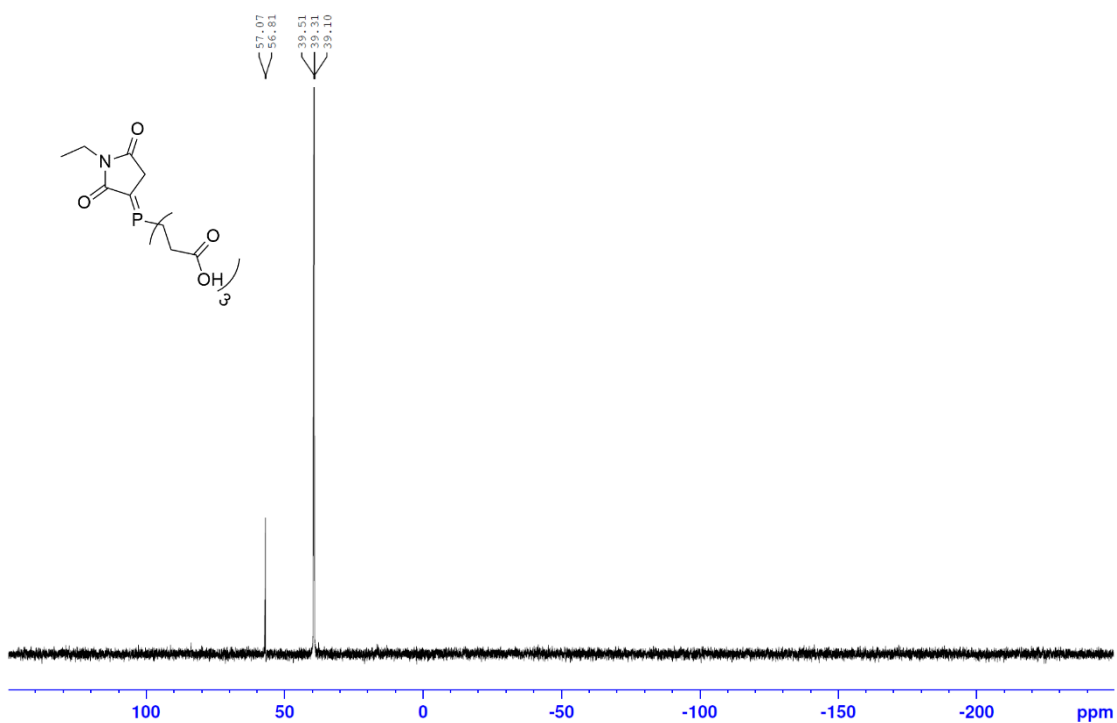
Figure A.16. ^{31}P NMR spectrum of NEM-TCEP (1 week) (solvent: ddH$_2$O).

Figure A.17. ^{31}P NMR spectrum of TPP (solvent: DMF).

NEM TPP in DMF
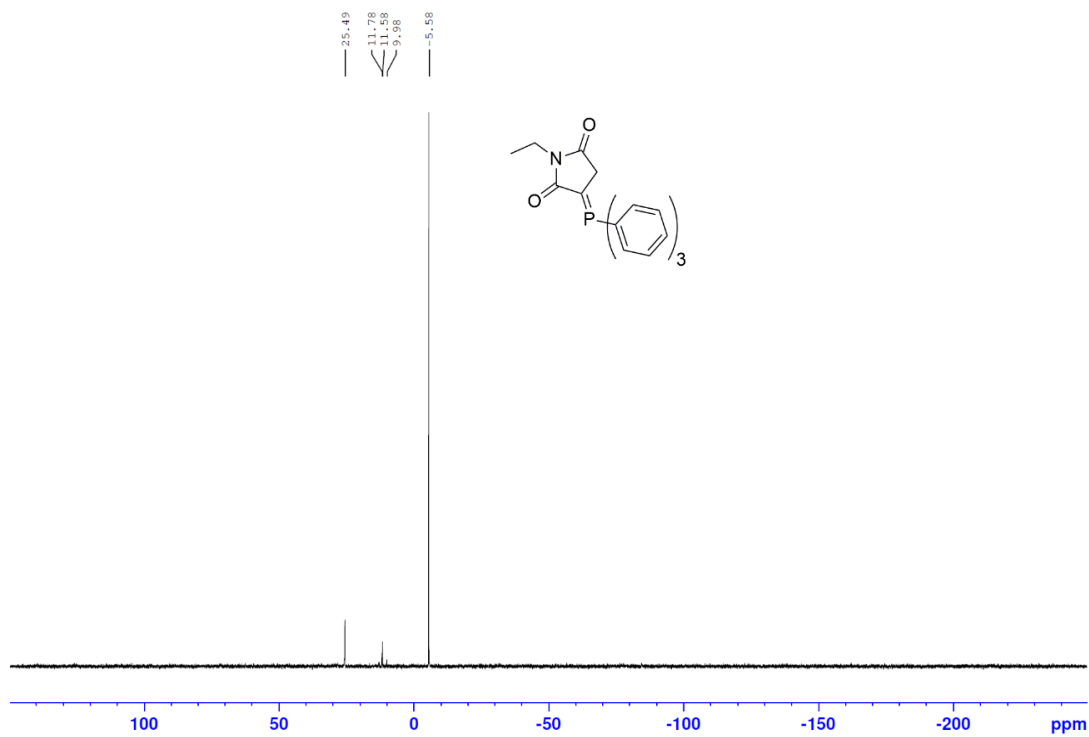
Figure A.18. ^{31}P NMR spectrum of NEM-TPP (solvent: DMF).
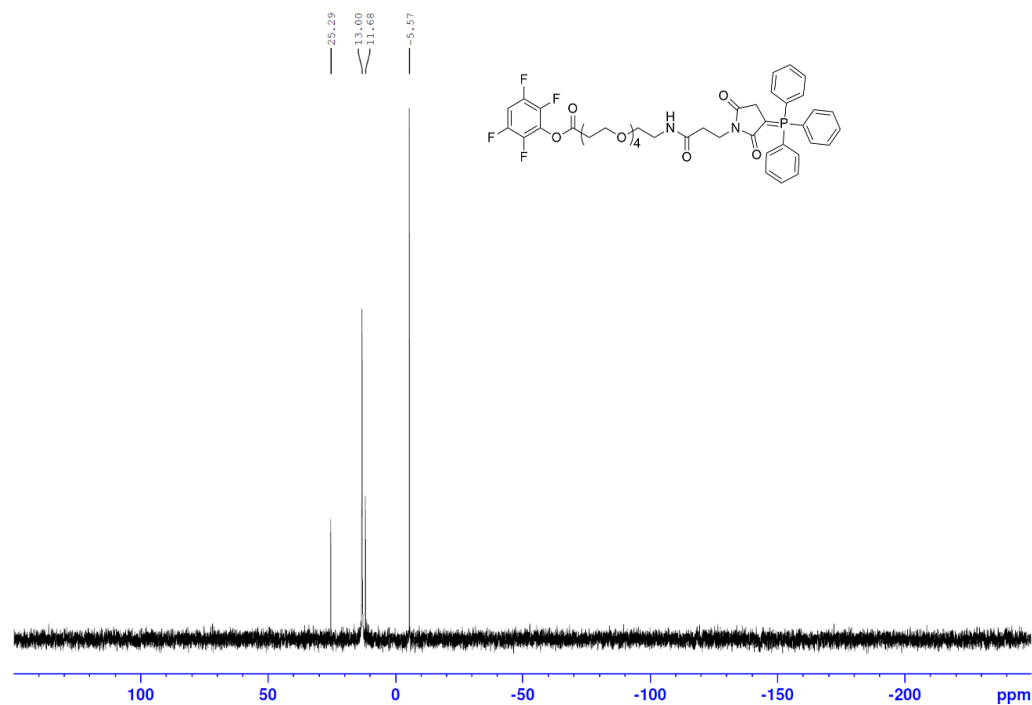
Figure A.19. ^{31}P NMR spectrum of TFP-PEG$_4$-MAL-TPP (0 hours) (solvent: DMF).
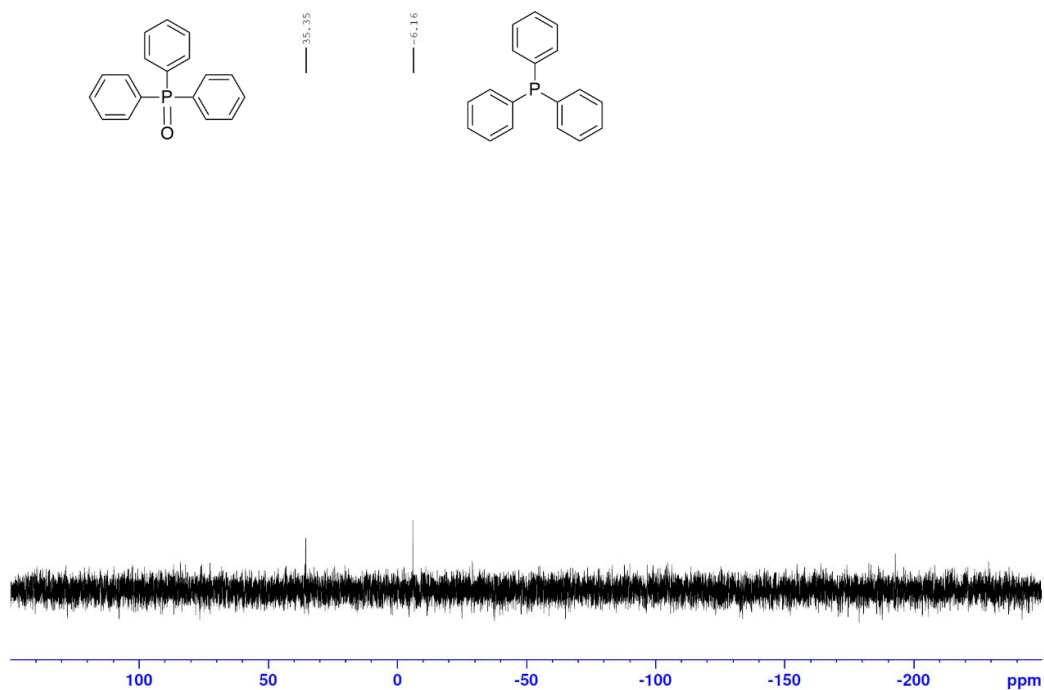
Figure A.20. ^{31}P NMR spectrum of TFP-PEG$_4$-MAL-TPP (2 hours) (solvent: ddH$_2$O). The chemical shift at δ = 35.3 ppm corresponds to the TPP oxide species and the chemical shift at δ = 6.1 ppm corresponds to unreacted TPP.
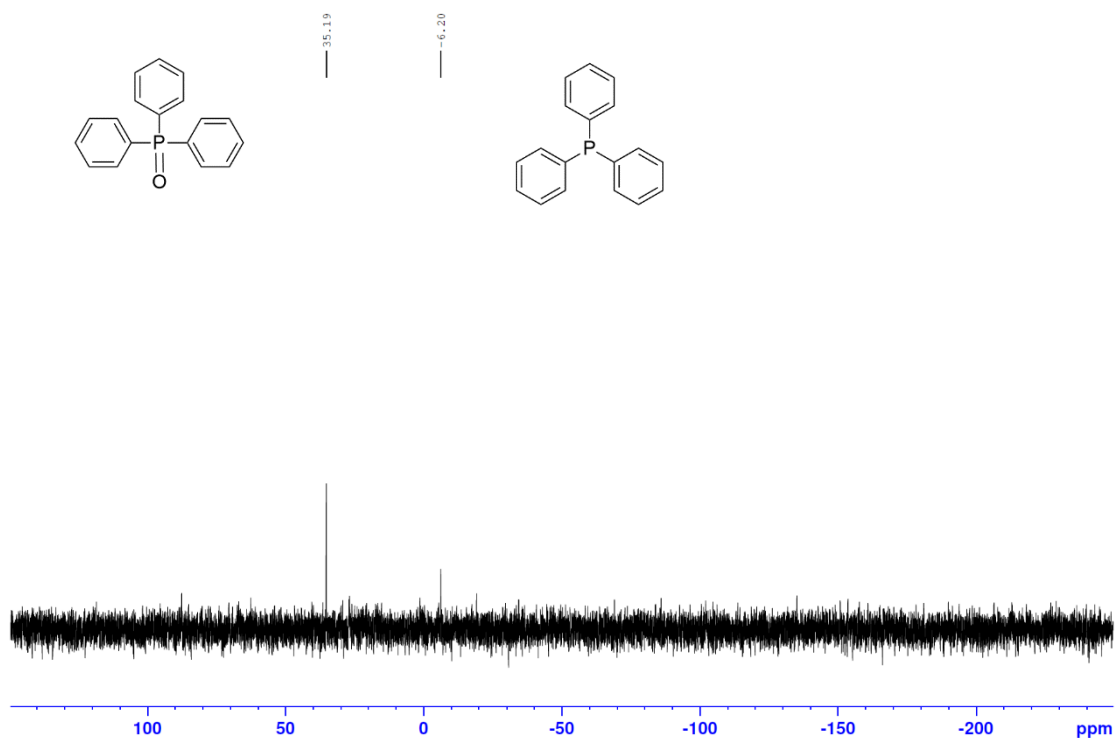
Figure A.21. ^{31}P NMR spectrum of TFP-PEG$_4$-MAL-TPP (24 hours) (solvent: ddH$_2$O). The chemical shift at $\delta = 35.2$ ppm corresponds to the TPP oxide species and the chemical shift at $\delta = 6.2$ ppm corresponds to unreacted TPP.

Sample #1
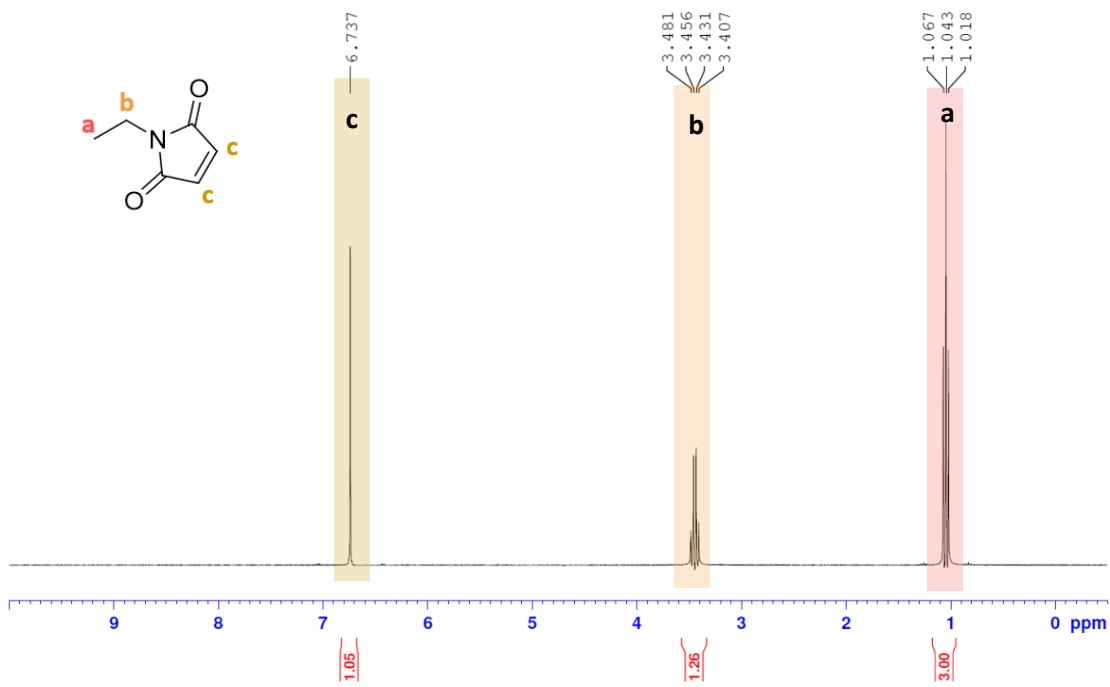
Figure A.22. ^{1}H NMR spectrum of NEM (solvent: CDCl$_3$).
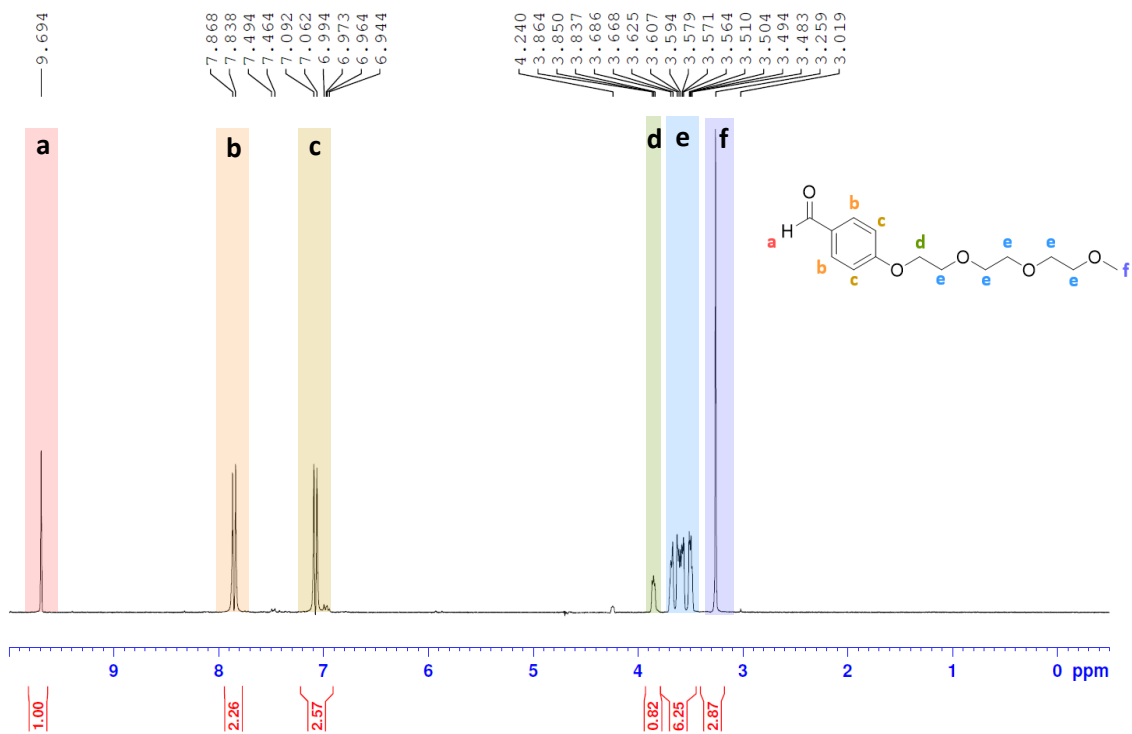
Figure A.23. ^{1}H NMR spectrum of mPEG$_4$BA (solvent: CDCl$_3$).
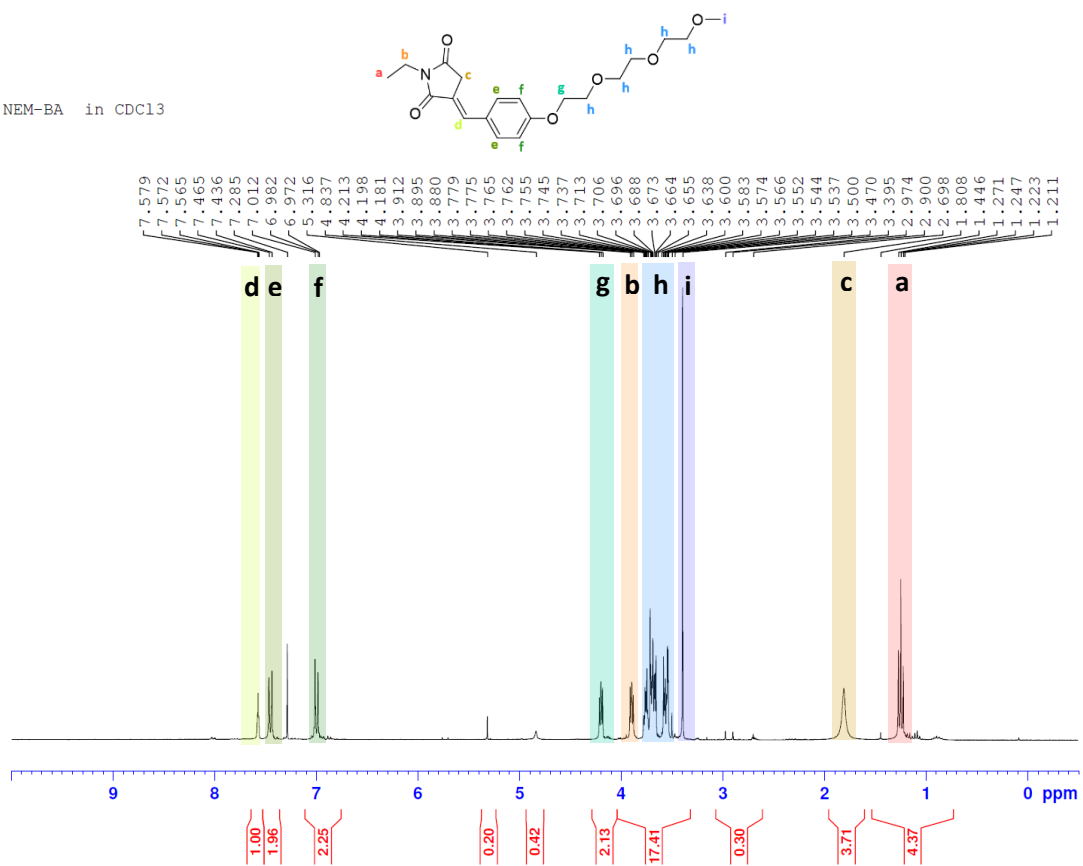
Figure A.24. ^{1}H NMR spectrum of NEM-mPEG$_4$BA (solvent: CDCl$_3$).
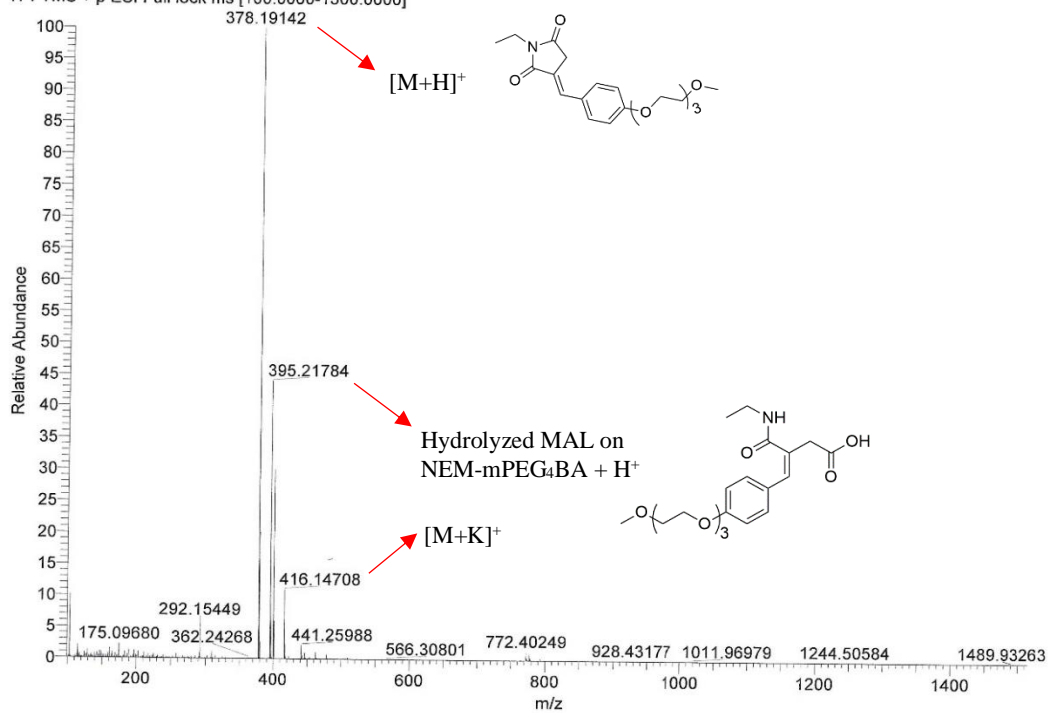
Figure A.25. High resolution ESI MS of NEM-mPEG4BA.
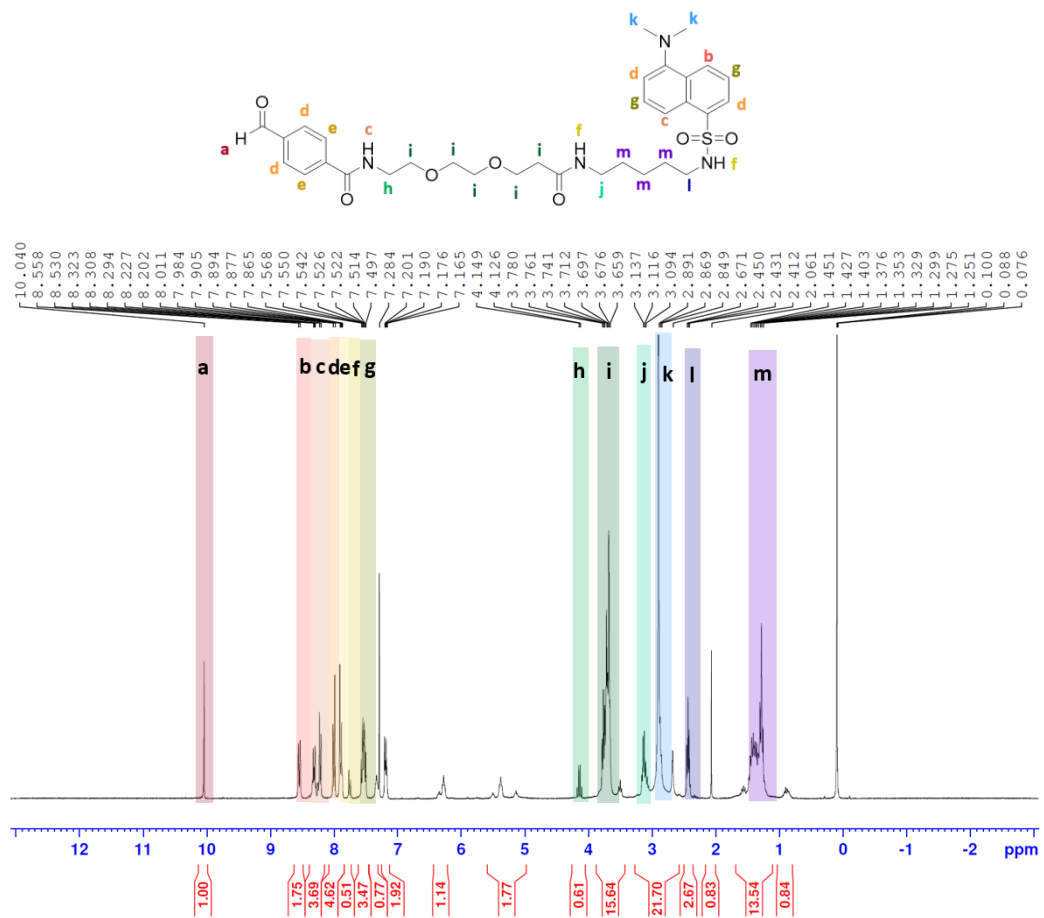
Figure A.26. ^{1}H NMR spectrum of **2a** (dansylcadaverine-PEG$_2$-Ph-Aldehyde) (solvent: CDCl$_3$).
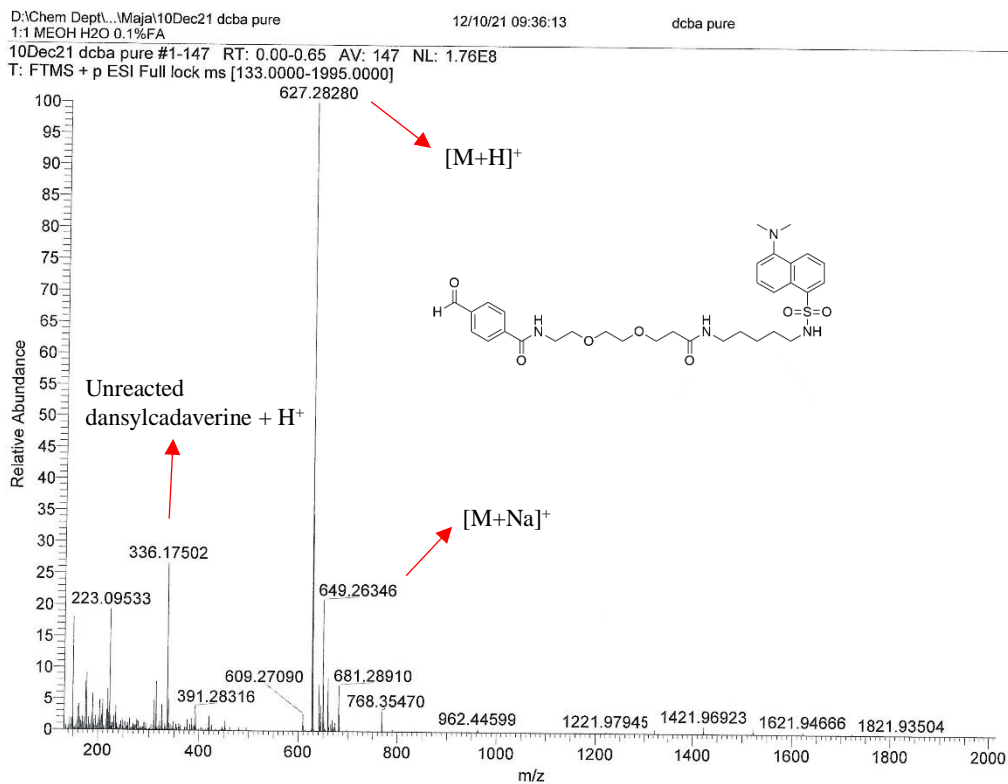
Figure A.27. High resolution ESI MS of **2a** (dansylcadaverine-PEG$_2$-Ph-Aldehyde).
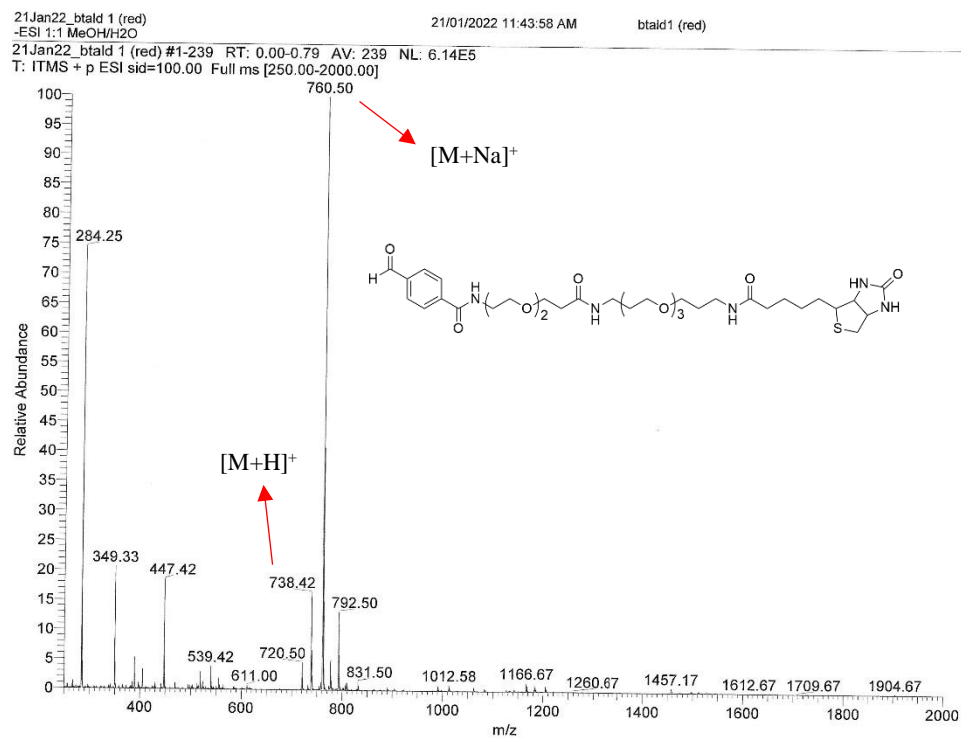
Figure A.28. Low resolution ESI MS of **2b** (biotin-PEG$_5$-Ph-Aldehyde).
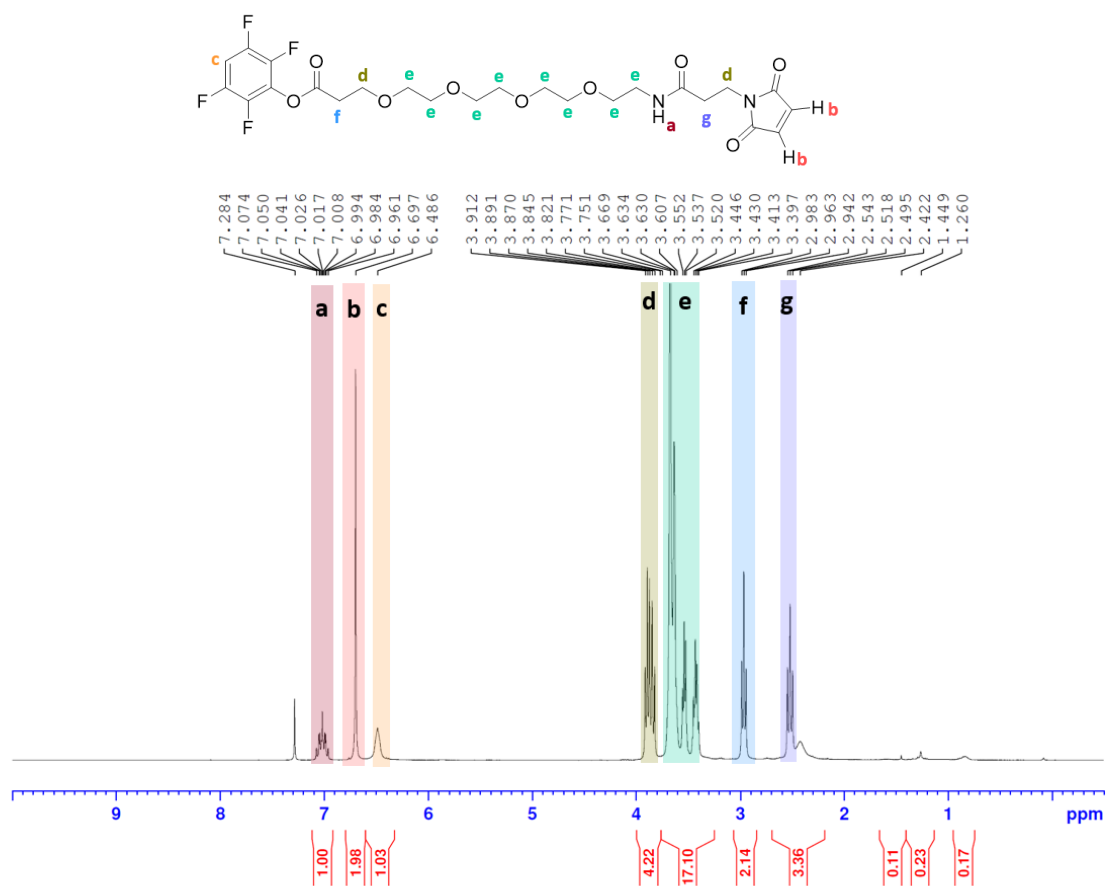
Figure A.29. ^{1}H NMR spectrum of TFP-PEG$_4$-MAL (solvent: CDCl$_3$).
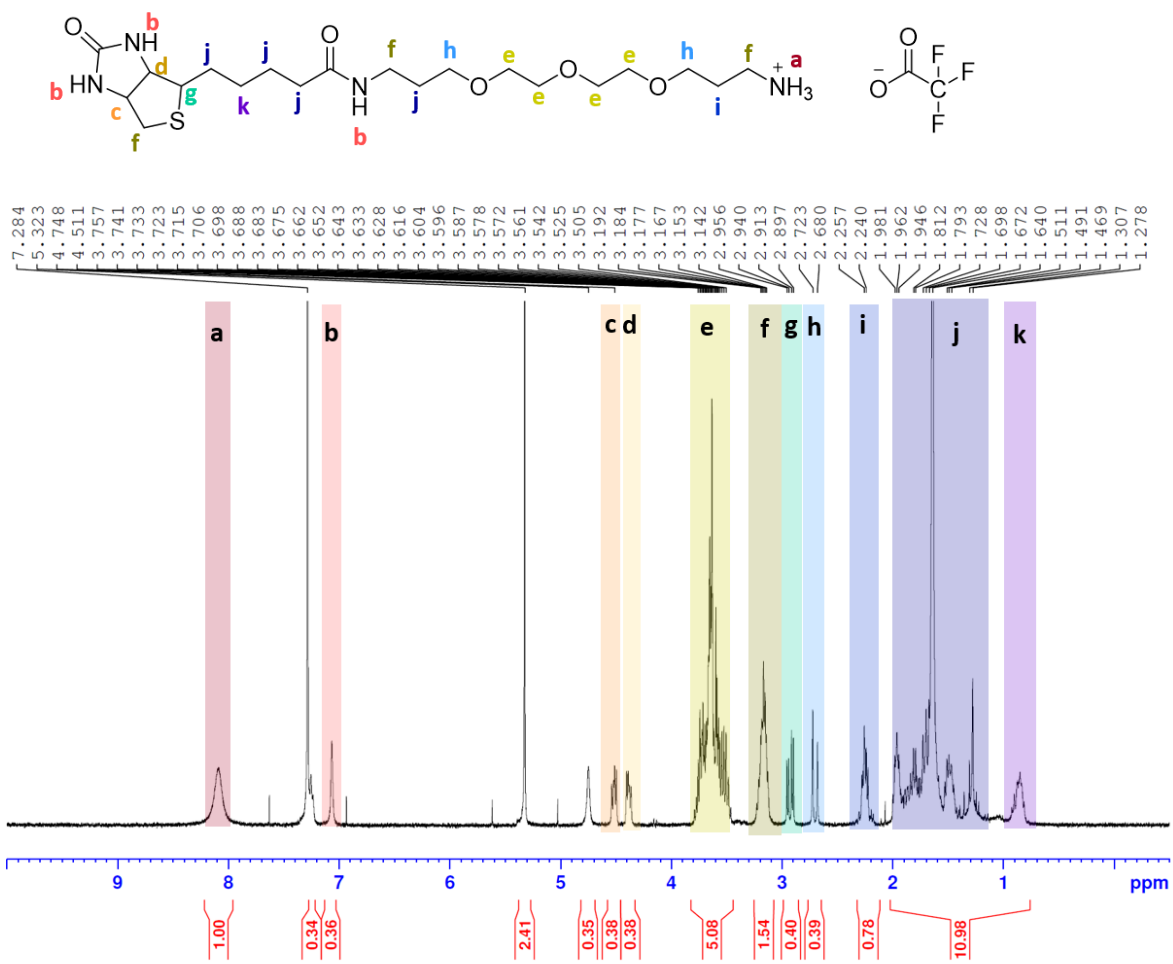
Figure A.30. ^{1}H NMR spectrum of biotin-PEG$_3$-NH$_3^{+-}$TFA (solvent: CDCl$_3$).
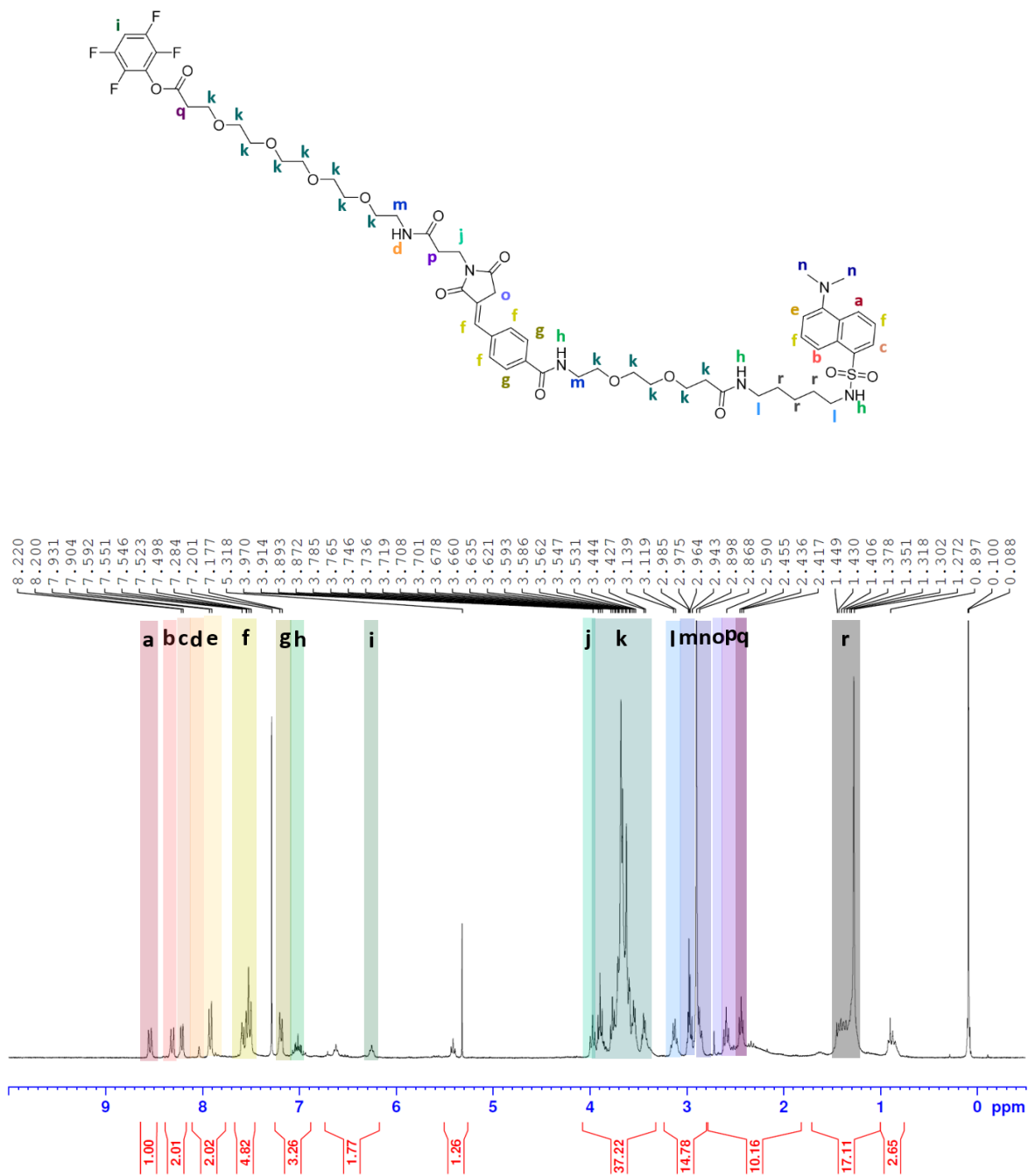
Figure A.31. ^{1}H NMR spectrum of **2f** (TFP-PEG$_4$-MAL-dansylcadaverine-PEG$_2$-Ph-Aldehyde Wittig) (solvent: CDCl$_3$).

Figure A.32. High resolution ESI MS of **2f** (TFP-PEG$_4$-MAL-dansylcadaverine-PEG$_2$-Ph-Aldehyde Wittig).
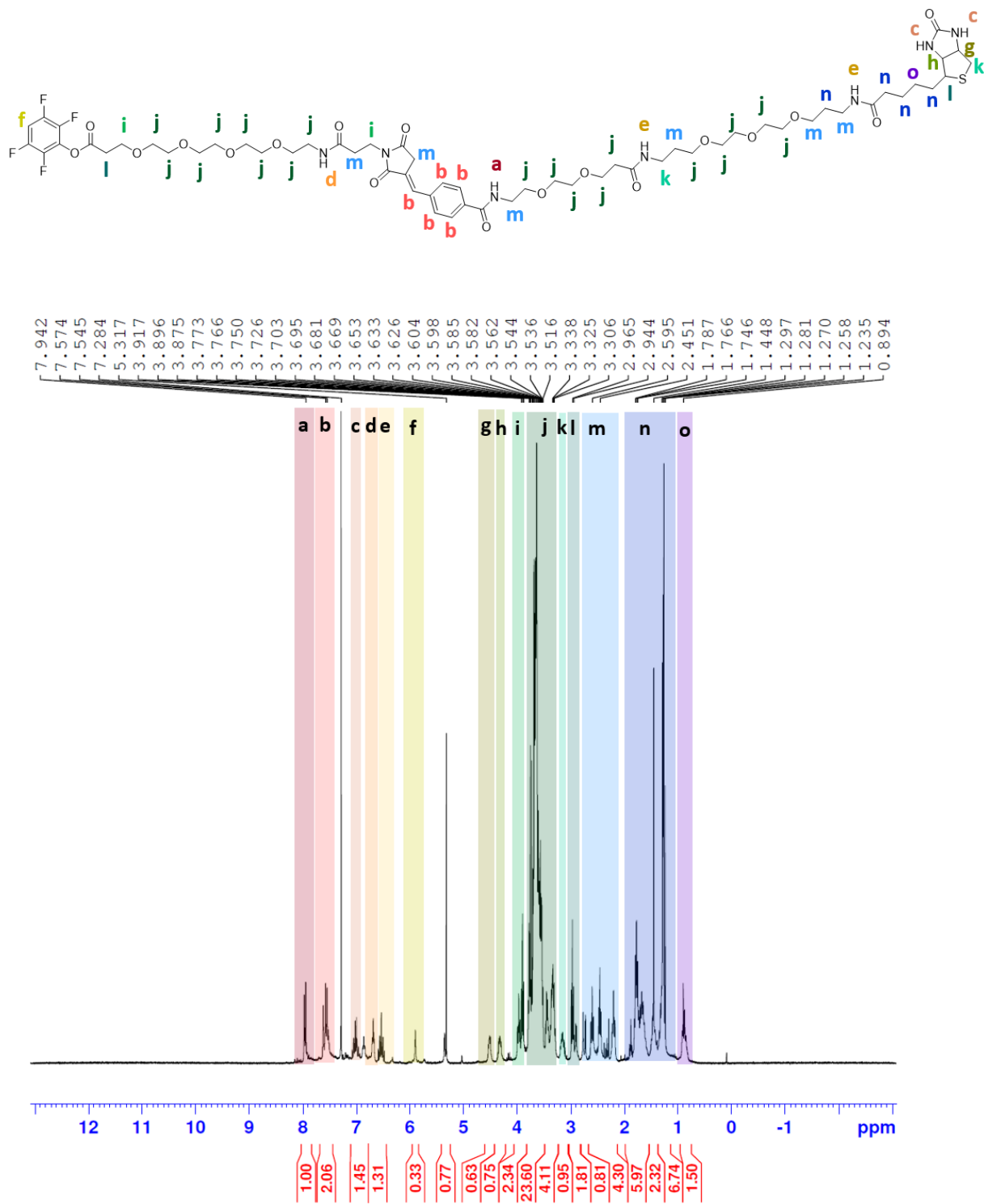
Figure A.33. ^{1}H NMR spectrum of **2g** (TFP-PEG$_4$-MAL-biotin-PEG$_5$-Ph-Aldehyde Wittig) (solvent: CDCl$_3$).
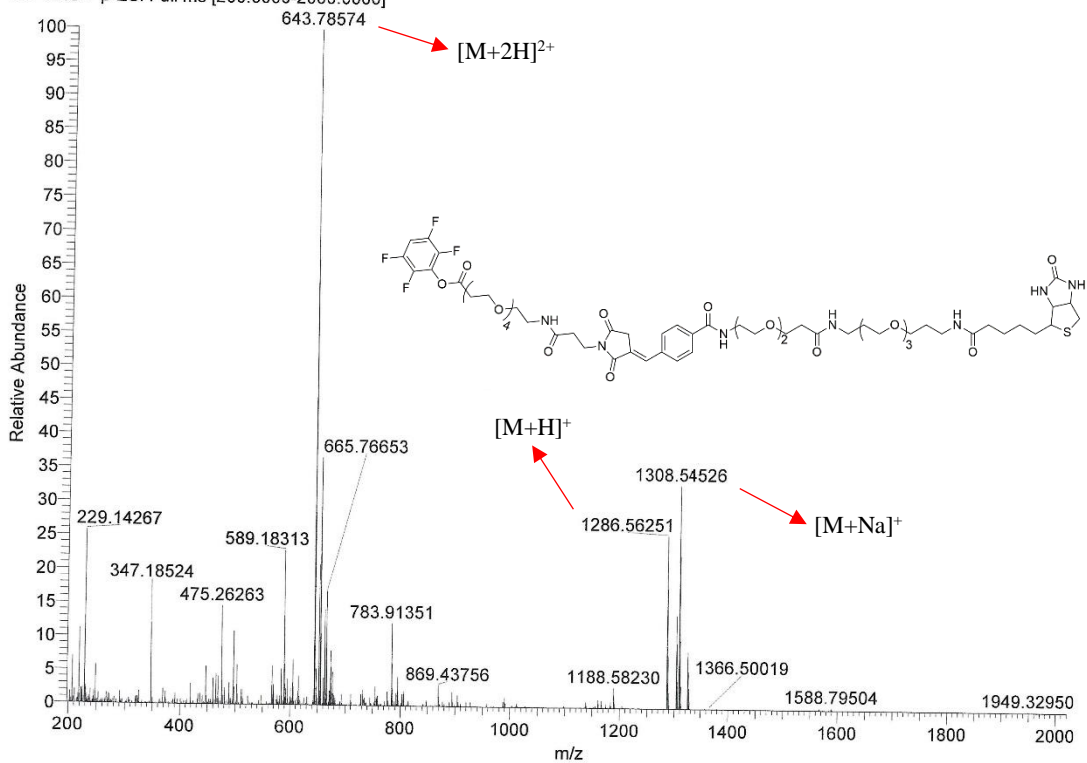
Figure A.34. High resolution ESI MS of **2g** (TFP-PEG₄-MAL-biotin-PEG₅-Ph-Aldehyde Wittig).
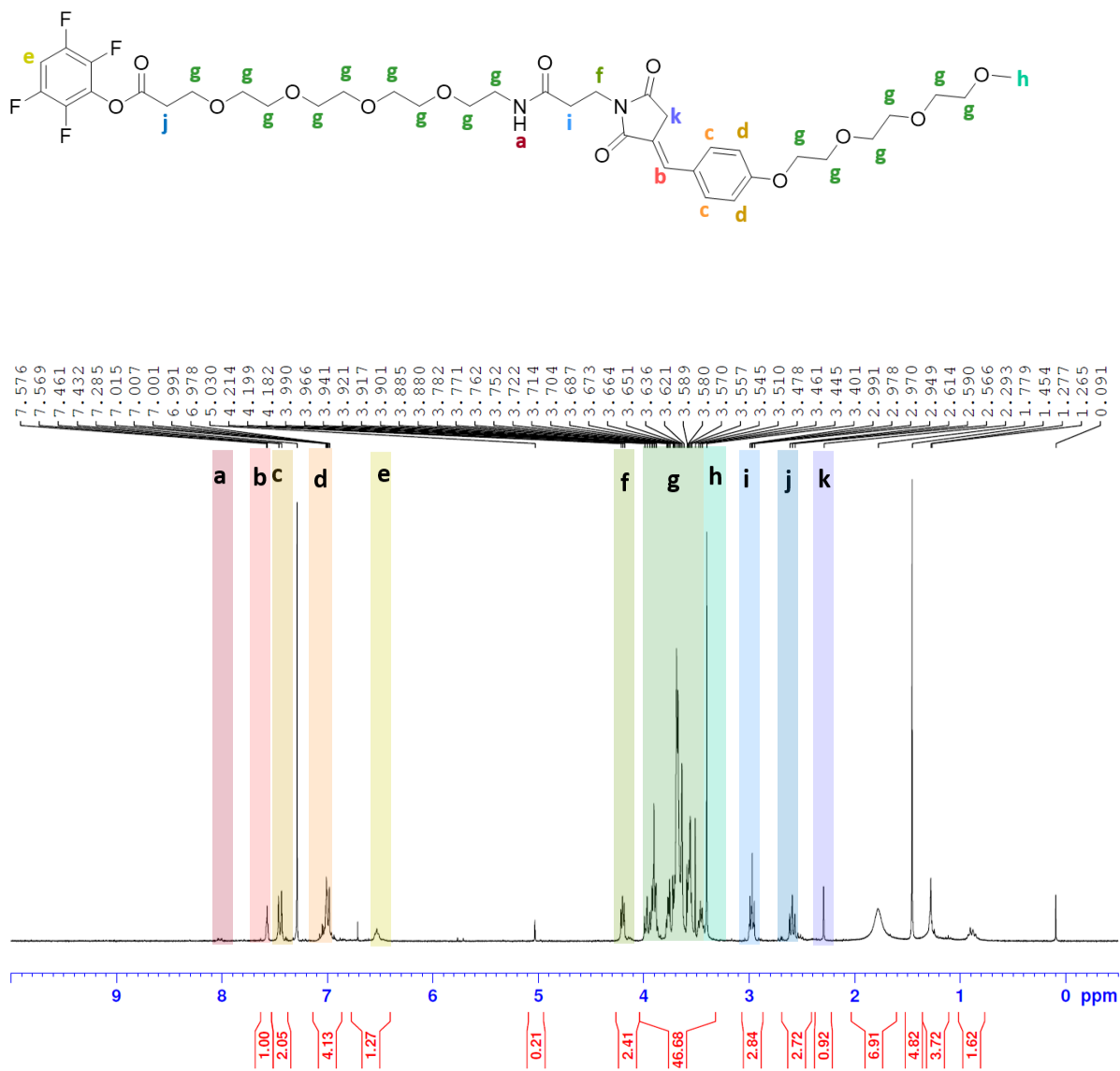
Figure A.35. ^{1}H NMR spectrum of **2h** (TFP-PEG$_4$-MAL-mPEG$_4$BA Wittig) (solvent: CDCl$_3$).
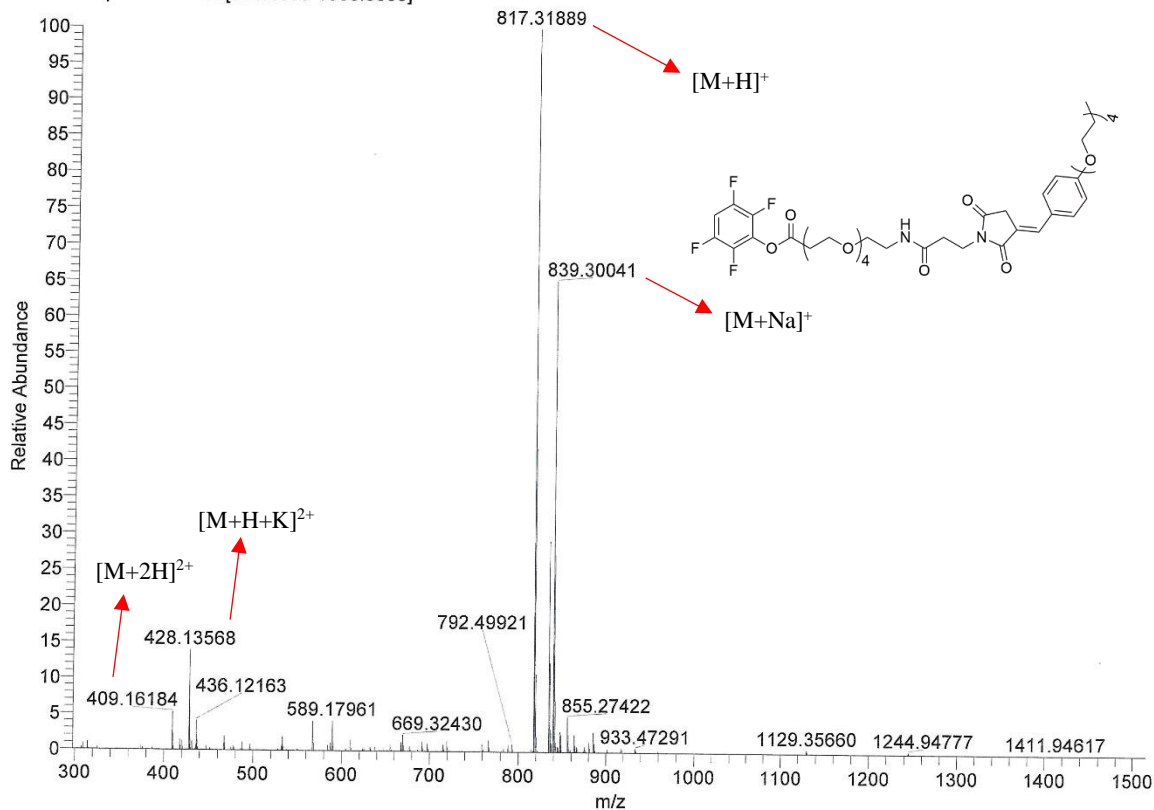
Figure A.36. High resolution ESI MS of **2h** (TFP-PEG₄-MAL-mPEG₄BAWittig).
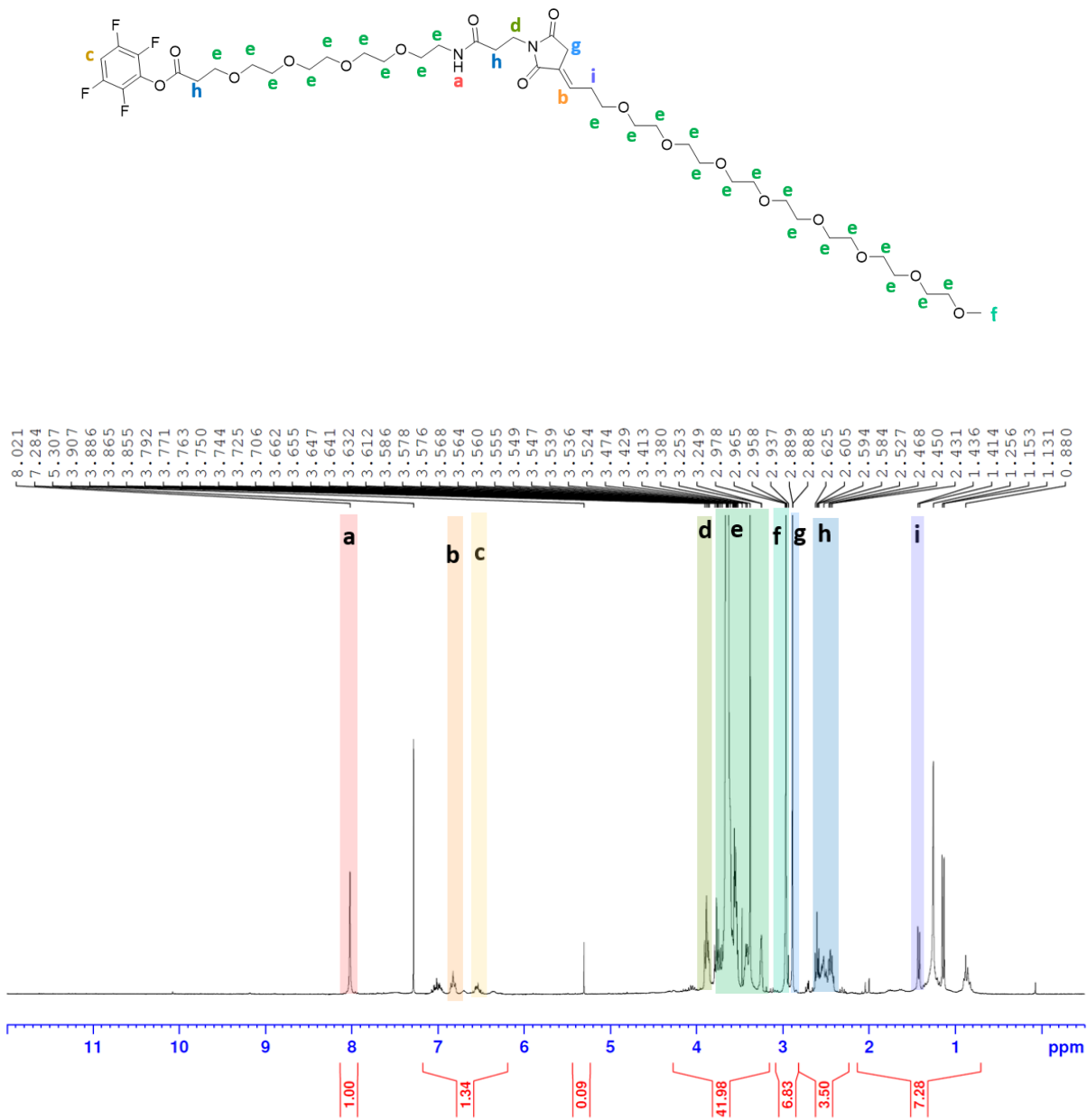
Figure A.37. ^{1}H NMR spectrum of **2i** (TFP-PEG$_4$-MAL-mPEG$_8$Aldehyde Wittig) (solvent: CDCl$_3$).
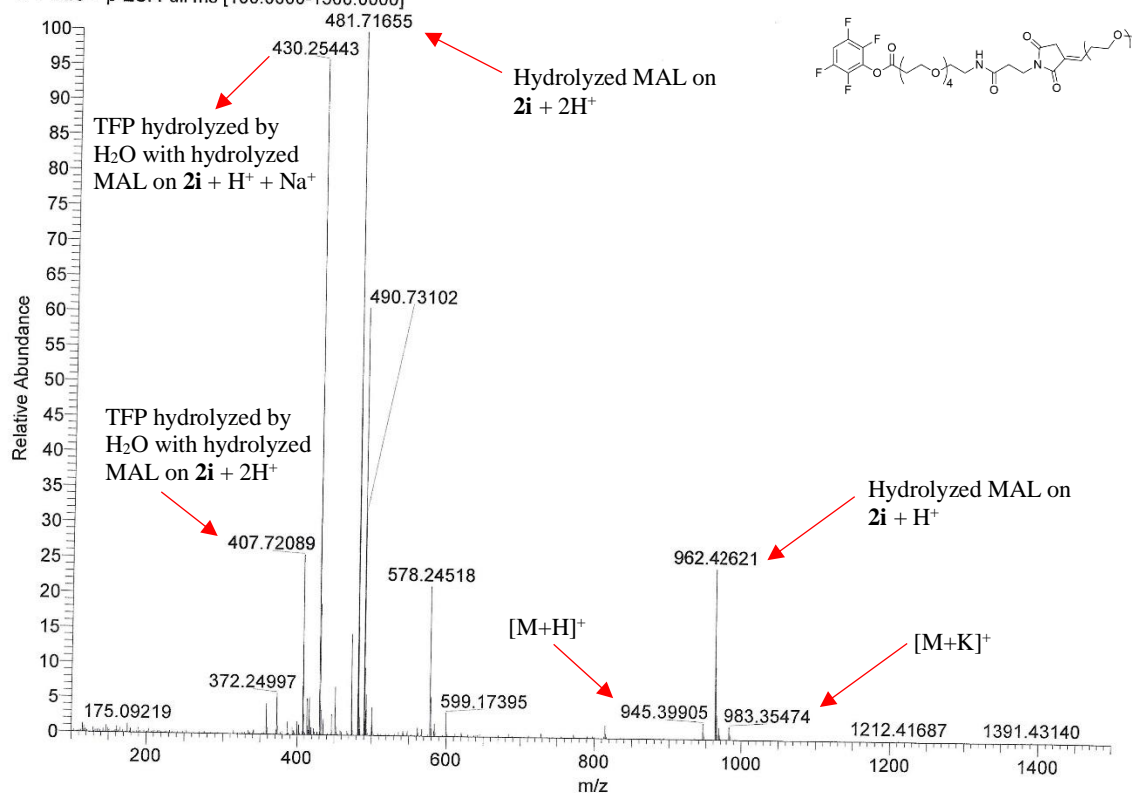
Figure A.38. High resolution ESI MS of **2i** (TFP-PEG$_4$-MAL-mPEG$_4$BAWittig).
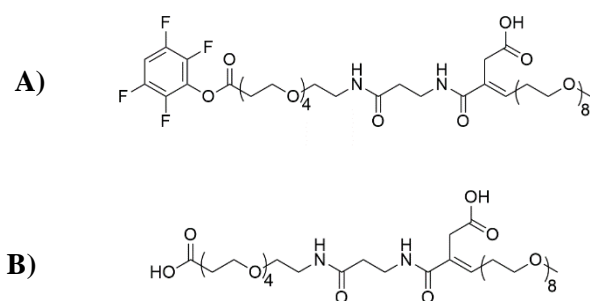
Figure A.39. Chemical structures of side products associated with **2i** (TFP-PEG$_4$-MAL-mPEG$_4$BAWittig) as detected by high resolution ESI MS. **A)** Hydrolyzed MAL on **2i** + H$^+$ (m/z = 962.4262 Da). **B)** TFP hydrolyzed by H$_2$O with hydrolyzed MAL on **2i** (for 2H$^+$ adduct: m/z = 407.7209 Da and for H$^+$ + Na$^+$ adduct: m/z = 430.2544.
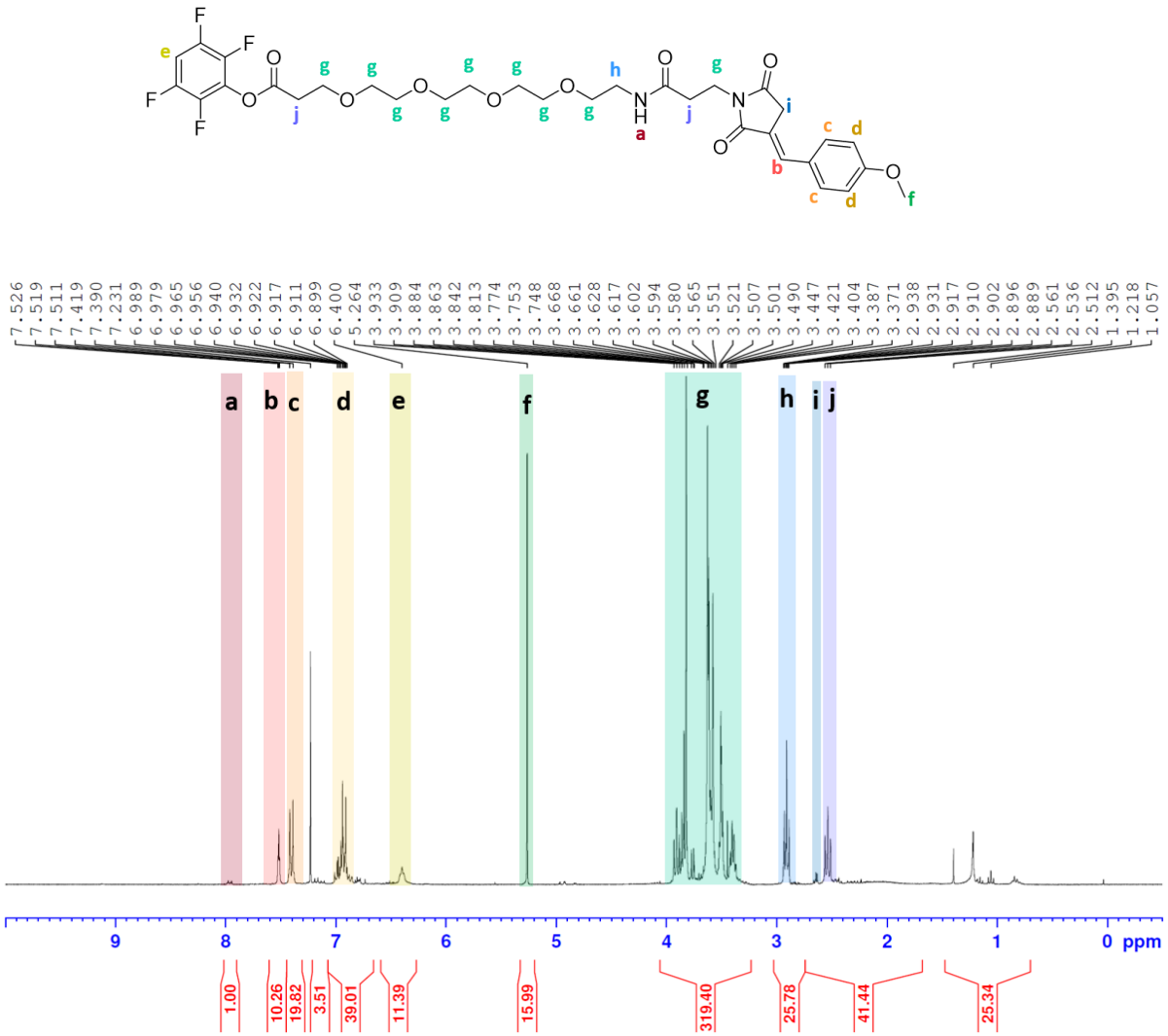
Figure A.40. ¹H NMR spectrum of **2j** (TFP-PEG₄-MAL-*p*-Anisaldehyde Wittig) (solvent: CDCl₃).
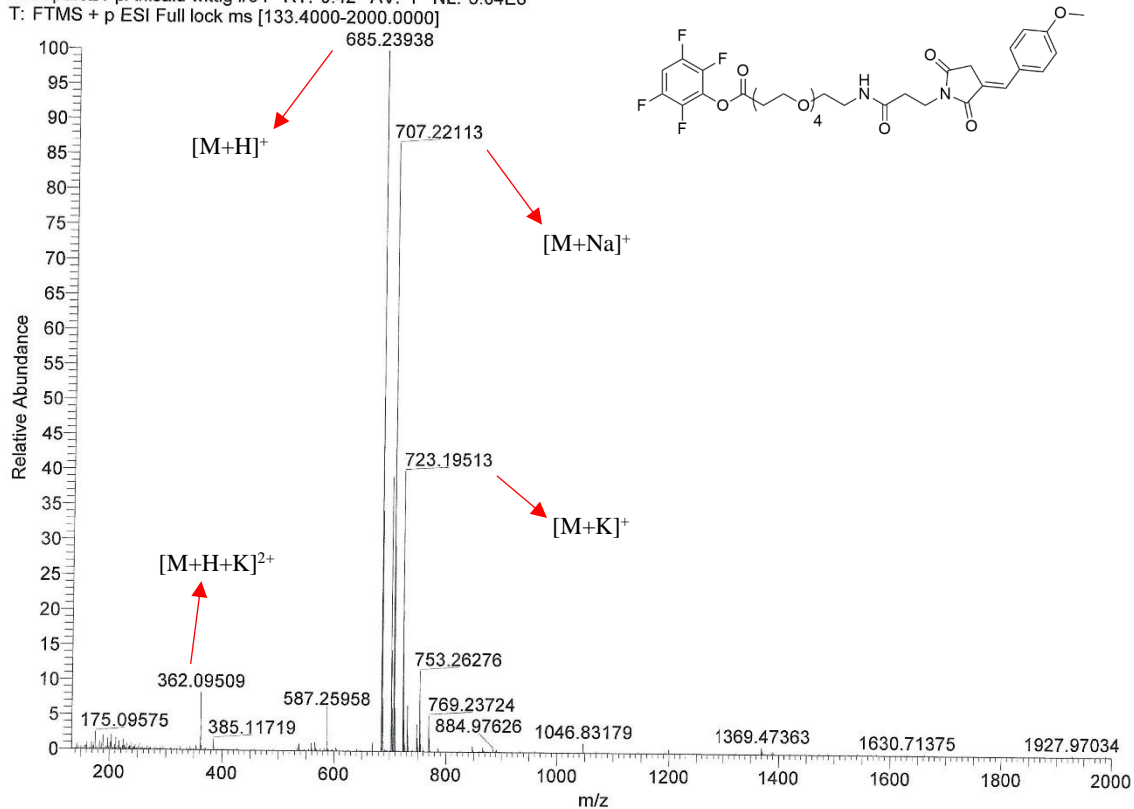
Figure A.41. High resolution ESI MS of **2j** (TFP-PEG$_4$-MAL-*p*-Anisaldehyde Wittig).
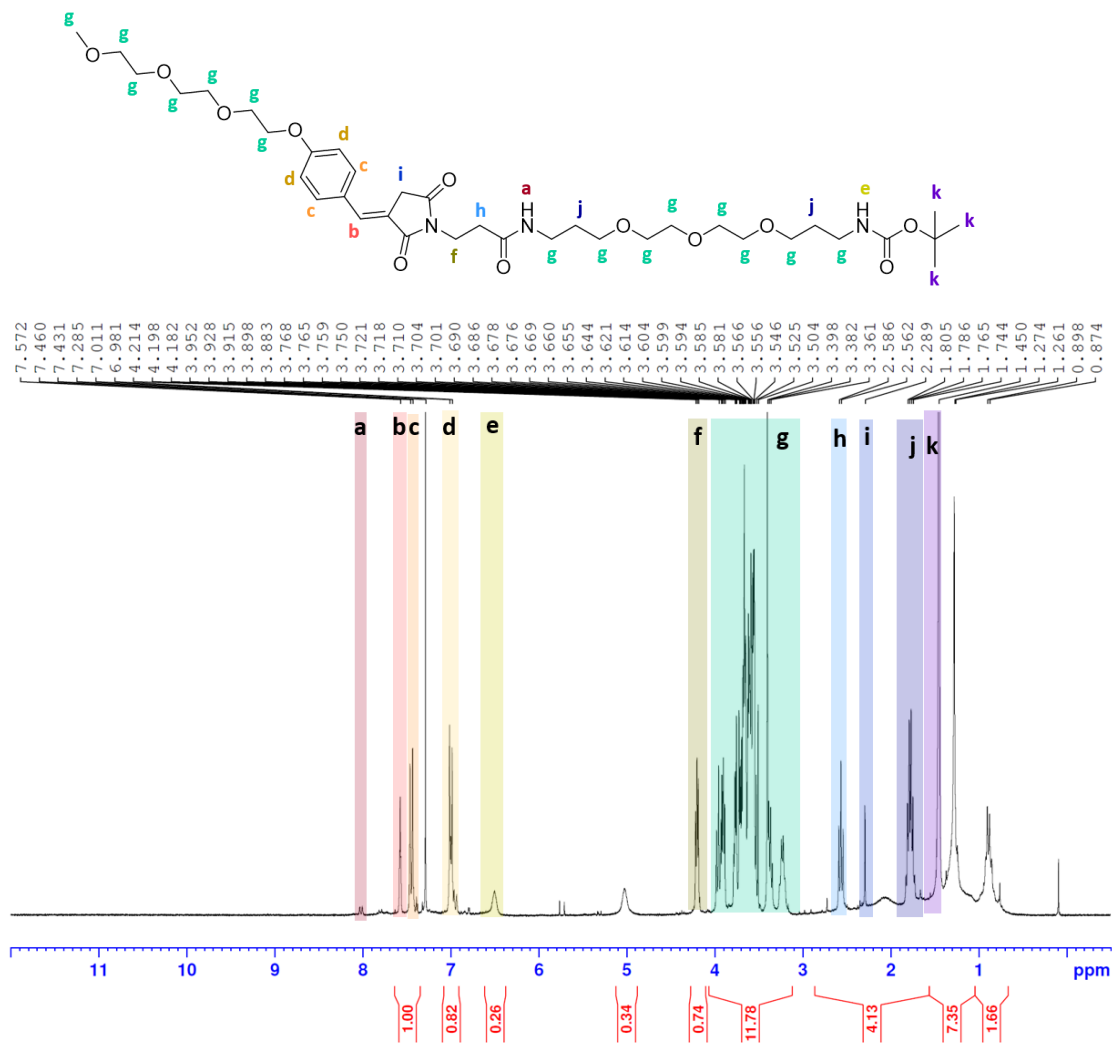
Figure A.42. ^{1}H NMR spectrum of **1b** (t-boc-amido-PEG$_3$-mPEG$_4$BA Wittig product) (solvent: CDCl$_3$).
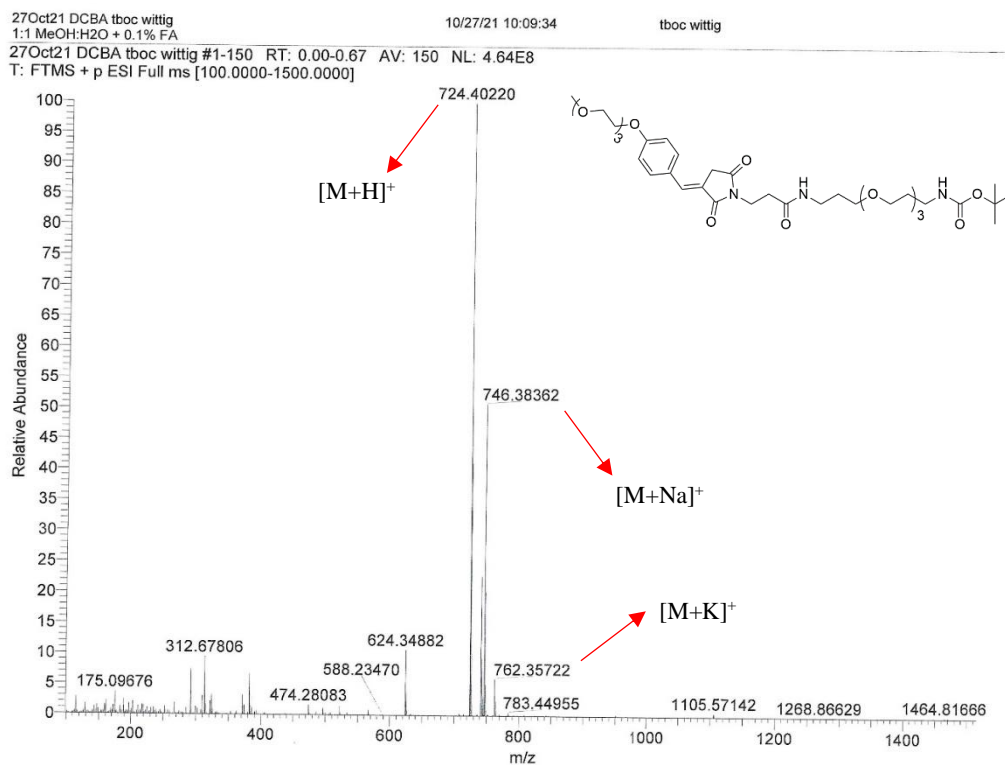
Figure A.43. High resolution ESI MS of **1b** (t-boc-amido-PEG$_3$-mPEG$_4$BA Wittig product).
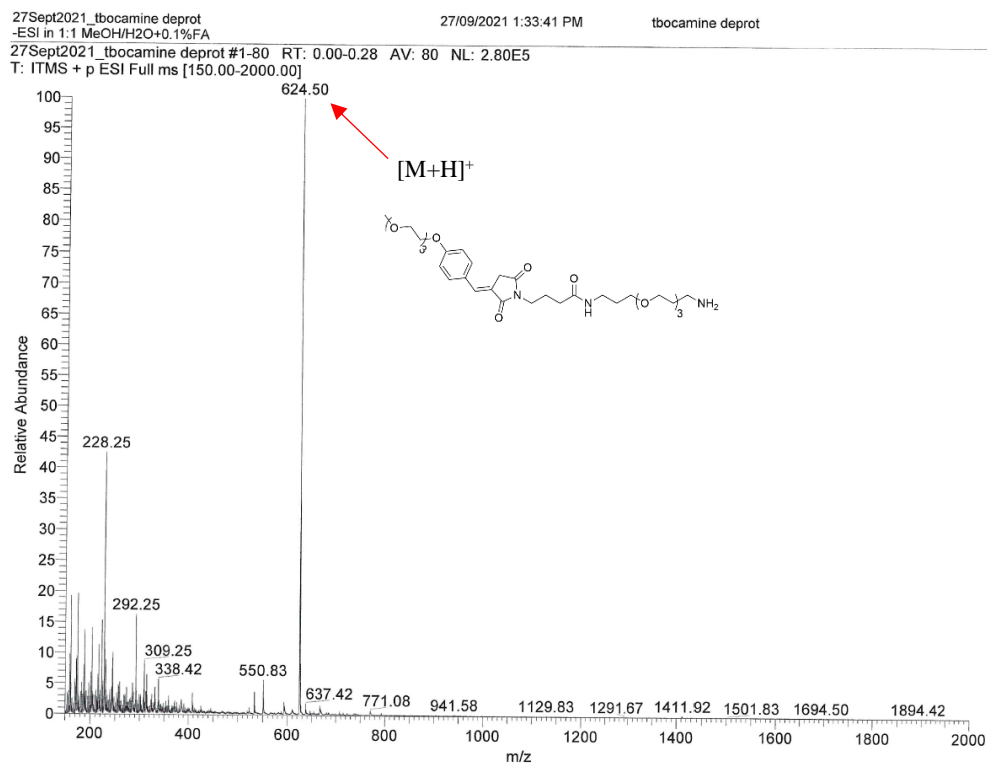

Figure A.44. Low resolution ESI MS of **1c** (amine-PEG$_3$-mPEG$_4$BA Wittig product).

Appendix B: Additional Information for Jaguar pKa Module Calculations

In Chapter 2, the pKas of various NEM-based phosphonium adducts were calculated using the Jaguar pKa module (Schrodinger LLC, 2021-4 Release) (Sections 2.3.5. and 2.4.5). The following presents a brief summary of the information provided by Schrodinger for the calculation of pKa values.[1]

The *ab initio* quantum chemical pKa calculation of a given molecule begins with the following thermodynamic cycle:
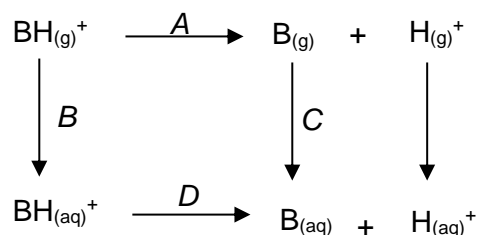
Scheme B.1. Thermodynamic cycle for the *ab initio* quantum chemical pKa calculation (Jaguar, Schrodinger LLC). Adapted from the Jaguar User Manual (Schrodinger LLC).[1]

The free energy changes of *A*, *B*, and *C* are calculated and summed to get *D* (along with the experimentally determined value of -259.5 kJ/mol), which is related to the pKa value by the following equation:

$$pK_a = \frac{1}{2.3\ RT}\ D \qquad \text{[Equation 1]}$$

The parameter *A* is calculated using the Gibbs free energy equation:

$$\Delta G = \Delta H - T\Delta S$$

$$= E_{B_{(g)}} - E_{B_{(BH)}} + \frac{5}{2}RT - T\Delta S \qquad \text{[Equation 2]}$$

In order to obtain the energy value in Equation 2, geometry optimizations of the protonated and deprotonated species must first be obtained. Schrodinger uses the B3LYP/6-31G* basis set. Next, accurate single point energies are obtained for each optimized geometry (using the cc-pVTZ(+) basis set). Finally, SCRF (self-consistent reaction field) calculations are used to calculate the solvation free energies of the protonated and deprotonated species using the optimized gas-phase geometries. Because a large database of experimental pKa values exist for a variety of functional groups, parameters for ions are fitted to the experimental pKa data. Finally, a correction scheme is applied to the raw data in order to remove any residual errors associated with the previous calculations.[2] The correction scheme is related to the linear equation shown below:

$$pK_a = a\, pK_a\,(raw) + b \quad \text{[Equation 3]}$$

The *a* term is added in the correction scheme in order to account for the variation in charge on ionizable groups. The *b* term is added in the correction scheme in order to account for surface tension corrections.

References

1. Schrodinger. Ab initio quantum chemical calculation of pKa values, **2021**. Jaguar User Manual. https://www.schrodinger.com/sites/default/files/s3/mkt/Documentation/2021-4/docs/Documentation.htm#jaguar_user_manual/jaguar_pka_theory_ab_initio.htm (accessed Feb 21, 2022).

2. Schrodinger. Empirical corrections for Jaguar pKa calculations, **2021**. Jaguar User Manual. https://www.schrodinger.com/sites/default/files/s3/mkt/Documentation/2021-4/docs/Documentation.htm#jaguar_user_manual/jaguar_pka_theory_empirical_corrections.htm (accessed Feb 21, 2022).